

ENZYMATIC SYNTHESIS OF PHENOLIC ACID GLUCOSYL ESTERS  
AND THEIR EFFECT IN CHOLANGIOCARCINOMA CELLS



EKO SUYANTO

A Thesis Submitted in Partial Fulfillment of the Requirements for the  
Degree of Doctor of Philosophy in Biochemistry and Biochemical Technology  
Suranaree University of Technology  
Academic Year 2023

การสังเคราะห์ด้วยเอนไซม์ของกรดฟีนอลิกกลูโคซิลเอสเทอร์และฤทธิ์ต่อเซลล์  
มะเร็งท่อน้ำดี



นายเอ็กโค สุยันโต

วิทยานิพนธ์นี้เป็นส่วนหนึ่งของการศึกษาตามหลักสูตรปริญญาวิทยาศาสตรดุษฎีบัณฑิต  
สาขาวิชาชีวเคมีและเทคโนโลยีชีวเคมี  
มหาวิทยาลัยเทคโนโลยีสุรนารี  
ปีการศึกษา 2566

ENZYMATIC SYNTHESIS OF PHENOLIC ACID GLUCOSYL ESTERS AND  
THEIR EFFECT IN CHOLANGIOCARCINOMA CELLS

Suranaree University of Technology has approved this thesis submitted in partial fulfillment of the requirement for the Degree of Doctor of Philosophy.

Thesis Examining Committee



(Dr. Kriengsak Lirdprapamongkol)

Chairperson



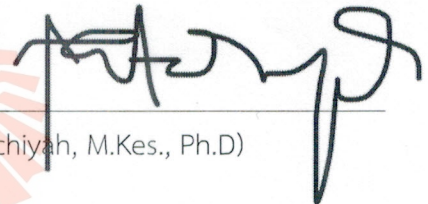
(Prof. Dr. James R. Ketudat-Cairns)

Member (Thesis Advisor)



(Assoc. Prof. Dr. Chutima Talabnin)

Member



(Prof. Fatchiyah, M.Kes., Ph.D.)

Member



(Assoc. Prof. Dr. Panida Khunkaewla)

Member



(Assoc. Prof. Dr. Mariena Ketudat-Cairns)

Member



(Assoc. Prof. Dr. Yupaporn Ruksakulpiwat)

Vice Rector for Academic Affairs

and Quality Assurance



(Prof. Dr. Santi Maensiri)

Dean of Institute of Science

เอ็กโค สุยน์โต : การสังเคราะห์ด้วยเอนไซม์ของกรดพีนอลิกกลูโคซิลเอสเทอร์และฤทธิ์ต่อเซลล์มะเร็งท่อน้ำดี (ENZYMATIC SYNTHESIS OF PHENOLIC ACID GLUCOSYL ESTERS AND THEIR EFFECT IN CHOLANGIOCARCINOMA CELLS). อาจารย์ที่ปรึกษา : ศาสตราจารย์ ดร. เจมส์ เกตุทัต-คาร์นส์, 155 หน้า.

คำสำคัญ : เบต้ากลูโคซิเดส; กลูโคซิลเอสเทอร์; กลูโคแกลลิน; มะเร็งท่อน้ำดี

Os9BGlu31 เป็นเอนไซม์ในข้าวกลุ่มไกลโคไซด์ไฮโดรเลส 1 (GH1) ซึ่งทำหน้าที่หลักในการเร่งปฏิกิริยาไฮโดรไลซิส และ Os9BGlu31 ยังเกี่ยวข้องกับกระบวนการทรานส์ไกลโคซิเลชันในการถ่ายโอนหมู่น้ำตาลไกลโคซิลเพื่อสังเคราะห์สารประกอบไกลโคซิเลตโดยเป็นปฏิกิริยาขั้นตอนเดียวและผลิตภัณฑ์มีความเสถียรมากขึ้น ละลายน้ำได้ มีความสามารถในการถูกดูดซึมสูง และมีฤทธิ์ทางชีวภาพสูง ดังนั้นสารประกอบไกลโคซิเลตอาจสามารถนำมาใช้เป็นสารออกฤทธิ์ในทางการแพทย์ รวมทั้งฤทธิ์ในการต้านมะเร็ง อย่างไรก็ตามยังไม่มีรายงานถึงฤทธิ์ของสารประกอบไกลโคซิเลต เช่น สารประกอบกรดพีนอลิก กลูโคซิลเอสเทอร์ต่อการเจริญของเซลล์มะเร็งท่อน้ำดี

ในการศึกษานี้เอนไซม์ Os9BGlu31 ถูกใช้ในกระบวนการสังเคราะห์สารประกอบกรดพีนอลิก กลูโคซิลเอสเทอร์ 8 ชนิด จากกรดพีนอลิกอิสระ จากนั้นสารที่สังเคราะห์ได้ถูกประเมินฤทธิ์ทางชีวภาพและศึกษากลไกที่เกี่ยวข้องในการยับยั้งการเจริญของเซลล์มะเร็งท่อน้ำดี เอนไซม์ Os9BGlu31 ดั้งเดิมและกลายพันธุ์ถูกผลิตโดยแบคทีเรีย *Escherichia coli* สายพันธุ์ Origami B(DE3) แล้วทำให้บริสุทธิ์โดยใช้คอลัมน์ IMAC จากนั้นผลิตภัณฑ์จากกระบวนการทรานส์ไกลโคซิเลชันของเอนไซม์ Os9BGlu31 และเอนไซม์กลายพันธุ์ถูกตรวจวัดโดยโครมาโตกราฟีเชิงวิเคราะห์แล้วทำให้บริสุทธิ์โดยใช้คอลัมน์เซฟาเดกซ์-แอลเอช20 โดยโครงสร้างของสารประกอบถูกวิเคราะห์โดยวิธีเอ็นเอ็มอาร์สเปกโทรสโกปี และผลิตภัณฑ์จากกระบวนการทรานส์ไกลโคซิเลชันถูกวัดความสามารถเบื้องต้นในการต้านอนุมูลอิสระและฤทธิ์ยับยั้งการเจริญในเซลล์มะเร็งท่อน้ำดี แล้วทดสอบความสามารถในการยับยั้งการแพร่กระจายของเซลล์มะเร็งท่อน้ำดีด้วยวิธีการตรวจจุลทรรศน์ เพื่อหาสารประกอบกรดพีนอลิกกลูโคซิลเอสเทอร์ที่มีฤทธิ์สูงที่สุดมาศึกษากลไกในการยับยั้งเซลล์มะเร็งท่อน้ำดีโดยการวิเคราะห์การเปลี่ยนแปลงวัฏจักรของเซลล์ การตายของเซลล์แบบอะพอโทซิส และวัดการแสดงออกในระดับเอ็มอาร์เอ็นเอของยีนที่เกี่ยวข้องกับกลไกดังกล่าว

จากการทดลองพบว่า Os9BGlu31 กลายพันธุ์สามารถสังเคราะห์ผลิตภัณฑ์จากกระบวนการทรานส์ไกลโคซิเลชันได้หลากหลายกว่าเอนไซม์ดั้งเดิมผ่านการถ่ายโอนหมู่น้ำตาลไปยังตำแหน่งของหมู่ไฮดรอกซิลหรือหมู่คาร์บอกซิล โดยผลิตภัณฑ์หลักมาจากการจับของหมู่น้ำตาลที่ตำแหน่งของหมู่คาร์บอกซิลของกรดพีนอลิก เอนไซม์ Os9BGlu31 กลายพันธุ์ที่ตำแหน่งกรดอะมิโน W243N และ W243L มีค่ากิจกรรมของเอนไซม์ในกระบวนการทรานส์ไกลโคซิเลชันต่อการเกิดผลิตภัณฑ์ที่สูงกว่าเอนไซม์ดั้งเดิมซึ่งผลิตภัณฑ์หลักที่พบคือ สารประกอบกรดพีนอลิกกลูโคซิลเอสเทอร์ โดยเฉพาะสารประกอบ กรดแกลลิกกลูโคซิลเอสเทอร์ (เบต้ากลูโคแกลลิน) ที่มีฤทธิ์ต้านอนุมูลอิสระค่า  $IC_{50}$  เท่ากับ  $3.6 \pm 0.1 \mu\text{g/mL}$

และเบต้ากลูโคสกลัยโคเจนยังมีฤทธิ์ยับยั้งการเจริญของเซลล์มะเร็งท่อน้ำดี KKU-213A KKU-055 และ KKU-100 โดยมีค่า  $IC_{50}$  ภายหลังบ่มสารกับเซลล์แต่ละกลุ่มเป็นเวลา 24 ชั่วโมง เท่ากับ  $67.3 \pm 1.3 \mu\text{M}$ ,  $19.8 \pm 1.3 \mu\text{M}$  และ  $178.7 \pm 4.1 \mu\text{M}$  ตามลำดับ รวมทั้งมีฤทธิ์ในการยับยั้งการแพร่กระจายของเซลล์มะเร็ง ทั้งตามปริมาณและระยะเวลาในการได้รับสาร รวมทั้งยังพบว่าเบต้ากลูโคสกลัยโคเจนไม่มีความเป็นพิษต่อเซลล์ปกติ จากการศึกษาการยับยั้งการเจริญของเซลล์มะเร็ง พบว่าเบต้ากลูโคสกลัยโคเจนทำให้เกิดการหยุดวัฏจักรของเซลล์ที่ระยะ S ไปยัง G2/M และระยะ G0/G1 ในเซลล์มะเร็งท่อน้ำดี KKU-213A และ KKU-055 ตามลำดับ และยังสามารถเหนี่ยวนำให้เกิดการตายแบบอะพอพโทซิสผ่านความเครียด เอนโดพลาสมิกเรติคูลัม โดยพบว่ามี การเพิ่มการแสดงออกของยีนในกลุ่มโปรตีนหลักของการควบคุมความเครียดเอนโดพลาสมิกเรติคูลัม และการตอบสนองของโปรตีนที่กางออก (unfolded protein response) คือ *XBP1*, *s-XBP1*, *ATF4*, *ATF6* และ *CHOP* ทั้งในเซลล์ KKU-055 และ KKU-213A ดังนั้นในการศึกษานี้สรุปได้ว่า เอนไซม์ Os9BGluc31 ทรานสเกลโคซิเดสในข้าวสามารถใช้ผลิตสารออกฤทธิ์ผ่านกระบวนการไกลโคซิเลชันเพียงขั้นตอนเดียว โดยเฉพาะ เบต้ากลูโคสกลัยโคเจน ที่พบว่ามีฤทธิ์ในการยับยั้งการเจริญและการแพร่กระจายของเซลล์มะเร็งท่อน้ำดีโดยไม่มีความเป็นพิษต่อเซลล์ปกติจึงเป็นอีกแนวทางหนึ่งในการนำใช้เป็นสารต้านมะเร็งทางเลือกใหม่เพื่อรักษามะเร็งท่อน้ำดีในอนาคต

สาขาวิชาเคมี  
ปีการศึกษา 2566

ลายมือชื่อนักศึกษา

ลายมือชื่ออาจารย์ที่ปรึกษา

EKO SUYANTO : ENZYMATIC SYNTHESIS OF PHENOLIC ACID GLUCOSYL ESTERS AND THEIR EFFECT IN CHOLANGIOCARCINOMA CELLS. THESIS ADVISOR : PROF. JAMES R. KETUDAT-CAIRNS, Ph.D. 155 PP.

Keywords:  $\beta$ -glucosidase; glucosyl ester;  $\beta$ -glucogallin; cholangiocarcinoma

Rice Os9BGlu31 is one of enzyme in glycoside hydrolase family 1 (GH1), an enzyme family that mostly catalyze hydrolysis reactions. In addition to weak hydrolysis activity, Os9BGlu31 has transglycosylation activity that can transfer a glycosyl moiety to other aglycone moiety to form glycosylated compounds through a retaining mechanism. In the transglycosylation reaction, the glycosylated compounds can be produced in a one-step reaction and the products often are more stable, soluble, bioavailable and has enhanced bioactivity. Therefore, the glycosylated compounds are promising functional compounds for human health purposes, including as anti-cancer agents. However, the effect of glycosylated compounds, such as phenolic acid glucosyl esters in cholangiocarcinoma cells has not been reported yet.

In this study, Os9BGlu31 was used to synthesize eight phenolic acid glucosyl esters, and their biological activities were evaluated in cholangiocarcinoma cells. The possible molecular mechanism of inhibition of cholangiocarcinoma cells by phenolic acid glucosyl ester was then investigated. Os9BGlu31 and its mutant variants were expressed in *Escherichia coli* strain Origami B(DE3), then purified by an IMAC column for further enzymatic reaction. The transglucosylation products were detected by analytical chromatography, produced, purified by Sephadex-LH20 resin column chromatography, and their structures were verified by NMR spectroscopy. Furthermore, the activity of transglucosylation products were evaluated, screened for anti-proliferative activity, then followed by a wound healing assay to assess anti-migration activity of selected-phenolic acid glucosyl ester. The possible molecular mechanism of inhibition of cholangiocarcinoma cells was investigated by cell cycle analysis, cell apoptosis analysis, and measured the mRNA expression level of related genes.

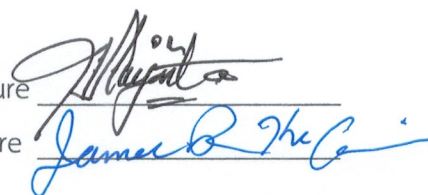
Os9BGlu31 wild type produced single transglucosylation product, whereas Os9BGlu31 mutants tend to produce multiple transglucosylation products, which can transfer a glucosyl moiety to a hydroxyl group or carboxyl group of certain compounds.

However, glucosyl moiety is preferentially attached on the carboxyl group of phenolic acid to produce major transglucosylation products. Os9BGlu31 W243N and W243L showed high activity and also produced high yields of major transglucosylation products than wild type enzyme. The major transglucosylation products were verified as phenolic acid glucosyl esters. Among these products, gallic acid glucosyl ester ( $\beta$ -glucogallin) had strong antioxidant activity with  $IC_{50}$  value of  $3.6 \pm 0.1 \mu\text{g/mL}$ .  $\beta$ -Glucogallin also showed anti-proliferative activity in cholangiocarcinoma cells with  $IC_{50}$  values of  $67.3 \pm 1.3 \mu\text{M}$ ,  $19.8 \pm 1.3 \mu\text{M}$ , and  $178.7 \pm 4.1 \mu\text{M}$  after incubation for 24 h in KKU-213A, KKU-055, and KKU-100, respectively. However,  $\beta$ -glucogallin showed no obvious anti-proliferative activity toward normal human fibroblast cells. It also inhibited the migration of cholangiocarcinoma cells in a time- and dose-dependent manner. Moreover,  $\beta$ -glucogallin induced inhibition of proliferation of cholangiocarcinoma cells through cell cycle arrest in S and G2/M phase in KKU-213A and G0/G1 phase in KKU-055. It also inhibited cholangiocarcinoma cells through up-regulating of gene expression of ER-stress and unfolded protein response (UPR) signaling markers, including *XBP1*, *sXBP1*, *ATF4*, *ATF6*, and *CHOP*, in both KKU-055 and KKU-213A. This study demonstrated that rice Os9BGlu31 transglucosidase is a promising enzyme for glycosylation and production of glycosylated compounds. It also provides evidence that  $\beta$ -glucogallin inhibits proliferation and migration of cholangiocarcinoma cells thus  $\beta$ -glucogallin is a potential agent in the treatment of cholangiocarcinoma cells.

School of Chemistry  
Academic Year 2023

Student's Signature

Advisor's Signature



The image shows two handwritten signatures in blue ink. The top signature is for the student, and the bottom signature is for the advisor, James R. The Co. The signatures are written over horizontal lines.

## ACKNOWLEDGEMENT

I would like to express my deepest gratitude to my advisor Prof. Dr. James R. Ketudat-Cairns for providing me an opportunity to pursue my degree in Doctor of Philosophy in Biochemistry and Biochemical Technology and for his guidance, enthusiastic encouragement, and support during my study. I would also like to express my sincere thanks to Assoc. Prof. Dr. Chutima Talabnin for giving me an opportunity to use cholangiocarcinoma cells and some materials in her lab. I'm very grateful to Prof. Fatchiyah, M.Kes, Ph.D who opened the way for my study and for her encouragement to me. I also sincerely thank to Assoc. Prof. Dr. Panida Khunkaewla, Assoc. Prof. Dr. Mariena Ketudat-Cairns, and Dr. Kriengsak Lirdprapamongkol for all suggestions and kindness to me. Thank you very much for all discussions from everyone that we had during my study.

I would also like to extend my deepest gratitude to all of my teachers and lecturers during my study from the kindergarten until doctoral program for all the valuable lessons and values that you taught me. May God bless all of you. All of my deepest gratitude to my wife and my daughters, you are the greatest wife and mother for me and our children, thank you very much for supporting me.

I sincerely thank to all post-doctoral fellow, students, research assistants, lab members and colleagues of JKC's lab as well as staff in Biochemistry and Biochemical Technology, School of Chemistry, Institute of Science, Suranaree University of Technology for their guidance, help, kindness, and good relationship during my study. I would like to thank Indonesian student community in Suranaree University of Technology (SUT-Indo) for their helping and friendship.

I would also like to thank OROG Scholarship from Suranaree University of Technology and International Research Network grant, IRN62W0004 for funding my doctoral academic and research. Finally, I would like to express my deepest gratitude to my parents and my sisters for giving me unlimited love, care, support, help, and cheering me up with the best wishes. Thank you very much for everyone who help me until now.

Eko Suyanto

# CONTENTS

	Page
ABSTRACT IN THAI .....	I
ABSTRACT IN ENGLISH .....	III
ACKNOWLEDGEMENT .....	V
CONTENTS .....	VI
LIST OF TABLES .....	X
LIST OF FIGURES .....	XI
LIST OF ABBREVIATIONS .....	XV
<b>CHAPTER</b>	
<b>I INTRODUCTION .....</b>	<b>1</b>
1.1 Background and significance .....	1
1.2 Research objectives .....	4
1.3 Research scope and limitations .....	4
<b>II LITERATURE REVIEWS .....</b>	<b>6</b>
2.1 Phenolic acids .....	6
2.1.1 Common characteristics of phenolic acids .....	6
2.1.2 Biosynthetic pathway of phenolic acids .....	7
2.1.3 Biological activities of phenolic acids .....	10
2.2 Glycosylation and glycosides .....	11
2.2.1 Glycosylation .....	11
2.2.2 Glycosides and their activities .....	13
2.3 Glycoside hydrolases family .....	14
2.3.1 Glycoside hydrolases .....	14
2.3.2 Mechanisms of glycoside hydrolases .....	15
2.3.3 $\beta$ -Glucosidases .....	17
2.3.4 Rice $\beta$ -glucosidase .....	20
2.3.5 Rice Os9BGlu31 transglucosidase .....	23
2.4 Mutagenesis and mutant variants .....	24

## CONTENTS (Continued)

	Page
2.5 Bile duct cancer .....	27
2.5.1 Cancers and metastasis .....	27
2.5.2 Cholangiocarcinoma .....	28
2.5.3 Epidemiology of cholangiocarcinoma .....	30
2.5.4 Carcinogenesis of Ov-associated cholangiocarcinoma .....	33
2.5.5 Treatment of cholangiocarcinoma .....	34
2.6 Cell death mechanisms .....	35
2.6.1 Programmed cell death .....	35
2.6.2 Apoptosis mechanisms .....	37
2.6.3 Apoptosis detection .....	41
2.7 Endoplasmic reticulum stress and unfolded protein response .....	41
2.8 Cell cycle .....	44
<b>III MATERIALS AND METHODS .....</b>	<b>48</b>
3.1 General materials .....	48
3.1.1 Plasmid and bacterial strain .....	48
3.1.2 Human cell lines .....	48
3.1.3 Oligonucleotide primers .....	48
3.1.4 Chemicals, reagents, and media .....	49
3.1.5 Instruments and equipment .....	52
3.2 General methods .....	53
3.2.1 Preparation of competent cells .....	53
3.2.2 Transformation of plasmid into competent cells .....	53
3.2.3 Protein expression and purification of Os9BGlu31 .....	54
3.2.4 Protein analysis by SDS-PAGE .....	55
3.2.5 Enzymatic assay .....	56
3.2.6 Detection and identification of transglucosylation products .....	56
3.2.6.1 Transglycosylation reaction .....	56
3.2.6.2 Thin layer chromatography .....	57

## CONTENTS (Continued)

	Page
3.2.6.3 Ultra-high performance liquid chromatography .....	57
3.2.7 Production and purification of major transglucosylation products .....	58
3.2.8 Structural analysis of major transglucosylation products .....	58
3.2.9 Evaluation of antioxidant activity .....	58
3.2.10 Mammalian cell culture .....	59
3.2.11 Evaluation and screening of anti-proliferative activity .....	59
3.2.12 Anti-proliferative activity of $\beta$ -glucogallin .....	60
3.2.13 Evaluation of anti-migration activity of $\beta$ -glucogallin .....	61
3.2.14 Colony formation assay .....	61
3.2.15 Cell apoptosis analysis .....	61
3.2.16 Cell cycle analysis .....	62
3.2.17 mRNA expression analysis by qRT-PCR .....	63
3.2.17.1 RNA extraction .....	63
3.2.17.2 Agarose gel electrophoresis .....	64
3.2.17.3 Reverse transcription of RNA to cDNA .....	64
3.2.17.4 Quantitative RT-PCR (qRT-PCR) .....	64
3.2.18 Statistical analysis .....	65
<b>IV RESULTS AND DISCUSSION</b> .....	<b>66</b>
4.1 Expression and purification of Os9BGlu31 wild type and its mutant variants .....	66
4.2 Activity of Os9BGlu31 wild type and its mutant variants .....	67
4.3 Transglucosylation activity and identification of products .....	69
4.4 Production of major transglucosylation products .....	79
4.5 Transglucosylation product structural confirmation .....	81
4.6 Activities of phenolic acid glucosyl esters .....	84
4.6.1 Antioxidant activity of phenolic acid glucosyl esters .....	84
4.6.2 Anti-proliferative activity of phenolic acid glucosyl esters .....	86
4.7 Anti-proliferative activity of $\beta$ -glucogallin .....	87

## CONTENTS (Continued)

	Page
4.8 Anti-migration activity of $\beta$ -glucogallin .....	90
4.9 $\beta$ -Glucogallin inhibit CCA proliferation by inducing apoptosis .....	92
4.10 $\beta$ -Glucogallin inhibit CCA proliferation via cell cycle arrest .....	95
4.11 $\beta$ -Glucogallin inhibit CCA proliferation via ER stress-induced cell death .....	98
<b>V CONCLUSION</b> .....	100
REFERENCES .....	102
APPENDICES .....	131
APPENDIX A PROTEIN PURIFICATION AND GLYCOSYLATED PRODUCTS .....	132
APPENDIX B PHENOLIC ACID GLUCOSYL ESTERS AND THEIR AGLYCONES .....	136
APPENDIX C NMR SPECTRA OF PHENOLIC ACID GLUCOSYL ESTERS .....	139
APPENDIX D PUBLICATION AND ACHIEVEMENT .....	153
CURRICULUM VITAE .....	155

## LIST OF TABLES

Table		Page
3.1	List of primer names and sequences for quantitative RT-PCR .....	49
3.2	List of chemicals, reagents, and media used in this study .....	49
4.1	Yield of major transglucosylation products in 100 mL of enzymatic reactions after purification .....	80



## LIST OF FIGURES

Figure	Page
2.1 Chemical structures of phenolic acids are classified into two major groups, hydroxybenzoic acid and hydroxycinnamic acid .....	6
2.2 The shikimate pathway in plants .....	8
2.3 Biosynthesis of phenolic acids via the phenylpropanoid pathway in plants that starts with deamination of phenylalanine .....	9
2.4 Schematic diagram of the hydrolysis reaction catalyzed by glycoside hydrolases .....	14
2.5 General mechanisms of (A) retaining and (B) inverting of $\beta$ -glucosidases ....	16
2.6 $\beta$ -Glucosidases catalyze both hydrolysis and transglycosylation reactions	18
2.7 Protein structures of $\beta$ -glucosidases from different families of GHs .....	18
2.8 Phylogenetic tree of predicted protein sequences of rice and <i>Arabidopsis</i> GH1 genes .....	22
2.9 Superposition of Os9BGlu31 on the Os3BGlu6 $\beta$ -glucosidase X-ray crystal structure covalent intermediate with 2-fluoro- $\alpha$ -D-glucoside (PDB ID: 3GNR) .....	26
2.10 Schematic representation of types of CCA in the liver based on localization .....	29
2.11 The classification of CCA according to its macroscopic growth pattern .....	29
2.12 The cholangiocarcinoma incidence in Thailand .....	31
2.13 The life cycle of the liver fluke (Ov) .....	32
2.14 The proposed mechanism of inflammation caused by liver flukes in related to cholangiocarcinogenesis .....	33
2.15 The morphological features of cell death mechanisms of apoptosis, autophagy, and necrosis .....	36
2.16 The caspase-dependent apoptosis mechanism can be divided into the extrinsic and intrinsic pathways .....	38
2.17 The caspase-independent apoptosis mechanism .....	40

## LIST OF FIGURES (Continued)

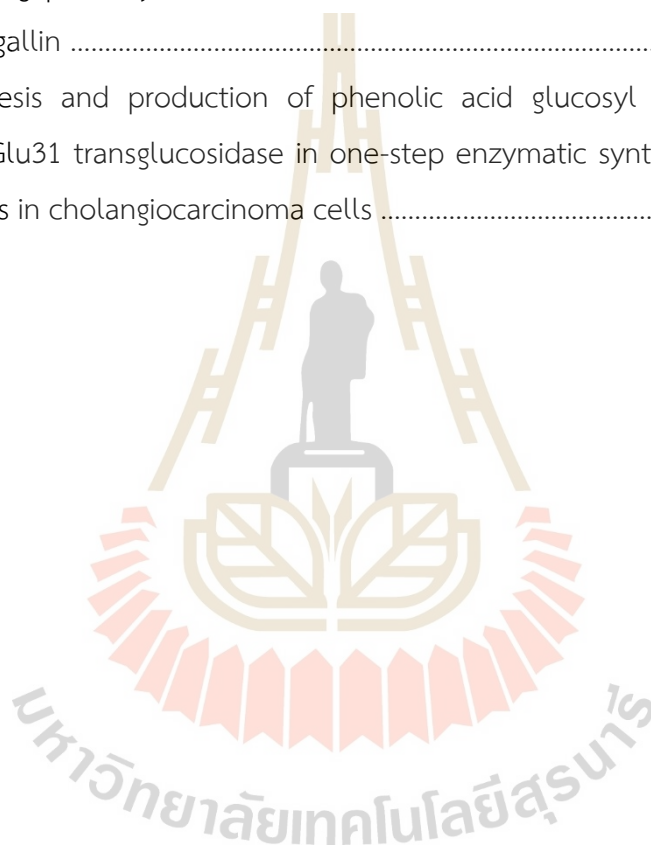
Figure	Page
2.18 The ER stress and unfolded protein response (UPR) signaling pathway .....	42
2.19 The general schematic of cell cycle in eukaryotic cells consisting several phases, including G1, S, G2, and M phase which are controlled by cell cycle regulators .....	45
4.1 SDS-PAGE analysis of Os9BGlu31 purification fractions .....	67
4.2 Enzyme activity of (A) Os9BGlu31 wild type and its mutant variants, including (B) W243H, (C) W243N, and (D) W243L with phenolic acids .....	68
4.3 Thin layer chromatography of transglucosylation products of enzymatic reactions catalyzed by Os9BGlu31 wild type and its mutant variants with ferulic acid (FA) and vanillic acid (VA) .....	70
4.4 UHPLC chromatogram profiles of transglucosylation products in the enzymatic reaction with ferulic acid (FA) and vanillic acid (VA) .....	71
4.5 Thin layer chromatography of transglucosylation products of enzymatic reactions catalyzed by Os9BGlu31 wild type and its mutant variants with 4-hydroxybenzoic acid (HBA) and <i>p</i> -coumaric acid (PCA) .....	72
4.6 UHPLC chromatogram profiles of transglucosylation products in the enzymatic reaction with 4-hydroxybenzoic acid (HBA) and <i>p</i> -coumaric acid (PCA) .....	73
4.7 Thin layer chromatography of transglucosylation products of enzymatic reactions catalyzed by Os9BGlu31 wild type and its mutant variants with <i>trans</i> -cinnamic acid (TCA) and syringic acid (SyrA) .....	74
4.8 UHPLC chromatogram profiles of transglucosylation products in the enzymatic reaction with <i>trans</i> -cinnamic acid (TCA) and syringic acid (SyrA) .....	75
4.9 Thin layer chromatography of transglucosylation products of enzymatic reactions catalyzed by Os9BGlu31 wild type and its mutant variants with sinapic acid (SinA) and gallic acid (GA) .....	76
4.10 UHPLC chromatogram profiles of transglucosylation products in the enzymatic reaction with sinapic acid (SinA) and gallic acid (GA) .....	77

## LIST OF FIGURES (Continued)

Figure	Page
4.11 General reaction scheme for the enzymatic synthesis of phenolic acid glucosyl esters in this study .....	78
4.12 Chemical structures of phenolic acid glucosyl esters that were verified by NMR spectroscopy .....	82
4.13 <sup>1</sup> H-NMR (500 MHz, CD <sub>3</sub> OD) spectra of gallic acid glucosyl ester ( $\beta$ -glucogallin) .....	82
4.14 <sup>13</sup> C-NMR (125 MHz, CD <sub>3</sub> OD) spectra of gallic acid glucosyl ester ( $\beta$ -glucogallin) .....	83
4.15 Antioxidant activity of phenolic acid glucosyl esters .....	85
4.16 Inhibitory effect of phenolic acid glucosyl esters in cell proliferation of KKU-213A at 24 h .....	86
4.17 Inhibitory effect of $\beta$ -glucogallin in cholangiocarcinoma cells at 24, 48 and 72 h and the morphological change of cells after $\beta$ -glucogallin treatment for 24 h were observed at 20X magnification .....	88
4.18 Inhibitory effect of $\beta$ -glucogallin in a normal human fibroblast cell line (IMR-90) at 24, 48, and 72 h .....	89
4.19 Inhibition of cell migration by $\beta$ -glucogallin at various times and doses in KKU-213A .....	90
4.20 Inhibition of cell migration by $\beta$ -glucogallin at various times and doses in KKU-055 .....	91
4.21 Inhibition of cell migration by $\beta$ -glucogallin at various times and doses in KKU-100 .....	91
4.22 Colony formation assay in (A) KKU-213A and (B) KKU-055 after treatment with $\beta$ -glucogallin .....	93
4.23 Apoptosis analysis in (A) KKU-213A and (B) KKU-055 after treatment with $\beta$ -glucogallin for 24 h .....	94
4.24 Cell cycle analysis in (A) KKU-213A and (B) KKU-055 after treatment with $\beta$ -glucogallin .....	96

## LIST OF FIGURES (Continued)

Figure	Page
4.25 Relative mRNA expression levels of cell cycle-related genes in KKU-213A and KKU-055 after treatment with $\beta$ -glucogallin .....	97
4.26 Relative mRNA expression levels of ER-stress genes related to UPR signaling pathway in KKU-213A and KKU-055 after treatment with $\beta$ -glucogallin .....	99
5.1 Synthesis and production of phenolic acid glucosyl esters by rice Os9BGlu31 transglucosidase in one-step enzymatic synthesis and their effects in cholangiocarcinoma cells .....	101



## LIST OF ABBREVIATIONS

<i>ACTB</i>	$\beta$ -actin gene
Annexin V-FITC	Annexin V conjugated with fluorescein isothiocyanate
APS	Ammonium persulphate
<i>ATF4</i>	Activating transcription factor 4 gene
<i>ATF6</i>	Activating transcription factor 6 gene
BCP	1-bromo-3-chloropropane
BSA	Bovine serum albumin
CAZy	Carbohydrate active enzymes
CCA	Cholangiocarcinoma
<i>CCNB1</i>	Cyclin B gene
<i>CCND1</i>	Cyclin D gene
<i>CCNE1</i>	Cyclin E gene
CD <sub>3</sub> OD	Deuterated methanol
<i>CDKNB1</i>	Cyclin-dependent kinase inhibitor 1B (p27 <sup>Kip1</sup> ) gene
cDNA	Complementary deoxyribonucleic acid
<i>CHOP</i>	C/EBP homologous protein gene
COX-2	Cyclooxygenase-2
Cs	<i>Clonorchis sinensis</i>
CV	Column volume
dCCA	Distal cholangiocarcinoma
DMEM	Dulbecco's Modified Eagle Medium
DMSO	Dimethyl sulfoxide
DNA	Deoxyribonucleic acid
DNase	Deoxyribonuclease
DPPH	2,2-diphenyl-1-picrylhydrazyl
EDTA	Ethylendiaminetetraacetic acid
EMEM	Eagle's minimum essential medium
ERK	Extracellular signal-regulated kinase
EtOH	Ethanol

## LIST OF ABBREVIATIONS (Continued)

FBS	Fetal bovine serum
GHs	Glycoside hydrolases
GlcCer	Glucosylceramide
GPs	Glycoside phosphorylases
GTs	Glycosyltransferases
h	Hour
HPLC	High performance liquid chromatography
iCCA	Intrahepatic cholangiocarcinoma
IMAC	Immobilized metal affinity chromatography
iNOS	Inducible nitric oxide synthase
IPTG	Isopropyl- $\beta$ -D-thiogalactopyranoside
JNK	Jun N-terminal kinase
kDa	Kilo Dalton
LB	Luria Bertani media
LDL	Low-density lipoprotein
LPH	Lactase-phloridzin hydrolase
MAPK	Mitogen-activated protein kinase
MeOH	Methanol
min	Minute
MMP	Matrix metalloproteinase
MW	Molecular weight
MWCO	Molecular mass cut off
NAFLD	Non-alcoholic fatty liver disease
NF- $\kappa$ B	Nuclear factor kappa B
NMR	Nuclear magnetic resonance
NOS	Nitrogen oxide species
Ov	<i>Opisthorchis viverrine</i>
PAGE	Polyacrylamide gel electrophoresis
PAL	Phenylalanine ammonia lyase
PBS	Phosphate-buffer saline

## LIST OF ABBREVIATIONS (Continued)

pCCA	Perihilar cholangiocarcinoma
PCD	Programmed cell death
PI	Propidium Iodide
PMSF	Phenylmethanesulfonyl fluoride
<i>p</i> NP	<i>p</i> -Nitrophenol
<i>p</i> NPG	<i>p</i> -Nitrophenyl- $\beta$ -D-glucopyranoside
ROS	Reactive oxygen species
rpm	Rotations per minute
SDS	Sodium dodecyl sulfate
SDS-PAGE	Sodium dodecyl sulfate-polyacrylamide gel electrophoresis
s	Second
SRB	Sulforhodamine B
<i>sXBP1</i>	spliced X-box binding protein 1 gene
TBS	Tris-buffer saline
TCA	Trichloroacetic acid
TEMED	Tetramethyl ethylenediamine
TGs	Transglycosidases
TLC	Thin layer chromatography
Tris	Tris-hydroxymethyl-aminoethane
UHPLC	Ultra-high performance liquid chromatography
UPR	Unfolded protein response
<i>XBP1</i>	X-box binding protein gene

# CHAPTER I

## INTRODUCTION

### 1.1 Background and significance

Glycosylation is a reaction to transfer glycosyl moieties to a hydroxyl group or other functional group of a glycosyl acceptor in order to form glycosylated compounds (glycosides or glycoconjugates). Glycosylation often able to enhance the stability, solubility, bioavailability and bioactivity of the compounds (Bujuq et al., 2018; Ferreyra et al., 2012; Liu et al., 2020; Moradi et al., 2016; Pourakbari et al., 2020; Vivekanandhan et al., 2016; Woo et al., 2012). Previous studies reported that glycosylation plays a critical role during interaction between a drug and its cellular target in drug pharmacodynamics, as it can change the cellular localization and physicochemical properties of the compounds, as well as their biological activities (Pandey et al., 2014). When the hydroxyl groups of non-sugar compounds are linked with glycosyl moieties, they formed glycosides, in which the glycone (the sugar portion) affects their solubility and bioactivity and could enhance the pharmacokinetic parameters so that they may become promising functional compounds, therapeutics and pharmaceuticals for human health purposes (Khan et al., 2019; Moradi et al., 2016; Velmurugan et al., 2020).

There are two methods to synthesize glycosides, by chemical and enzymatic glycosylation. Generally, a chemical glycosylation reaction needs cycles of protection and deprotection, and strict reaction conditions to produce the glycosylated products, leading to high costs of synthesis and purification (Li et al., 2014; Moradi et al., 2016; Thapa et al., 2019). In contrast, enzymatic glycosylation copes with these issues by using unprotected sugar moieties and providing absolute stereocontrol to generate feasible routes to synthesize glycosides. Enzymatic glycosylation can be catalyzed by many enzymes to synthesize glycosides, including glycosyltransferases (GTs), glycoside phosphorylases (GPs), and transglycosidases (TGs), as well as glycoside hydrolases (GHs) (Lairson and Withers, 2004; Pergolizzi et al., 2017).

Glycoside hydrolases (GHs) are a group of enzymes, which catalyze hydrolysis reaction of the glycosidic bond and are currently split into 183 families based on the protein sequences and specificities of these enzymes. Among those families, 11 families contains  $\beta$ -glucosidases, including GH1, GH2, GH3, GH5, GH16, GH30, GH39, GH116, GH131, GH175, and GH180 (Cantarel et al., 2009; Ketudat-Cairns et al., 2015, CAZy, 2023). Most plant  $\beta$ -glucosidases (E.C. 3.2.1.21) fall in GH family 1 (GH1), in which most of the members catalyze hydrolysis reaction. In addition to hydrolysis activity, previous studies revealed that many GH1 enzymes also have high transglycosylation activity and related enzymes have been found to act as transglucosidases, which act to transfer a glucosyl moiety from glucosyl donors to glucosyl acceptors with little hydrolysis through a retaining mechanism to form glycosylated compounds (Ketudat-Cairns et al., 2015; Luang et al., 2013; Matsuba et al., 2010; Opassiri et al., 2003, 2004).

One transglucosidase is named Os9BGlu31, based on its position on rice chromosome 9 and its being a member of GH1, which primarily contains  $\beta$ -glucosidases. It has high activity in reactions containing phenolic acid glucose esters, such as feruloyl glucose as glucosyl donor and a suitable acceptor (Luang et al., 2013). Os9BGlu31 is also able to use apigenin as a glucosyl acceptor and apigenin 7-O-glucoside as a glucosyl donor. Previous studies revealed that Os9BGlu31 mutant variants can transfer a glucosyl moiety from a glucosyl donor to several phenolic acids and flavonoids, including kaempferol to produce multiple kaempferol glycosides as products (Komvongsa et al., 2015a; Tran et al., 2019). Further study about the application of those glycosylated products for human health purposes has yet to be reported.

Glycosylated compounds are known to have many activities, such as antioxidant, anti-inflammatory, anti-cancer, and anti-diabetic, as well as anti-bacterial (Kang et al., 2015; Park and Song, 2019; Pourakbari et al., 2020). For instance, apigenin-7-O-glucoside, a flavonoid glycoside, has the ability to promote cell apoptosis and inhibits cell migration of HeLa human cervical cancer cells (Liu et al., 2020). In HCT116 human colon cancer cells, it can reduce cell viability and induce apoptosis (Smiljkovic et al., 2017). It also has been reported to stimulate production of reactive oxygen species

(ROS) in human gastric cancer cells (Sun et al., 2018). In another example, 4-O- $\beta$ -galactopyranosyl derivatives of phenolic acid esters (methyl vanillate and methyl ferulate) have higher cytotoxic activity in MCF-7 breast cancer cells and in PC-3 prostate cancer cells than the parental esters (Bujug et al., 2018). However, the effect of glycosylated compounds, particularly phenolic acid glucosyl esters in human cholangiocarcinoma cells has not been reported yet.

There are many types of cancers depending, in part, on the location or organ system in the body where the cancer begins. One of the aggressive cancers is cholangiocarcinoma, a cancer of the human epithelial cells of the bile duct in the liver, which has the highest incidence in northeastern Thailand and parts of Laos and Cambodia (Sithithaworn et al., 2014). Previous studies reported that around 700 million people in the world are at risk of liver flukes infection (Brindley et al., 2021; Sripa et al., 2007, 2011; Zheng et al., 2017). The major risk factor for cholangiocarcinoma development in this area is infection of liver fluke (*Opisthorchis viverrine*, Ov) (Sripa and Pairojkul, 2008). Chronic inflammation caused by Ov in the liver may also trigger a failure of the immune response, which contributes to the progression of cholangiocarcinogenesis.

Generally, the therapy for cancers involves surgery, drug chemotherapy, immunotherapy, and radiotherapy (Ma et al., 2019; Shao-qiang et al., 2009). However, commonly, these methods have various adverse effects (Mansoori et al., 2017; Small et al., 2017), and most of the chemotherapeutic drugs, such as cisplatin, are non-specific so that their administration often affects the normal tissues in the body (Astolfi et al., 2013). Therefore, many people are trying to find effective ways to inhibit cancer cell proliferation in the body without any side effects. The use of phytochemicals or bioactive compounds as anti-cancer agents is a promising way to inhibit cancer cell proliferation.

In this present study, enzymatic synthesis was performed with rice Os9BGlu31 transglucosidase and its mutant variants for the production of sufficient quantities of phenolic acid glucosyl esters, which was not previously reported. The major transglucosylation products were purified, then their identities and purity were verified

by NMR spectroscopy. This included enzymatic synthesis of gallic acid glucosyl ester, also named  $\beta$ -glucogallin, which was not previously reported. The activity of major transglucosylation products were evaluated and one of transglucosylation product ( $\beta$ -glucogallin) with high anti-proliferative activity was selected in order to study its effect and possible molecular mechanism in the inhibition of cholangiocarcinoma cells.

## 1.2 Research objectives

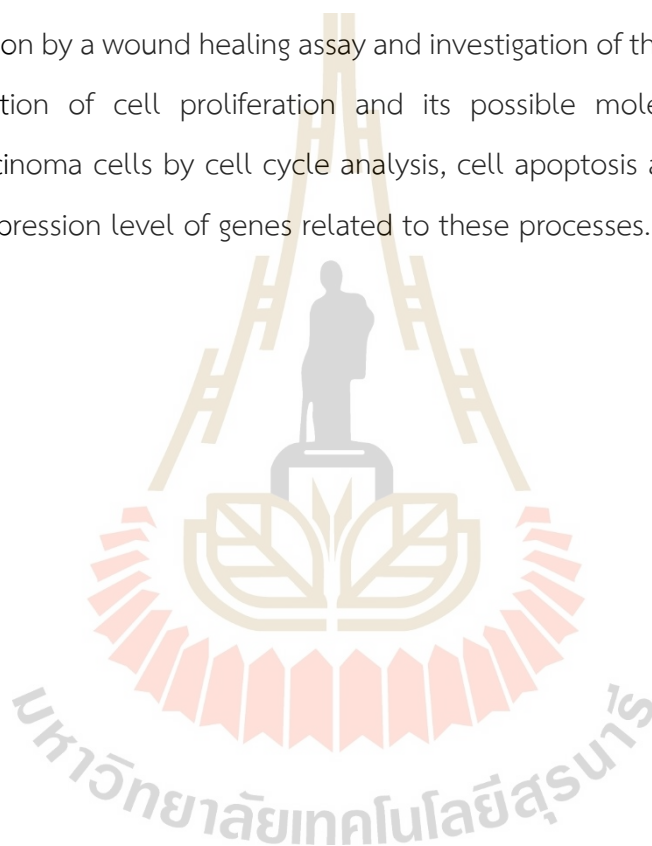
This study has several objectives, including:

1. To investigate the ability of Os9BGlu31 and its mutant variants in glycosylation of phenolic acids for the production of phenolic acid glucosyl esters,
2. To purify and verify the phenolic acid glucosyl esters from transglucosylation reactions,
3. To evaluate and screen the activity of phenolic acid glucosyl esters,
4. To investigate the effect of  $\beta$ -glucogallin in the inhibition of cell migration in cholangiocarcinoma cells,
5. To investigate the effect of  $\beta$ -glucogallin in the inhibition of cell proliferation and its possible molecular mechanism in cholangiocarcinoma cells.

## 1.3 Research scope and limitations

This study focused on the production of phenolic acid glucosyl esters from phenolic acids as glucosyl acceptors, including ferulic acid, hydroxybenzoic acid, vanillic acid, *p*-coumaric acid, *trans*-cinnamic acid, gallic acid, sinapic acid, and syringic acid by enzymatic synthesis using Os9BGlu31 wild type and its mutant variants as catalyst to produce sufficient quantities of major transglucosylation products for bioactivity testing. It also focused on the investigation of the action of a selected-phenolic acid glucosyl ester ( $\beta$ -glucogallin) in the inhibition of cell migration and cell proliferation, and its possible molecular mechanism in cholangiocarcinoma cells. Protein expression and purification of Os9BGlu31 and its mutant variants were performed to express and purify the enzymes, and the phenolic acid glucosyl esters were produced by enzymatic synthesis then purified by Sephadex LH-20 column

chromatography. The transglucosylation products were identified by analytical chromatography, including TLC and UHPLC, and verified by NMR spectroscopy. Furthermore, the phenolic acid glucosyl esters were evaluated for antioxidant activity and screened for cytotoxicity activity in cholangiocarcinoma cells to obtain the candidate of major transglucosylation product that has high cytotoxicity activity in these cells. A selected-phenolic acid glucosyl ester,  $\beta$ -glucogallin, was used for further experiments. These included investigation of the effect of  $\beta$ -glucogallin in the inhibition of cell migration by a wound healing assay and investigation of the role of  $\beta$ -glucogallin in the inhibition of cell proliferation and its possible molecular mechanism in cholangiocarcinoma cells by cell cycle analysis, cell apoptosis analysis, and measure the mRNA expression level of genes related to these processes.



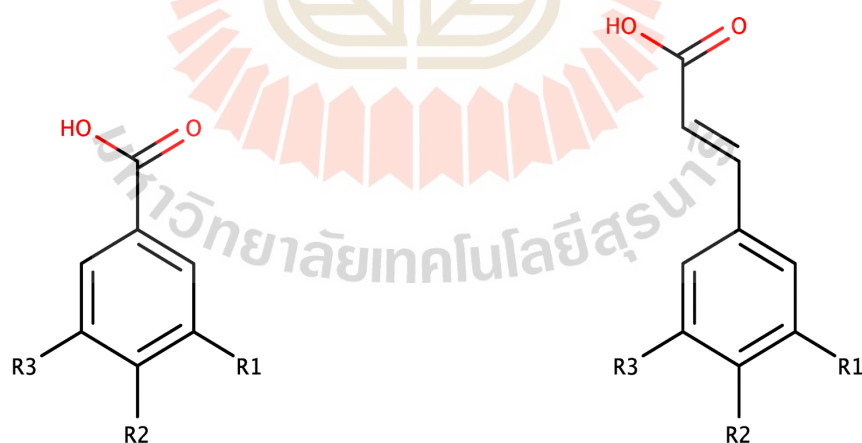
## CHAPTER II

### LITERATURE REVIEWS

#### 2.1 Phenolic acids

##### 2.1.1 Common characteristics of phenolic acids

Phenolic compounds are found in plants as the most widely distributed secondary metabolites, especially in fruits and vegetables (Tian et al., 2004). They are a component in the cell wall, involved in nutrient uptake and support the seed during germination under abiotic stress. They also have many roles in the plants, such as protection against pathogens, predators, and ultraviolet radiation, as well as attraction of pollinating animals and mechanical support (Parr and Bolwell, 2000). Generally, phenolic compounds are categorized into polyphenols, such as tannins, oligophenols, such as flavonoids, and monophenols or phenolic acids, such as benzoic acid and cinnamic acid and their hydroxylated derivatives.



1, R1 = R2 = R3 = H, Benzoic acid

2, R1 = R2 = R3 = OH, Gallic acid

3, R1 = R2 = OH, R3 = H, Protocatechuic acid

4, R1 = R3 = H, R2 = OH, *p*-Hydroxybenzoic acid

5, R1 = OCH<sub>3</sub>, R2 = OH, R3 = H, Vanillic acid

6, R1 = R2 = R3 = H, Cinnamic acid

7, R1 = R2 = OH, R3 = H, Caffeic acid

8, R1 = R3 = H, R2 = OH, *p*-Coumaric acid

9, R1 = OCH<sub>3</sub>, R2 = OH, R3 = H, Ferulic acid

10, R1 = R3 = OCH<sub>3</sub>, R2 = OH, Sinapic acid

**Figure 2.1** Chemical structures of phenolic acids are classified into two major groups, hydroxybenzoic acid and hydroxycinnamic acid (Silva et al., 2020).

In general, the phenolic acids have an aromatic ring, a carboxylic acid group, and one or more hydroxyl substituents in their chemical structure (Tsao, 2010). Based on chemical structure, phenolic acids can be grouped into hydroxycinnamic acid and hydroxybenzoic acid and their derivatives (Figure 2.1) (Kumar and Goel, 2019; Shao and Bao, 2015; Verma and Srivastav, 2020). Hydroxycinnamic acid derivatives have a C6-C3 structure, including cinnamic acid, ferulic acid, *p*-coumaric acid, caffeic acid, chlorogenic acid, and sinapic acid (Lin and Lai, 2011; Rattanachitthawat et al., 2010; Shao and Bao, 2015). Ferulic acid and *p*-coumaric acid usually are found in soluble conjugates, insoluble bound form or free form. In rice, they are primary phenolic acids with high abundance (Irakli et al., 2012; Park et al., 2012; Zaupa et al., 2015). On the other hand, *p*-hydroxybenzoic acid, vanillic acid, gallic acid, protocatechuic acid and syringic acid are other phenolic acids that are derived from hydroxybenzoic acid so that they have a C6-C1 structure (Ciulu et al., 2018; Goufo and Trindade, 2014; Kumar and Goel, 2019; Shao and Bao, 2015).

### 2.1.2 Biosynthetic pathways of phenolic acids

In plants, there are two fundamental metabolic pathways for phenolic acid biosynthesis, including the shikimate pathways and the malonate pathway. The shikimate pathway (also called the shikimic acid pathway) participates in the most phenolic acid biosynthesis in higher plants rather than the malonate. The shikimate pathway produces aromatic amino acids, such as phenylalanine (Phe), tyrosine (Tyr) and tryptophan (Trp) from chorismate (precursor of aromatic amino acids) via converting erythrose-4-phosphate (E4P) from the pentose phosphate pathway, and phosphoenolpyruvate (PEP) from the glycolytic pathway (Zabalza et al., 2017). This occurs in plastids and the products are exported to the cytosol to sustainably produce other products derived from the shikimate pathway, such as phenolic compounds, proteins, and other compounds (Figure 2.2).

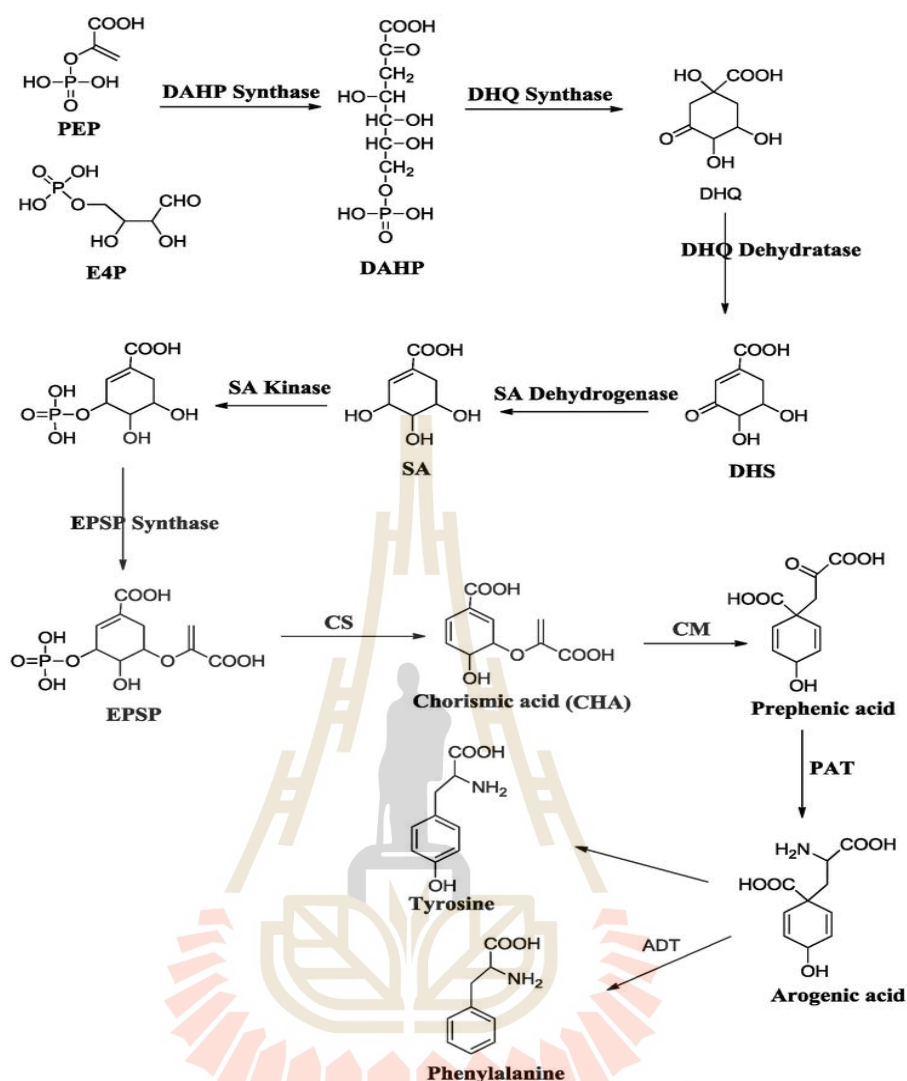


**Figure 2.2** The shikimate pathway in plants. The shikimate pathway synthesizes aromatic amino acids, such as phenylalanine (Phe), tyrosine (Tyr), and tryptophan (Trp) (Rehan, 2021).

There are many steps in the shikimate pathway and involves many enzymes. In the first step of the shikimate pathway is condensation of E4P and PEP into 3-deoxy-D-arabinoheptulosonate 7-phosphate (DAHP) by DAHP synthase (DAHPS), then DAHP is cyclized to form 3-dehydroquinic acid (DHQ) by DHQ synthase (DHQS). In the next step, DHQ is converted to form 3-dehydroshikimate (DHS) by dehydration, followed by serial enzymatic reactions to form shikimate, in which catalyzed by 3-dehydroquinic acid dehydratase/shikimate dehydrogenase (DHQD/SDH), shikimate 3-phosphate (S3P)

catalyzed by shikimate kinase (SK), 5-enolpyruvylshikimate 3-phosphate (EPSP) via condensation of S3P and catalyzed by EPSP synthase (EPSPS), respectively. Then, chorismate (chorismic acid) is synthesized by chorismate synthase (CS) via dephosphorylating of EPSP. Moreover, chorismate mutase (CM) catalyzed biosynthesis of prephenic acid, then prephenate aminotransferase (PAT) converted prephenic acid into aroenic acid. Finally, aroenate dehydrogenase (ADT) is a last step enzyme of phenylalanine biosynthesis, which catalyzes of aroenic acid into phenylalanine. In addition, quinic acid (QA), and phenolic acids, such as protocatechuic acid (PCA), and gallic acid (GA) can be directly synthesized from the DHS intermediate of the shikimate pathway in the plastid (Marchiosi et al., 2020).

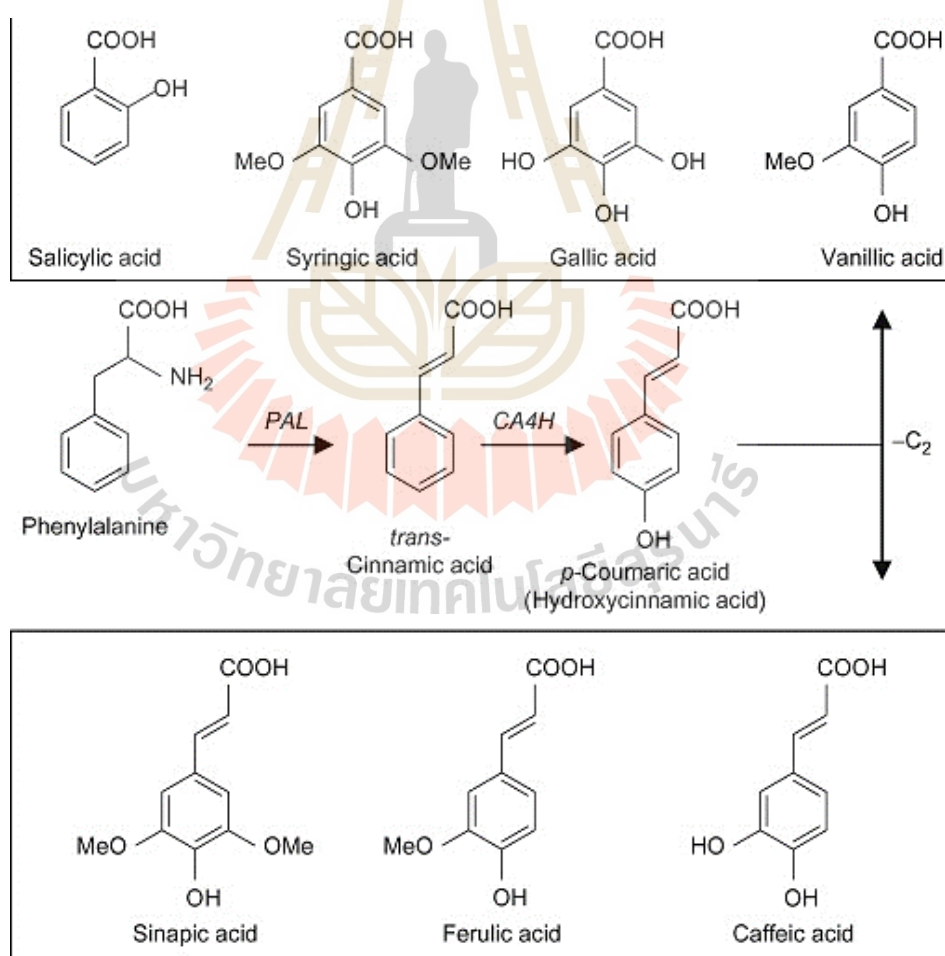


**Figure 2.3** Biosynthesis of phenolic acids via the phenylpropanoid pathway in plants that starts with deamination of phenylalanine (Iriti and Faoro, 2010).

Another metabolic pathway to synthesize phenolic acids is the phenylpropanoid pathway (Figure 2.3). It is a pathway to synthesize most of phenolic acids in plants that begins from deamination reaction of phenylalanine catalyzed by phenylalanine ammonia-lyase (PAL) to form cinnamic acid. In the presence of cinnamate 4-hydroxylase (CH4), cinnamic acid can be converted to form *p*-coumaric acid by hydroxylation of cinnamic acid at the C4 position of the aromatic ring. In grasses, tyrosine can be converted to form *p*-coumaric acid by tyrosine ammonia-lyase (TAL). In the next step, *p*-coumaric acid or a *p*-coumaroyl residue is hydroxylated by *p*-coumaroyl (shikimate/quinic acid) 3-hydroxylase (C3H) at C3 position to generate caffeoyl residue or caffeic acid (Barros et al., 2019). Then, ferulic acid and sinapic acid are synthesized by oxymethylation using cinnamyl (caffeate) *O*-methyltransferase (COMT) from caffeic acid and 5-hydroxy-ferulate, respectively. On the other hand, cinnamic acid is transformed into benzoic acid by losing two carbon atoms in the structure of cinnamic acid, then benzoic acid is converted to salicylic acid, *p*-hydroxybenzoic acid, and vanillic acid, respectively (Kumar and Goel, 2019; Mandal et al., 2010).

### 2.1.3 Biological activities of phenolic acids

Phenolic acids are known to have many biological activities for human health purposes, such as inhibiting cancer cell proliferation, preventing oxidative damage of lipids and low-density lipoproteins, reducing the risk of coronary heart disease, and acting as anti-microbials (Alves et al., 2013; Carocho and Ferreira, 2013; Morton et al., 2000). The biological activities of phenolic acids are associated with their bioavailability because they are mostly present in forms bound with fiber through ester bonds to arabinoxylan chains or ether bonds to lignin in cereals so that they have poorly bioavailable and cannot be hydrolyzed by human digestive enzymes in the intestinal tract. On the other hand, the bioavailability of phenolic acids is higher in fruits and vegetables because they are present in free forms or as conjugates with tartaric acid, quinic acid, and malic acid or sugar moieties so that they can be hydrolyzed by enzymes during digestion in the upper intestinal tract (Hole et al., 2012). In oral administration, phenolic acids undergo metabolism by enzymatic

processes in the body and are absorbed by the cells. Free forms of phenolic acids can be released in the stomach, while conjugated forms require the activity of intestinal enzymes during hydrolysis reactions for releasing free phenolic acids before it can be absorbed by the intestine and enter into the blood circulation for distributing to the cell targets in the body to perform their physiological action (Andreasen et al., 2001).

Previous studies reported that phenolic acids exerted biological activities in cardiovascular disease, type 2 diabetes mellitus, metabolic syndromes, neuroprotective effects, inhibiting oxidation of low-density lipoprotein (LDL), reducing cholesterol level, and curing and preventing cancer, as well as other chronic diseases (Chandrasekara and Shahidi, 2011; El-Seedi et al., 2012; Heitman and Ingram, 2017; Kumar and Goel, 2019; Loader et al., 2017; Santana-Gálvez et al., 2017; Upadhyay and Rao, 2013). Phenolic acids also have antioxidant properties which can be expressed by their reducing properties as hydrogen- or electron-donating agents that can act as free radical scavengers, as well as metal chelating agents. Their antioxidant activity depends on the hydroxyl group positions, in relation to the carboxyl functional group and also depend on the number of hydroxyl groups in the structure (Balasundram et al., 2006; Zheng et al., 2020).

## 2.2 Glycosylation and glycosides

### 2.2.1 Glycosylation

Glycosylation is a reaction to transfer simple carbohydrate (glycosyl) moieties to hydroxyl groups or other functional groups of glycosyl acceptors or molecules in order to form glycosylated compounds (glycoconjugates). The major groups of glycoconjugates are glycosides and acyl sugar esters, and more complex forms are glycoproteins, glycopeptides, peptidoglycans, glycolipids, and lipopolysaccharides. Glycosides are known as molecules with glycosidic bonds that link between a sugar (glycone) and another functional group from non-sugar compound (aglycone). Glycosides can be linked by an *S*-glycosidic, *C*-glycosidic, *N*-glycosidic or *O*-glycosidic

bond to the glycone anomeric carbon which as  $\alpha$  or  $\beta$ -form with mostly in the  $\beta$ -form (Wang et al., 2023).

Glycosylation plays critical roles in drug pharmacodynamics, particularly in the interaction between a drug and its cellular target. It can change the cellular localization, physicochemical, and biological properties of the compounds (Pandey et al., 2014). In the human body, glycans are important compounds in cell-to-cell interactions, including cell-to-matrix interactions and cell-to-cell recognition. In plants, glycosylation can control the bioactivity of plant metabolites, thus it is an important mechanism for the defense and regulation of phytohormones (Wei et al., 2013). Glycosylation also can enhance the bioactivity, stability, solubility, bioavailability, physicochemical and physiological properties of the glycosides, so that they become promising functional compounds, therapeutics and pharmaceuticals for human health purposes (Bujug et al., 2018; Ferreyra et al., 2012; Liu et al., 2020; Moradi et al., 2016; Pourakbari et al., 2020; Vivekanandhan et al., 2016; Woo et al., 2012).

There are two types of methods to synthesize glycosides, chemical glycosylation and enzymatic glycosylation with advantages and disadvantages for each method. Generally, a chemical glycosylation reaction usually needs many cycles including protection and deprotection reactions (Rather and Mishra, 2013). It also requires strict reaction conditions to produce the products, has high costs and an extensive purification process. Meanwhile, it is hard to achieve high stereospecificity or regioselectivity in the reaction, due to the diverse and distributed reactive sites of the sugar substrates (Li et al., 2014; Moradi et al., 2016; Thapa et al., 2019). On the other hand, enzymatic glycosylation has been recognized to cope with these issues as a feasible tool to synthesize glycosides under friendly environmental conditions while using unprotected sugar moieties and providing absolute stereocontrol to generate feasible routes in one step reaction. Enzymatic glycosylation can be catalyzed by many enzymes. In cases where the availability of carbohydrates is limited by difficult synthesis or inadequate natural supply, the enzymatic glycosylation approach can help with synthesizing complex glycans in a selective and specific way. There are several enzymes that can catalyze glycosylation reaction to form glycosides, such as

transglycosidases (TGs), glycoside hydrolases (GHs), and glycosyltransferases (GTs), as well as glycoside phosphorylases (GPs) (Lairson and Withers, 2004; Pergolizzi et al., 2017). These enzymes are catalogued in the CAZy (Carbohydrate-Active enZymes) database, where enzymes are categorized by sequence, structure, and mechanistic similarities (Cantarel et al., 2009; CAZy, 2023).

In particular, GTs, due to their high regio- and stereo-specificity, are often the only choice to transfer a glucosyl moiety to an acceptor to form specific glycosidic bonds. Challenges in the use of GTs include their availability, their expensive sugar-nucleotide donors and feedback inhibition (Lim et al., 2005). However, other enzymes are promising candidates for glycoside productions, including GHs. GHs are found with high abundance in nature, exhibit robustness and allow the use of cheaper glycosyl donor substrates. Previous studies showed the use of GHs, particularly  $\beta$ -glucosidases that were found to have higher activity for transglycosylation besides hydrolysis (Adari et al., 2016; Luang et al., 2013; Nam et al., 2017).

### 2.2.2 Glycosides and their activities

Glycosides are known to have many biological activities, such as antioxidant, anti-inflammatory, anti-cancer, and anti-diabetic, as well as anti-bacterial (Kang et al., 2015; Park and Song, 2019; Pourakbari et al., 2020; Wang et al., 2023). For instance, 4-O- $\beta$ -galactopyranosyl derivatives of phenolic acid esters (methyl vanillate and methyl ferulate) have higher cytotoxic activity in MCF-7 human breast cancer cells and in PC-3 human prostate cancer cells than their parental esters (Bujuq et al., 2018). On the other hand, a glycoside form of apigenin, namely apigenin-7-O-glucoside, has ability to promote cell apoptosis and inhibits cell migration in HeLa human cervical cancer cells (Liu et al., 2020). In HCT116 human colon cancer cells, it can similarly reduce cell viability and induce apoptosis (Smiljkovic et al., 2017). It also has been reported to stimulate production of reactive oxygen species (ROS) in human gastric cancer cells (Sun et al., 2018). Another flavonoid glycoside, luteolin-7-O-glucoside inhibited cell migration and invasion in human oral cancer cells by regulating matrix metalloproteinase-2 (MMP-2) expression (Velmurugan et al., 2020). It can also increase

apoptosis of cancer cells, sensitize cancer cells in chemotherapies, and reduce cancer cell proliferation and angiogenesis (Park and Song, 2019). Quercetin-3-*O*-glucoside was also reported to inhibit cell migration in CFPAC-1 pancreatic cancer cells (Lee et al., 2016).

## 2.3 Glycoside hydrolases family

### 2.3.1 Glycoside hydrolases

The glycoside hydrolases (GHs) (EC 3.2.1.x) are a group of enzymes that can catalyze hydrolysis reactions at the anomeric carbon of *O*-glycosides, leading to a hemiacetal or hemiketal and free aglycones (Figure 2.4) (Henrissat, 1991). These enzymes can catalyze the hydrolysis of *O*-linked glycosides. There are many studies that reported about the biological functions of GHs in essential processes of living organisms, including hydrolysis of structural compounds or storage polysaccharides, protecting against many pathogens, and turnover of cell surface carbohydrate (Bourne and Henrissat, 2001; Henrissat and Davies, 2000). In addition, they also have great potential for the future, because they are useful to improve food quality from plants by releasing nutrient and flavor compounds, make desirable sugars by converting certain sugars, and converting cellulose biomass as well as other polysaccharide wastes to get useful products (Sharma et al., 2013).

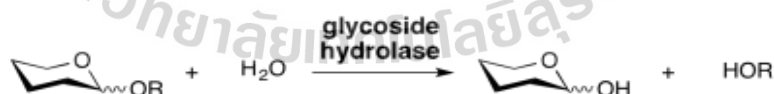


**Figure 2.4** Schematic diagram of the hydrolysis reaction catalyzed by glycoside hydrolases (www.cazypedia.org).

The Enzyme Commission (EC) system classifies GHs based on their substrate specificities and reactions. Henrissat suggested another classification system of glycoside hydrolase which is based on the similarity of sequences of amino acids and structures (Henrissat, 1991). This classification system gives more insight and explanation about the catalytic mechanisms. According to this system, enzymes can

be grouped in the same family if the enzymes have similarity of amino acid sequences and well-conserved sequence motifs that identify the family. Structures in a family can be used as appropriate search models for molecular replacement and homology modelling of proteins with related sequences.

There are about 183 sequence-based families of GHs which have been grouped and all of those families are available on the CAZy website ([www.cazy.org](http://www.cazy.org)), which is regularly updated and allows us to learn about the active site residues, reliable mechanism prediction (retaining or inverting), and possible substrates of reactions (Cantarel et al., 2009; Lombard et al., 2014; CAZy, 2023). Glycoside hydrolases (GHs) also can be classified into clans (clan A to R) of related enzymes based on their 3-dimensional (3D) structures, similarity of catalytic domain structures, and catalytic mechanisms, as well as conserved-catalytic amino acids. The GH-A clan is the largest group of families and consist of GH1, 2, 5, 10, 17, 26, 30, 35, 39, 42, 50, 51, 53, 59, 72, 79, 86, 113, 128, 140, 147, 148, 157, 158, 164, 167, 169, and 173 (CAZy, 2023). Each of those families contains enzymes that possess different substrate specificities.

### 2.3.2 Mechanism of glycoside hydrolases

Generally, hydrolysis of glycosidic bonds by GHs occurs through general acid/base catalysis which requires a proton donor and a nucleophile/base. Catalysis by GHs is performed with 2 types of mechanisms, resulting in retention or inversion of the anomeric oxygen configuration, depending on the mechanism utilized. The GHs are also divided into retaining and inverting enzymes based on the stereochemical outcome of the hydrolysis reaction (Figure 2.5).

The most common retaining mechanism uses two acidic amino acid residues, Asp or Glu, located  $\sim 5.5 \text{ \AA}$  apart in the active site, which is closer than the catalytic residues of enzymes using an inverting mechanism,  $\sim 10 \text{ \AA}$ . The retaining mechanism often occurs by double displacement, in which retaining GHs catalyze the reaction through two reaction steps, called glycosylation and deglycosylation, respectively. In the glycosylation step, the catalytic acid/base facilitates departure of the leaving group by donating a proton to the glycosidic bond oxygen atom, while the

nucleophile residue attacks the anomeric carbon to form an enzyme-glycone covalent intermediate. In the deglycosylation step, the process is reversed with a water molecule attacking with basic support from the catalytic acid/base to displace the catalytic nucleophile from the glycone. In contrast, inverting GHs generally use single displacement, where the catalytic acid residue donates a proton to the glycosidic bond oxygen, while the catalytic base residue removes a proton from a water molecule, increasing its nucleophilicity to facilitate its attack on the anomeric center on the opposite side to the departing glycosidic bond (Figure 2.5).

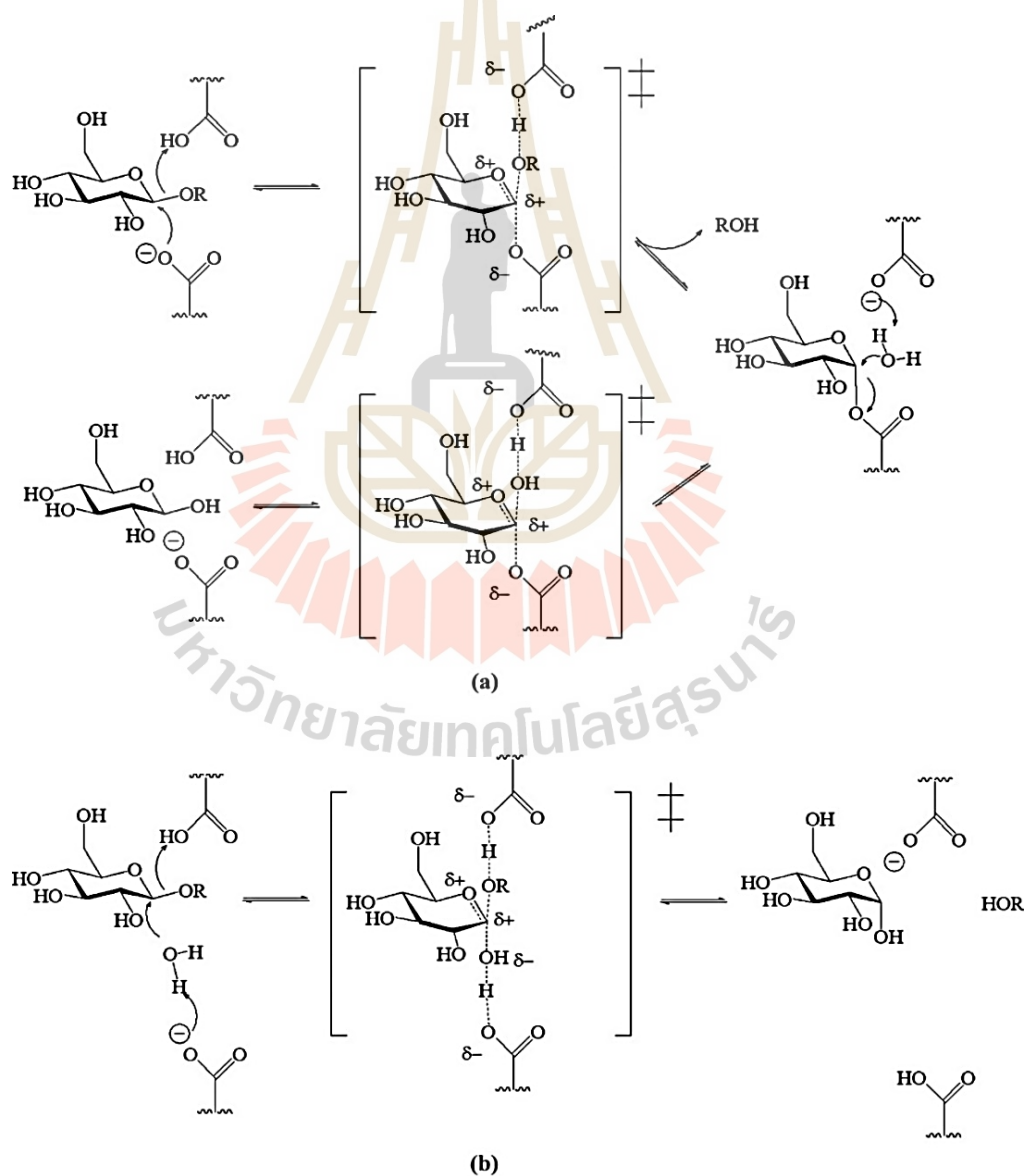


**Figure 2.5** General mechanisms of (A) retaining and (B) inverting of  $\beta$ -glucosidases. O-R is an alkyl or aryl group that acts as the leaving group (Rempel and Withers, 2008).

Many retaining GH are able to catalyze both hydrolysis and transglycosylation reactions. Unfortunately, there is not much information about what is the factor that determines the ratio between the hydrolysis and transglycosylation (Teze et al., 2014). The transglycosylation reaction can be applied to produce high value products from simple substrates. Significantly, efforts are still being made to try to increase the activity of transglycosylation by GHs and to improve the product, due to the high demands to synthesize glycosides for many purposes since GHs substrates have lower relative expense than nucleotide sugar substrates of GTs.

### 2.3.3 $\beta$ -Glucosidases

$\beta$ -Glucosidases (E.C. 3.2.1.21) are a member of GHs that catalyze hydrolysis of glycosidic bonds to non-reducing  $\beta$ -D-glucopyranoside moieties (Figure 2.6). Based on the protein sequences and specificities, there are 11 families of GHs containing  $\beta$ -glucosidases, such as GH1, GH2, GH3, GH5, GH16, GH30, GH39, GH116, GH131, GH175, and GH180 (Cantarel et al., 2009; Ketudat-Cairns et al., 2015; CAZy, 2023). Many  $\beta$ -glucosidases are grouped into GH1 together with  $\beta$ -mannosidases,  $\beta$ -galactosidases, thioglucosidases, phospho- $\beta$ -galactosidases, and phospho- $\beta$ -glucosidases (Ketudat-Cairns and Esen, 2010). Most plant  $\beta$ -glucosidases fall in GH1, which contain highly conserved amino acid sequences at the catalytic acid/base (T(F/L)NEP) and at the catalytic nucleophile ((I/V)TENG) (Ketudat-Cairns et al., 2012).

The GH1, GH2, GH5, GH30 and GH39 families are grouped into GH-A clan, which have the proton-donor and nucleophile at the end of  $\beta$ -strands 4 and 7, respectively, of the  $(\beta/\alpha)_8$  barrel structure of the catalytic domain (Jenkins et al., 1995; Ketudat-Cairns and Esen, 2010). In contrast, GH116 family members have  $(\alpha/\alpha)_6$  solenoid structures, while GH3 family have a  $(\beta/\alpha)_8$  barrel structure and a  $(\beta/\alpha)_6$  sandwich domain (Ketudat-Cairns and Esen 2010; Charoenwattanasatien et al., 2016; CAZy, 2023). In addition to hydrolysis activity, many  $\beta$ -glucosidases also have high transglycosylation activity (Ketudat-Cairns et al., 2012; Opassiri et al., 2003, 2004). In fact, related enzymes have been found to act as transglucosidases, which act to transfer glucosyl moiety from glucoconjugates to other glucosyl acceptors with little hydrolysis through a

retaining mechanism to form glycosides (Figure 2.6) (Ketudat-Cairns et al., 2012, 2015; Luang et al., 2013; Matsuba et al., 2010; Moellering et al., 2010).

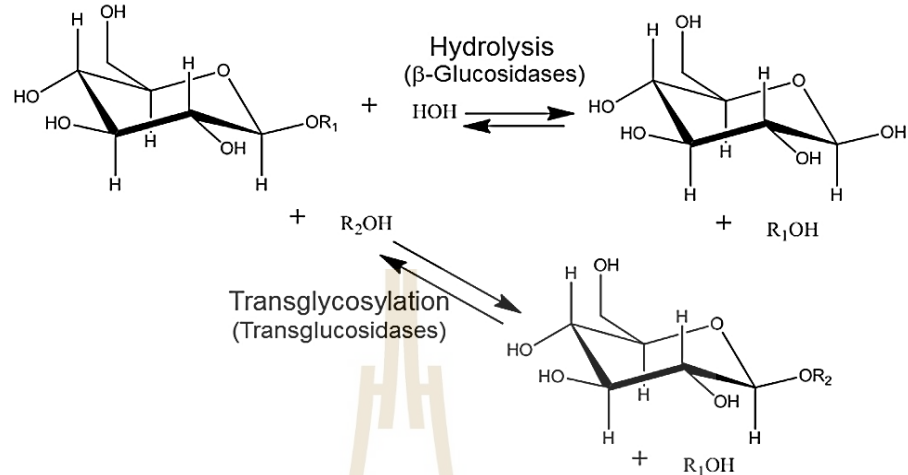


**Figure 2.6**  $\beta$ -Glucosidases catalyze both hydrolysis and transglycosylation reactions (Ketudat-Cairns et al., 2015).

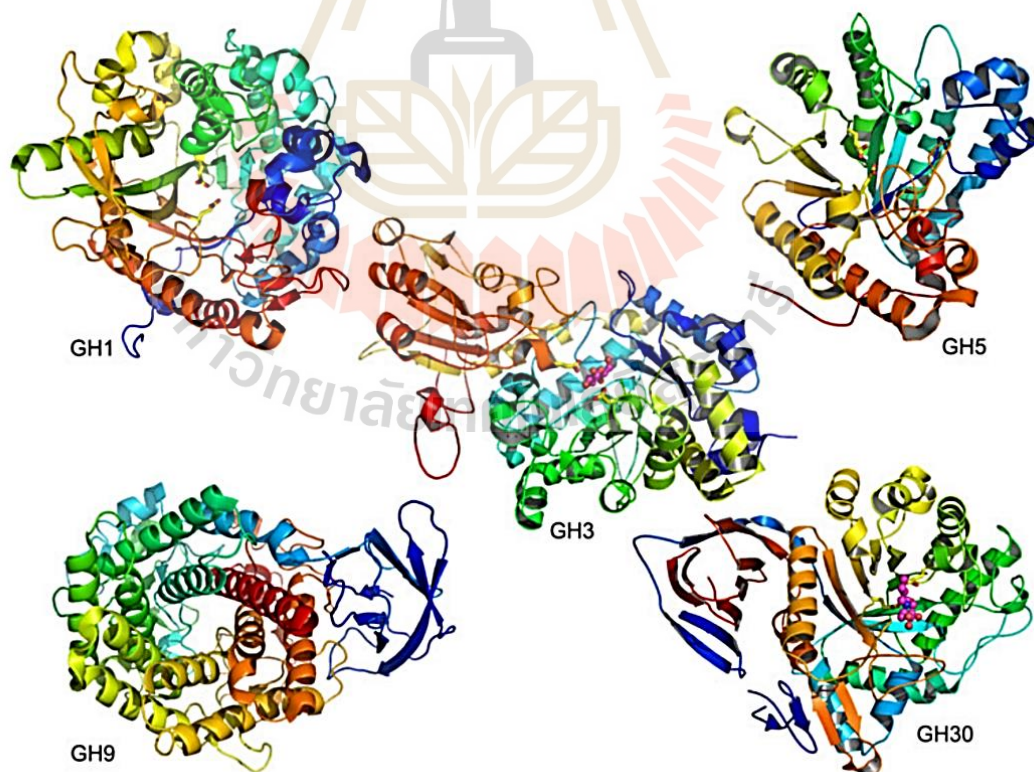


**Figure 2.7** Protein structures of  $\beta$ -glucosidases from different families of GHs (Ketudat-Cairns and Esen, 2010).

$\beta$ -Glucosidases and related enzymes can be found in many living organisms and they have different specificities, depending on their roles in animals, plants, and microorganisms, including in lignification, defense, catabolism of cell wall-derived oligosaccharides, activation of phytohormone conjugates and releasing of scent in plants, breakdown of glycolipids and exogenous glucosides in animals, and biomass conversion in microorganisms, as well as acting in plant-microbe and plant-insect interactions (Ketudat-Cairns and Esen, 2010; Seshadri et al., 2009). In mammals, there are several  $\beta$ -glucosidases, including GH1 cytoplasmic  $\beta$ -glucosidase, GH1 lactase-phloridzin hydrolase (LPH), GH30 human lysosomal acid  $\beta$ -glucosidase (GBA1), and GH116 bile acid  $\beta$ -glucosidase (GBA2) (Ketudat-Cairns and Esen, 2010). Both GBA1 and GBA2 showed activity to release glucose and ceramide by cleaving glucosylceramide (GlcCer) (Matern et al., 2001). Previous studies revealed that *GBA1* gene can undergo mutations that cause Gaucher disease, a lysosomal storage disorder characterized by accumulation of GlcCer in macrophages (Hruska et al., 2008), while GBA2 defects cause hereditary spastic paraplegia (Martin et al., 2013) and autosomal recessive congenital ataxia with spasticity (Hammer et al., 2013). In contrast, GH1 cytoplasmic  $\beta$ -glucosidase has low activity toward glucosylceramide, and it appears to mainly function on exogenous plant glucosides. The intestinal hydrolase LPH functions in food digestion and has both  $\beta$ -galactosidase activity for digestion of lactose and  $\beta$ -glucosidase activity toward exogenous glucosides (Ketudat-Cairns and Esen, 2010).

The *Drosophila melanogaster* genome only has one GH1 gene, but other insects have adapted glycosides and glycoside hydrolases from the plants on which they feed for protection and digestive purposes. In insects,  $\beta$ -glucosidases play a key role in metabolism, including degradation of glycolipids and dietary glycosides, as well as in cellular signaling (Marana et al., 2001). Myrosinases, which are a type of thio- $\beta$ -glucosidase found in certain insects and plants, hydrolyze non-toxic glucosinolates into toxic defense compounds. In microorganisms, especially cellulolytic microorganisms, cellulase induction and cellulose hydrolysis involve  $\beta$ -glucosidases, due to their hydrolysis activity. In fungi,  $\beta$ -glucosidases are a part of the cellulose degrading enzymes that divide cellobiose into two glucose molecules to complete the glucan-

breakdown work of endoglucanases and cellobiohydrolases. The action of  $\beta$ -glucosidases can protect these enzymes from the product inhibition effect of cellobiose. Therefore,  $\beta$ -glucosidases are critical to convert high cellulose biomass to fermentable sugars in the production of biofuel, such as ethanol (Chen et al., 2007; Sharma et al., 2013).

Plant  $\beta$ -glucosidases are found mainly in GH1 and GH3 although putative GH5 and GH116  $\beta$ -glucosidases are also found in plants. Plant GH1  $\beta$ -glucosidases have diverse specificities, which are involved in pigment metabolism, defense, fruit ripening, phytohormone metabolism, and  $\beta$ -glucan synthesis in cell wall development. These enzymes tend to have high specificity and activity against their aglycones, which include sugars, phytohormones, flavonoids and several phenolic acids (Luang et al., 2013; Opassiri et al., 2004; Tran et al., 2019), although they also showed hydrolysis activity on non-physiological substrates, such as *p*-nitrophenol- $\beta$ -D-glucopyranoside (*p*NPG) (Ketudat-Cairns and Esen, 2010; Komvongsa et al., 2015a; Tran et al., 2019). The activity of these enzymes is determined by their substrate specificity, localization of the enzymes with respect to potential substrates, as well as the activities of the substrates and products. Previous studies revealed that these enzymes have activity to hydrolyze a variety of *p*-nitrophenyl- $\beta$ -D-glycosides and a variety of natural glycosides at low levels, which demonstrates some flexibility in sugar binding. It also showed strong hydrolysis and glucosyltransferase activity with  $\beta$ -1,3- and  $\beta$ -1,4-linked glucooligosaccharides (Opassiri et al., 2004).

#### 2.3.4 Rice $\beta$ -glucosidase

Glycoside hydrolase family 1 (GH1) contains many enzymes that catalyze hydrolysis *O*-glycosidic bond to release simple carbohydrates, such as  $\beta$ -D-glucose,  $\beta$ -D-galactose and  $\beta$ -D-mannose (CAZy, 2023). For instance, rice BGlu1 (Os3BGlu7) acts to hydrolyze  $\beta$ -1,3-linked oligosaccharides and  $\beta$ -1,3-linked oligosaccharides. It also has transglucosylation activity to synthesis pyridoxine 5'-*O*- $\beta$ -D-glucoside from pyridoxine (vitamin B6) (Opassiri et al., 2004, 2006). Mutation of this enzyme at glutamate residue 414 showed that it is the catalytic nucleophile and 3 mutant variants of this enzyme,

including E414G, E414S and E414A, have transglucosylation activity with  $\alpha$ -glucosyl fluoride as glucosyl donor and *p*NP-cellobioside as glucosyl acceptor of which E414G had higher activity than other mutant variants (Hommalai et al., 2007).

The relationship between rice and *Arabidopsis* GH1 protein sequences is described by the phylogenetic tree of predicted protein sequences (Opassiri et al., 2006). There are forty *Arabidopsis* (*Arabidopsis thaliana*) and thirty-four rice (*Oryza sativa*) genes encoding apparently functional GH1 proteins separated into eight amino acid-sequence-based phylogenetic clusters that contain both *Arabidopsis* and rice genes. In some cases, enzymes that conduct the same or similar functions are grouped together in the same phylogenetic cluster. For instance, enzymes which act on monolignol glycosides, includes rice Os4BGlu14, Os4BGlu16 and Os4BGlu18, as well as *Arabidopsis* BGlu45, BGlu46 and BGlu47, are grouped with *Pinus contorta* coniferin/syringin  $\beta$ -glucosidase (PC AAC69619). A previous study reported that Os4BGlu16 and Os4BGlu18 preferentially hydrolyze monolignol glycosides and discussed their possible role in lignification (Baiya et al., 2014, 2018).

All putative rice GH1  $\beta$ -glucosidase protein sequences contain putative catalytic acid/base and nucleophilic glutamate residues, except for Os4BGlu14 and Os9BGlu33, which have the acid/base glutamate replaced with glutamine, as seen in thioglucosidases (Opassiri et al., 2006). The catalytic acid/base and nucleophile consensus sequences are: W-X-T/I-F/L/I/V/S/M-N/A/L/I/D/G-E/Q-P/I/Q and V/I/L-X-E-N-G, respectively (Czjzek et al., 2000; Hofmann et al., 1999; Hulo et al., 2006).  $\beta$ -Glucosidases in which glutamate is replaced with glutamine at the acid/base position have been shown to be effective transferases in the presence of a glucoside with a good leaving group aglycone and a nucleophilic acceptor (Mullegger et al., 2005).

Currently, several rice  $\beta$ -glucosidases from different At/Os phylogenetic clusters have been isolated and characterized. Rice BGlu1 (Os3BGlu7) and its close relatives Os3BGlu8 and Os7BGlu26, from the At/Os4 phylogenetic cluster, were found to release glucose and mannose from oligosaccharides generated in cell wall remodeling at various stages of plant development (Kuntothom et al., 2009; Opassiri et al., 2003). In contrast, the At/Os1 cluster representative Os3BGlu6 has little activity on  $\beta$ -1,4-linked

oligosaccharides and prefers hydrophobic glycosides (Seshadri et al., 2009) and was later shown to have relatively high activity toward gibberellin GA<sub>4</sub> 1-*O*-acyl glucose ester compared to other rice enzymes (Hua et al., 2013). Os3BGLu6 also reported to act as a glucocylceramidase to catalyze the hydrolysis of glucosylceramide to ceramide, in which Os3BGLu6 had high activity for glucosylceramides containing (4*E*,8*Z*)-sphingadienine (Koga et al., 2021).

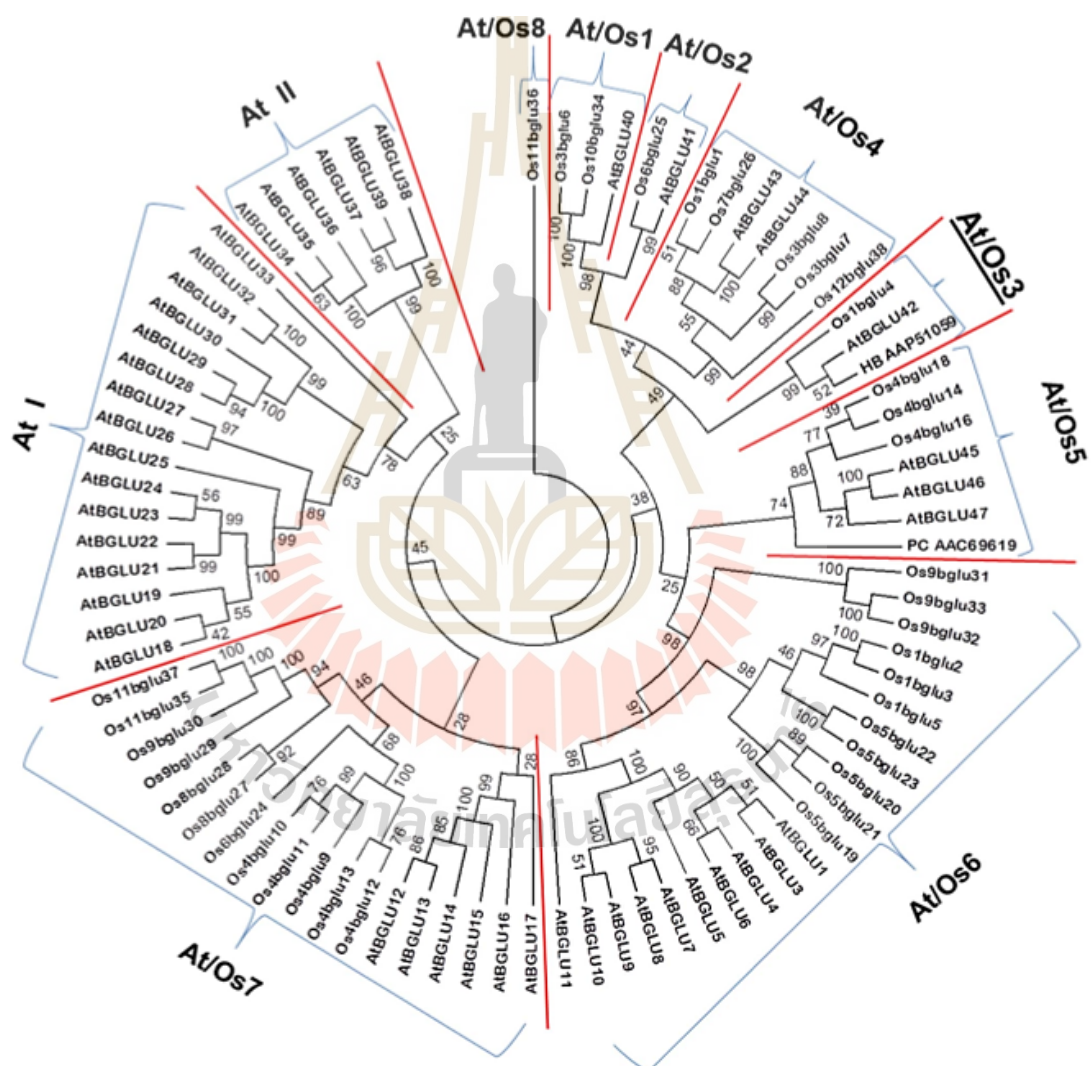


**Figure 2.8** Phylogenetic tree of predicted protein sequences of rice and *Arabidopsis* GH1 genes (Rouyi et al., 2014).

While, Os4BGLu12  $\beta$ -glucosidase in phylogenetic cluster At/Os7 was characterized and found to have high exoglucanase activity, consistent with a role in cell wall

metabolism (Opassiri et al., 2010). This enzyme was also implicated in the release of the phytohormones, such as tuberonic acid and salicylic acid from their glucosides, suggesting roles in phytohormone and oligosaccharide metabolism (Wakuta et al., 2011). The *Arabidopsis* At/Os8 representative, sensitive to freezing 2 (SFR2), was shown to be the chloroplast galactolipid: galactolipid galactosyltransferase (GGGT), which disproportionate the galactosyl residues of galactosyl diacyl glycerides to produce diacyl glycerol and  $\beta$ -linked oligogalactosyl diacyl glyceride from monogalactosyl diacyl glycerides (Moellering et al., 2010). Os11BGlu36, the rice At/Os8 representative, is expected to have the same function, GGGT, although active protein has yet to be produced by recombinant methods.

### 2.3.5 Rice Os9BGlu31 transglucosidase

Previous studies reported that many GH1 transglycosidases act to catalyze transglycosylation with or without hydrolysis, which consist of transgalactosidases and transglucosidases (Matsuba et al., 2010; Moellering and Benning, 2011). One transgalactosidase, named galactolipid-galactolipid galactosyl transferase (GGGT), where found to act to transfer galactose from monogalactosyl diacyl glyceride (MGDG) as donor to digalactosyl diacyl glyceride (DGDG) or other MGDG as acceptor to form glycolipids, containing long oligosaccharide chains at the outer membrane of chloroplast (Moellering and Benning, 2011). On the other hand, acyl glucose-dependent anthocyanin glucosyl transferases (AAGT), which is a GH1 transglucosidase, can transfer a glucosyl moiety from 1-*O*- $\beta$ -D-vanillyl-glucose to cyanidin 3-*O*-glucoside in carnation at the 5 position and delphinium without hydrolysis (Matsuba et al., 2010; Sasaki et al., 2014). Together with serine carboxypeptidase-like (SCPL) acyl glucose-dependent acyl transferases, AAGT and *Arabidopsis* GH1 enzyme AtBGLU10 is responsible for building large anthocyanins by transferring sugar moieties and acyl groups to the anthocyanin backbone. AtBGLU10 acts to transfer the glucosyl moiety from sinapoylglucose (acyl-glucose ester) as glucosyl donor during sinapoylation and glucosylation to *p*-coumaroyl moiety on the anthocyanin A11 in *Arabidopsis* (Miyahara et al., 2013; Nishizaki et al., 2013; Sasaki et al., 2014).

Another At/Os6 cluster member that is a transglucosidase, named Os9BGlu31, based on its position on rice chromosome 9 and its being a member of GH1 which primarily contains  $\beta$ -glucosidases, acts to transfer glucose from glucosyl donors to the glucosyl acceptors to form glycosides (Luang et al., 2013). It had high activity in reaction containing phenolic acid esters, such as feruloyl glucose and similar phenolic acid glucose esters, including 4-coumaroyl-glucose and sinapoyl-glucose as glucosyl donors. These glucose esters are known to serve as donors in acyl and glucosyl transfer reactions in the vacuole, where Os9BGlu31 is accumulated (Nishizaki et al., 2013). Even free phenolic acids of these esters also act as excellent acceptor substrates to form their glucosyl esters (Ketudat-Cairns et al., 2015; Luang et al., 2013). Os9BGlu31 is also able to use apigenin as an acceptor and apigenin 7-O-glucoside as a glucosyl donor. It also can produce multiple kaempferol glycosides as products (Komvongsa et al., 2015a). These enzymes have potential to be applied to *in vitro* glycodiversification without the need for a nucleotide sugar intermediate (Gantt et al., 2011).

#### 2.4 Mutagenesis and mutant variants

In protein engineering, mutagenesis is a strategy to modify protein sequence to study and obtain suitable structure or function of a protein. Proteins contain a sequence of residues, which primarily comprise 20 amino acids. This is a simple architecture of protein and can be expanded by post-translational modifications. Modified polypeptides can be produced by recombinant DNA and other methods of mutagenesis. One of method for mutagenesis is site-saturated mutagenesis, in which a single amino acid can be substituted to any other 19 possible amino acid substituents and the mutagenesis products with many variants are collected in a library with having a different codon in the targeted position. On the other hand, site-directed mutagenesis is commonly applied to learn the function of single amino acid residues in the protein, by which a single amino acid is substituted with a specific amino acid of interest to generate a desired mutation (Siloto and Weselake, 2012). Therefore, site-directed mutagenesis can be used to learn the importance of specific amino acid residues, such as the role of their residues in enzyme catalysis.

Site-directed mutagenesis was developed by Kunkel, with use of a strain deficient in dUTPase and uracil deglycosylase and the uracil-containing wild type DNA can be degraded by recipient *E. coli* (Kunkel, 1985). Currently, polymerase chain reaction (PCR)-based method is applied for mutagenesis of the gene encoding a protein, which requires a thermostable DNA polymerase, a plasmid vector as template and mutagenic primers containing the desired mutation for both strands of the targeted position. By using this method, the mutagenic primers can be annealed to the DNA template, then the plasmid DNA replicated to produce DNA containing the mutagenic primers to generate a mutagenic product in a mixture between mutant and parental plasmid DNA. In the next step, *DpnI* is often used to remove the template methylated DNA from the newly synthesized demethylated mutant DNA, then followed by transformation into *E. coli* cells.

Previous study reported the use of site-directed mutagenesis to modify the activities of GH enzymes and even identify the catalytic residues in active sites, which mutation did not cause complete elimination the activity of enzyme, but altered the catalytic mechanism of enzyme significantly depending on the specific mutation and type of amino acid substitution (Peracchi, 2001). Therefore, this method can be applied to modify the specificity, mechanism or activity of an enzyme for many desired applications. For instance, mutagenesis of Os9BGlu31 by substitution three amino acid residues by site-directed mutagenesis at the catalytic acid/base (E169Q and E169A), putative catalytic nucleophile (E387A), and residue preceding catalytic nucleophile (H386T) showed decreased of enzyme activity compared wild type. The wild type enzyme displays an unusual lack of inhibition by mechanism-based inhibitors of GH1  $\beta$ -glucosidases that utilize a double displacement retaining mechanism (Luang et al., 2013).

Moreover, Os9BGlu31 was mutated at amino acid residues in the acceptor binding region of active site by site-directed mutagenesis using specific primers based on homology model with Os3BGlu6 as template to produce Os9BGlu31 mutant variants, such as I172T, L183Q, W243N, W243A, W243D, W243F, W243M, and W243Y (Komvongsa et al., 2015a). While I172T and L183Q mutants decreased the enzyme

activity, the W243 mutants had variable effects on enzyme activity depending on their acceptor substrate compared with wild type. However, the W243N mutant had higher activity than wild type on phenolic acids and kaempferol. Interestingly, W243N mutant could produce multiple products of kaempferol glucosides (Komvongsa et al., 2015a). Os9BGlu31 also can transfer a glucosyl moiety to unsaturated fatty acids, such as oleic acid and linoleic acid, to form 1-*O*-acyl glucose esters (Komvongsa et al., 2015b). The W243 residue seems critical to the specificity of substrate and product of Os9BGlu31, so that its mutation allows for production of a range transglucosylation products (glucosides). The corresponding residue in active site cleft of Os3BGlu6 is within 8.7 Å of the acceptor water binding site. Moreover, a double mutant of Os9BGlu31, L241D/W243N, was reported to have very high activity on ferulic acid with high level of hydrolysis (Tran et al., 2019).

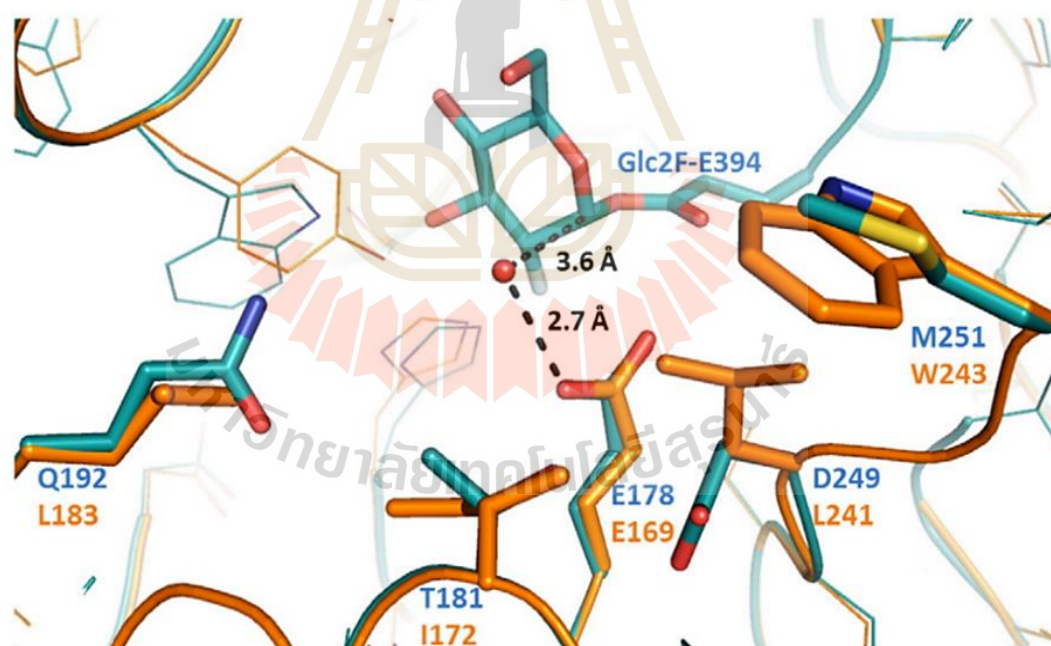


**Figure 2.9** Superposition of Os9BGlu31 on the Os3BGlu6  $\beta$ -glucosidase X-ray crystal structure covalent intermediate with 2-fluoro- $\alpha$ -D-glucoside (PDB ID: 3GNR). Orange carbon = Os9BGlu31, cyan carbon = Os3BGlu6, red sphere = putative nucleophilic water in the Os3BGlu6 complex, ribbon form = protein backbones, thick stick = the catalytic acid base and surrounding residues, and the 2-fluoroglucose-bound nucleophile of Os3BGlu6 (Komvongsa et al., 2015a).

## 2.5 Bile duct cancer

### 2.5.1 Cancers and metastasis

Cancers comprise a large group of diseases that are characterized by development of abnormal cells that grow uncontrollably in almost any tissue and organ in the body. Cancer can also easily invade adjoining parts, then spread to other organs in the body. It is the second leading cause of death globally in the human population. Cancer cells can spread from the primary site to the other organs in the body, thus causing abnormal proliferation and metastasis, which is characterized by cell migration, invasion, and adhesion. During metastasis, particularly in the invasion step, cancer cells will break the basement membrane through the extracellular matrix and need an epithelial-mesenchymal transition (EMT) for invasion. Cancer cells can synthesize several proteases, such as serine proteases and matrix metalloproteinases (MMPs), including MMP-2 and MMP-9, which are involved in this step to break the basement membrane (Liu et al., 2020; Sun et al., 2020; Velmurugan et al., 2020; Vo et al., 2020). Therefore, MMPs have become vital protein targets for treatment strategies against cancer aggressiveness.

Previous studies reported that there are protein kinases, called mitogen-activated protein kinase (MAPKs), consisting of p38 MAP kinase (p38 MAPK), Jun N-terminal kinase 1/2/3 (JNK1/2/3), and extracellular signal-regulated kinase 1/2 (ERK1/2), which are associated with cancer cell proliferation, migration and invasion, as well as apoptosis (Chowdhury et al., 2019; Nam et al., 2008; Tang et al., 2019). Overexpression of p38 MAPK can increase metastasis by increasing expression of MMPs in prostate cancer and in neoplastic squamous epithelial cells (Koul et al., 2013; Xu et al., 2006). In oral cancer cells, the lack of p38 MAPK expression can reduce MMP-9 expression, and reduce the rate of metastasis in breast cancer cells and also reduce MMP-2 expression (Buck et al., 2004; Velmurugan et al., 2020). In contrast, stimulation of ERK phosphorylation tends to increase cancer metastasis (Nokin et al., 2019; Shen et al., 2019). Moreover, in human lung cancer cells, metastasis can be suppressed by downregulation of the ERK/p38 signaling pathway, which is implicated for inhibition of MMPs, including MMP-2 and MMP-9 activities (Yue et al., 2019). Because metastasis is dangerous, metastasis

needs to be inhibited by the treatment methods that trigger programmed cell death, including apoptosis through the extrinsic or intrinsic death receptor pathway.

Cancers can develop through carcinogenesis by accumulation of genetic alterations in cells. Generally, the characteristics of cancer can be modeled in several ways, which are called the “hallmarks” of cancer that require the acquisition of 6 fundamental properties. Currently, this hallmarks have been developed to include 10 fundamental properties, including inducing or accessing vasculature, genome instability and mutation, resisting cell death, deregulating cellular metabolism and sustaining proliferative signaling, evading growth suppressors, avoiding immune destruction, enabling replicative immortality, tumor-promoting inflammation, and activating invasion and metastasis (Hanahan, 2022).

### **2.5.2 Cholangiocarcinoma**

There are several types of cancer based on the location or organ system in the body and specific cell type. One of the cancers is cholangiocarcinoma (CCA), an aggressive cancer of the epithelial cells of the bile duct inside the liver which has highest incidence in northeastern Thailand. It has very poor prognosis because it is aggressive and the symptoms are unobservable and undetectable until the bile duct is blocked by a tumor (Banales et al., 2020). Cholangiocarcinoma can be classified into 2 types, including intrahepatic and extrahepatic cholangiocarcinoma depending on their anatomic location (Figure 2.10). The intrahepatic cholangiocarcinoma (iCCA) arises from the bile duct epithelial cells within the liver parenchyma, whereas extrahepatic cholangiocarcinoma occurs between the bile duct and cystic duct of the liver and is separated into perihilar cholangiocarcinoma (pCCA) and distal cholangiocarcinoma (dCCA) (Brindley et al., 2021; Khan et al., 2019; Sripa et al., 2011). Moreover, extrahepatic cholangiocarcinoma can be classified according to the Bismuth classification into types I to IV (Blechacz and Gores, 2008; Ghouri et al., 2015). Another classification of cholangiocarcinoma is according to its macroscopic growth pattern, consisting of mass forming, periductal-infiltrating and intraductal growth (Figure 2.11) (Sripa et al., 2007; Sripa and Pairojkul, 2008; Zheng et al., 2017).

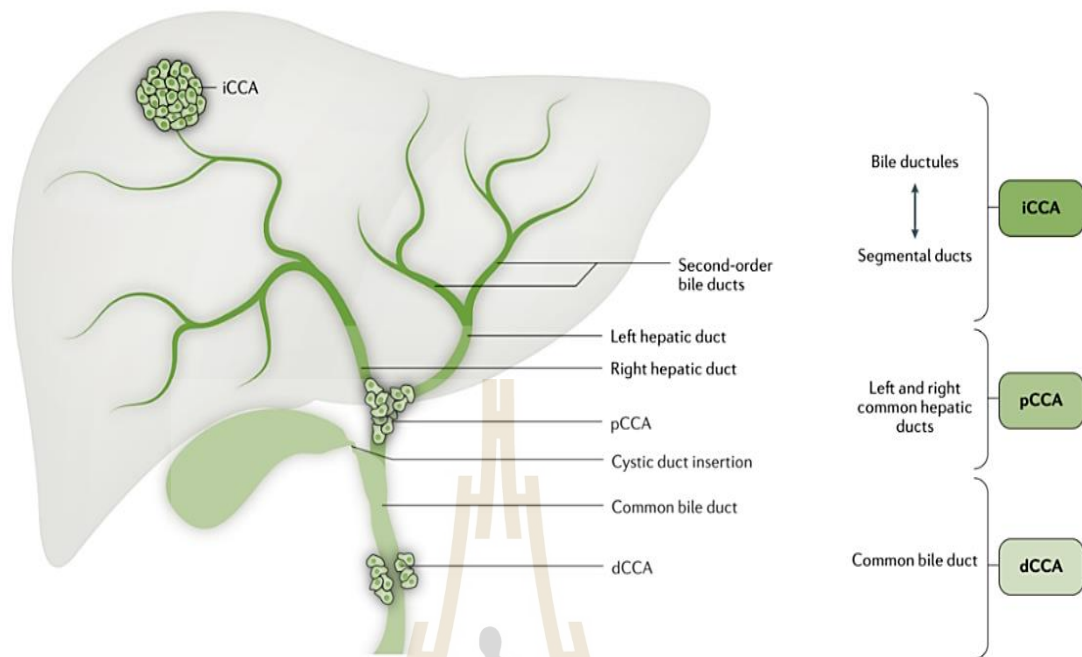


**Figure 2.10** Schematic representation of types of CCA in the liver based on localization. It is classified according to anatomic location as intrahepatic CCA (iCCA), perihilar CCA (pCCA), and distal CCA (dCCA) (Brindley et al., 2021).

CCA Subtype	Dimensions	Location (Intra or Extra-hepatic)	Pathology	Method of Spread	Symptoms of Bile Duct Obstruction?
Mass forming	Central mass; depends on location (IH up to 15 cm; EH 1–2 cm)	Intra-hepatic Extra-hepatic	<ul style="list-style-type: none"> <li>• Gray white mass</li> <li>• Poor cellular differentiation</li> <li>• Well defined, wavy, or lobulated borders</li> <li>• May have central fibrosis and necrosis</li> </ul>	<ul style="list-style-type: none"> <li>• Grows outward into lumen</li> <li>• Invades liver parenchyma through peribiliary venous plexus</li> <li>• Intrahepatic metastasis is common in advanced stages</li> </ul>	Symptoms occasionally occur
Periductal-infiltrating	0.5–8 cm long (up to 1cm in the case of EH tumors)		<ul style="list-style-type: none"> <li>• Concentric thickening of bile duct wall</li> <li>• Later stages appear branch-like</li> <li>• Usually highly differentiated</li> </ul>	<ul style="list-style-type: none"> <li>• Invades bile duct wall</li> <li>• Spreads along axis of bile ducts</li> </ul>	Viscous mucus produced by the tumor can impede bile flow and produce intermittent obstructive symptoms
Intraductal growing	Usually small and flat; later stages may fill bile duct lumen		<ul style="list-style-type: none"> <li>• Tumors within lumen</li> <li>• Frond-like foldings</li> </ul>	<ul style="list-style-type: none"> <li>• Spreads superficially along mucosal surface</li> <li>• Sloughing of tumor cells can initiate secondary tumors</li> <li>• Invasive intraductal CCA can also occur</li> </ul>	Narrowing of bile ducts eventually leads to symptoms

**Figure 2.11** The classification of CCA according to its macroscopic growth pattern. CCA can be classified into mass forming, periductal-infiltrating and intraductal growth (Sripa et al., 2007).

There are many types of CCA cells that isolated from CCA patients, including KKU-213, KKU-055, and KKU-100. KKU-213 cells were isolated from intrahepatic bile duct specimens of a 58-year-old Northeast Thai man who infected by *Opisthorchis viverrine* (Ov) with CCA at stage-4B. KKU-213 was classified as adenosquamous carcinoma and separated into KKU-231A, KKU-213B, and KKU-213C. KKU-213A was derived from well-differentiated, and has small and spindle-shaped cells, whereas KKU-213B has irregular polygonal cells, high nucleus to cytoplasmic ratio, and patch-like structure. While KKU-213C has irregular polygonal cells, and high nucleus to cytoplasmic ratio. However, both of those cells have similar doubling-time was around 24 h. KKU-213A showed the highest migration and invasion abilities approximately 3.5 times higher than KKU-213B and KKU-213C. Therefore, KKU-213A was more aggressiveness and fast growth with high metastatic (Isidan et al., 2022; Sripa et al., 2020).

KKU-055 cells were isolated from intrahepatic bile duct specimens of a 56-year-old Northeast Thai man who infected by Ov with poorly differentiated primary cholangiocarcinoma adenocarcinoma tissue. KKU-055 was more sensitive toward chemotherapeutic drugs and slow growth (Panawan et al., 2023; Tepsiri et al., 2005) While, KKU-100 cells were isolated from extrahepatic bile duct specimens of a 65-year-old Northeast Thai woman who infected by Ov with cholangiocarcinoma of the *porta hepatis* (Sripa et al., 2005). KKU-100 was derived from poorly differentiated tubular adenocarcinoma, the common histologic type of cholangiocarcinoma reported in Thailand. It possesses compact and polygonal-shaped epithelial cells with the individual KKU-100 cells had a large nucleus containing 2-5 nucleoli and a clear cytoplasm. The cholangiocarcinoma cell line, KKU-100, was established 4 month after the primary culture-population doubling time was 72 h, and least sensitive cell line toward chemotherapeutic drugs and slow growth (Sripa et al., 2005; Tepsiri et al., 2005).

### 2.5.3 Epidemiology of cholangiocarcinoma

Commonly, infection by liver fluke (*Opisthorchis viverrine*, Ov) is known as a

major risk factor for CCA development in Asia, but in other countries, liver flukes are not endemic, so that it is not a major risk factor for CCA development in those areas. The incidence of CCA in other countries is caused by non-fluke-related CCA risk factors, including cirrhosis, primary sclerosing cholangitis, hepatitis B, Caroli disease, choledochal cyst, non-alcoholic fatty liver disease (NAFLD), and choledocholithiasis (Brindley et al., 2021). According to the previous studies, the incidence of CCA is rare worldwide but it is steadily increasing in Thailand, especially in northeastern Thailand (Figure 2.12) (Brindley et al., 2021; Sithithaworn et al., 2014).

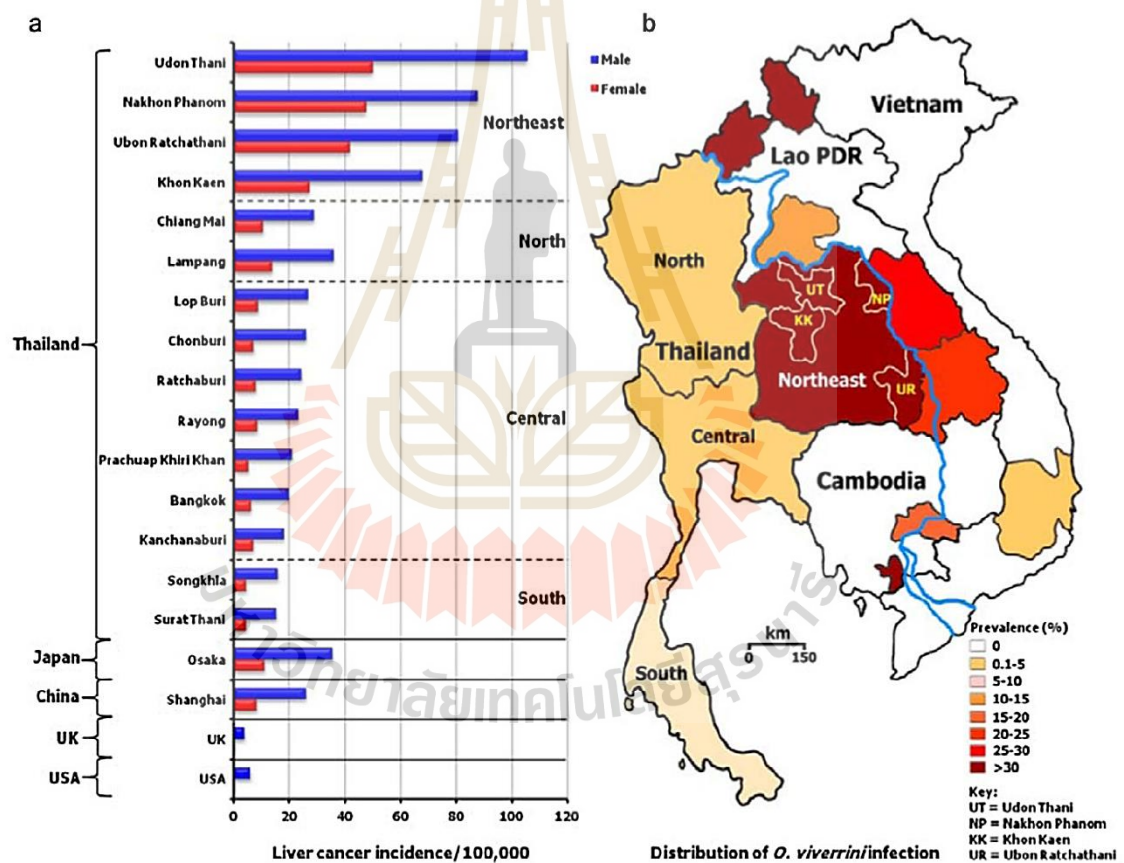


**Figure 2.12** The cholangiocarcinoma incidence in Thailand. (A) Geographical locations of cholangiocarcinoma incidence, and (B) distribution of liver fluke (*Ov*) in Thailand (Sithithaworn et al., 2014).

The incidence of CCA is 10-15% of all liver cancers and 3% of gastrointestinal cancers in human. Mostly, CCA is the second most common type of liver cancer after

hepatocellular carcinoma (Banales et al., 2020). Previous studies reported that around 700 million people are at risk of liver fluke infection in the world (Brindley et al., 2021; Sripa and Pairojkul, 2008; Zheng et al., 2017). The highest incidence has been reported in Khon Kaen province in Thailand with age-standardized incidence rate (ASRs) at 39.4 and 94.8 per 100,000 in the years 1991-1998 in females and males, respectively (Sripa et al., 2007; Sripa and Pairojkul, 2008).

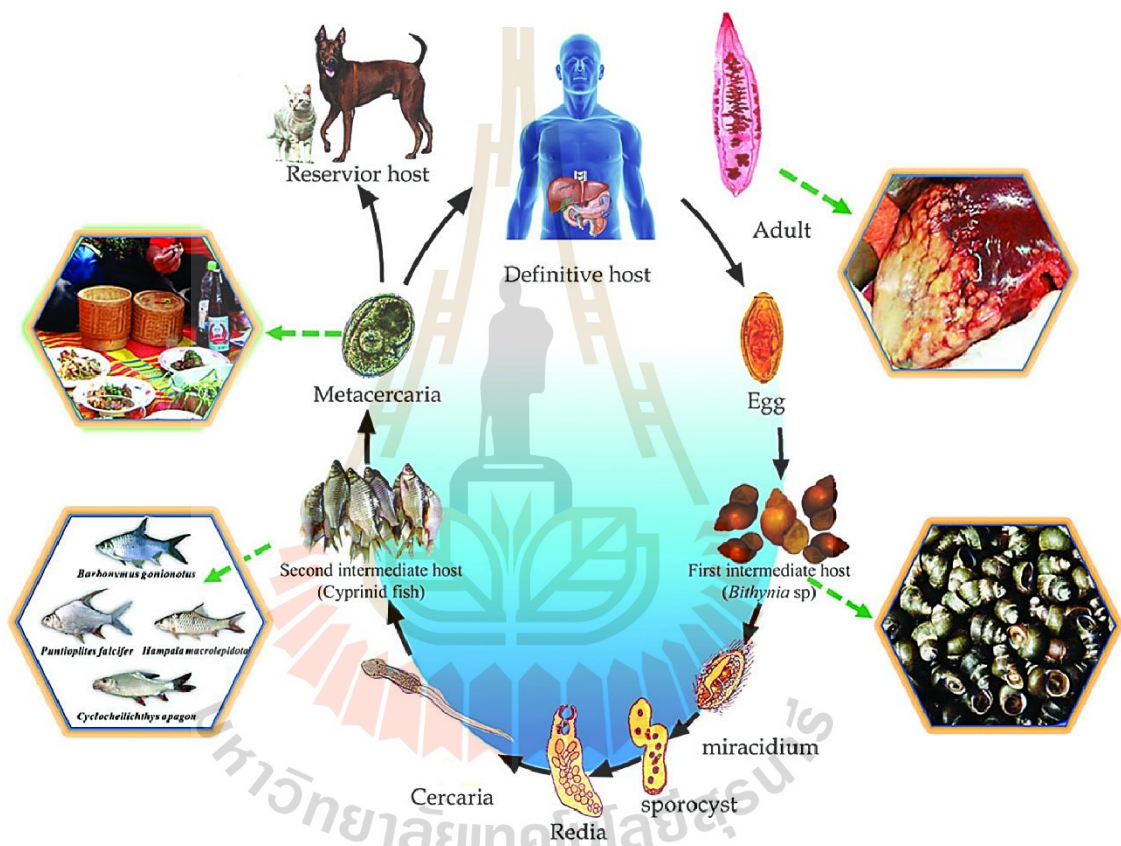


**Figure 2.13** The life cycle of the liver fluke (*Ov*) (Sithithaworn et al., 2014).

Infection of bile duct by liver fluke can be started from the food. The liver flukes, *Opisthorchis viverrine* (*Ov*) and *Clonorchis sinensis* (*Cs*), can migrate into the body of humans who eat raw or undercooked freshwater cyprinid fish that carrying the larvae of liver flukes, called metacercaria (Figure 2.13). This juvenile larvae migrates through the ampulla of Vater (hepatopancreatic duct) into the bile duct and intrahepatic bile duct then they can live many years in there (Brindley et al., 2021; Sripa et al., 2007, 2011; Yongvanit et al., 2012). Infection of *Ov* is a major risk

factor of CCA in Thailand, Cambodia and Laos, whereas Cs is found in China, Korea, Vietnam, Taiwan and Japan (Yongvanit et al., 2012).

#### 2.5.4 Carcinogenesis of Ov-associated cholangiocarcinoma

The mechanism of inflammation caused by liver fluke infection in related to cholangiocarcinogenesis was proposed (Figure 2.14). Chronic inflammation was caused by infection of Ov in the human liver can increase the levels of proinflammatory cytokines, which are generated by cyclooxygenase-2 (COX-2) and increase transcription factors, such as nuclear factor kappa B (NF- $\kappa$ B), as well as inducible oxide activities that disturb the homeostasis of oxidant/antioxidant and DNA repair enzymes. These oxidative and nitrative stresses can induce an increase of reactive oxygen species (ROS) and nitrogen species (NOS) production in inflamed target cells, thus increasing the level of oxidized DNA and DNA bases modified by lipid peroxidation products in human tissues (Yongvanit et al., 2012).

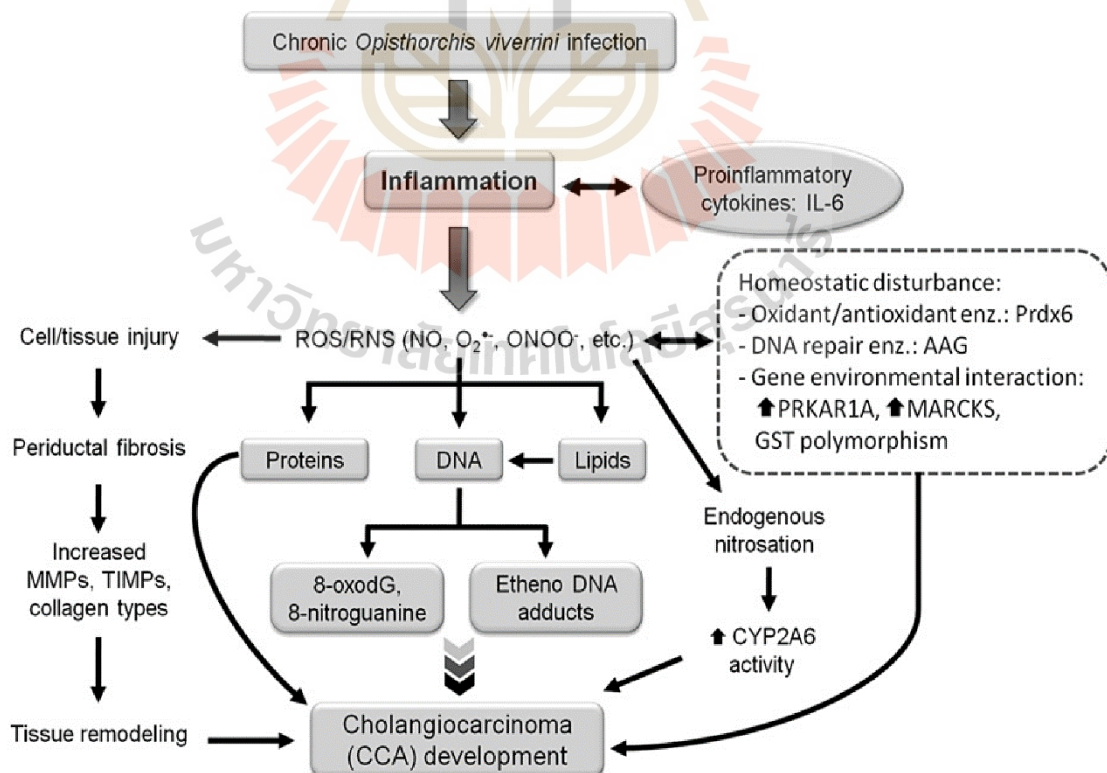


**Figure 2.14** The proposed mechanism of inflammation caused by liver flukes in related to cholangiocarcinogenesis (Yongvanit et al., 2012).

The production of endogenous nitric oxide is catalyzed by inducible nitric oxide synthase (iNOS), an enzyme mainly produced by inflammatory cells, especially macrophages that are induced by inflammatory cytokines (Jaiswal et al., 2000). Previous studies reported that Ov-infection in an animal model caused oxidative and nitrosative DNA damage as judged by the presence of 8-oxo-7,8-dihydro-2'-deoxyguanosine (8-oxodG) and 8-nitroguanine, which are biomarkers for DNA damage in the liver (Pinlaor et al., 2003; Thanan et al., 2008; Yongvanit et al., 2012). Furthermore, a high level of 8-oxodG is found in liver tissues of CCA patients and in urine and leukocytes of Ov-infected patients (Thanan et al., 2008). Also, chronic inflammation caused by Ov may trigger a failure of the immune response which contributes to the progression of cholangiocarcinogenesis.

A study of metastasis of cholangiocarcinoma reported that mannose glycans with terminating  $\alpha$ -1,2-mannose residues triggered cholangiocarcinoma metastasis by down-regulation of the Golgi  $\alpha$ -mannosidase I (MAN1A1 gene). Inhibition of  $\alpha$ -mannosidase I caused reshaping of the glycome that resulted in increasing capability of migration and invasion. Molecular modelling revealed that a conformational change of the helical domain of transferrin receptor protein 1 can extend mannose glycosylation and improve noncovalent interaction energies to trigger the enhancement of cell migration in metastatic cholangiocarcinoma (Park et al., 2020). Another study found potential biomarkers of CCA in serum for monitoring, prognosis and recurrence. Mostly, a carbohydrate antigen (CA 19-9) can be used as a serum marker for CCA but other antigens, including CYFRA21-A, MUC5AC, CA-S1212, IL-6, and RCAS1 also represent potential biomarkers (Silsirivanit et al., 2013).

### **2.5.5 Treatment of cholangiocarcinoma**

Generally, the therapies for malignant tumors include surgery, drug chemotherapy, immunotherapy, and radiotherapy (Ma et al., 2019; Rizvi et al., 2018; Rizvi and Gores, 2013). Surgical resection remains the main potential therapy for CCA patients. There are 2 types of surgery for bile duct cancer, including curative surgery and palliative surgery to relieve symptoms, such as blockage of the bile duct (Rizvi et

al., 2018). Curative surgery can only be used at the early stage (Patel, 2011; Razumilava and Gores, 2014). Meanwhile, the early diagnosis process remains painful for patients, so that the patients are diagnosed in advanced stages of CCA, at which point it is impossible to undergo surgical restorative treatment (Patel, 2011).

Other therapies are radiation therapy and chemotherapeutics for CCA patients. Radiation therapy or adjuvant therapy uses high-energy electromagnetic rays to destroy the cancer cells at identified tumors. Meanwhile, chemotherapy is the treatment to kill the cancer cells by drugs that are usually given into a vein. The drugs that can be used to treat the cancer cells include 5-fluorouracil (5-FU), gemcitabine, cisplatin, capecitabine, and oxaliplatin (Valle et al., 2010). To get more effective treatment, usually 2 or more drugs are combined. For instance, a combination of gemcitabine and cisplatin may help the CCA patients live longer than treatment with one drug, because they show a synergistic effect that is associated with longer overall survival and greater response (Valle et al., 2010). The evidence suggests that gemcitabine-cisplatin extends overall survival approximately 5 to 12 months compared with mono-therapeutic drug treatment (Astolfi et al., 2013; Valle et al., 2010). By using this therapy, non-cancer cells can be affected, which can lead to side effects, including hair loss, loss of appetite, nausea, vomiting, diarrhea, neuropathy and so on (Binder et al., 2007). Many researchers try to find new types of treatment which can be tested in clinical trials, including immunotherapy and targeted therapy, as well as treatment with bioactive compounds to reduce the side effects of chemotherapeutic drugs and potentially improve their ability to kill the cancer cells.

## 2.6 Cell death mechanisms

### 2.6.1 Programmed cell death

In general, programmed cell death (PCD) is a genetically or biochemical regulated process of cell suicide, which is an important process for the homeostasis of tissues, development, elimination of abnormal or unwanted cells, and integrity of multicellular organisms. Therefore, PCD induction is an interesting therapeutic strategy of drugs or treatments to kill cancer cells and suppress the cancer cell development

in the body. There are three major types of cell death mechanisms, including apoptosis, autophagy, and necrosis (Chaabane et al., 2013). Apoptosis is considered a programmed cell death because it is a result of a tightly regulated and genetically regulated process in the cells. In contrast, necrosis occurs accidentally through disruption of cell structure without plan or organization. Autophagy is a cell death mechanism that involves cell degradation through degradation of cellular component, such as organelle, cytoplasm, and protein by lysosomes. However, previous studies described that PCD is consist of apoptosis, autophagy, and regulated or programmed necrosis (necroptosis) (Christofferson and Yuan, 2010; Han et al., 2011; Tan et al., 2014). The cell death mechanisms can be induced within in the same tissue which apoptosis is faster than autophagy and necrosis that appear only when apoptosis is inhibited (Los et al., 2002).

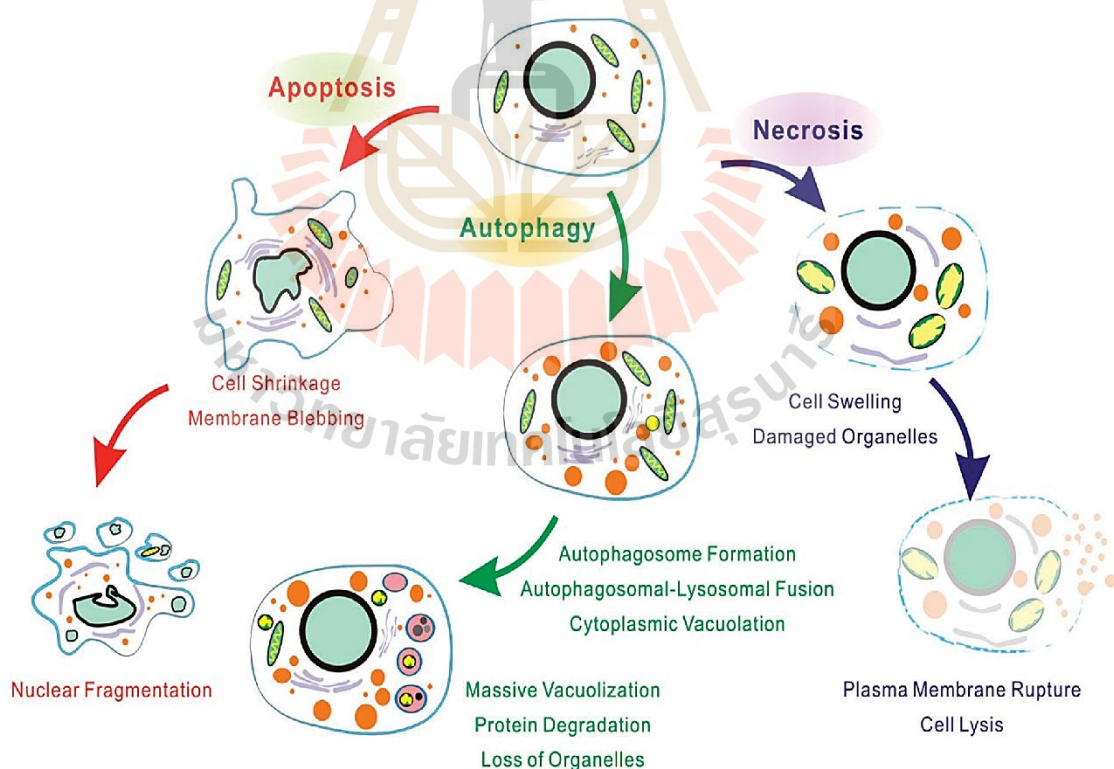


**Figure 2.15** The morphological features of cell death mechanisms of apoptosis, autophagy, and necrosis (Tan et al., 2014).

Commonly, the differences between apoptosis, autophagy, and necrosis are based on morphological and biochemical alterations (Figure 2.15). Cells undergoing apoptosis tend to show cell morphological changes, including cell shrinkage, membrane blebbing, nuclear fragmentation, chromatin condensation, organelle relocation and compaction, and formation of apoptotic bodies. The general biochemical process of apoptosis involves degradation of cellular constituents, including DNA degradation by activation of caspases, DNA fragmentation by endogenous DNases resulted DNA fragments (180-200 bp), energy (ATP)-dependent apoptotic processes, and translocation of phosphatidylserine to the extracellular side of the membrane (Tan et al., 2014). However, other studies reported that apoptosis can also be caused in a caspase-independent manner (Chipuk and Green, 2005; Tait and Green, 2008). In contrast, necrosis is caused by lethal disruption of cell structure and activity, which is characterized by cytoplasm and mitochondria or cell swelling, damaged organelles, and plasma membrane rupture, ending with cell lysis. The biochemical feature of necrosis, include random digestion of DNA, loss of ion homeostasis, and no energy requirement. Autophagy is characterized by the formation and accumulation of autophagosomes and autophagolysosomes from fusion between autophagosome with lysosome (Tan et al., 2014). This involves action of autophagy-related proteins (ATG), of which ATG-6 (Beclin-1) and microtubule-associated protein 1 light chain 3 (LC3) are two major components for autophagic cell death (Mizushima and Yoshimori, 2007).

### 2.6.2 Apoptosis mechanisms

Activation of caspases cascade is a common biochemical feature of apoptosis, called caspase-dependent apoptosis mechanism. However, there is another mechanism of apoptosis, called caspase-independent apoptosis mechanism (Chipuk and Green, 2005; Tait and Green, 2008; Tan et al., 2014). In caspase-dependent apoptosis, caspase signaling pathway can be activated through either by intrinsic (mitochondria-mediated) or extrinsic (death receptor-mediated) pathway (Figure 2.16).

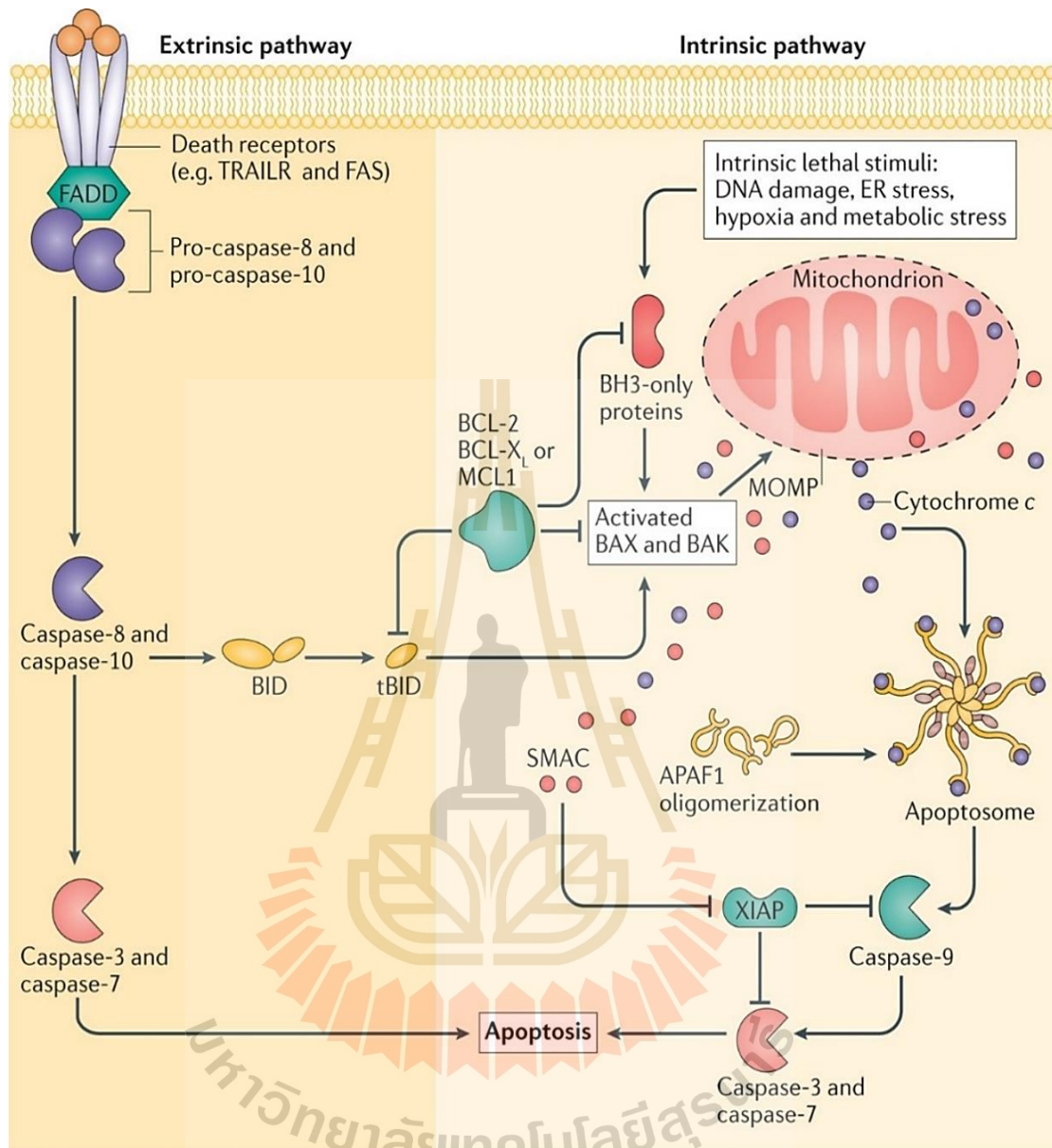


**Figure 2.16** The caspase-dependent apoptosis mechanism can be divided into the extrinsic and intrinsic pathways (Ichim and Tait, 2016).

The extrinsic apoptotic pathway is mediated by external stimulation, which death ligands (tumor necrosis factor (TNF) ligand or Fas ligand (type II transmembrane protein)) bind to a death receptor, such as TNF-related apoptosis-inducing ligand (TRAIL) receptor 1 (TRAILR1), TRAILR2, Fas receptor (CD95), or TNF receptor 1 (TNFR 1). The death receptors, which have an intracellular death domain can activate initiator caspases (caspase-8 and caspase-10) from pro-caspase forms through dimerization

mediated by adaptor proteins (Fas-associated death domain (FADD) protein and TNF receptor-associated death domain (TRADD) protein). The adaptor FADD also result in the formation of the death-inducing signaling complex (DISC). The activated form of caspase-8 and caspase-10 initiates apoptosis by cleaving and activating the effector caspases (caspase-3 and caspase-7) thereby leading to apoptosis. The extrinsic and intrinsic apoptotic pathways can be connected at the level of caspase-8 by cleavage of Bcl-2-homology domain 3 (BH3) interacting-domain death agonist (BID) to form its active form, truncated BID (tBID), which is mediated by caspase-8. This leads to the intrinsic apoptotic pathway via activation of Bax and Bak, which trigger mitochondrial outer membrane permeabilization (MOMP) (Adams and Cory, 2007; Ichim and Tait, 2016).

The intrinsic apoptotic pathway is often deregulated in cancer and is triggered by Internal stimuli in the cells, such as oxidative stress, high concentrations of cytosolic  $Ca^{2+}$ , hypoxia, irreparable DNA damage, and endoplasmic reticulum (ER) stress. These internal stimuli induced dysfunction of mitochondria, including the mitochondrial membrane potential (MMP), and change the inner mitochondrial membrane and mitochondrial permeability, as well as formation of pore in the mitochondrial membrane (Kroemer et al., 2007). This pathway is regulated by the Bcl-2 proteins family. There are three groups of the Bcl-2 proteins, named the pro-apoptotic Bcl-2 homology domain 3 (BH3)-only protein (p53 upregulated modulator of apoptosis (PUMA), BID, and Bim), the pro-apoptotic effector proteins (Bax, Bak, Bad, Bcl-Xs, Bid, Bik, and Hrk), and the anti-apoptotic proteins (Bcl-2, Bcl-XL, Bcl-W, Bfl-1, and Mcl-1) (Czabotar et al., 2014). The anti-apoptotic proteins regulate apoptotic pathway via blocking activation of pro-apoptotic effector proteins, tBID and BH3-only protein, which block the mitochondrial release of cytochrome c (Llambi et al., 2011). In contrast, in the cell stresses, the internal lethal stimuli activate the pro-apoptotic protein (BH3)-only protein, which leads to activation of pro-apoptotic proteins such as Bax and Bak. These trigger mitochondrial outer membrane permeabilization (MOMP) to release cytochrome c and apoptosis-inducing factors (AIF) into the cytoplasm (Wang et al., 2005). Following this, mitochondrial intermembrane space proteins, such as second

mitochondria-derived activator of caspases (SMAC), Omi/HtrA2, and endonuclease G are also released into the cytoplasm (Kim et al., 2006). Cytochrome *c* interacts and activates apoptotic protease activating factor 1 (APAF1) and pro-caspase-9 to form the apoptosome, which induces and activates caspase-9. Then, active caspase-9 form can activate the effector caspases (caspase-3 and caspase-7), then leading to apoptosis. On the other hand, SMAC promotes activation of caspase by blocking the caspase inhibitor X-linked inhibitor of apoptosis protein (XIAP), which leads to disruption of the interaction of XIAP with the effector caspases (caspase-3 and caspase-7) and caspase-9 (Figure 2.17) (Adams and Cory, 2007; Ichim and Tait, 2016).

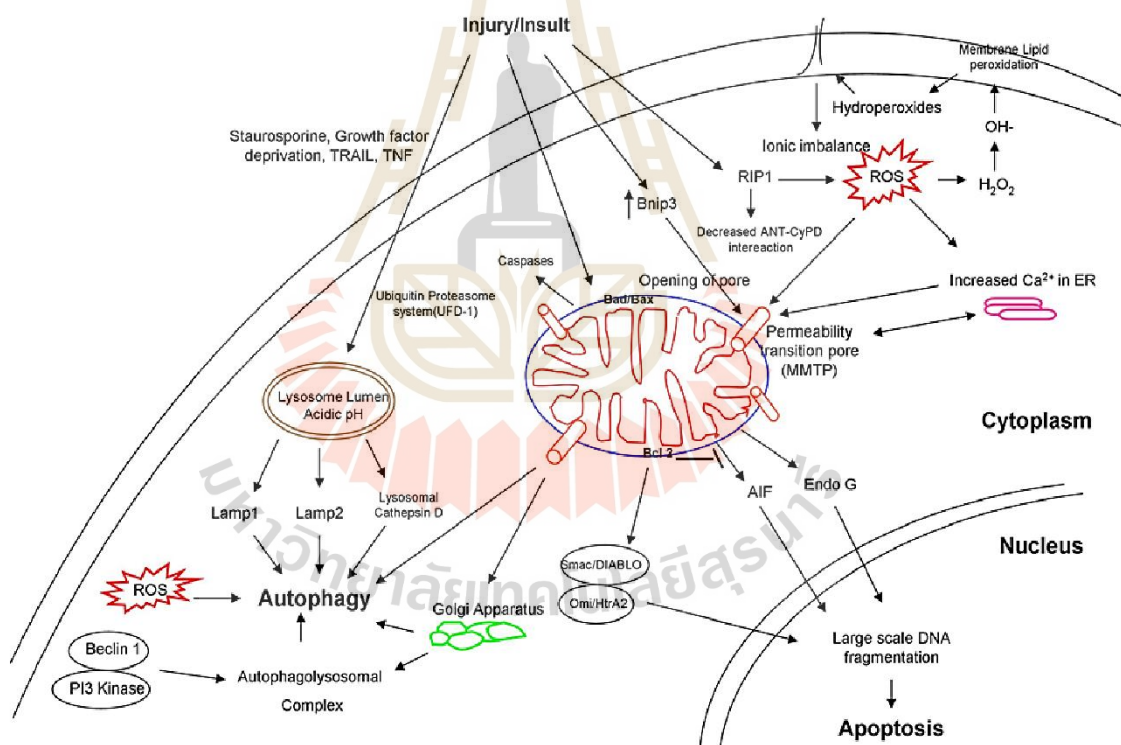


**Figure 2.17** The caspase-independent apoptosis mechanism (Bae et al., 2008)

The caspase-independent apoptosis mechanism involves the mitochondria, lysosome, and endoplasmic reticulum (ER) (Figure 2.17). As with the caspase-dependent apoptosis, mitochondria are a key regulator, and pro-apoptotic proteins, such as Bax and Bak, translocate to the mitochondria from the cytoplasm in a process

caused by activation of cathepsins. These are proteins that are released by lysosomes when triggered by ER stress through activating influx of  $\text{Ca}^{2+}$  into the cytoplasm (Martínez-Torres et al., 2018). Furthermore, cathepsin activity causes the cleavage of AIF to form truncated AIF (tAIF), after which tAIF is translocated into the nucleus, and together with endonuclease G and Omi/HtrA2 triggers condensation of chromatin and DNA fragmentation to induce apoptosis (Bhadra, 2022; Chipuk and Green, 2005). On the other hand, dysfunction of mitochondria also induces ROS production, which can mediate activation of poly (ADP-ribose) polymerase-1 (PARP-1). PARP-1 is required for releasing AIF to cytoplasm from mitochondria, meaning that ROS production is also involved in caspase-independent apoptosis (Kang et al., 2004).

### 2.6.3 Apoptosis detection

Apoptosis detection can be performed by morphological observation and several assays of apoptotic cell death that analyze either biochemical or morphological changes, including detecting the phosphatidylserine and release of cytochrome c by flow cytometry, observing nuclear morphology change by Hoechst staining or DAPI staining, analyzing fragmentation of DNA by its ladder pattern with gel electrophoresis, and caspase enzyme activation by western blot. Commonly, detecting the phosphatidylserine was performed by Annexin V/PI staining, since phosphatidylserine, a phospholipid, was found in the extracellular side of the plasma membrane of apoptotic cells and can be detected by Annexin V staining. A previous study reported that a technique using Fourier-transform infrared spectroscopy (FTIR) can also be applied to detect apoptotic and necrotic cell death in human leukemia U937 and CCRF-CEM cells (Zelig et al., 2009).

## 2.7 Endoplasmic reticulum stress and unfolded protein response

The endoplasmic reticulum (ER) has many functions in cells, such as playing a role in protein synthesis, post-translational modification and protein folding, and balancing concentrations in homeostasis. The ER also plays an important role in cell death, since it is a cellular sensor of stress and can induce releasing of pro-apoptotic

proteins in the apoptotic pathway, particularly in caspase-independent apoptosis (Mathiasen et al., 2002). Alteration of ER integrity and misfolded protein caused by extensively damaged ER, lead to ER stress that can initiate PCD through the unfolded protein response (UPR) signaling pathway or respiratory chain dysfunction or release of calcium into the cytoplasm (Mehmet, 2000; Wang et al., 2001).

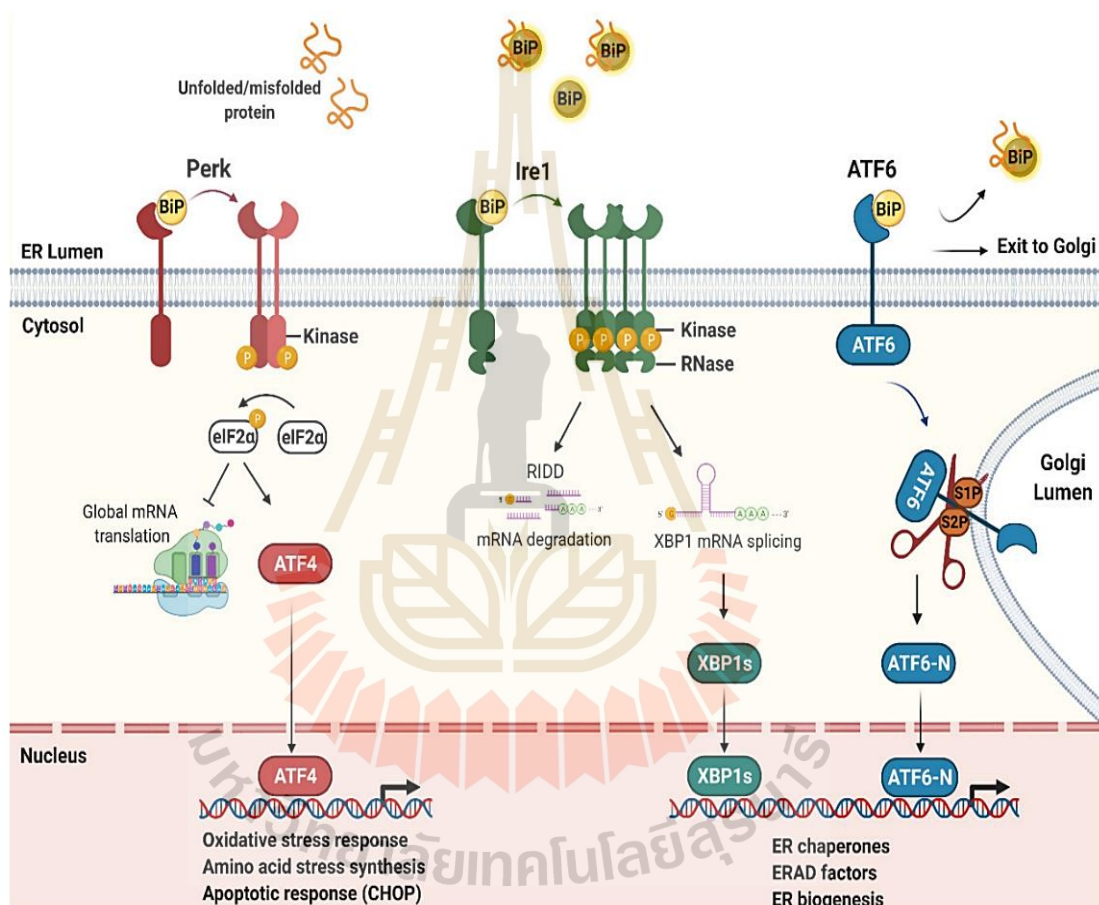


**Figure 2.18** The ER stress and unfolded protein response (UPR) signaling pathway (Alshareef et al., 2021).

The unfolded protein response (UPR) is an intracellular signaling cascade initiated by misfolded protein in the ER lumen (Figure 2.18). There are three major UPR signaling pathways that can be activated by protein regulators in the ER membrane, including activating transcription factor-6 (ATF6), inositol-requiring 1 $\alpha$  (IRE1), and protein kinase RNA-like ER kinase (PERK) (Bhattarai et al., 2020; Hetz, 2012; Hetz et al., 2020). During

ER stress, the unfolded or misfolded protein activate binding of BiP/GRP78 (major ER chaperone/glucose-regulated protein with size 78 kDa) dissociation from three ER transmembrane-associated sensors in the ER membrane, including PERK, IRE1, and ATF6, which allows these protein sensors to initiate downstream signaling (Alshareef et al., 2021; Bhattarai et al., 2020; Wodrich et al., 2022). The three UPR signaling pathways can be activated simultaneously, but others can be selectively activated or suppressed.

PERK is a kinase that activates phosphorylation of the eukaryotic translation initiation factor-2 $\alpha$  (eIF2 $\alpha$ ) to attenuate mRNA translation in the cytoplasm so as to reduce ER protein overload, but phosphorylated eIF2 $\alpha$  increases mRNA translation of activating transcription factor-4 (ATF4) through upstream open reading frames (uORFs) in its 5' untranslated region (UTR). ATF4 then activates transcription of pro-apoptotic CCAAT/enhancer-binding protein (C/EBP) homologous protein (CHOP). In comparison, IRE1 is the most conserved signal transducer and a bi-functional kinase/endoribonuclease (RNase), which acts to cleaves X-box binding protein-1 (XBP1) mRNA through autophosphorylation of IRE1 in the cytoplasm and generates spliced X-box binding protein 1 (sXBP1) mRNA, a strong active transcription factor. The sXBP1 mRNA translocates to the nucleus, then induces up-regulated transcription of ER chaperone genes and ER-associated degradation (ERAD) factors.

IRE1 also undergoes a process, called regulated IRE1-dependent degradation (RIDD) to degrade other ER-targeted mRNAs (Alshareef et al., 2021). IRE1 has been reported to interact with tumor necrosis factor (TNF) receptor-associated factor-2 (TRAF2) and activate apoptosis signal-regulating kinase 1 (ASK1), which leads it to activate c-Jun N-terminal kinase (JNK), a protein kinases family that plays an important role in stress signaling pathway related to gene expression, to promote apoptosis (Bhattarai et al., 2020). On the other hand, ATF6 translocates to the Golgi membrane from the ER membrane and is cleaved by site-1 proteases (S1P) and site-2 proteases (S2P) to generate its N-terminal transcription factor domain (ATF6-N). Then, ATF6-N translocates to the nucleus and together with or without sXBP1 mRNA acts to upregulates transcription of ER stress-responsive genes, such as ER chaperone genes

and ER-associated degradation (ERAD) factors (Alshareef et al., 2021; Bhattarai et al., 2020).

## 2.8 Cell cycle

In eukaryotic organisms, cell cycle is a series of fundamental biological processes to initiate cell division, which plays a crucial role in progression and proliferation of cells. In general, cell cycle can be divided into two periods, interphase and mitosis (M phase). Interphase is a longest period than mitosis phase, which comprised of three main phases, including G1 phase (cells grow up and become larger), S phase (DNA synthesis), and G2 phase (completion of DNA replication and prepare for mitosis) with various cell cycle checkpoints to ensure the critical processes for each phase are engaged prior to the next phase, such as G1/S checkpoint (restriction point), G2/M checkpoint (DNA damage checkpoint), and spindle assembly checkpoint (SAC) (Barnum and O'Connell, 2014; Gao et al., 2020; Wang, 2021). While, M phase can be divided into prophase, prometaphase, metaphase, anaphase, and telophase, then followed by cytokinesis. The proper completion of each phase in cell cycle is very important for further cell cycle progression. A cell can decide to grow or enter to G0 phase, a phase of quiescence (Leal-Esteban and Fajas, 2020; Wang, 2021). A cell can also grow through G1 phase from the preceding M phase directly or from G0 phase, which need mitogenic signals, such as epidermal growth factor (EGF) and platelet-derived growth factor (PDGF) to activate signal transduction pathways (Limas and Cook, 2019; Wang, 2021).

In cell cycle (Figure 2.19), cyclin-dependent kinases (CDKs) and their regulatory cyclin subunits (Cyc), CDK inhibitors (CKI), and retinoblastoma protein (pRb), are crucial components to control and regulate cell cycle progression. In the transition of each phase, the regulatory cyclin can bind to their specific CDKs and activate it to form active heterodimeric complexes and leading to cell cycle progression. In contrast, the CDKs also can be inhibited by CKI thus cell cycle progression depends on switching status of CDKs, which associated with cyclin or CKIs. There are many CDKs in cell cycle, among them, CDK4/6, CDK2, and CDK1 are serine/threonine kinases

and play main roles as regulators in cell cycle progression (Lim and Kaldis, 2013). Cyclins are cell cycle regulators and having a cyclin box (100 amino acids domain that form five  $\alpha$ -helices) at N-terminal, which responsible for the binding to CDKs. When cyclin bind to the C-helix of the CDKs, generates a conformational change that allowing more interactions, which exposes the threonine at T-loop, so it can be phosphorylated and activated. There are many cyclin, including cyclin A, B, D, and E, which their expression level are fluctuate depend on synthesis and degradation, so that cyclically activating CDKs (Leal-Esteban and Fajas, 2020). While, retinoblastoma protein (pRb) is a tumor suppressor protein that negatively regulates the cell cycle progression (Figure 2.19).

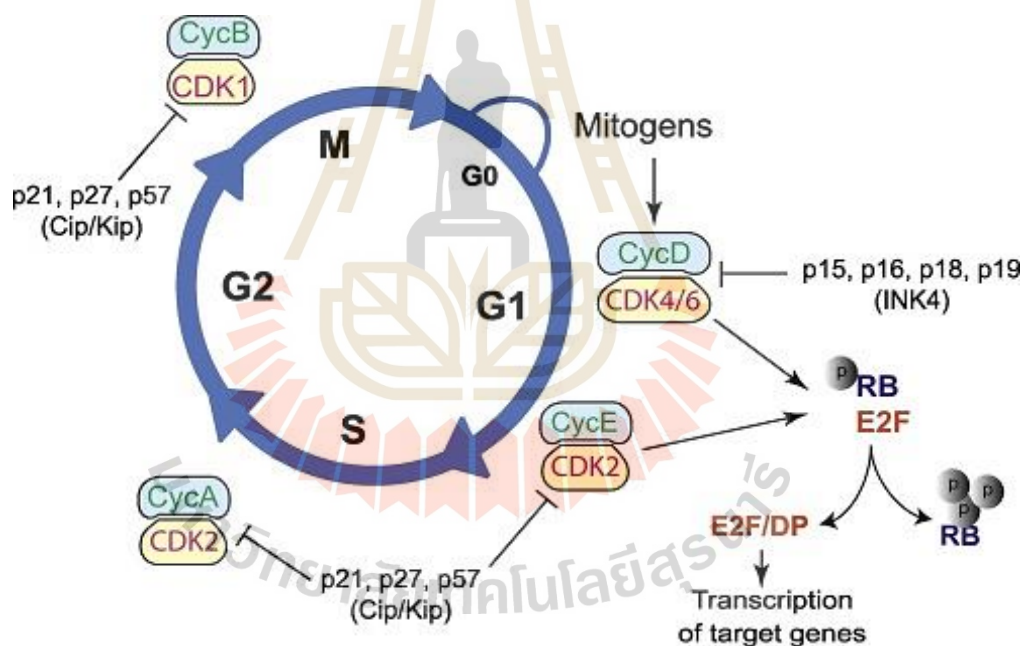


**Figure 2.19** The general schematic of cell cycle in eukaryotic cells consisting several phases, including G1, S, G2, and M phase which are controlled by cell cycle regulators (Leal-Esteban and Fajas, 2020).

Typically, in the quiescent phase (G0 phase), hypophosphorylated pRb associate with E2F transcription factors (pRb-E2F) that act to repress transcriptional activity. It means that when pRb is unphosphorylated, the E2F transcription factors are repressed by inhibiting their trans-activation domain and by recruiting histone deacetylase (HDAC)

(Leal-Esteban and Fajas, 2020). In contrast, in cell cycle progression from G<sub>0</sub>, extracellular mitogen activated mitogenic signaling that can promote the transcription and translation of cyclin D gene (*CCND*), and expression of cyclins D (D1, D2, and D3) and starting the cell cycle machinery. Cyclin D bind to their specific CDK, CDK4 or CDK6, to make CycD-CDK4/6 complex and induce the cell cycle progression during G<sub>1</sub> phase. CycD-CDK4/6 complex phosphorylates pRb at its C-terminal region and initiate an intramolecular interaction with pocket tumor suppressor protein (pRb, p107, and p103), and inhibit the binding of histone deacetylase (HDAC) resulting its pRb inactivate and disassociation from E2F transcription factors. Then, the hyperphosphorylated pRb release E2F transcription factors and initiate transcription of target genes, including cyclin E gene (*CCNE*) and cyclin A gene (*CCNA*) for S phase progression (Julian and Blais, 2015). Cyclin E can bind with CDK2 to make CycE-CDK2 complex and become active to continue hyperphosphorylated pRb, so that create a positive feedback loop and also release E2F transcription factors and their dimeric partners (DPs) to fully activate the gene expression of cyclin that guarantee cell cycle progression (Alimbetov et al., 2018; Connell-Crowley et al., 1997). After that, the subsequent phases of the cell cycle are not responsive to extrinsic factors, thus called the restriction point (G<sub>1</sub>/S checkpoint).

In the next step, at the onset of S phase, cyclin A bind and activate CDK2 to regulate S phase, which phosphorylates the proteins involved in DNA replication, and drive transition from S phase to G<sub>2</sub> phase. Finally, at the late of G<sub>2</sub> phase, Cyclin B (B1 and B2) bind and activate CDK1 to ensure the proper cell cycle progression in G<sub>2</sub> phase and enter into M phase to drive completion of mitosis by phosphorylating several proteins that participate in DNA replication, centrosome, and chromosome function and organization of structures required for cytokinesis. During the whole cell cycle, the activation and function of the different Cyc-CDKs complexes are negatively regulated by CKIs protein families, including INK4 and CDK-interacting protein/kinase inhibitory proteins (Cip/Kip). The INK4 family consist of p15 (CDKN2B), p16 (CDKN2A), p18 (CDKN2C), and p19 (CDKN2D), while the Cip/Kip protein family includes p21 (CDKN1A), p27 (CDKN1B), and p57 (CDKN1C) (Hydbring et al., 2016; Leal-Esteban and Fajas, 2020).

Cyclin D-, E-, A-, and B-dependent kinase complexes can be inhibited by the Cip/Kip protein family which it obstruct their interaction with their substrates. The expression of Cip/Kip inhibitor can be induced by different stimuli. For instance, the expression of p27 can be increased by inhibitory signals, such as transforming growth factor  $\beta$  (TGF $\beta$ ), while the expression of p21 can be increased by DNA damage (Besson et al., 2007; Sherr and Roberts, 1999).



## CHAPTER III

### MATERIALS AND METHODS

#### 3.1 General materials

##### 3.1.1 Plasmid and bacterial strain

The Os9BGlu31 cDNA was previously cloned into the pET32a(+)/DEST expression vector to produce N-terminally thioredoxin-, His<sub>6</sub>-, and S-tagged fusion proteins with enterokinase and tobacco etch virus (TEV) protease cleavage sites between the N-terminal fusion tag and tag free protein (mature Os9BGlu31) (Tran et al., 2019). This construct was transformed into *Escherichia coli* strain Origami™ B(DE3) competent cells for recombinant protein expression. Several Os9BGlu31 mutant variants, including W243H, W243L, and W243N from previous work were used to optimize the production of phenolic acid glucosyl esters (Komvongsa et al., 2015a; Tran et al., 2019).

##### 3.1.2 Human cell lines

Several human cell lines were used to perform experiments, including three human cholangiocarcinoma (CCA) cell lines, such as KKU-213A, KKU-055, and KKU-100, which were previously isolated from patients with CCA and liver fluke infection admitted to Srinagarind Hospital, Khon Kaen University, Khon Kaen province, Thailand, and IMR-90, a normal human fibroblast cell line. All CCA cell lines have been characterized at the Liver Fluke and Cholangiocarcinoma Research Center, Khon Kaen University, Khon Kaen, Thailand, and authenticated, then the certificates were obtained from the Japanese Collection of Research Bioresources Cell Bank (Sripa et al., 2005, 2020). IMR-90 cell line was purchased from the American Type Culture Collection (Manassas, VA, USA).

##### 3.1.3 Oligonucleotide primers

Several oligonucleotide primers were used for quantitative RT-PCR, including cell

cycle regulator gene primers and ER-stress related gene primers as shown in Table 3.1.

**Table 3.1** List of primer names and sequences for quantitative RT-PCR.

Primers	Forward primer 5'-3'	Reverse primer 5'-3'
<i>CCNE1</i>	5'-GAAATGGCCAAAATCGACAG-3'	5'-TCTTTGTCAGGTGTGGGGA-3'
<i>CCNB1</i>	5'-GACAACCTTGAGGAAGAGCAAGC-3'	5'-ATGGTCTCCTGCAACAACCT-3'
<i>CDKNB1</i>	5'-TGGAGAAGCACTGCAGAGAC-3'	5'-GCGTGTCCCTCAGAGTTAGCC-3'
<i>CCND1</i>	5'-AACTACCTGGACCGCTTCCT-3'	5'-CCACTTGAGCTTGTTCCACCA-3'
<i>ATF4</i>	5'-TCAAACCTCATGGGTTCTCC-3'	5'-GTGTCATCCAACGTGGTCAG-3'
<i>ATF6</i>	5'-GAACCATTGCTTTACATTCTCCAC-3'	5'-CTGCTTGACTTGGTCCTTTCTACTTC-3'
<i>CHOP</i>	5'-TGAACGGCTCAAGCAGGAAATCG-3'	5'-GGATTGAGGGTCACATCATTGGCACT-3'
<i>XBP1</i>	5'-TTACGAGAGAAAATCATGGCC-3'	5'-GGGTCCAAGTTGTCCAGAATGC-3'
<i>sXBP1</i>	5'-TGCTGAGTCCGAGCAGGTG-3'	5'-TGGGTCCAAGTTGTCCAGAATGC-3'
<i>ACTB</i>	5'-GATCAGCAAGCAGGAGTATGACG-3'	5'-AAGGGTGTAAACGCAACTAAGTCATAG-3'

Description of primers:

*CCNE1* = cyclin E, *CCNB1* = cyclin B, *CDKNB1* = Cyclin-dependent kinase inhibitor 1B (p27<sup>Kip1</sup>), *CCND1* = cyclin D, *ATF4* = Activating transcription factor 4, *ATF6* = Activating transcription factor 6, *CHOP* = C/EBP homologous protein, *XBP1* = X-box binding protein, *sXBP1* = spliced X-box binding protein, *ACTB* =  $\beta$ -actin.

### 3.1.4 Chemicals, reagents, and media

Chemicals, reagents and media that were used in the experiments are shown in Table 3.2.

**Table 3.2** List of chemicals, reagents, and media used in this study.

Chemicals, reagents and media	Sources
2-mercaptoethanol	Acros Organics
Coomassie brilliant blue R250	
Triton X-100	
Imidazole	Affymetrix
2,2-diphenyl-1-picrylhydrazyl	Alfa Aesar
Ammonium persulfate	Amresco

**Table 3.2** List of chemicals, reagents, and media used in this study (Continued).

Ampicillin sodium salt	Bio Basic
HPLC grade water	
Isopropyl- $\beta$ -D-thiogalactopyranoside	
Kanamycin sulfate	
Tetracycline-HCl	
Tetramethyl ethylenediamine	
Lysozyme	
6x purple loading dye	BioLabs
5-Fluorouracil	Boryung Pharmaceutical
Acetic acid	Carlo Erba
Acetic acid glacial	
Chloroform	
Citric acid	
Cobalt (II) chloride	
Ethanol	
Ethylenediaminetetraacetic acid disodium salt	
Formic acid	
Glycerol	
Hydrochloric acid	
Isopropanol	
Methanol	
<i>n</i> -butanol	
Potassium chloride	
Potassium dihydrogen phosphate	
Sodium chloride	
Sodium dodecyl sulfate	
Tris (hydroxymethyl)-aminomethane	
DNA ladder 1 kb	Fermentas
Sodium citrate	Fluka

**Table 3.2** List of chemicals, reagents, and media used in this study (Continued).

IMAC Sepharose 6 fast flow resin	GE Healthcare
Sephadex LH-20 resin	
0.25% trypsin-EDTA	Gibco
1% Penicillin-streptomycin	
10% Fetal bovine serum	
Dulbecco's Modified Eagle Medium	
Eagle's Minimum Essential Medium	
Agar bacteriological	Himedia
Glycine	
Peptone	
Yeast extract	
Propidium Iodide	Invitrogen
TRIzol reagent	
TEV protease	Lab's stock
Acetonitrile	Labscan
Annexin V-FITC/PI Apoptosis Detection Kit	MedChem Express
1-bromo-3-chloropropane (molecular chloroform)	Merck
Disodium hydrogen phosphate	
Methanol-D4 (CD <sub>3</sub> OD)	
Silica gel 60 F254 TLC plate	
Sodium hydroxide	
Sulforhodamine B	
Trichloroacetic acid	
Acrylamide	Pacific Science
<i>bis</i> -acrylamide	
DNAse I	Thermo Fisher
H <sub>2</sub> O grade PCR	Roche Molecular system
LightCycler 480 SYBR Green I Master	

**Table 3.2** List of chemicals, reagents, and media used in this study (Continued).

Dimethyl sulfoxide	Pharmacia Biotech
4-hydroxybenzoic acid	Sigma-Aldrich
Ferulic acid	
Gallic acid	
<i>p</i> -Coumaric acid	
Phenylmethylsulfonyl fluoride	
<i>p</i> -nitrophenyl- $\beta$ -D-glucopyranoside	
<i>p</i> -nitrophenol	
Sinapic acid	
Syringic acid	Sigma-Aldrich
<i>trans</i> -Cinnamic acid	
Vanillic acid	
Agarose powder	Vivantis
Low molecular weight protein marker	
Nuclease free water	
Viva cDNA synthesis kit	
ViSafe red gel staining	

### 3.1.5 Instruments and equipment

Instruments used in the experiments include laminar air flow cabinet, fume hood, autoclave (HYSC, Korea), centrifuges (ThermoScientific), FreeZone® Console freeze dryer (LabConco), freezer, oven (JP Selecta), hot air (drying) oven (RedLINE), EcoTemp TW20 water bath (Julabo), UV light transilluminator (Anatech), Techne® Prime thermal cycler, Multiskan GO microplate reader (ThermoScientific), Incubator, compact shaking incubator (JSR, Korea), humidified incubator (containing CO<sub>2</sub>), inverted microscope (Olympus IX51), Attune™ NxT Acoustic Focusing Flow Cytometer (ThermoScientific), Nanodrop 2000 spectrophotometer (ThermoScientific), T80+ UV-Vis spectrophotometer (PG instrument), G4220 Ultra high performance liquid chromatography (UHPLC) (Agilent), Nuclear Magnetic Resonance (NMR) spectrometer

(Bruker Avance 500), CFX Opus 96 Real-time PCR system (BioRad). Equipment that were used in the experiments include glassware, petri dish, pipet tips, polypropylene tubes, centrifuge tubes, microtubes, PCR tubes, autopipettes, ice box, vortex, chromatography column packing, hot air gun, TLC tank, cell culture plates, cell culture flasks, hemocytometer, hand tally counter, low profile PCR plates, and plate seal.

## 3.2 General methods

### 3.2.1 Preparation of competent cells

Glycerol stock of *E. coli* strain Origami™ B(DE3) was streaked onto a plate of LB agar medium containing 12.5 µg/mL tetracycline and 15 µg/mL kanamycin, then incubated at 37°C for 16-18 h. After incubation, a single colony was picked and inoculated into 5 mL of LB broth medium containing the same antibiotics as above, then incubated at 37°C, 200 rpm, for 16-18 h, followed by transferring 100 µL of culture starter to 50 mL of LB broth medium containing the same antibiotics as above and incubated at 37°C, 200 rpm until the cell density reached a level that gave an optical density at 600 nm wavelength of 0.4-0.6. The cell culture was chilled on ice for 5-10 min in sterile polypropylene tubes and the cell pellets were harvested by centrifugation at 4,000 rpm, 4°C, for 10 min. The cell pellets were resuspended with 10 mL of pre-cooled 0.1 M CaCl<sub>2</sub> and incubated on ice for 20 min, followed by centrifugation at 4,000 rpm, 4°C, for 10 min. Finally, the cell pellets were resuspended with 1 mL of 0.1 M CaCl<sub>2</sub> containing 15% glycerol and incubated on ice for 1 h, then aliquoted to be 50 µL per 1.5 mL microcentrifuge tube and stored at -80°C.

### 3.2.2 Transformation of plasmid into competent cells

An aliquot of competent cells from the previous step was thawed on ice for 10 min and 1 µL of recombinant plasmid encoding Os9BGlu31 wild type or its mutants (50-100 ng) was added into the competent cell suspension for transformation and gently mixed. The cell suspension containing the recombinant plasmid was incubated on ice for 30 min and transformed by heat shocking the cells at 42°C for 45 s then quickly chilled on ice for 2-5 min. The cell suspension was mixed with 200 µL of LB

broth medium and incubated at 37°C for 1 h with shaking. Then, 100-200 µL of cell suspension was spread on LB agar medium containing 12.5 µg/mL tetracycline, 15 µg/mL kanamycin, and 50 µg/mL ampicillin and incubated at 37°C for 16-18 h.

### 3.2.3 Protein expression and purification of Os9BGlu31

The recombinant cells containing the Os9BGlu31 expression vector were picked and streaked onto a plate of LB agar medium containing the same antibiotics as in section 3.2.2 (12.5 µg/mL tetracycline, 15 µg/mL kanamycin, and 50 µg/mL ampicillin) and incubated at 37°C for 16-18 h. After that, a single colony was picked and inoculated into 50 mL of LB broth medium containing the same antibiotics, then incubated at 37°C, 200 rpm, for 16-18 h as starter. The starter (1% v/v) was inoculated into LB broth medium containing the same antibiotics for large scale protein production, then incubated at 37°C, shaking at 200 rpm until the cell density was reached an optical density of 0.4-0.6 at 600 nm wavelength. Protein expression in the cell culture was induced by adding 0.4 mM IPTG, then the culture was incubated at 20°C, 200 rpm for 18 h. The cell pellets were harvested by centrifugation at 4,000 rpm, 4°C, for 20 min and stored at -80°C to help break the cells and store until ready to use.

The cell pellets were thawed at 30°C for 30 min and resuspended by pipetting in the extraction buffer (20 mM Tris-HCl pH 8, 150 mM sodium chloride, 200 µg/mL lysozyme, 1% (v/v) Triton X-100, 1 mM PMSF, and 5 µg/mL DNase I) and incubated at room temperature for 60 min, followed by centrifugation at 12,000 rpm, 4°C, for 20 min to remove insoluble debris. The soluble extracts (crude extract of enzyme) were transferred into a new tube and kept on ice, then the protein was purified in 2 steps by immobilized metal-affinity chromatography (IMAC) Sepharose on cobalt-equilibrated resin. The resin in 20% EtOH was prepared by loading it into sterilized column packing and washed with 5 column volumes (CV) of sterilized distilled H<sub>2</sub>O. Then, 5 CV of 0.1 M CoCl<sub>2</sub> was added into the column until the resin color changed to pink. The resin was washed with 5 CV of distilled H<sub>2</sub>O, then with 5 CV of 0.3 M NaCl, then with 5 CV of distilled H<sub>2</sub>O, followed by equilibrating with 5 CV of equilibration buffer (150 mM NaCl, 20 mM Tris-HCl pH 8).

The soluble extracts were loaded into the IMAC resin column for the first round of IMAC and washed with 5 CV of equilibration buffer, followed sequentially by 5 CV each of 5 mM, 10 mM, and 20 mM in equilibration buffer and eluted with 250 mM imidazole in equilibration buffer. All purified fractions containing protein were collected and each fraction was assayed for the enzymatic activity to identify the fraction containing Os9BGlu31 by setting 140  $\mu$ L reactions consisting of 10  $\mu$ L of purified fraction samples, 5 mM *p*NPG in 50 mM citrate buffer pH 4.5. The reactions were incubated at 30°C for 30 min and stopped by adding 75  $\mu$ L of 2 M Na<sub>2</sub>CO<sub>3</sub>, then the released *p*-nitrophenol (*p*NP) was measured by a microplate reader at 405 nm (Tran et al., 2019). Then, all fractions were analyzed by SDS-PAGE to visualize the protein bands. The fractions containing Os9BGlu31 fusion protein were collected and imidazole was removed by ultrafiltration 3-4 times in 30 kDa MWCO Centricon centrifugal filter (Millipore, USA) with dilution in equilibration buffer after each round. Then, TEV protease was added into the Os9BGlu31 fusion protein to cleave and remove N-terminal fusion tag from the Os9BGlu31 fusion protein and incubated at 7°C for 16 h.

A second round of IMAC was performed as described above to remove cleaved tag and other contaminant proteins. The tag free Os9BGlu31 protein in the flow-through and wash fractions was pooled and concentrated by ultrafiltration, as described above and protein absorbance was measured by Nanodrop 2000 spectrophotometer at 280 nm. Then, the protein concentration was calculated with the extinction coefficient for each enzyme which was obtained from protein parameter program on the EXPASY ([www.expasy.org](http://www.expasy.org)), followed by analysis of protein purity using SDS-PAGE analysis. The extinction coefficient used for Os9BGlu31 wild type is 1.72 and its mutant variants are 1.63. Finally, the pure protein was aliquoted into 1.5 mL microcentrifuge tube and stored at -80°C.

#### **3.2.4 Protein analysis by SDS-PAGE**

The protein profile in the fractions were analyzed by SDS-PAGE on 12% polyacrylamide separating gels with 5% stacking gels. The protein samples were

prepared by mixing protein samples with 6x loading dye (50 mM Tris-HCl pH 6.8, 10% (w/v) SDS, 50% (v/v) glycerol, 0.2 mg/mL bromophenol blue, 20% (v/v) 2-mercaptoethanol) at a 5:1 ratio in microtube and boiled at 100°C for 5 min to denature the protein, then loaded into wells in the gel and electrophoresed in 1x running electrode buffer (25 mM Tris base, 192 mM glycine, 0.1% (w/v) SDS, pH 8.3) with a constant voltage 140 volts, 400 mA, for 60 min or until the dye front neared the bottom of the gel. The gels were put into a tank containing a staining solution (0.1% (w/v) Coomassie brilliant blue R-250, 40% (v/v) MeOH, and 10% (v/v) acetic acid). The staining step was performed for 1 h and it was replaced with de-staining solution (40% (v/v) EtOH and 10% (v/v) acetic acid) for 1 h to remove the staining solution, then washed with water and incubated at room temperature with gentle shaking overnight. The low molecular weight protein marker was used to compare band positions and to estimate the molecular weights of protein bands.

### 3.2.5 Enzymatic assay

Enzymatic reactions and determination of enzyme activity of Os9BGlu31 and its mutant variants were assayed with or without several phenolic acids including gallic acid, syringic acid, 4-hydroxybenzoic acid, vanillic acid, ferulic acid, *trans*-cinnamic acid, sinapic acid, and *p*-coumaric acid as glucosyl acceptors by setting 150 µL of enzymatic reactions consisting of 0.25 mM glucosyl acceptors, 1 µg of Os9BGlu31 wild type or its mutant variants, 5 mM *p*NPG as glucosyl donor in 50 mM citrate buffer pH 4.5. The enzymatic reactions were incubated at 30°C for 30 min and stopped by adding 75 µL 2 M Na<sub>2</sub>CO<sub>3</sub> to alkalize the enzymatic reaction and produce yellow color from nitrophenol, then the released *p*-nitrophenol (*p*NP) was measured by a microplate reader at 405 nm. In these experiments, reactions without enzymes were used as blanks. All measurements were performed in triplicate.

### 3.2.6 Detection and identification of transglucosylation products

#### 3.2.6.1 Transglycosylation reactions

The transglycosylation reactions were performed with 0.25 mM phenolic acids

(gallic acid, syringic acid, 4-hydroxybenzoic acid, vanillic acid, ferulic acid, *trans*-cinnamic acid, sinapic acid, and *p*-coumaric acid) as glucosyl acceptors, 5 mM *p*NPG as glucosyl donor, and 1 µg of Os9BGlu31 wild type or its mutant variants in 50 mM citrate buffer pH 4.5. The enzymatic reactions were incubated at 30°C for 2 h and stopped by adding 1% (v/v) formic acid, then the transglucosylation products were analyzed by analytical chromatography, including thin layer chromatography (TLC) and ultra-high performance liquid chromatography (UHPLC).

### 3.2.6.2 Thin layer chromatography

The transglucosylation products were detected from transglycosylation reactions samples by thin layer chromatography (TLC) analysis. The samples of enzymatic reaction and standard compounds, such as glucose, *p*NPG, and glucosyl acceptors were spotted on silica gel 60 F254 TLC plates, and separated by chloroform:MeOH (8:2) and *n*-butanol:acetic acid:water (6:2:2) as the mobile phases. The plates were observed under UV light at 254 nm and stained with 10% H<sub>2</sub>SO<sub>4</sub> in EtOH, then charred at 120°C.

### 3.2.6.3 Ultra-high performance liquid chromatography

The transglucosylation products were further characterized by Ultra-High Performance Liquid Chromatography (UHPLC) on an Agilent Technologies G4220 system with a diode array detector (DAD) and separation through a ZORBAX RRHD SB C18 column (pore size 1.8 µm, length 2.1×150 mm) with column temperature at 40°C. The flow rate was maintained at 0.2 mL/min with injection volume 5 µL and the solvent system consisting of 0.1% formic acid in water (solvent A) and acetonitrile (solvent B). The standard compounds and samples were filtered at 0.22 µm, then eluted and separated with a gradient program of 95% A/5% B, 0-2 min; 5-50% B, 2-13 min; 50-70% B, 13-14 min; 70-100% B, 14-16 min; 100-5% B, 16-20 min; 5% B, 20-25 min. The signal was monitored by a diode array detector (DAD) at wavelength 254 nm.

### 3.2.7 Production and purification of major transglucosylation products

Scaled up production of major transglucosylation products was performed to obtain suitable amounts for structural analysis and evaluation of their activities. In this experiment, 100 mL of transglycosylation reactions consisted 2 mM phenolic acids (gallic acid, syringic acid, 4-hydroxybenzoic acid, vanillic acid, ferulic acid, *trans*-cinnamic acid, sinapic acid, and *p*-coumaric acid) as glucosyl acceptors, 5 mM *p*NPG as glucosyl donor, and 1 mg of Os9BGlu31 wild type or its mutant variants in 50 mM citrate buffer pH 4.5. The reactions were incubated at 30°C and evaporated by freeze dryer, then fractionated by Sephadex LH-20 resin column chromatography with elution in distilled H<sub>2</sub>O as mobile phase to obtain pure transglucosylation products. The major transglucosylation products were detected by TLC as described above in section 3.2.6.2, and the fractions containing a single spot of major transglucosylation products were pooled and evaporated by freeze dryer, then stored at 4°C for subsequent analysis.

### 3.2.8 Structural analysis of major transglucosylation products

At least 4 mg of major transglucosylation products were dissolved in 600 µL of deuterated methanol (CD<sub>3</sub>OD) in NMR tube and analyzed by <sup>1</sup>H-NMR and <sup>13</sup>C-NMR spectrometer. The <sup>1</sup>H-NMR spectra were recorded at 500 MHz and <sup>13</sup>C-NMR spectra at 125 MHz on a Bruker Avance III 500 MHz instrument with a Cryoprobe Prodigy and chemical shifts are given in parts per million and coupling constants in hertz. All spectra were analyzed by MestReNova software (Mestrelab Research). This analysis was used to verify the structure and purity of the major transglucosylation products.

### 3.2.9 Evaluation of antioxidant activity

Since the major transglucosylation products were verified as phenolic acid glucosyl esters, the activity of phenolic acid glucosyl esters were further evaluated for antioxidant activity by the 2,2-diphenyl-1-picryl-hydrazil (DPPH) radical scavenging assay. This assay was used in order to measure the free radical scavenging activity of the compounds (Brand-Williams et al., 1995; Zhang et al., 2019). Ascorbic acid, which

served as a positive control, and phenolic acid glucosyl esters were dissolved in EtOH. The reactions were prepared by mixing 180  $\mu\text{L}$  of 0.1 mM DPPH solution in EtOH with 20  $\mu\text{L}$  of samples, including various concentrations of phenolic acid glucosyl esters (0.5, 1, 2, 4, 8, 16, 32, 64, 128, 256  $\mu\text{g}/\text{mL}$ ), 20  $\mu\text{L}$  of ascorbic acid at the same concentrations, and 20  $\mu\text{L}$  of EtOH as negative control in 96-well plates. The reactions were incubated in a dark room at 30°C, shaking at 200 rpm for 30 min, then the absorbance was measured at 517 nm by a microplate reader. All measurements were performed in triplicate. The half-maximal inhibitory concentration ( $\text{IC}_{50}$ ) values of phenolic acid glucosyl esters were calculated by GraphPad Prism software version 8.0 (GraphPad Software, Inc). The radical scavenging activity was calculated by the formula: DPPH radical scavenging activity (%) = 
$$\frac{[(\text{absorbance of control} - \text{absorbance of sample}) / (\text{absorbance of control})] \times 100\%}{}$$

### 3.2.10 Mammalian cell culture

The CCA cells were cultured in Dulbecco's Modified Eagle's Medium (DMEM), while the IMR-90 cells were cultured in Eagle's Minimum Essential Medium (EMEM). All media were supplemented with 1% penicillin/streptomycin and 10% Fetal Bovine Serum (FBS). The cells were incubated at 37°C in a humidified incubator containing 5%  $\text{CO}_2$  until 70-80% confluence and detached by digestion with 0.25% trypsin-EDTA, then sub-cultured in the same media. Some of cells were kept in freezing medium containing DMEM:FBS:DMSO (4:5:1) and stored at -80°C as stock of cells for further experiments. Mycoplasma contamination was detected by PCR detection according to Uphoff (Uphoff et al., 2012).

### 3.2.11 Evaluation and screening of anti-proliferative activity

The anti-proliferative activity of phenolic acid glucosyl esters were evaluated and screened by a sulforhodamine B (SRB) assay in CCA cells (Talabnin et al., 2020). The SRB assay has ability to determine cell density based on the cellular protein content (Thongsom et al., 2017; Vichai and Kirtikara, 2006). In this experiment, evaluation and screening of anti-proliferative activity of phenolic acid glucosyl esters were performed

in KKU-213A since it is known has high aggressiveness and fast growth. The cells were seeded at  $7 \times 10^3$  cells/well in 96-well plates in complete medium and incubated at  $37^\circ\text{C}$  for overnight, then cultured in medium-supplemented with or without various concentrations of phenolic acid glucosyl esters (0, 1, 10, 100, 1000  $\mu\text{M}$ ), followed by incubation at  $37^\circ\text{C}$  for 24 h. The adherent cells were fixed by addition 100  $\mu\text{L}$  of 10% (v/v) trichloroacetic acid (TCA) and incubation at  $4^\circ\text{C}$  for overnight, then washed with 200  $\mu\text{L}$  of distilled water 5 times. The cells were stained with 100  $\mu\text{L}$  of 0.4% (w/v) SRB solution in 1% (v/v) acetic acid and incubated in a dark room at room temperature for 30 min, then washed with 200  $\mu\text{L}$  of 1% (v/v) acetic acid 5 times and dried at  $37^\circ\text{C}$ . The protein-bound dye was solubilized by adding 100  $\mu\text{L}$  of 10 mM Tris solution pH 10 for 20 min on a shaker, then the absorbance was measured in a microplate reader at 564 nm. The experiments were performed in three independent replications. The cell viability was calculated by the formula:

$$\text{Cell viability (\%)} = (\text{absorbance of treatment/absorbance of control}) \times 100\%$$

### 3.2.12 Anti-proliferative activity of $\beta$ -glucogallin

Based on the screening of anti-proliferative activity results, one of phenolic acid glucosyl esters which had highest anti-proliferative activity was selected and used for further experiments to investigate the anti-proliferative effect of the selected-phenolic acid glucosyl ester (gallic acid glucosyl ester or  $\beta$ -glucogallin) in three human CCA cells, including KKU-213A, KKU-055, and KKU-100, as well as IMR-90 normal human fibroblast cell line. The CCA cells and normal human cells were seeded at  $7 \times 10^3$  cells/well in 96-well plates and incubated at  $37^\circ\text{C}$  for overnight, then cultured in medium-supplemented with or without various concentrations of  $\beta$ -glucogallin (0-200  $\mu\text{M}$ ), and incubated at  $37^\circ\text{C}$  for 24, 48, and 72 h. The anti-proliferative activity of  $\beta$ -glucogallin was determined by a sulforhodamine B (SRB) assay as described above in section 3.2.11. The experiments were performed in three independent replications and morphological change of the cells were observed under an inverted microscope (Olympus IX51). The half-maximal inhibitory concentration ( $\text{IC}_{50}$ ) values of  $\beta$ -glucogallin were calculated by GrapPad Prism software version 8.0 (GraphPad Software, Inc).

### 3.2.13 Evaluation of anti-migration activity of $\beta$ -glucogallin

Anti-migration activity was evaluated by a wound healing assay. The CCA cells were seeded at  $3 \times 10^5$  cells/well in 24-well plates and incubated at  $37^\circ\text{C}$  for overnight to make a monolayer. The monolayer of cells was scratched with a sterile 200  $\mu\text{L}$  pipette tip on the middle area of each well to create a linear wound. The cells were washed with 1X PBS and cultured in serum free medium-supplemented with or without  $\beta$ -glucogallin, then incubated at  $37^\circ\text{C}$ . The wound closure or migration of CCA cells into the wound area was observed and photographed at 0, 6, 12, 24, 48, and 72 h under a light microscope, then analyzed by ImageJ software to evaluate the degree of wound healing. The experiments were performed in three independent replications. The wound healing was calculated by the formula:

Wound healing =

(area of original wound – area of wound during healing)/area of original wound.

### 3.2.14 Colony formation assay

KKU-213A and KKU-055 were selected for further experiments, including colony formation assay to visualize the colonies of cells for survival and proliferative activities. The cells were seeded at  $2 \times 10^3$  cells/well in 6-well plates and incubated at  $37^\circ\text{C}$  for overnight, then washed with 1X PBS and cultured in medium-supplemented with or without  $\beta$ -glucogallin. After that, the medium was discarded and replaced with fresh medium, then followed by incubation at  $37^\circ\text{C}$  for 14 days. The SRB assay as described above in section 3.2.11 was used in this experiment. After SRB staining, the colonies of cells were captured by camera and the protein-bound dye was solubilized by adding 100  $\mu\text{L}$  of 10 mM Tris solution pH 10 for 20 min on a shaker, then the absorbance was measured in a microplate reader at 564 nm to visualize colony formation. The experiments were performed in three independent replications.

### 3.2.15 Cell apoptosis analysis

Cell apoptosis analysis was performed to investigate the apoptotic cells after CCA cells were treated with  $\beta$ -glucogallin. The CCA cells were seeded at  $4 \times 10^5$

cells/well in 6-well plates and incubated at 37°C for overnight, then washed with 1X PBS and cultured in serum free medium-supplemented with or without  $\beta$ -glucogallin, followed by incubation at 37°C for 24 h. The cell culture medium containing floating cells were collected and adherent cells were detached by digestion with 0.25% trypsin-EDTA. Both of floating cells and adherent cells were mixed and harvested by centrifugation at 1,300 rpm, 4°C for 5 min, then cells were washed once with 1X PBS and centrifuged at 1,300 rpm, 4°C for 5 min. The cells were stained with Annexin V-FITC/PI apoptosis detection kit following the manufacturer's protocol for cell apoptosis analysis. The cells were mixed with 1 mL of pre-cooled 1X PBS and homogenized by pipetting to make a single cell suspension, then centrifuged at 1,300 rpm, 4°C for 3 min and supernatant was discarded. The cells were resuspended in 195  $\mu$ L of binding buffer and stained with 5  $\mu$ L of Annexin V-FITC, then mixed with 10  $\mu$ L of propidium iodide (PI), followed by incubation at room temperature for 10-20 min in a dark area. The apoptotic cells were detected by Attune™ NxT Acoustic Focusing Flow Cytometer and the data was analyzed by Attune™ NxT Software. The experiments were performed in three independent replications.

### 3.2.16 Cell cycle analysis

Cell cycle analysis was performed to investigate inhibition mechanism of CCA proliferation by  $\beta$ -glucogallin via cell cycle arrest. The CCA cells were seeded at  $4 \times 10^5$  cells/well in 6-well plates and incubated at 37°C for overnight, then washed with 1X PBS and cultured in serum free medium-supplemented with or without  $\beta$ -glucogallin, followed by incubation at 37°C for 24 h. The cell culture medium containing floating cells were collected and adherent cells were detached by digestion with 0.25% trypsin-EDTA. Both floating cells and adherent cells were mixed and harvested by centrifugation at 1,300 rpm, 4°C for 5 min, then cells were washed once with 1X PBS and centrifuged at 1,300 rpm, 4°C for 5 min, then supernatant was discarded. The cells were resuspended in 500  $\mu$ L of 1X PBS and homogenized by pipetting to make a single cell suspension, which was kept on ice. The cell suspension was mixed with 3 mL of pre-cooled sterile 70% (v/v) EtOH with shaking, followed by incubation on ice for 2 h,

then centrifuged at 1,300 rpm, 4°C for 3 min. The supernatant was discarded and washed once with 1X PBS, then centrifuged at 1,300 rpm, 4°C for 5 min. The cells were stained with 0.5 mL of propidium iodide (PI) staining solution (20 µg/mL PI, 0.1% (v/v) Triton-X 100, and RNase A (20 µg/mL)), which freshly prepared and incubated on ice for 60 min in a dark area (Naradun et al., 2022). The DNA content was detected by Attune™ NxT Acoustic Focusing Flow Cytometer and data were analyzed by Flowing Software version 2.5.1 (Cell Imaging Core, Turku Centre for Biotechnology). The experiments were performed in three independent replications.

### 3.2.17 mRNA expression analysis by qRT-PCR

The mRNA expression levels analysis of molecular marker were performed to investigate the role of  $\beta$ -glucogallin in the molecular mechanism of inhibition of CCA proliferation via cell cycle arrest and ER stress-induced cell death signaling. The CCA cells were seeded at  $4 \times 10^5$  cells/well in 6-well plates and incubated at 37°C for overnight, then washed with 1X PBS and cultured in serum free medium-supplemented with or without  $\beta$ -glucogallin, followed by incubation at 37°C for 24 h. The experiments were performed in three independent replications.

#### 3.2.17.1 RNA extraction

After incubation for 24 h, the cell culture medium was discarded and the cells washed once with 1X PBS. The adherent cells in the wells were mixed with 1 mL of TRIzol reagent for total RNA extraction and incubated at room temperature for 5 min, then homogenized by pipetting. The cell lysate was transferred into a sterile microtube and mixed with 0.2 mL of 1-bromo-3-chloropropane (BCP), then homogenized by vortex and incubated at room temperature for 3 min before centrifugation at 12,000 rpm for 15 min. The aqueous phase (upper layer) was collected in a new sterile microtube and supplemented with 0.5 mL of isopropanol, then the tube was inverted by hand several times, followed by incubation at room temperature for 10 min. The total RNA was collected by centrifugation at 12,500 rpm, 4°C for 20 min and the supernatant was discarded. Then, 1 mL of sterile 75% (v/v) EtOH was added into the

microtube, followed by centrifugation at 10,000 rpm, 4°C for 20 min, after which the supernatant was discarded. The total RNA was collected and dried at room temperature. Then, the total RNA was resuspended in 20-50 µL of nuclease free water and the RNA were stored at -80°C.

#### **3.2.17.2 Agarose gel electrophoresis**

The absorbance of the total RNA concentration was measured by Nanodrop 2000 spectrophotometer and the quality of total RNA was analyzed by agarose gel electrophoresis on 0.8% agarose gels containing fluorescent nucleic acid dye (ViSafe red gel staining, Vivantis). The ladder (1 kb DNA ladder) or RNA samples were prepared by mixing the samples with 6x purple loading dye at a 1:1 ratio and loaded into the wells of an agarose gel in a chamber containing 1X TAE buffer. Agarose gel electrophoresis was performed at a constant voltage of 100 volts for 30 min. The RNA bands were visualized under UV irradiation on a transilluminator.

#### **3.2.17.3 Reverse transcription of RNA to cDNA**

The cDNA was synthesized by a Viva cDNA synthesis kit. The RNA-primer mixtures were prepared by mixing 2 µg of total RNA and 1 µL of oligo d(T)<sub>18</sub> primer and 1 µL of dNTPs, then nuclease free water was added up to 10 µL. The mixtures were centrifuged briefly and incubated at 65°C for 5 min, then chilled on ice for 2 min. After that, the solutions were mixed with 10 µL of cDNA synthesis mix (2 µL of 10X M-MULV buffer, 0.5 µL of reverse transcriptase, and 7.5 µL of nuclease free water) and homogenized by pipetting, then incubated at 42°C for 60 min. The reactions were terminated by incubation at 85°C for 5 min, then chilled on ice for 10 min and the cDNA were stored at -20°C.

#### **3.2.17.4 Quantitative RT-PCR (qRT-PCR)**

Quantitative RT-PCR was performed to investigate the mRNA expression levels of the genes of interest with LightCycler 480 SYBR Green I Master mix and a CFX Opus 96 Real-time PCR system. The master solution per reaction was prepared by mixing 10

$\mu\text{L}$  of 2X SYBR green, 1  $\mu\text{L}$  of 10  $\mu\text{M}$  primers mix (forward and reverse) and 1  $\mu\text{L}$  of PCR grade  $\text{H}_2\text{O}$ , which was mixed with 5  $\mu\text{L}$  of 10 ng cDNA samples (total concentration 25-50 ng) in low profile PCR plates. The target genes were amplified with the primers listed in Table 3.1 by initial denaturation at 95°C for 5 min, followed by 45 cycles of denaturation at 95°C for 10 s, annealing at 55°C or 60°C for 10 s and extension at 72°C for 20 s. The annealing temperature was 55°C for *CCNB1*, *CCNE1*, *CDKNB1*, *ATF4*, *ATF6*, and *CHOP*, and 60°C for *CCND1*, *XBP1* and *sXBP1*. The gene expression values were normalized against the housekeeping gene,  $\beta$ -*actin*. Relative gene expressions were calculated by the  $2^{-\Delta\Delta\text{CT}}$  method (Livak and Schmittgen, 2001). The experiments were performed in three independent replications.

### 3.2.18 Statistical analysis

All experiments were performed in three independent replications and GraphPad Prism 8.0.1 (GraphPad software Inc) was used for statistical analysis. The significance values ( $p$  value) were calculated by one-way ANOVA and two-way ANOVA, followed by Bonferroni's test for multiple comparison datasets. The results are presented as means  $\pm$  standard deviation (SD) and  $p$  value  $< 0.05$  was accepted as a statistically significant difference which were indicated as \*  $p < 0.05$ , \*\*  $p < 0.01$ , \*\*\*  $p < 0.001$ , \*\*\*\*  $p < 0.0001$ .

## CHAPTER IV

### RESULTS AND DISCUSSION

#### 4.1 Expression and purification of Os9BGlu31 wild type and its mutant variants

The Os9BGlu31 mutant variants (W243N, W243H, and W243L) were previously produced by site-directed mutagenesis (Komvongsa et al., 2015a; Tran et al., 2019). The cDNA of Os9BGlu31 wild type and its mutant variants were cloned into pET32a(+)/DEST expression vector and expressed in *E. coli* strain Origami™ B(DE3) competent cells. The His-tagged fusion protein of Os9BGlu31 was induced by the optimum concentration of 0.4 mM IPTG and incubated at 20°C for 18 h. In initial experiments, after Os9BGlu31 fusion protein was eluted by imidazole and purified by a 1<sup>st</sup> IMAC step with Co<sup>2+</sup> equilibrated resin, the fractions contained target protein bands (Os9BGlu31 and tags fusion protein) with a size of 70 kDa and non-target protein bands based on SDS-PAGE analysis (Appendix A, Figure A.1-A.4). It means that the fractions had impurities because it still contained many contaminant protein bands. In later experiments, after the 1<sup>st</sup> IMAC step, the fusion tags were cleaved from Os9BGlu31 by TEV protease and purified by a 2<sup>nd</sup> IMAC step with Co<sup>2+</sup> equilibrated resin, which bound the tag but not cleaved Os9BGlu31. The result showed that I obtained Os9BGlu31 tag-free protein with a size of 50 kDa, which was pooled from 0-5 mM imidazole wash fractions based on SDS-PAGE analysis (Appendix A, Figure A.1-A.4). This protein was used for further experiments, including for the production of phenolic acid glucosyl esters. Therefore, I succeeded to generate Os9BGlu31 wild type and its mutant variants with protein purity apparently greater than 90% (Figure 4.1).

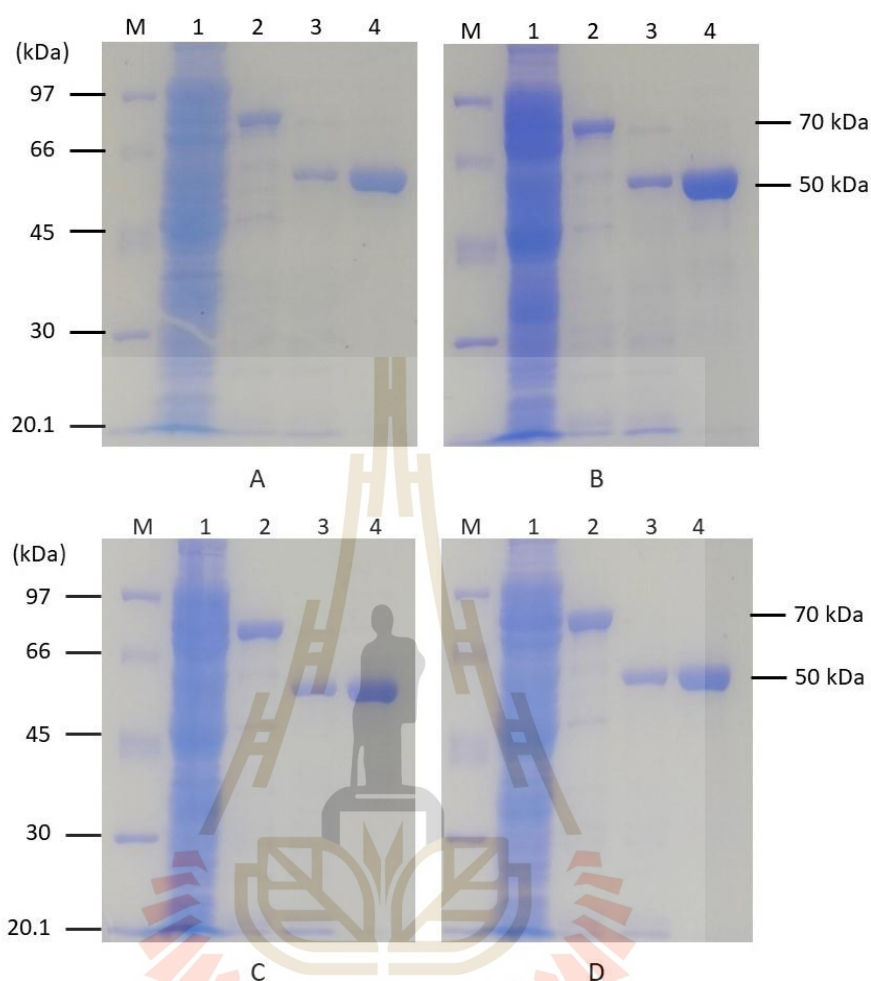


**Figure 4.1** SDS-PAGE analysis of Os9BGlu31 purification fractions. (A) Os9BGlu31 wild type, (B) Os9BGlu31 W243H, (C) Os9BGlu31 W243N, (D) Os9BGlu31 W243L. Os9BGlu31 wild type and its mutant variants were purified by IMAC Sepharose with  $\text{Co}^{2+}$  equilibrated resin. Lane M = molecular weight marker, lane 1 = soluble crude enzyme, lane 2 = Os9BGlu31 protein after it was purified by 1<sup>st</sup> IMAC, lane 3 = protein after cleavage, lane 4 = Os9BGlu31 protein after it was purified by 2<sup>nd</sup> IMAC.

## 4.2 Activity of Os9BGlu31 wild type and its mutant variants

Then, I measured the activity of Os9BGlu31 wild type and its mutant variants on several phenolic acids as substrates, including gallic acid, to investigate the effect of mutations of Os9BGlu31 on its enzyme activity. Previous study proved that active site cleft residues of Os9BGlu31 surrounding the aglycone and acceptor binding site play

an important role in the transglucosidase specificity (Komvongsa et al., 2015a; Tran et al., 2019). The mutations of tryptophan at position 243 (W243) to several amino acids increasing or decreasing the polarity and decreasing the size of amino acid side chain at the active site that can increase the transglycosylation activity and allow it to produce multiple kaempferol glycosides (Komvongsa et al., 2015a).

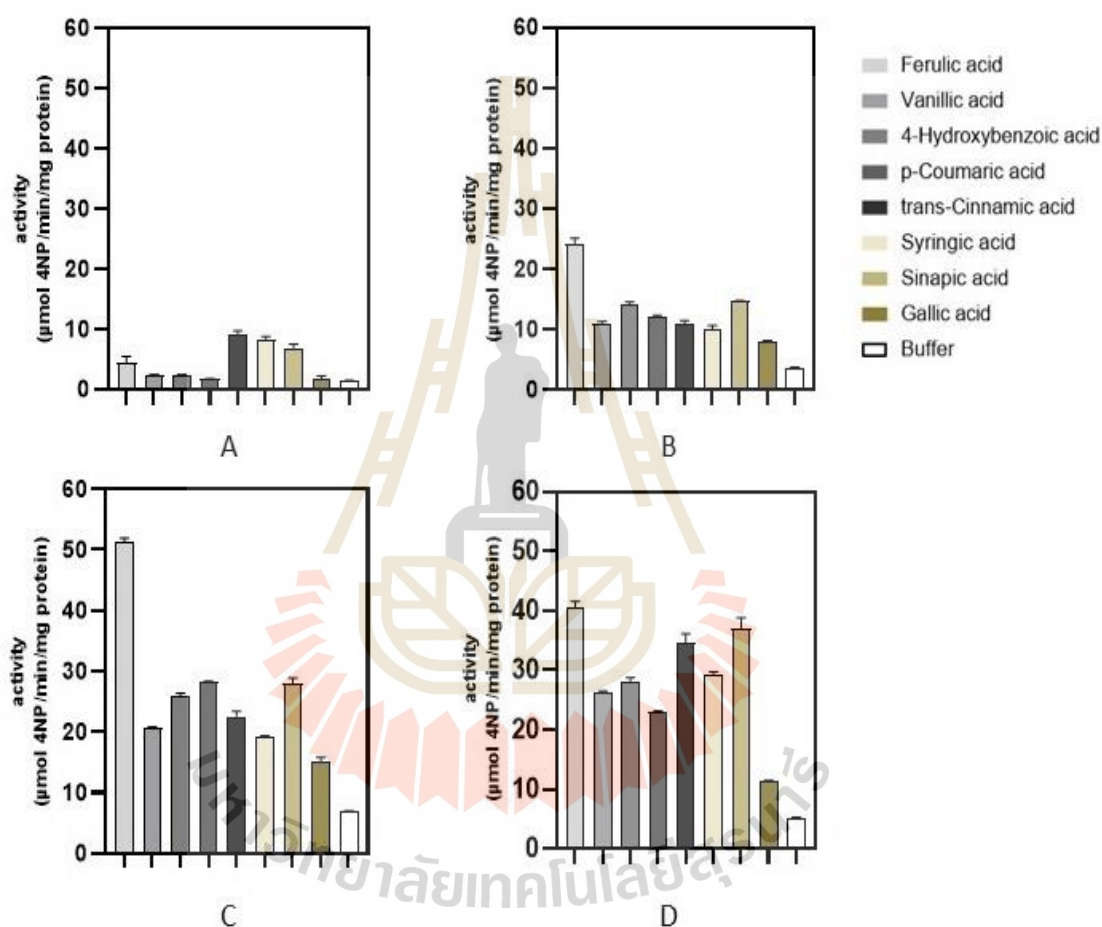


**Figure 4.2** Enzyme activity of (A) Os9BGlu31 wild type and its mutant variants, including (B) W243H, (C) W243N, and (D) W243L with various phenolic acids as glucosyl acceptors.

In this study, as shown in Figure 4.2, the enzyme activity of Os9BGlu31 wild type was lower than all mutant variants in the presence of phenolic acids in enzymatic reactions. Most of the Os9BGlu31 mutant variants showed high activity and different acceptor specificity in enzymatic reactions depending on the amino acid substituted for W243. The W243L mutant had higher activity than other mutants with vanillic acid,

4-hydroxybenzoic acid, *trans*-cinnamic acid, syringic acid, and sinapic acid. In contrast, W243N mutant had highest activity with ferulic acid, *p*-coumaric acid, and gallic acid, while W243H showed intermediate activity compared with other mutants. In the presence of phenolic acids, Os9BGlu31 wild type and its mutant variants showed different rates of *p*NP release from *p*NPG with different glucosyl acceptors specificity compared with buffer alone, and showed low activity with gallic acid compared with ferulic acid and other phenolic acids tested. However, Os9BGlu31 mutant variants had higher activity with ferulic acid compared to other phenolic acids as glucosyl acceptors. These phenomena indicated that ferulic acid is a specific substrate for these mutant enzymes, as previously noted (Komvongsa et al., 2015a; Tran et al., 2019). We hypothesized that the Os9BGlu31 mutant variants should have more hydrolysis activity than wild type due to amino acid residues were converted to more hydrophilic amino acids for water binding, but the mutants still have high transglucosylation activity to transfer glucosyl moiety to phenolic acids as glucosyl acceptors for the production of transglucosylation products. Interestingly, W243L mutant, is known more hydrophobic, also showed an increased activity with most phenolic acids, which consistent with previous result (Tran et al., 2019).

### 4.3 Transglucosylation activity and identification of products

In addition to slight hydrolysis activity, Os9BGlu31 has transglucosylation activity, which acts to transfer glucosyl moiety from glucosyl donor to the glucosyl acceptor to form glucosides (Luang et al., 2013). Here, I studied the transglucosylation activity of Os9BGlu31 wild type and its mutant variants on phenolic acids, including gallic acid as glucosyl acceptor, which was not previously reported, to produce sufficient quantities of major transglucosylation products for testing in cholangiocarcinoma cells. Os9BGlu31 acts as a transglucosidase to transfer glucosyl moiety from *p*-nitrophenyl  $\beta$ -D-glucopyranoside (*p*NPG) to carboxyl group of phenolic acids to form phenolic acid glucosyl esters, and release *p*-nitrophenol (*p*NP), which can be observed on TLC plates under UV-light and after sulfuric acid treatment and charring at 120°C as shown in Figures 4.3, 4.5, 4.7, and 4.9.

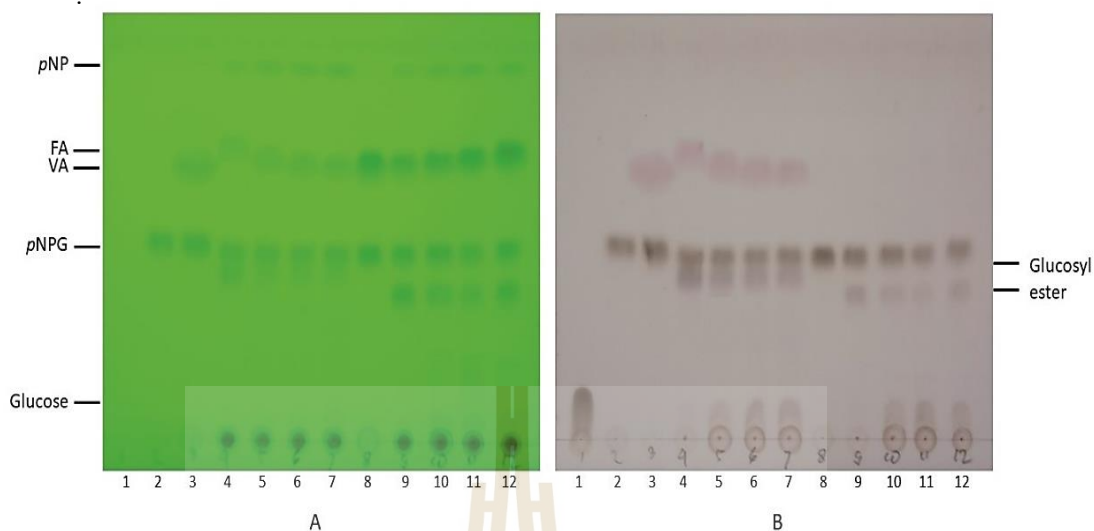


**Figure 4.3** Thin layer chromatography of transglucosylation products of enzymatic reactions catalyzed by Os9BGlu31 wild type and its mutant variants with ferulic acid (FA) and vanillic acid (VA). (A) The products were observed on a TLC plate under UV-light at 254 nm, and (B) after sulfuric acid treatment and charring at 120°C. Enzymatic reaction mixtures were separated by silica gel 60 TLC with mobile phase, chloroform:methanol (8:2, v/v). Lane 1 = glucose, lane 2 = pNPG, lane 3 = reaction with FA without Os9BGlu31, lane 4 = enzymatic reaction with FA and Os9BGlu31 wild type (WT), lane 5 = enzymatic reaction with FA and Os9BGlu31 W243H, lane 6 = enzymatic reaction with FA and Os9BGlu31 W243N, lane 7 = enzymatic reaction with FA and Os9BGlu31 W243L, lane 8 = reaction with VA without Os9BGlu31, lane 9 = enzymatic reaction with VA and Os9BGlu31 wild type (WT), lane 10 = enzymatic reaction with VA and Os9BGlu31 W243H, lane 11 = enzymatic reaction with VA and Os9BGlu31 W243N, lane 12 = enzymatic reaction with VA and Os9BGlu31 W243L.

Moreover, Os9BGlu31 mutant variants tend to produce multiple products compared with wild type, which surmised as glucosides of phenolic acids in addition to the glucosyl esters in the enzymatic reaction with phenolic acids as glucosyl acceptors, including ferulic acid and vanillic acid (Figure 4.4). According to the UHPLC results, the retention time of peaks of pNP was 12.1 min and pNPG was 8.1 min, while ferulic acid was at 10.2 min and vanillic acid was at 8.5 min. The major

transglucosylation products of ferulic acid and vanillic acid were glucosyl esters and it can be seen at 8.2 min and 6.7 min, respectively. The Os9BGlu31 mutant variants also produced glucosides of ferulic acid at 7.4 min and vanillic acid at 5.9 min, as well as bis-glucosides of ferulic acid at 6.3 min and vanillic acid at 4.7 min in some cases (Figure 4.4).

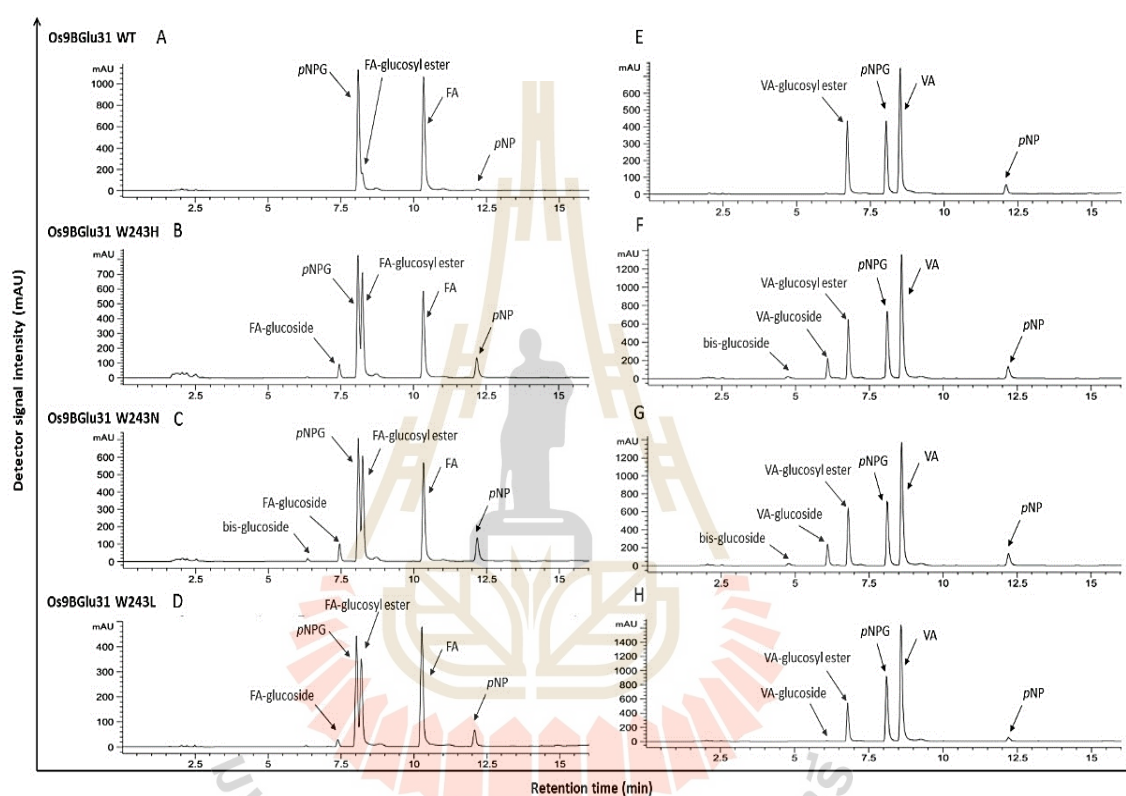


**Figure 4.4** UHPLC chromatogram profiles of transglucosylation products in the enzymatic reaction with ferulic acid (FA) and vanillic acid (VA). Transglucosylation reactions of FA are with (A) Os9BGlu31 wild type, (B) W243H mutant, (C) W243N mutant, and (D) W243L mutant. Transglucosylation reactions of VA are with (E) Os9BGlu31 wild type, (F) W243H mutant, (G) W243N mutant, and (H) W243L mutant. The major transglucosylation products were identified as phenolic acid glucosyl ester with DAD wavelength at 254 nm.

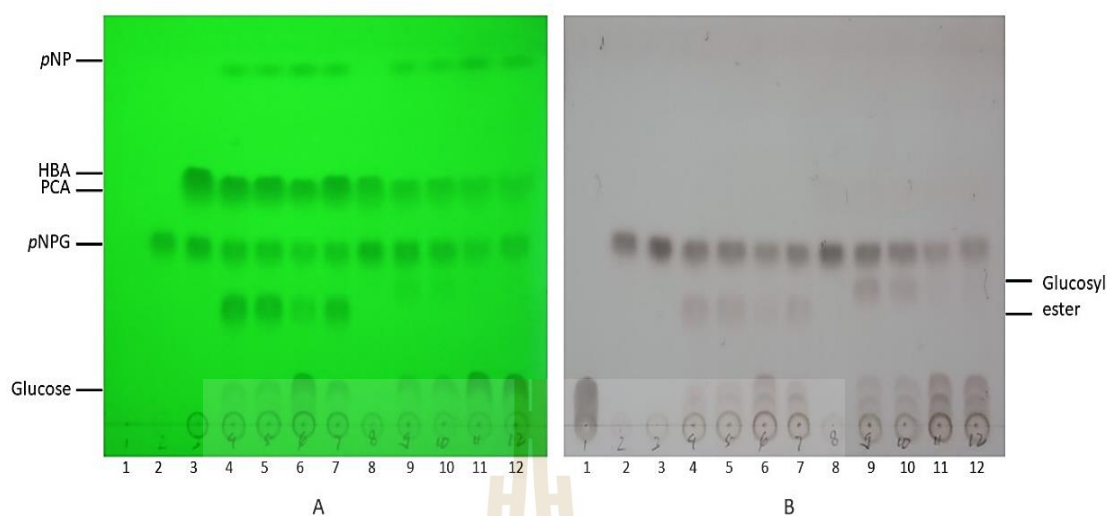


**Figure 4.5** Thin layer chromatography of transglucosylation products of enzymatic reactions catalyzed by Os9BGlu31 wild type and its mutant variants with 4-hydroxybenzoic acid (HBA) and *p*-coumaric acid (PCA). (A) The products were observed on a TLC plate under UV-light at 254 nm, and (B) after sulfuric acid treatment and charring at 120°C. Enzymatic reaction mixtures were separated by silica gel 60 TLC with mobile phase, chloroform:methanol (8:2, v/v). Lane 1 = glucose, lane 2 = *p*NPG, lane 3 = reaction with HBA without Os9BGlu31, lane 4 = enzymatic reaction with HBA and Os9BGlu31 wild type (WT), lane 5 = enzymatic reaction with HBA and Os9BGlu31 W243H, lane 6 = enzymatic reaction with HBA and Os9BGlu31 W243N, lane 7 = enzymatic reaction with HBA and Os9BGlu31 W243L, lane 8 = reaction with PCA without Os9BGlu31, lane 9 = enzymatic reaction with PCA and Os9BGlu31 wild type (WT), lane 10 = enzymatic reaction with PCA and Os9BGlu31 W243H, lane 11 = enzymatic reaction with PCA and Os9BGlu31 W243N, lane 12 = enzymatic reaction with PCA and Os9BGlu31 W243L.

The Os9BGlu31 mutant variants also produced multiple products compared with wild type on 4-hydroxybenzoic acid and *p*-coumaric acid as glucosyl acceptors. According to the UHPLC results, the retention time of peaks of 4-hydroxybenzoic acid was at 7.8 min and *p*-coumaric acid was at 9.7 min. The major transglucosylation products of 4-hydroxybenzoic acid and *p*-coumaric acid were glucosyl esters that can

be seen at 6.2 min and 7.8 min, respectively. The O9BGlu31 mutant variants also produced apparent glucosides of 4-hydroxybenzoic acid at 4.9 min and *p*-coumaric acid at 6.9 min, as well as bis-glucosides of 4-hydroxybenzoic acid at 3.3 min and *p*-coumaric acid at 5.9 min (Figure 4.6).

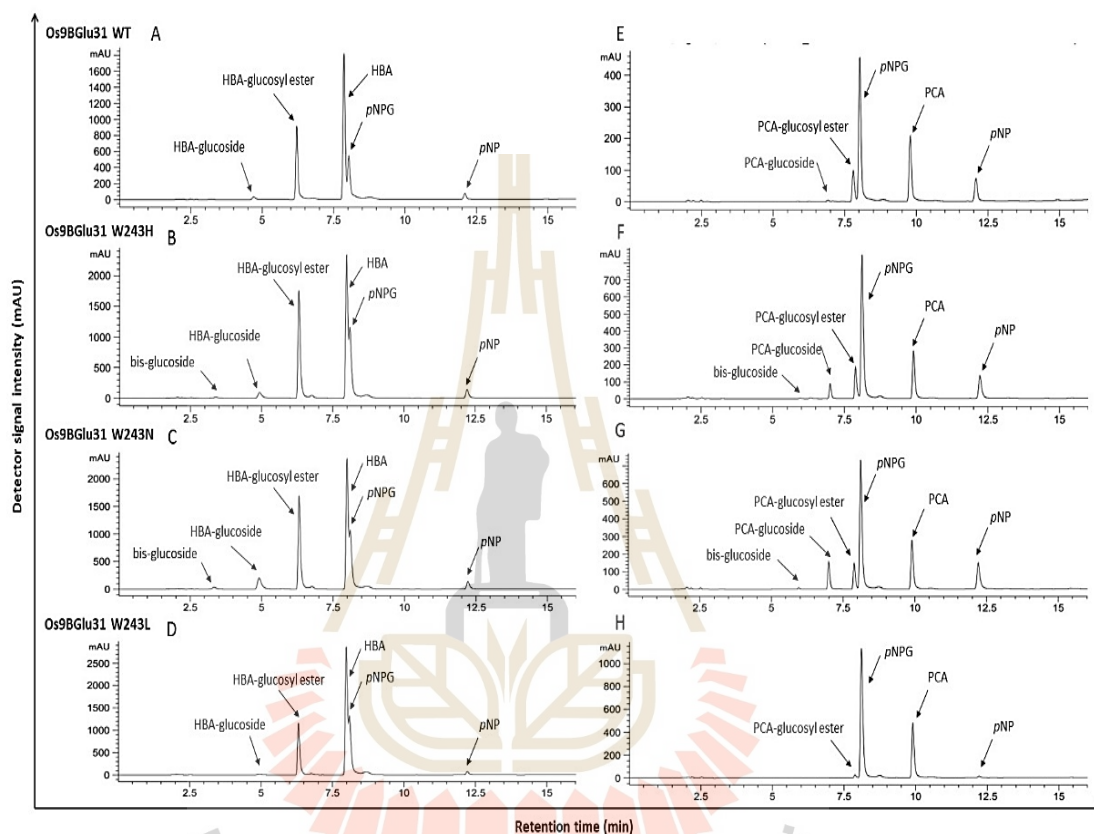


**Figure 4.6** UHPLC chromatogram profiles of transglucosylation products in the enzymatic reaction with 4-hydroxybenzoic acid (HBA) and *p*-coumaric acid (PCA). Transglucosylation reactions of HBA are with (A) Os9BGlu31 wild type, (B) W243H mutant, (C) W243N mutant, and (D) W243L mutant. Transglucosylation reactions of PCA are with (E) Os9BGlu31 wild type, (F) W243H mutant, (G) W243N mutant, and (H) W243L mutant. The major transglucosylation products were identified as phenolic acid glucosyl ester with DAD wavelength at 254 nm.

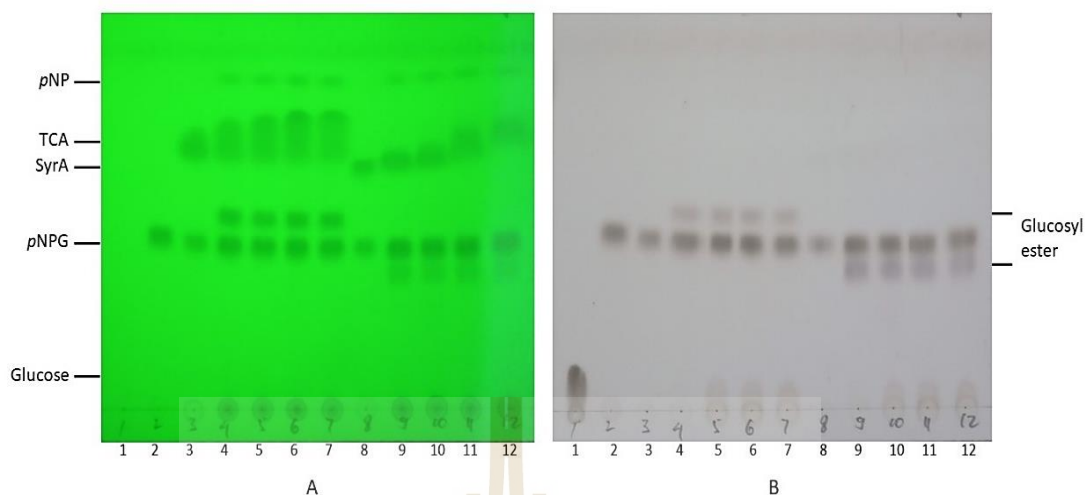


**Figure 4.7** Thin layer chromatography of transglucosylation products of enzymatic reactions catalyzed by Os9BGlu31 wild type and its mutant variants with *trans*-cinnamic acid (TCA) and syringic acid (SyrA). (A) The products were observed on a TLC plate under UV-light at 254 nm, and (B) after sulfuric acid treatment and charring at 120°C. Enzymatic reaction mixtures were separated by silica gel 60 TLC with mobile phase, chloroform:methanol (8:2, v/v). Lane 1 = glucose, lane 2 = pNPG, lane 3 = reaction with TCA without Os9BGlu31, lane 4 = enzymatic reaction with TCA and Os9BGlu31 wild type (WT), lane 5 = enzymatic reaction with TCA and Os9BGlu31 W243H, lane 6 = enzymatic reaction with TCA and Os9BGlu31 W243N, lane 7 = enzymatic reaction with TCA and Os9BGlu31 W243L, lane 8 = reaction with SyrA without Os9BGlu31, lane 9 = enzymatic reaction with SyrA and Os9BGlu31 wild type (WT), lane 10 = enzymatic reaction with SyrA and Os9BGlu31 W243H, lane 11 = enzymatic reaction with SyrA and Os9BGlu31 W243N, lane 12 = enzymatic reaction with SyrA and Os9BGlu31 W243L.

The Os9BGlu31 mutant variants tested also produced multiple products compared with wild type on syringic acid as glucosyl acceptor, while the Os9BGlu31 mutant variants produced glucosyl ester only on *trans*-cinnamic acid because it only has a carboxyl group that can act as an acceptor in its structure, thus additional products cannot be found. According to the UHPLC results, the retention time of peaks of *trans*-cinnamic acid was at 13.4 min and syringic acid was at 8.7 min. The major

transglucosylation products of *trans*-cinnamic acid and syringic acid were glucosyl esters and can be seen at 10.3 min and 7 min, respectively. Additionally, O9BGlu31 mutant variants produced apparent glucosides of syringic acid at 6.5 min and bis-glucosides at 5.5 min (Figure 4.8). Moreover, the Os9BGlu31 mutant variants tested also produced multiple products compared with wild type on sinapic acid and gallic acid as glucosyl acceptors. According to the UHPLC results, the retention time of peaks of sinapic acid was at 10.3 min and gallic acid was at 3.8 min. The major transglucosylation products of sinapic acid and gallic acid included their glucosyl esters that eluted at 8.3 min and 2.8 min, respectively (Figure 4.10).

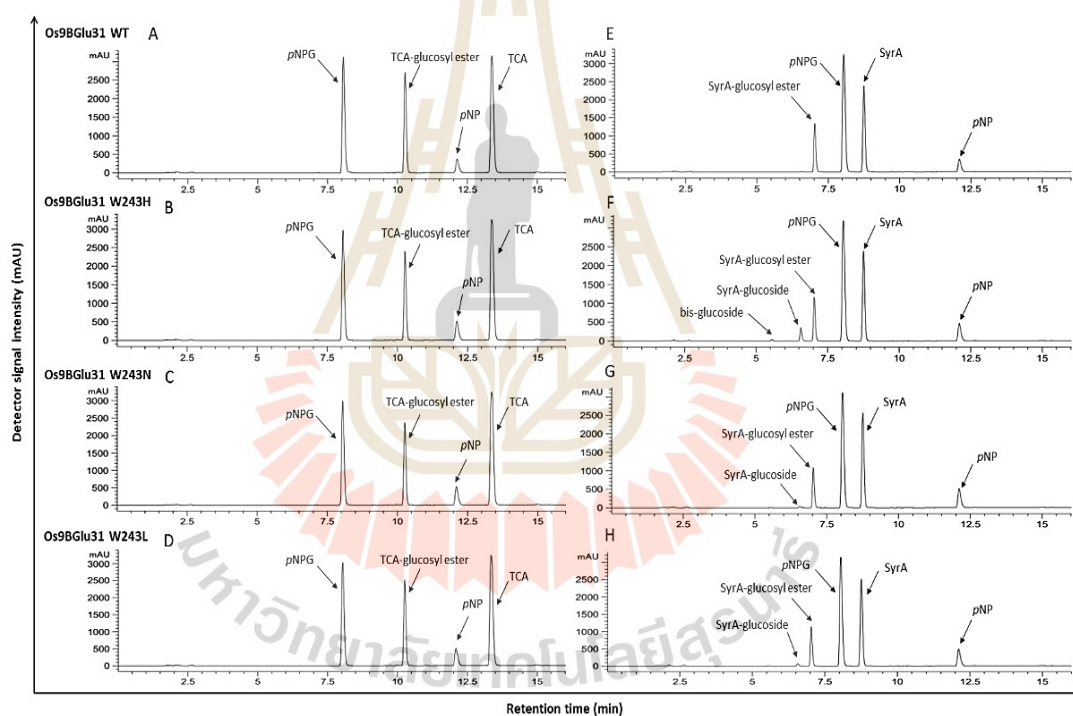


**Figure 4.8** UHPLC chromatogram profiles of transglucosylation products in the enzymatic reaction with *trans*-cinnamic acid (TCA) and syringic acid (SyrA). Transglucosylation reactions of TCA are with (A) Os9BGlu31 wild type, (B) W243H mutant, (C) W243N mutant, and (D) W243L mutant. Transglucosylation reactions of SyrA are with (E) Os9BGlu31 wild type, (F) W243H mutant, (G) W243N mutant, and (H) W243L mutant. The major transglucosylation products were identified as phenolic acid glucosyl ester with DAD wavelength at 254 nm.

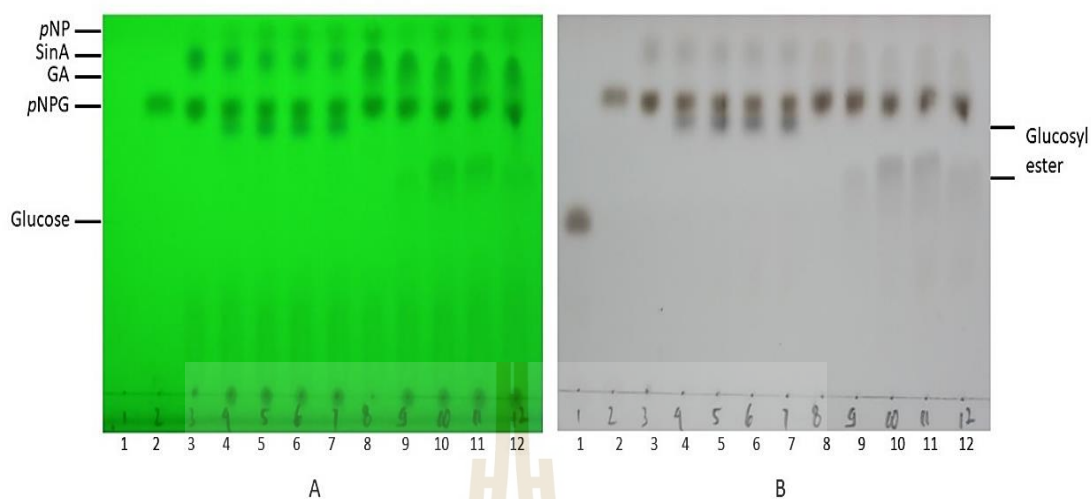


**Figure 4.9** Thin layer chromatography of transglucosylation products of enzymatic reactions catalyzed by Os9BGlu31 wild type and its mutant variants with sinapic acid (SinA) and gallic acid (GA). (A) The products were observed on a TLC plate under UV-light at 254 nm, and (B) after sulfuric acid treatment and charring at 120°C. Enzymatic reaction mixtures were separated by silica gel 60 TLC with mobile phase, *n*-butanol:acetic acid:water (6:2:2, v/v/v). Lane 1 = glucose, lane 2 = *p*NPG, lane 3 = reaction with SinA without Os9BGlu31, lane 4 = enzymatic reaction with SinA and Os9BGlu31 wild type (WT), lane 5 = enzymatic reaction with SinA and Os9BGlu31 W243H, lane 6 = enzymatic reaction with SinA and Os9BGlu31 W243N, lane 7 = enzymatic reaction with SinA and Os9BGlu31 W243L, lane 8 = reaction WITH GA without Os9BGlu31, lane 9 = enzymatic reaction with GA and Os9BGlu31 wild type (WT), lane 10 = enzymatic reaction with GA and Os9BGlu31 W243H, lane 11 = enzymatic reaction with GA and Os9BGlu31 W243N, lane 12 = enzymatic reaction with GA and Os9BGlu31 W243L.

In these experiments, the standards of glucosyl esters and glucosides were not used to determine the transglucosylation products. However, the peaks of products were tentatively identified based on their relative elution times and further identification can be obtained by LC-MS/MS on an electrospray ionization (ESI)-Quadruple Time of Flight (QToF) MS/MS as reported in previous studies (Komvongsa

et al., 2015a; Tran et al., 2019). The elution times of products were used to identify them, since most of glucoside products elute before the glucosyl esters product due to their higher polarity that was caused by the unconjugated carboxyl group is blocked by glucose in the esters.

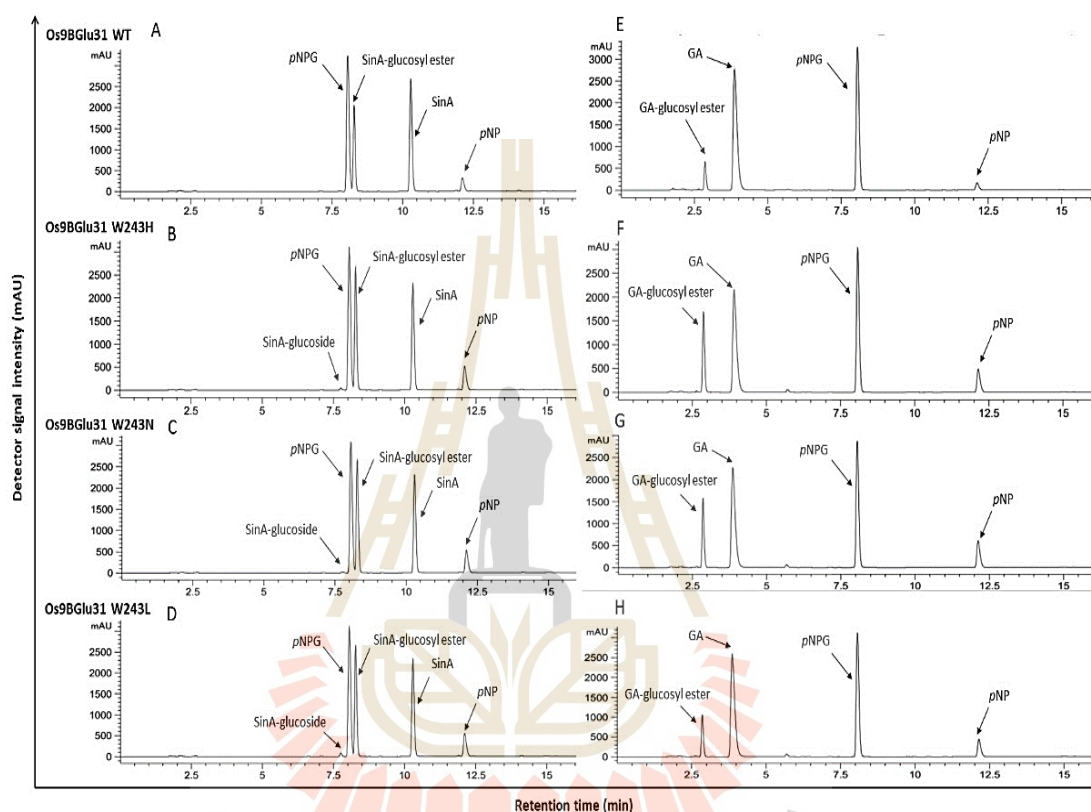


**Figure 4.10** UHPLC chromatogram profiles of transglucosylation products in the enzymatic reaction with sinapic acid (SinA) and gallic acid (GA). Transglucosylation reactions of SinA are with (A) Os9BGlu31 wild type, (B) W243H mutant, (C) W243N mutant, and (D) W243L mutant. Transglucosylation reactions of GA are with (E) Os9BGlu31 wild type, (F) W243H mutant, (G) W243N mutant, and (H) W243L mutant. The major transglucosylation products were identified as phenolic acid glucosyl ester with DAD wavelength at 254 nm.

The Os9BGlu31 mutant variants had higher hydrolysis activity than wild type, but still showed high transglucosylation activity, which is consistent with previous reports (Komvongsa et al., 2015a; Luang et al., 2013; Tran et al., 2019). This enzymatic reaction

showed high activity with phenolic acid glucose esters, particularly feruloyl glucose, as glucosyl donor. In the enzymatic reaction without glucosyl acceptors, Os9BGlu31 showed slow hydrolysis of *p*NPG to release *p*NP and glucose, whereas when low concentrations of free phenolic acids were present, it mainly acts to transfer glucosyl moiety to phenolic acids via a retaining mechanism (Luang et al., 2013). The reaction involves complex interactions between active site amino acid residues and the water network as the glucosyl acceptor binds to the active site of enzyme, so that increasing the hydrophilicity of the surrounding amino acid residue may not be sufficient to convert a transglucosidase to glucosidase (Pengthaisong and Cairns, 2014; Teze et al., 2013; Tran et al., 2019). The hydrolysis activity of Os9BGlu31 is about 10% of its transglycosylation activity, but is negligible in the presence of efficient acceptors (Luang et al., 2013). The enzyme activity is increased by several mutations of W243, thus mutant variants with all 20 possible amino acids at this position have been tested, and W243N and W243L had highest activity (Komvongsa et al., 2015a; Tran et al., 2019). These properties suggested that Os9BGlu31 mutant variants would be useful for the production of glucoconjugates for bioactivity testing.

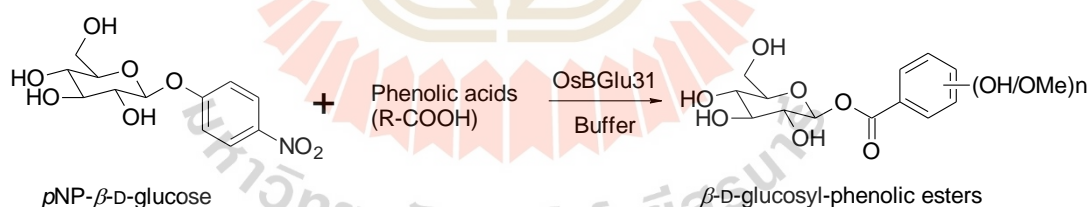


**Figure 4.11** General reaction scheme for the enzymatic synthesis of phenolic acid glucosyl esters in this study.

In general, Os9BGlu31 wild type tend to produce a single product, while Os9BGlu31 mutant variants tends to produce multiple products (Table A.1). However, phenolic acid glucosyl esters are major transglucosylation products in the enzymatic reactions with higher intensity than additional products. In this study, Os9BGlu31 mutant variants can transfer a glucosyl moiety to the carboxyl group of phenolic acids to form 1-*O*-glucosyl esters as the major transglucosylation products and to hydroxyl

groups to form glucosides as the additional products, while the wild type enzyme produced phenolic acid glucosyl esters only in detectable amount. In the presence of carboxyl group and hydroxyl group in structure of phenolic acids, Os9BGlu31 preferable to transfer glucosyl moiety to carboxyl group rather than to hydroxyl group, because it is related to regioselectivity that refers to the process of selection, where an atom is selected over other atoms and it was caused by steric effect and steric hindrance. Oxygen atom of carboxyl group is far away from the backbone of the aromatic ring, whereas the oxygen atom of hydroxyl group is attached at the backbone of aromatic ring and it has more substitution of hydroxyl group so that make it crowded, thus the enzymes need high energy and is not easy to transfer glucosyl moiety to hydroxyl group at aromatic ring of phenolic acids.

The major transglucoylation products can be detected on a TLC and UHPLC, but the additional products can be detected on UHPLC chromatograms only, since the products are low intensity, thus they are not detectable on TLC plates. The additional peaks seen in reactions with mutant enzymes were previously identified as glucosides and bis-glucosides of phenolic acids, including ferulic acid, vanillic acid, 4-hydroxybenzoic acid, *p*-coumaric acid, syringic acid, and sinapic acid (Komvongsa et al., 2015a; Tran et al., 2019). This reaction produced glycosylated compounds, which may be more stable and soluble, and have higher bioavailability than their free aglycones (Méndez-Liter et al., 2019; Moradi et al., 2016; Vivekanandhan et al., 2016; Woo et al., 2012). Therefore, it is very interesting and useful for poorly-soluble compounds in medical applications. Despite the more complex product mixtures with the Os9BGlu31 mutant variants, the yields of phenolic acid glucosyl esters were also higher after purification from enzymatic reactions catalyzed by Os9BGlu31 mutant variants than by wild type (Table 4.1). Therefore, Os9BGlu31 mutant variants were preferred for scale up production of phenolic acid glucosyl ester for bioactivity testing.

#### 4.4 Production of major transglucosylation products

Then, I produced the major transglucosylation products by enzymatic reactions using Os9BGlu31 wild type and its mutant variants as catalyst in 100 mL enzymatic

reactions to investigate which mutant and glucosyl acceptor can produced high yield of major transglucosylation products that were required for structural analysis and evaluation of biological activities (Table 4.1). The enzymatic reactions were evaporated by freeze dryer, since the reactions contains 5% DMSO and the major transglucosylation products were purified by LH-20 column chromatography with elution in distilled H<sub>2</sub>O as mobile phase. This mobile phase was selected because it generated the best purification process during a preliminary purification experiment and also the transglucosylation products are more polar than their free aglycones, thus the transglucosylation products are soluble in the water during purification.

**Table 4.1** Yield of major transglucosylation products in 100 mL of enzymatic reactions after purification.

Substrates (Glucosyl acceptors)	Yield of phenolic acid glucosyl esters (%)			
	Os9BGlu31	Os9BGlu31	Os9BGlu31	Os9BGlu31
	Wild type	W243H	W243N	W243L
Ferulic acid	3.1	13.1	22.03	15.9
Vanillic acid	1.7	6.8	12.4	14.9
4-Hydroxybenzoic acid	2.8	9.2	15.7	17.1
<i>p</i> -Coumaric acid	2.1	6.4	15.1	12.1
<i>trans</i> -Cinnamic acid	4.7	6.6	13.5	16.9
Syringic acid	3.6	4.9	9.4	13.2
Sinapic acid	2.7	6.6	11.3	13.2
Gallic acid	2.4	4.8	9.6	6.5

All fractions were spotted on TLC plates for further purification and the fractions containing a single spot of major transglucosylation products without any visible contaminants were pooled then dried by freeze dryer and the masses of the products were weighed to obtain the yields of major transglucosylation products. In order to ensure the purity of these products, TLC analysis was performed to match the spot of products that showing only single spots of products without any contaminant spots

on TLC plates from the fractions that were pooled, and by using physical comparison which in this case, the pure products have white color without any other colors from *p*NP because it conjugated with glucose. The NMR spectrometer also was used to verify the structure and purity of products. The result showed that Os9BGlu31 mutants enzyme produced higher yields of major transglucosylation products than wild type enzyme (Table 4.1). These results are in line with the enzyme activity of Os9BGlu31 in small scale (analytical) reactions, which the highest yield percentage can be produced by W243N with ferulic acid in 100 mL of enzymatic reaction.

#### 4.5 Transglucosylation product structural confirmation

The structures and purity of products were verified by  $^1\text{H-NMR}$  and  $^{13}\text{C-NMR}$ . According to the NMR spectra, the major transglucosylation products were verified and identified as phenolic acid glucosyl esters, including gallic acid glucosyl ester ( $\beta$ -glucogallin), syringic acid glucosyl ester, 4-hydroxybenzoic acid glucosyl ester, vanillic acid glucosyl ester, ferulic acid glucosyl ester, *trans*-cinnamic acid glucosyl ester, sinapic acid glucosyl ester, and *p*-coumaric acid glucosyl ester (Figure 4.12). In general, the  $^1\text{H-NMR}$  spectra of all phenolic acid glucosyl esters showed the common characteristic of a chemical shift of the anomeric proton peak at around 5.5 ppm as a clear doublet peak, which indicates the beta configuration of the glycosidic linkage (Figure 4.13). The aromatic ring protons give peaks that appear with chemical shifts between 6 ppm to 8.5 ppm and the unprotected glucose protons give peaks with chemical shift between 3 ppm to 4 ppm.

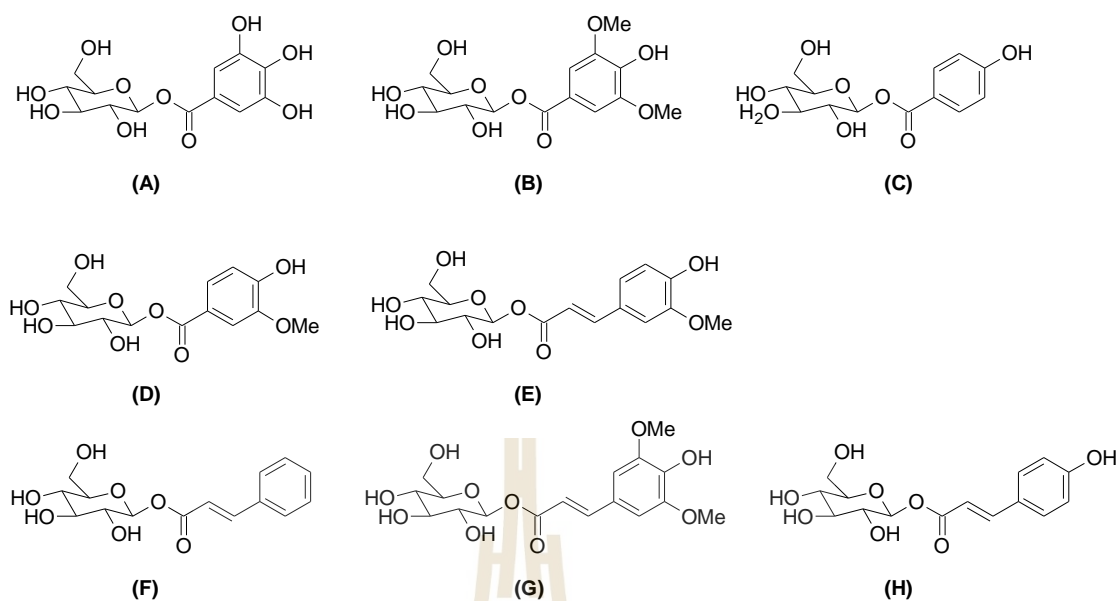


**Figure 4.12** Chemical structures of phenolic acid glucosyl esters that were verified by NMR spectroscopy. (A) gallic acid glucosyl ester ( $\beta$ -glucogallin), (B) syringic acid glucosyl ester, (C) 4-hydroxybenzoic acid glucosyl ester, (D) vanillic acid glucosyl ester, (E) ferulic acid glucosyl ester, (F) *trans*-cinnamic acid glucosyl ester, (G) sinapic acid glucosyl ester, and (H) *p*-coumaric acid glucosyl ester.

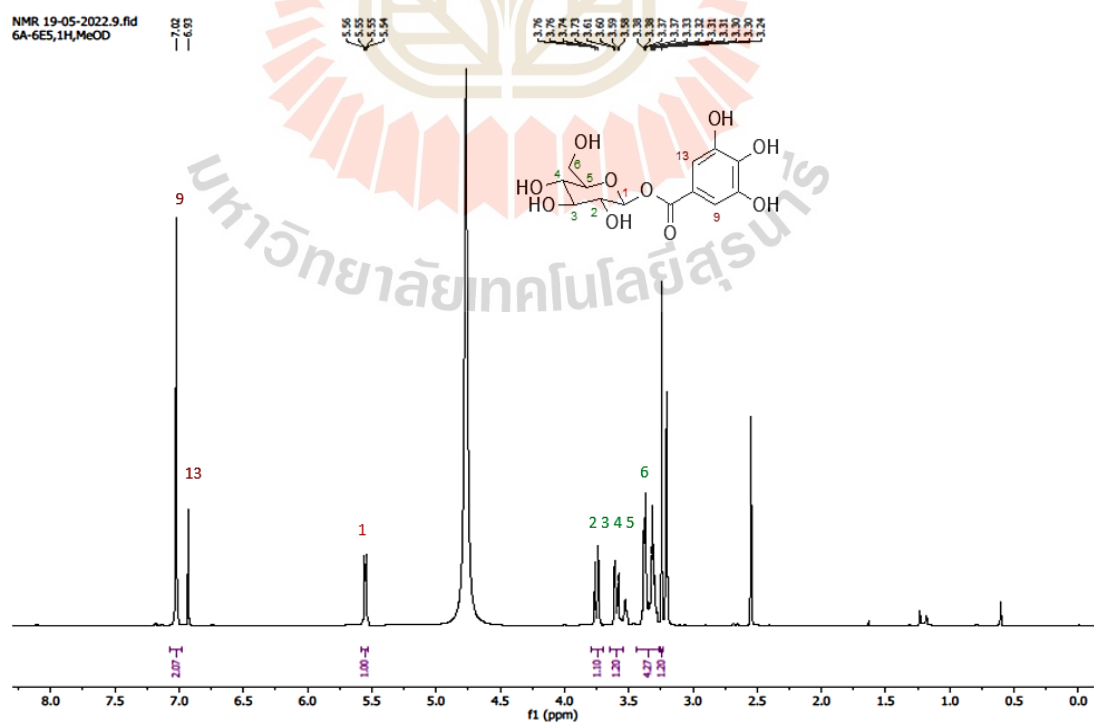


**Figure 4.13**  $^1\text{H-NMR}$  (500 MHz,  $\text{CD}_3\text{OD}$ ) spectra of gallic acid glucosyl ester ( $\beta$ -glucogallin). Solvent:  $\text{CD}_3\text{OD}$ , Frequency: 500 MHz.

Additionally, the  $^{13}\text{C}$ -NMR spectra of all phenolic acid glucosyl esters showed the common characteristics of a peak for the anomeric carbon at a chemical shift around 94 ppm, and the ester carbonyl carbon at around a chemical shift of 165 ppm, which confirms the ester linkage (Figure 4.14). The peaks for the carbon position in glucose can be identified between the chemical shift range of 60 ppm to 75 ppm, and the phenolic hydroxyl attached carbon peak can be identified at chemical shift between 140 ppm to 155 ppm for all phenolic acid glucosyl esters. Meanwhile, the peak of aromatic ring proton attached carbons appear with chemical shift between 110 ppm to 140 ppm (Figure 4.13, 4.14, and Appendix C Figure C.1-C.14).

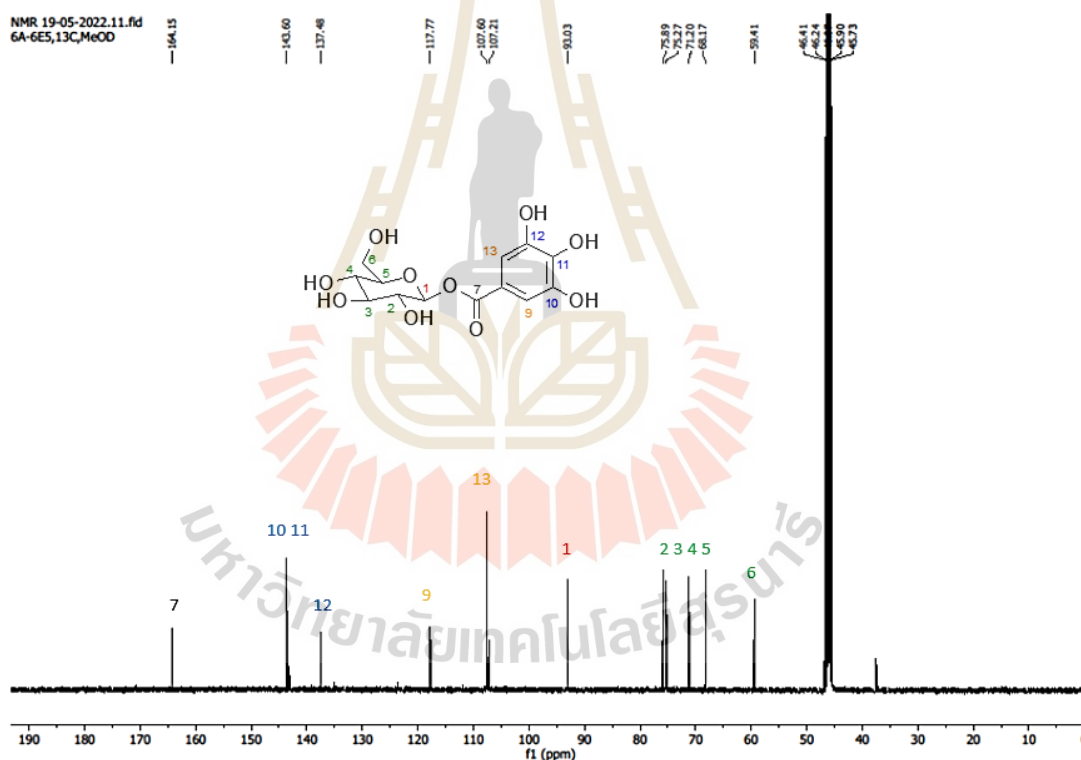


**Figure 4.14**  $^{13}\text{C}$ -NMR (125 MHz,  $\text{CD}_3\text{OD}$ ) spectra of gallic acid glucosyl ester ( $\beta$ -glucogallin). Solvent:  $\text{CD}_3\text{OD}$ , Frequency: 125 MHz.

The purified  $\beta$ -glucogallin showed NMR spectra with peaks, as follow:  $^1\text{H}$  NMR (500 MHz,  $\text{CD}_3\text{OD}$ )  $\delta$  7.02 (s, 2H), 5.55 (dd,  $J = 5.5, 7.5$  Hz, 1H), 3.75 (dd,  $J = 12.2, 1.9$  Hz, 1H), 3.59 (dd,  $J = 12.1, 4.5$  Hz, 1H), 3.44 – 3.26 (m, 4H), and 3.24 (s, 1H);  $^{13}\text{C}$  NMR (125 MHz,  $\text{CD}_3\text{OD}$ )  $\delta$  164.15, 143.60, 137.48, 117.77, 107.60, 107.21, 93.03, 75.89, 75.27, 71.20,

68.17, and 59.41. The anomeric protons coupling constant value at a chemical shift of 5.5 ppm (doublet peak), which indicates the beta configuration of the glycosidic linkage (Figure 4.13). The anomeric carbon is shown at a chemical shift of 93.03 ppm (Figure 4.14), and the ester carbonyl carbon characteristic peak at around 164.15 ppm, which confirms the ester linkage. This spectra was similar to the NMR spectra of  $\beta$ -glucogallin in the previous study (Puppala et al., 2012). The  $^1\text{H-NMR}$  and  $^{13}\text{C-NMR}$  spectroscopy data for other major transglucosylation products are provided to establish the formation of phenolic acid glucosyl ester and to assess the actual ratio of components. The  $^1\text{H-NMR}$  and  $^{13}\text{C-NMR}$  spectra of those phenolic acid glucosyl esters are provided in Appendix C Figure C.1-C.14, which correspond to the expected structures.

## 4.6 Activities of phenolic acid glucosyl esters

### 4.6.1 Antioxidant activity of phenolic acid glucosyl esters

Generally, antioxidant activity is found in hydrogen- or electron-donating agents that can act as free radical scavengers, as well as metal chelating agents, which can suppress metal-catalyzed free radical formation. The antioxidant activity of the compounds depends on the hydroxyl group positions, in relation to the carboxyl functional group and also depends on the number of hydroxyl groups in the structure of compounds (Balasundram et al., 2006; Zheng et al., 2020). However, the antioxidant activity of phenolic acid glucosyl esters have not been reported yet. Therefore, the measurement of antioxidant activity was incorporated into this study. There are many methods to evaluate antioxidant activity, including measurement of DPPH, which is known as common method for evaluating antioxidant properties due to it being feasible, simple, and sensitive (Deng et al., 2011; Li et al., 2015; Zhang et al., 2019).

I evaluated the antioxidant activity of phenolic acid glucosyl esters and their free aglycones by the DPPH scavenging assay (Figure 4.15, Figure B.1 and Table B.1). The free radical scavenging activities of the phenolic acid glucosyl esters were compared to ascorbic acid, as presented in Figure 4.15. Among the phenolic acid glucosyl esters, gallic acid glucosyl ester (GA-GE) or  $\beta$ -glucogallin exhibited high antioxidant capacity with a half-maximal inhibitory concentration ( $\text{IC}_{50}$ ) value of  $3.6 \pm 0.1 \mu\text{g/mL}$ . It was

similar to the antioxidant activity of ascorbic acid ( $IC_{50}$   $2.4 \pm 0.1$   $\mu\text{g/mL}$ ). Ferulic acid glucosyl ester (FA-GE), sinapic acid glucosyl ester (SinA-GE), and syringic acid glucosyl ester (SyrA-GE) also have significant antioxidant activities with  $IC_{50}$  values of  $45.2 \pm 1.2$   $\mu\text{g/mL}$ ,  $41.7 \pm 0.1$   $\mu\text{g/mL}$  and  $70.1 \pm 1.9$   $\mu\text{g/mL}$ , respectively. In contrast, *p*-coumaric acid glucosyl ester (PCA-GE), 4-hydroxybenzoic acid glucosyl ester (HBA-GE), vanillic acid glucosyl ester (VA-GE) and *trans*-cinnamic acid glucosyl ester (TCA-GE) had low or negligible antioxidant activities, even at 256  $\mu\text{g/mL}$ .

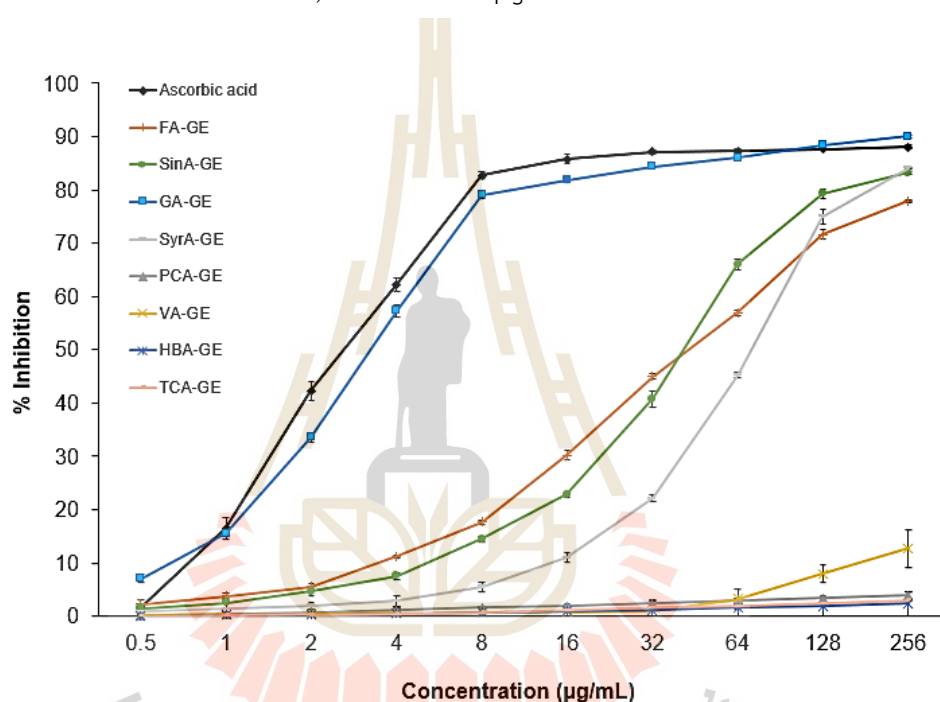


**Figure 4.15** Antioxidant activity of phenolic acid glucosyl esters. The radical scavenging activity was determined by DPPH assay. The values are expressed as mean  $\pm$  SD (shown as error bars) of three independent experiments.

The antioxidant assay showed an excellent antioxidant activity for  $\beta$ -glucogallin, which had an  $IC_{50}$  value similar to that of ascorbic acid. It suggests that  $\beta$ -glucogallin is a potential antioxidant agent for human health applications, since ascorbic acid has been reported as an excellent antioxidant and anti-cancer agent in the treatment and prevention of cancers (Bhattacharya, 2021; Du et al., 2012; Kumar et al., 2017; van Gorkom et al., 2019). Moreover, a previous study reported a correlation between antioxidant and cytotoxicity activity in cancer cells (Sammar et al., 2019). In addition,

previous studies also revealed that phenolics and flavonoids showed antioxidant activities and display anti-cancer activity (Chahar et al., 2011; Ghasemzadeh and Jaafar, 2013; Perillo et al., 2020; Yang et al., 2018).

#### 4.6.2 Anti-proliferative activity of phenolic acid glucosyl esters

To evaluate and investigate the effect of phenolic acid glucosyl esters in the inhibition of CCA cell proliferation, the cell viability was evaluated with an SRB assay after the CCA cells were treated with phenolic acid glucosyl esters. This experiment also screening the anti-proliferative activity of phenolic acid glucosyl ester in CCA cells. I used KKU-213A in this experiment for screening the anti-proliferative activity, since it is known to have high aggressiveness and fast growth.

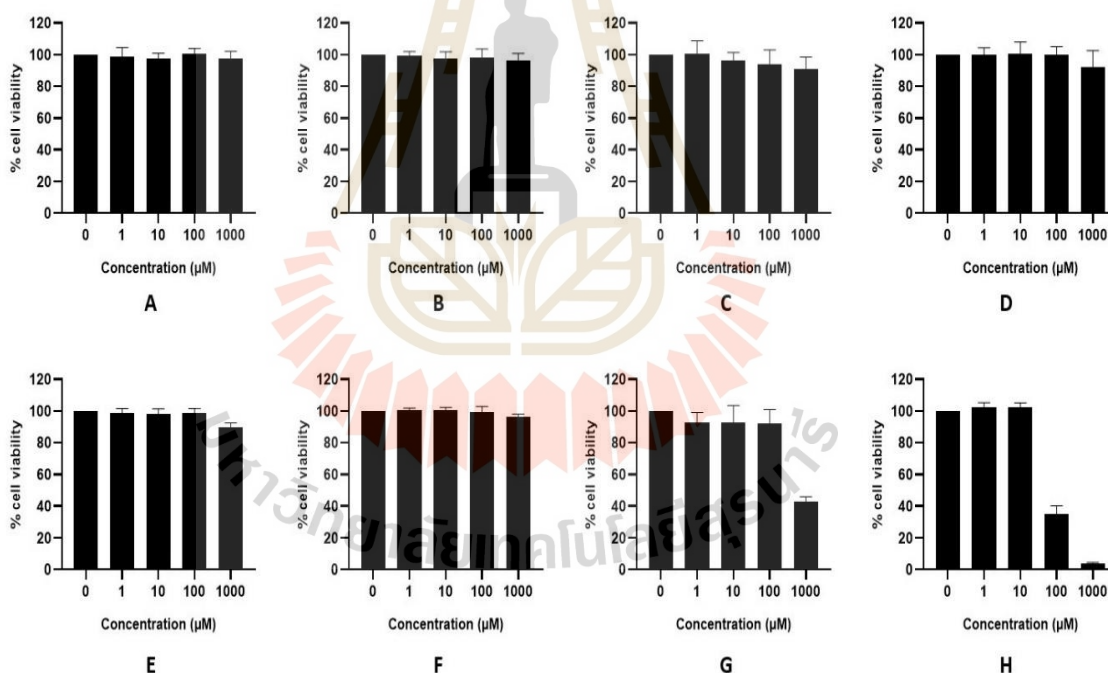


**Figure 4.16** Inhibitory effect of phenolic acid glucosyl esters in cell proliferation of KKU-213A at 24 h. (A) ferulic acid glucosyl ester, (B) vanillic-acid glucosyl ester, (C) 4-hydroxybenzoic acid glucosyl ester, (D) *p*-coumaric acid glucosyl ester, (E) *trans*-cinnamic acid glucosyl ester, (F) syringic acid glucosyl ester, (G) sinapic acid glucosyl ester, and (H) gallic acid glucosyl ester ( $\beta$ -glucogallin). The cell viability was determined by the SRB assay. The values are expressed as mean  $\pm$  SD (shown as error bars) of three independent experiments.

Among phenolic acid glucosyl esters,  $\beta$ -glucogallin exerted the highest inhibitory effect in K KU-213A, which was dose-dependent in the concentration range between 0-1000  $\mu$ M and caused more than 60% loss of cell viability at 100  $\mu$ M, while sinapic acid glucosyl ester caused around 50% loss of cell viability at 1000  $\mu$ M (Figure 4.16). On the other hand, no inhibitory effect was observed with other phenolic acid glucosyl esters in K KU-213A even at 1000  $\mu$ M. Since  $\beta$ -glucogallin had the highest inhibitory effect in K KU-213A, we decided to select this compound for further experiments. I also evaluated the anti-proliferative activity of phenolic acids in K KU-213A as additional knowledge for this study (Figure B.2).

#### 4.7 Anti-proliferative activity of $\beta$ -glucogallin

Then, I determined the anti-proliferative activity of  $\beta$ -glucogallin in three human CCA cell lines, including K KU-213A, K KU-055, and K KU-100, as well as a normal human fibroblast cell line to ensure whether  $\beta$ -glucogallin has anti-proliferative activity in different cells or not. As shown in Figure 4.17,  $\beta$ -glucogallin exerted significant inhibition of CCA cells in a time- and dose-dependent manner with different  $IC_{50}$  values (Table B.2). The anti-proliferative activity of  $\beta$ -glucogallin in K KU-213A cells has  $IC_{50}$  values of  $67.3 \pm 1.3 \mu$ M at 24 h,  $57.8 \pm 1.6 \mu$ M at 48 h, and  $51.7 \pm 0.4 \mu$ M at 72 h (Figure 4.17A).  $\beta$ -Glucogallin exerted higher anti-proliferative activity in K KU-055 with  $IC_{50}$  values of  $19.8 \pm 1.3$ ,  $18.1 \pm 0.7$  and  $17.6 \pm 1.7 \mu$ M at 24, 48, and 72 h, respectively (Figure 4.17C), but showed lower anti-proliferative activity in K KU-100 with  $IC_{50}$  values of  $178.7 \pm 4.1$ ,  $170.9 \pm 4.9$ , and  $140.7 \pm 1.6 \mu$ M at 24, 48, and 72 h, respectively (Figure 4.17E). These results indicate that K KU-055 is more sensitive toward  $\beta$ -glucogallin than K KU-213A and K KU-100, whereas K KU-100 is least sensitive. I also evaluated the anti-proliferative activity of 5-fluorouracil in CCA cells as additional knowledge for this study (Figure B.3).

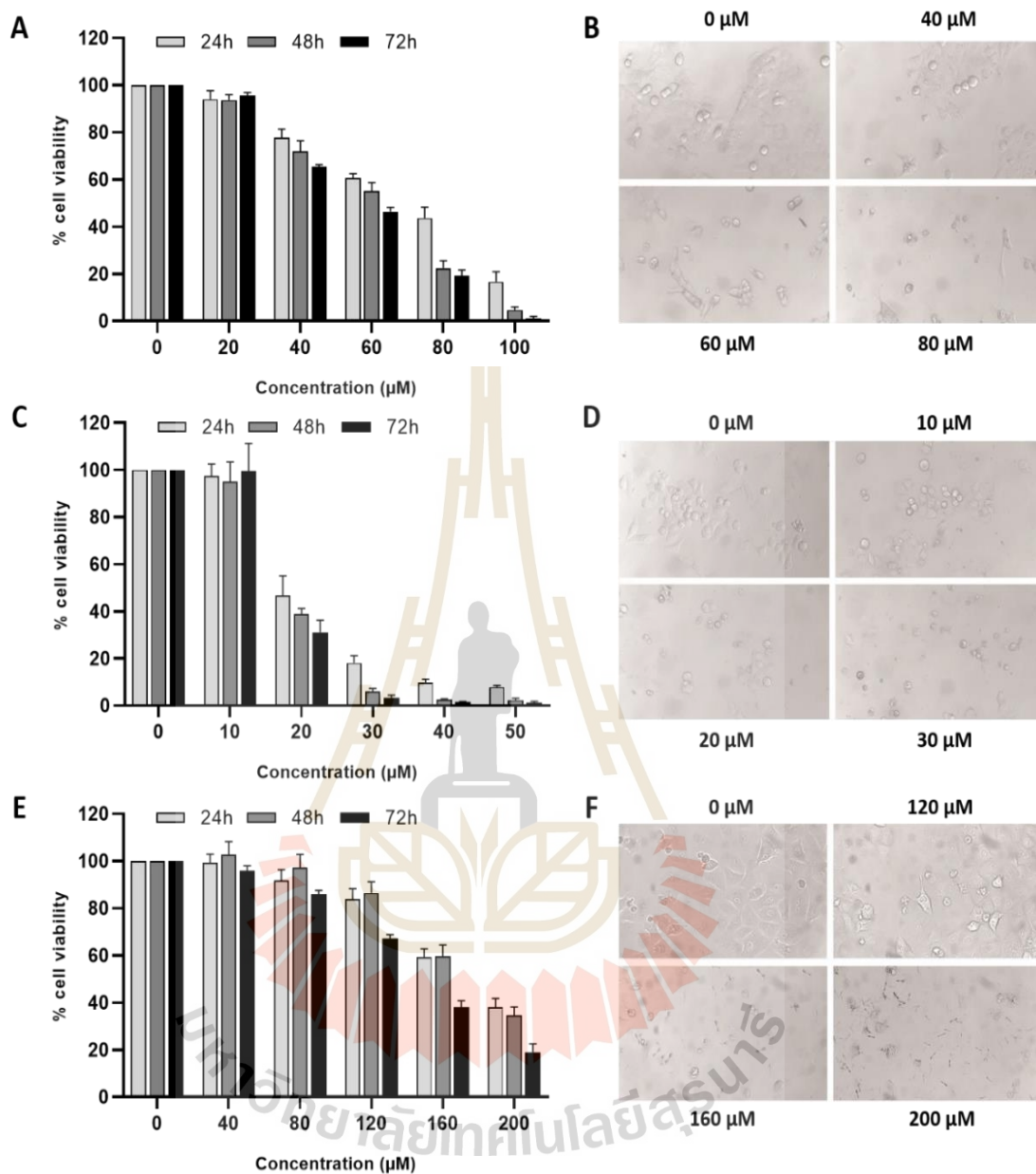


**Figure 4.17** Inhibitory effect of  $\beta$ -glucogallin in cholangiocarcinoma cells at 24, 48 and 72 h and the morphological change of cells after  $\beta$ -glucogallin treatment for 24 h were observed at 20X magnification. (A,B) KKU-213A, (C,D) KKU-055, and (E,F) KKU-100. The cell viability was determined by SRB assay. The values are expressed as mean  $\pm$  SD (shown as error bars) of three independent experiments.

Previous studies reported that  $\beta$ -glucogallin is known as aldose reductase inhibitor (Chang et al., 2013; Lee et al., 2011; Puppala et al., 2012). Interestingly, our

result found that  $\beta$ -glucogallin showed anti-proliferative activity that indicated by inhibition of cancer cell proliferation in CCA cells at lower concentration compared with other phenolic acid glucosyl esters (Figure 4.16). Additionally,  $\beta$ -glucogallin treatment showed higher anti-proliferative activity in KKU-055 than KKU-213A and KKU-100 in a time- and dose-dependent manner. In contrast, there was no cell morphology change in the normal human fibroblast cell line (IMR-90) as control after  $\beta$ -glucogallin treatment within concentrations in the range of 0-200  $\mu$ M. All of IMR-90 cells were still alive at that concentration range at 24 h, indicating that  $\beta$ -glucogallin showed low anti-proliferative activity toward normal cells (Figure 4.18). These phenomena are consistent with the observed cell morphological changes, since the CCA cell morphology was changed and the number of floating cells was increased in a time- and dose-dependent manner compared with control, indicating that cell death was induced by  $\beta$ -glucogallin in CCA cells. Mostly, after treatment with  $\beta$ -glucogallin, the adherent cells morphology was changed to be rounded with cell shrinkage, membrane blebbing and formation of many small apoptotic bodies and bright spherical cells (Figure 4.17B, D, F).

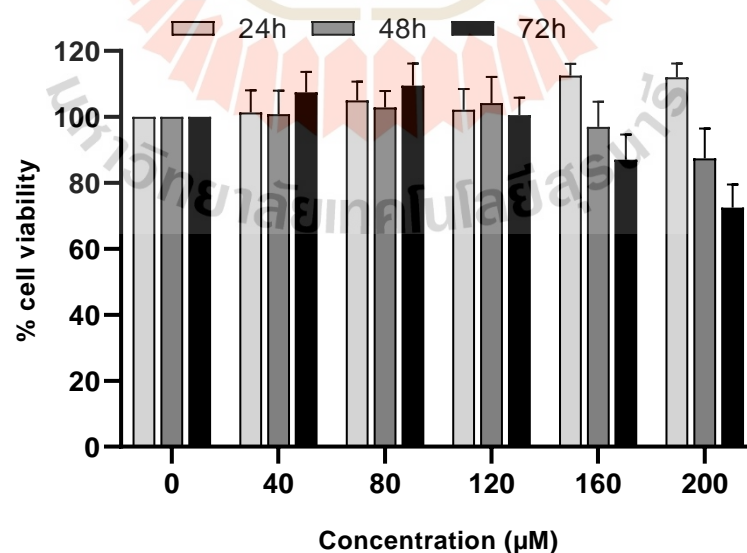


**Figure 4.18** Inhibitory effect of  $\beta$ -glucogallin in a normal human fibroblast cell line (IMR-90) at 24, 48, and 72 h. The cell viability was determined by SRB assay. The values are expressed as mean  $\pm$  SD (shown as error bars) of three independent experiments.

#### 4.8 Anti-migration activity of $\beta$ -glucogallin

In order to explore and evaluate the anti-migration activity of  $\beta$ -glucogallin in CCA cells, a wound healing assay was performed to observe CCA cells migration. The wound healing assay was used to observe the wound closure of cell monolayer on the surface of the culture plate meaning that I observed the cell migration on horizontal direction without any chemo-attractant. Therefore, the cells that have fast growth will migrate more faster to close the wound area based on the growth activity of cells. In this experiment, I evaluated the anti-migration activity of  $\beta$ -glucogallin in KKU-213A, KKU-055 and KKU-100. Each of CCA cells have different characteristics, which KKU-213 is more aggressive and fast growing, while KKU-055 is more sensitive but slow growing, and KKU-100 is less sensitive and slow growing. I also used low concentrations of  $\beta$ -glucogallin that were less than the  $IC_{50}$  values in each CCA cells to reduce the cytotoxic effect. As shown in Figure 4.19, KKU-213A cells quickly migrated into the wound area within 48 h in the untreated cells, whereas the cell migration of KKU-055 and KKU-100 was slower (Figure 4.20 and 4.21).

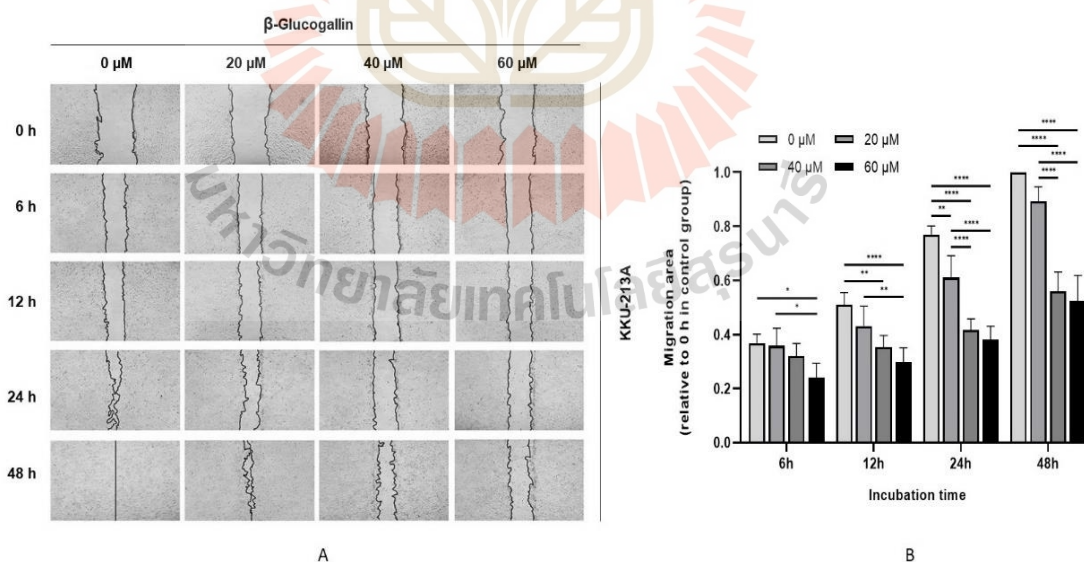


**Figure 4.19** Inhibition of cell migration by  $\beta$ -glucogallin at various times and doses in KKU-213A. (A) Cell migration after treatment with  $\beta$ -glucogallin. (B) Quantification of wound healing rate in KKU-213A after treatment with  $\beta$ -glucogallin. The values are expressed as mean  $\pm$  SD (shown as error bars) of three independent experiments. \*  $p < 0.05$ , \*\*  $p < 0.01$ , \*\*\*  $p < 0.001$ , \*\*\*\*  $p < 0.0001$ .

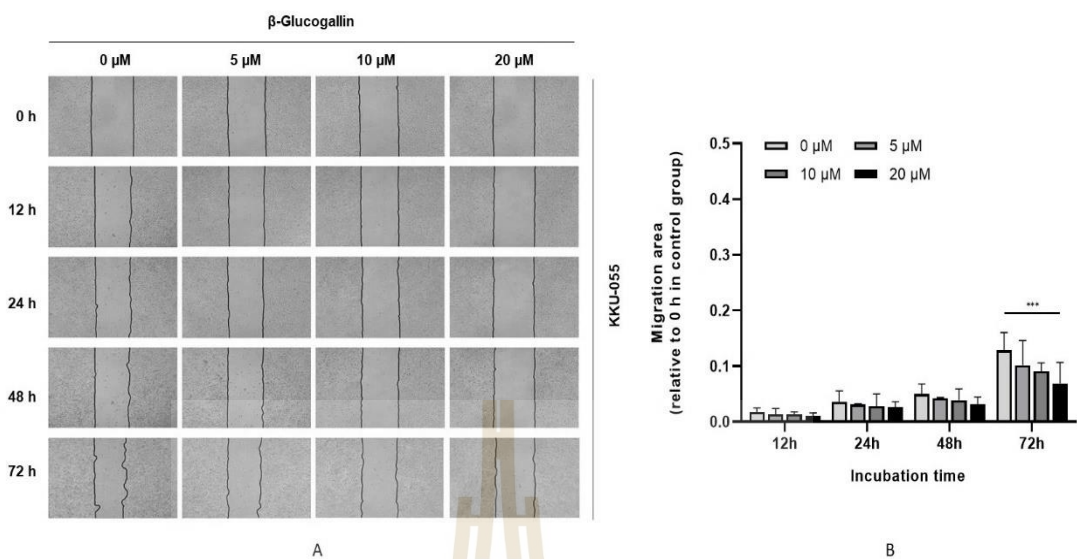


**Figure 4.20** Inhibition of cell migration by  $\beta$ -glucogallin at various times and doses in KKU-055. (A) Cell migration after treatment with  $\beta$ -glucogallin. (B) Quantification of wound healing rate in KKU-055 after treatment with  $\beta$ -glucogallin. The values are expressed as mean  $\pm$  SD (shown as error bars) of three independent experiments. \*  $p < 0.05$ , \*\*  $p < 0.01$ , \*\*\*  $p < 0.001$ , \*\*\*\*  $p < 0.0001$ .

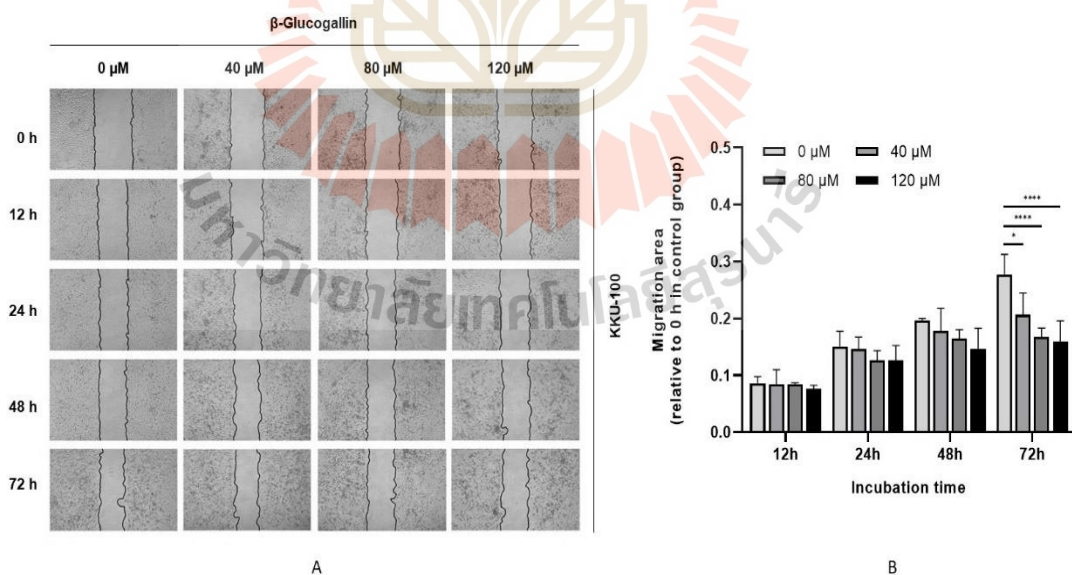


**Figure 4.21** Inhibition of cell migration by  $\beta$ -glucogallin at various times and doses in KKU-100. (A) Cell migration after treatment with  $\beta$ -glucogallin. (B) Quantification of wound healing rate in KKU-100 after treatment with  $\beta$ -glucogallin. The values are expressed as mean  $\pm$  SD (shown as error bars) of three independent experiments. \*  $p < 0.05$ , \*\*  $p < 0.01$ , \*\*\*  $p < 0.001$ , \*\*\*\*  $p < 0.0001$ .

In general, for these results, compared with the untreated cells, the healing rate (wound closure or migration area) of the treated group was slower with increasing concentration of  $\beta$ -glucogallin. Therefore,  $\beta$ -glucogallin inhibits CCA cell migration in a time- and dose-dependent manner, which indicated that  $\beta$ -glucogallin possesses anti-migration activity.

#### 4.9 $\beta$ -Glucogallin inhibit CCA proliferation by inducing apoptosis

In order to corroborate the finding about the anti-proliferative activity of  $\beta$ -glucogallin in CCA cells and to understand the survival and proliferative activities of CCA cells after treatment with  $\beta$ -glucogallin, I further investigated the cell survival and proliferative activities of CCA cells by a cell colony formation assay (clonogenic assay). This assay is important to understand whether the cells are able to survive and proliferate after  $\beta$ -glucogallin treatment and is related to the drug resistance because the propensity of a single cell to form a colony over long time periods is a hallmark of cancer. In this experiment, I selected K KU-213A and K KU-055 to representing CCA cells with different characteristics, in that K KU-213A is more aggressive and fast growing, while K KU-055 is more sensitive and slow growing. I used a concentration of  $\beta$ -glucogallin near the  $IC_{50}$  value and double this concentration in K KU-213A (0, 70, and 140  $\mu$ M) and K KU-055 (0, 20, and 40  $\mu$ M) to ensure that their effects on the survival and proliferative activities were measurable but that the concentrations were still safe in the normal human fibroblast cell line, then the cells were incubated in these concentrations for 14 days. The result showed that K KU-213A and K KU-055 formed fewer colonies in  $\beta$ -glucogallin compared with untreated cells as control in a dose-dependent manner. This indicates that the cells were unable to survive and proliferate after  $\beta$ -glucogallin treatment and there is no drug resistance in the cells (Figure 4.22).

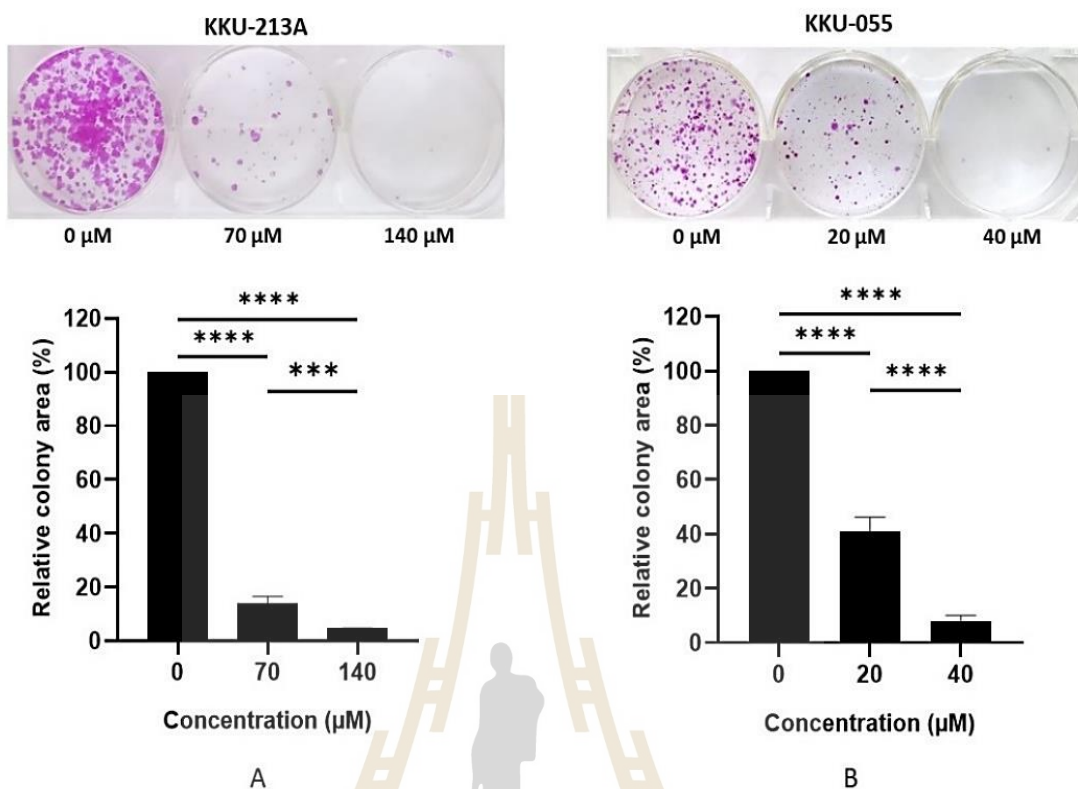


**Figure 4.22** Colony formation assay in (A) KKU-213A and (B) KKU-055 after treatment with  $\beta$ -glucogallin. The cells were seeded at  $2 \times 10^3$  cell/well and incubated for 14 days at  $37^\circ\text{C}$  after treatment with  $\beta$ -glucogallin. The values are expressed as mean  $\pm$  SD (shown as error bars) of three independent experiments. \*  $p < 0.05$ , \*\*  $p < 0.01$ , \*\*\*  $p < 0.001$ , \*\*\*\*  $p < 0.0001$ .

In order to confirm the role of  $\beta$ -glucogallin in cell death of CCA cells, I further investigated the apoptotic cells of CCA by Annexin-V/PI staining using flow cytometry. The morphological change of the cells is associated with a change of membrane permeability. When cells undergo apoptosis, phosphatidylserine, a phospholipid embedded in the inner leaflet of the plasma membrane, is exposed on the surface, so it can be detected by Annexin V (a 36 kDa calcium-binding protein) staining. Annexin V can bind to phosphatidylserine in the presence of calcium ions, whereas PI stains the DNA.

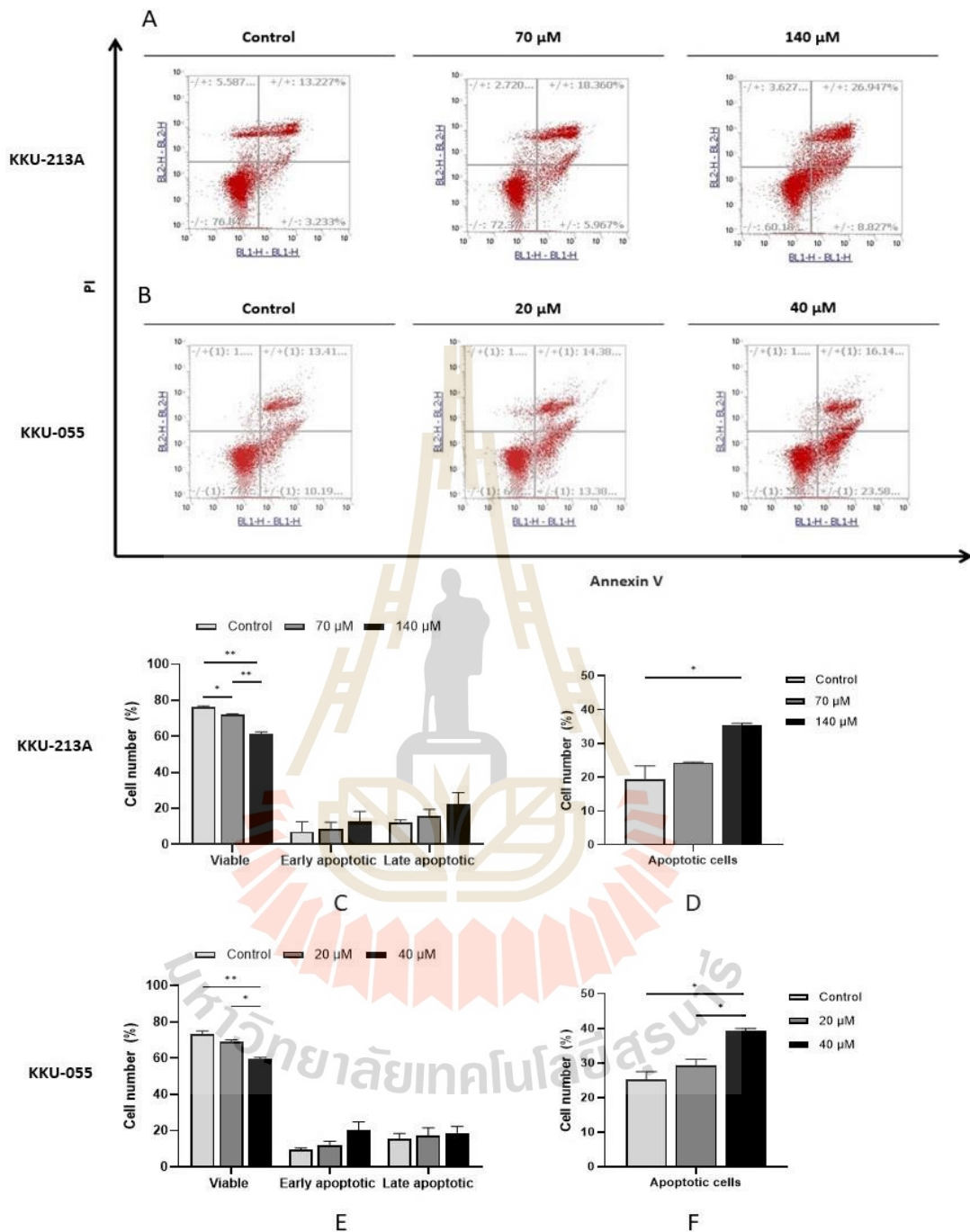


**Figure 4.23** Apoptosis analysis in (A) KKU-213A and (B) KKU-055 after treatment with  $\beta$ -glucogallin for 24 h. The proportion of apoptotic cells were quantified, (C, D) KKU-213A and (E, F) KKU-055. The apoptotic cell was detected by Annexin V/PI staining and evaluated by flow cytometry. The values are expressed as mean  $\pm$  SD (shown as error bars) of three independent experiments. \*  $p < 0.05$ , \*\*  $p < 0.01$ , \*\*\*  $p < 0.001$ , \*\*\*\*  $p < 0.0001$ .

The result showed that the proportion of apoptotic cells (early apoptotic and late apoptotic cells) was increased compared with control in both K KU-213A and K KU-055. In K KU-213A, the cell numbers was increasing from 19.3% in control to 24.3% and 35.3% after treatment with 70  $\mu$ M and 140  $\mu$ M of  $\beta$ -glucogallin, respectively. In comparison, the apoptotic cell numbers of K KU-055 increased from 25.3% in control to 29.2% and 39.3% after treated with 20  $\mu$ M and 40  $\mu$ M of  $\beta$ -glucogallin, respectively (Figure 4.23). This result indicated that  $\beta$ -glucogallin induced apoptosis, although the percentage of apoptotic cells seems to not be high. The higher apoptotic cells in control may be caused by the cell culture condition, in which the cells were incubated in medium without serum, as noted in a previous study (Naradun et al., 2022).

#### 4.10 $\beta$ -Glucogallin inhibit CCA proliferation via cell cycle arrest

In order to investigate the effect of  $\beta$ -glucogallin in CCA cells proliferation and to understand whether  $\beta$ -glucogallin led to inhibition of cell growth, I performed cell cycle analysis by PI staining and flow cytometry in K KU-213A and K KU-055 after treatment with  $\beta$ -glucogallin. I also evaluated the expression of cell cycle-related genes, including *CCND1*, *CCNE1*, *CCNB1*, and *CDKNB1* by qRT-PCR. As shown in Figure 4.24, cell cycle analysis demonstrated the proportion of cell accumulation of K KU-213 in the S and G2/M phase was significantly increased in a dose-dependent manner indicating that  $\beta$ -glucogallin caused cell cycle arrest in S and G2/M phase. In K KU-213A control, the proportion of cell accumulation was 7% and 19% in S and G2/M phase, respectively. In treated cells, the cell accumulation was increased to 9% and 17% in S phase after treatment with 70  $\mu$ M and 140  $\mu$ M  $\beta$ -glucogallin, respectively, while the cell accumulation in G2/M phase increased to 23% and 27% after treatment with 70  $\mu$ M and 140  $\mu$ M  $\beta$ -glucogallin, respectively. In contrast, the proportion of cell accumulation of G0/G1 phase in K KU-055 was increased from 69% in control to 75% in 20  $\mu$ M and 79% in 40  $\mu$ M  $\beta$ -glucogallin. Meanwhile, in S-phase and G2/M phase showed decreased cell accumulation in a dose-dependent manner. This result indicated that  $\beta$ -glucogallin caused cell cycle arrest in G0/G1 phase in K KU-055.

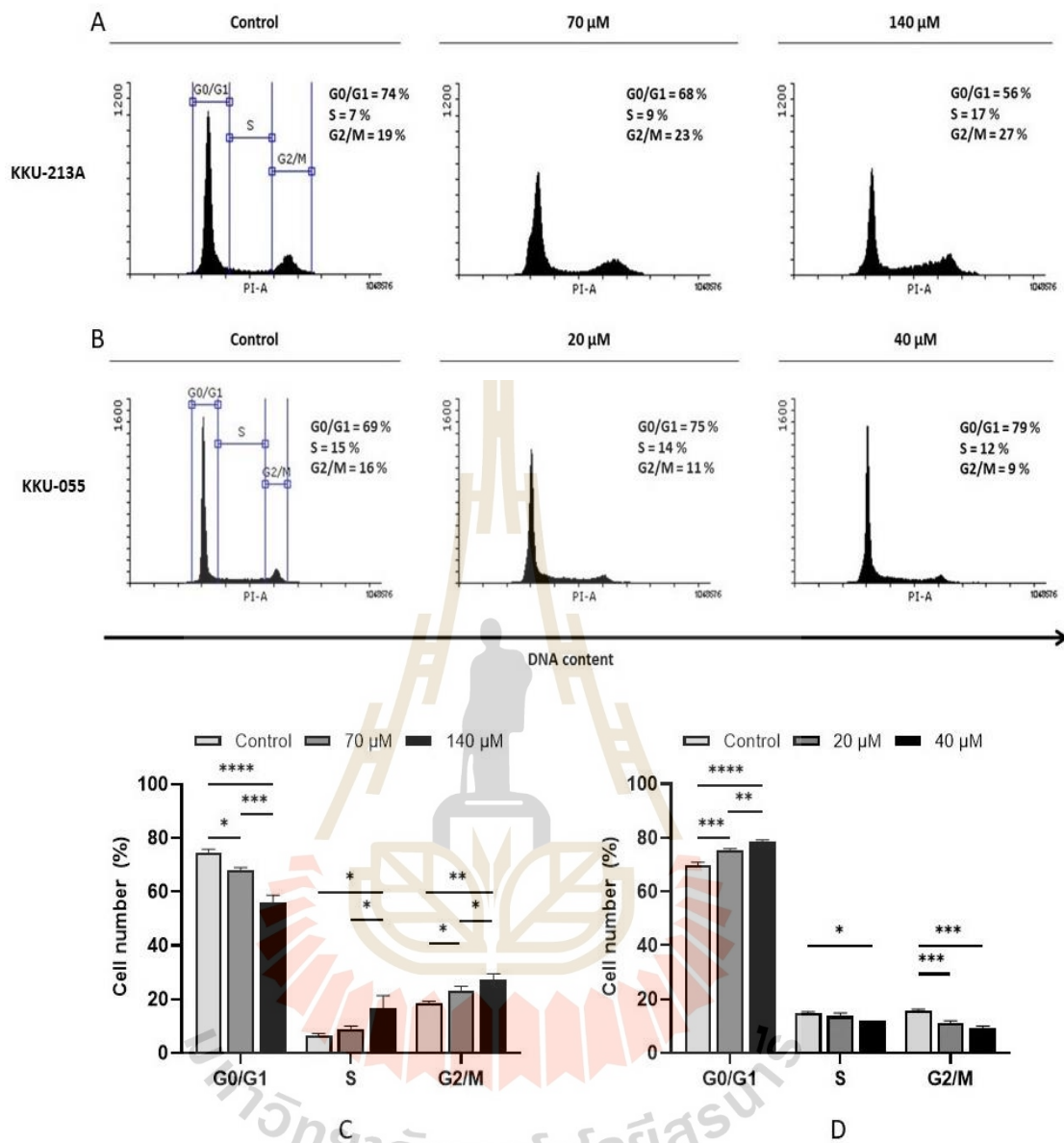


**Figure 4.24** Cell cycle analysis in (A) KKU-213A and (B) KKU-055 after treatment with  $\beta$ -glucogallin.  $\beta$ -Glucogallin appeared to induce inhibition of CCA cell proliferation via cell cycle arrest in KKU-213A and KKU-055. The cell number were quantified, (C) KKU-213A and (D) KKU-055. The DNA content was detected by propidium iodide staining using flow cytometer. The values are expressed as mean  $\pm$  SD (shown as error bars) of three independent experiments. \*  $p < 0.05$ , \*\*  $p < 0.01$ , \*\*\*  $p < 0.001$ , \*\*\*\*  $p < 0.0001$ .

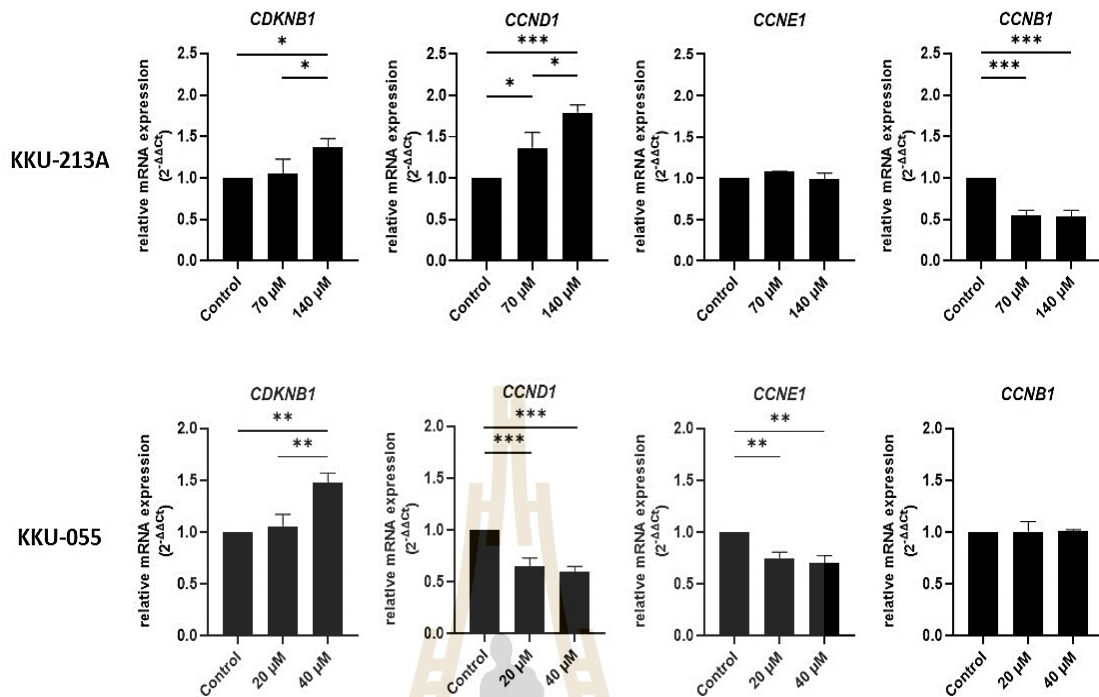


**Figure 4.25** Relative mRNA expression levels of cell cycle-related genes in KKU-213A and KKU-055 after treatment with  $\beta$ -glucogallin. The values are expressed as mean  $\pm$  SD (shown as error bars) of three independent experiments. \*  $p < 0.05$ , \*\*  $p < 0.01$ , \*\*\*  $p < 0.001$ , \*\*\*\*  $p < 0.0001$ .

In order to confirm these results, I investigated the mRNA expression level of cell cycle regulator genes by quantitative reverse-transcription, qRT-PCR. According to the results,  $\beta$ -glucogallin down-regulated gene expression of *CCNB1* (cyclin B) in KKU-213A, and *CCND1* (cyclin D) and *CCNE1* (cyclin E) in KKU-055 in a dose-dependent manner. These results suggested that the low expression of those genes may have led to the low expression of cyclin proteins as cell cycle regulators, thus decreased the binding to CDKs to regulate cell cycle progression, which was caused by the effect of  $\beta$ -glucogallin in CCA cells (Figure 4.25). Cyclin D is a cell cycle regulator in the G0/G1 phase, thus the highly expression of *CCND1* in KKU-213 is associated with cell cycle progression during G1 phase, which over expression of *CCND1* was triggered by mitogen, then cyclin D bind to their specific CDK (CDK4 or CDK6) to make CycD-CDK4/6 complex and induce cell cycle progression during G1 phase. In contrast, the expression of *CCND1*

and *CCNE1* was down-regulated by  $\beta$ -glucogallin in KKU-055, which  $\beta$ -glucogallin inhibited transcription of *CCND1* and *CCNE1*. While, cyclin B is a cell cycle regulator in the G2/M phase for cell development and proliferation. In the cell cycle, the cell transformation from G1 phase to S phase is regulated by cyclin A, cyclin D and cyclin E, as well as cyclin dependent kinase (CDK) 2/6 and their activities are controlled by CDK inhibitors (Niyonizigiye et al., 2019; Zhang et al., 2019). Interestingly, the down-regulating of gene expression was followed by up-regulated of *CDKNB1* expression level in both KKU-213A and KKU-055. The *CDKNB1* is known as cyclin-dependent kinase inhibitor 1B (p27<sup>Kip1</sup>) gene which can bind to cyclin-CDK complexes (CycE-CDK2, CycA-CDK2, and CycB-CDK1), then inhibit the catalytic activity thus inhibit cell cycle progression.

#### 4.11 $\beta$ -Glucogallin inhibit CCA proliferation via ER-stress-induced cell death

Additionally, in order to investigate the possible cell death mechanism in inhibition of CCA by  $\beta$ -glucogallin, I investigated the mRNA expression levels of ER-stress genes related to the unfolded protein response (UPR) signaling pathway.  $\beta$ -Glucogallin induced up-regulating of gene expression of ER-stress and UPR signaling markers, including *XBP1*, *sXBP1*, *ATF4*, *ATF6* and *CHOP*, in both KKU-055 and KKU-213A (Figure 4.26).  $\beta$ -Glucogallin appeared to induce ER-stress by splicing *XBP1* to form *sXBP1* mRNA, since the expression of *sXBP1* is increased approximately 5-fold and 10-fold after treatment with 70  $\mu$ M and 140  $\mu$ M  $\beta$ -glucogallin, respectively. These phenomena showed that treatment of CCA cells with  $\beta$ -glucogallin induced ER-stress and UPR signaling pathway, then activated proapoptotic genes in the nucleus to trigger apoptosis via ER stress-induced cell death. This finding was supported by the previous results, suggested that another cell death mechanism for further study, because the inability of protein folding and misfolded protein will lead to ER-stress, unfolded protein response (UPR) and ER-associated degradation (ERAD), which these interact with the ubiquitin-proteasome system (UPS) (Mao et al., 2019). If the protein accumulation is persistent by inhibiting the proteasome system, it would turn the

signaling from pro-survival to pro-apoptotic, meaning that  $\beta$ -glucogallin has potential as a proteasome inhibitor.

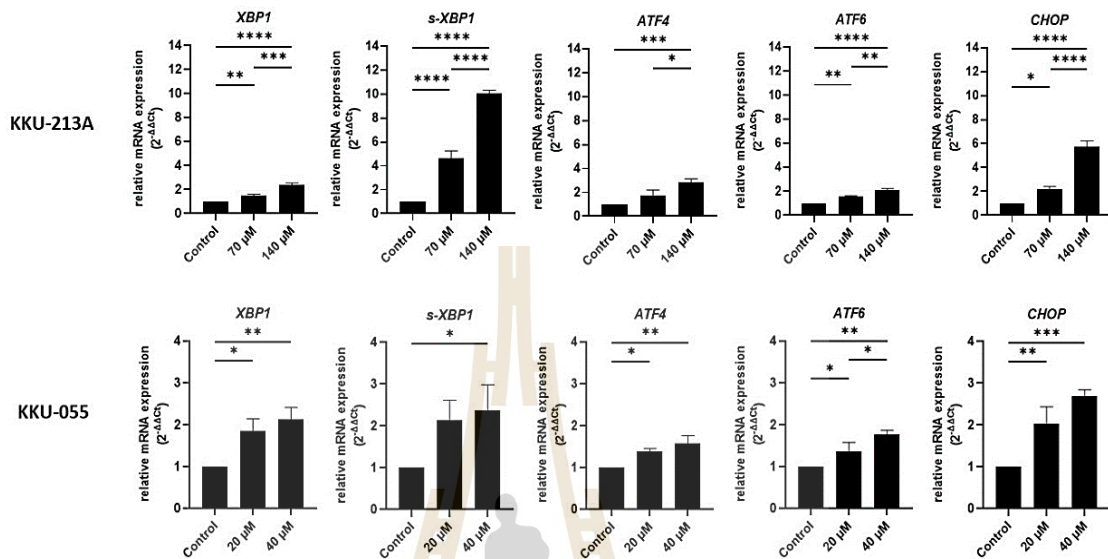


**Figure 4.26** Relative mRNA expression levels of ER-stress genes related to UPR signaling pathway in KKU-213A and KKU-055 after treatment with  $\beta$ -glucogallin. The values are expressed as mean  $\pm$  SD (shown as error bars) of three independent experiments. \*  $p < 0.05$ , \*\*  $p < 0.01$ , \*\*\*  $p < 0.001$ , \*\*\*\*  $p < 0.0001$ .

## CHAPTER V

### CONCLUSION

This study showed that rice Os9BGlu31 transglucosidase is a promising enzyme for glycosylation of compounds of interest and it can be used to synthesize sufficient quantities of products for bioactivity testing. Os9BGlu31 transferred glucosyl moiety from *p*NPG as glucosyl donor to phenolic acids as glucosyl acceptors to produce phenolic acid glucosyl esters in one-step enzymatic synthesis. Mutation of Os9BGlu31 at suitable positions improved the enzymatic activity and allowed it to transfer glucosyl moiety to the carboxyl groups of phenolic acids at higher rates thus it can produce phenolic acid glucosyl esters as major transglucosylation products. The mutant variants also transfer glucosyl moiety to hydroxyl groups, thus produced other derivative transglucosylation products although in lower quantities. The W243N and W243L mutants of Os9BGlu31 are the best mutant variants in this study, since they produced high yield of phenolic acid glucosyl esters, while also resulting additional transglucosylation products, including glucoside and bis-glucoside. Despite these additional products, their high rates made W243N and W243L mutant variants are the enzymes of choice for the production of phenolic acid glucosyl esters, since these could readily be purified away from other products.

This study also provided evidence that among phenolic acid glucosyl esters tested,  $\beta$ -glucogallin displays excellent antioxidant activity, and inhibition of cell proliferation and cell migration of cholangiocarcinoma cells without inhibiting cell proliferation of normal human fibroblast cells.  $\beta$ -Glucogallin induced inhibition of cholangiocarcinoma cells via ER stress-induced cell death by up-regulating of gene expression of ER-stress and unfolded protein response signaling markers, leading to inhibit cell cycle progression via down-regulating of gene expression of cell cycle regulators, then induced apoptotic pathway to promote apoptosis. This finding revealed that  $\beta$ -glucogallin is a potential anti-cancer and anti-migration agent in the treatment of cholangiocarcinoma, which may offer an opportunity to develop it as a supplemental ingredient in cholangiocarcinoma treatments. Although these results are

promising, further study is needed to investigate further molecular mechanisms by which  $\beta$ -glucogallin inhibits cholangiocarcinoma cells.

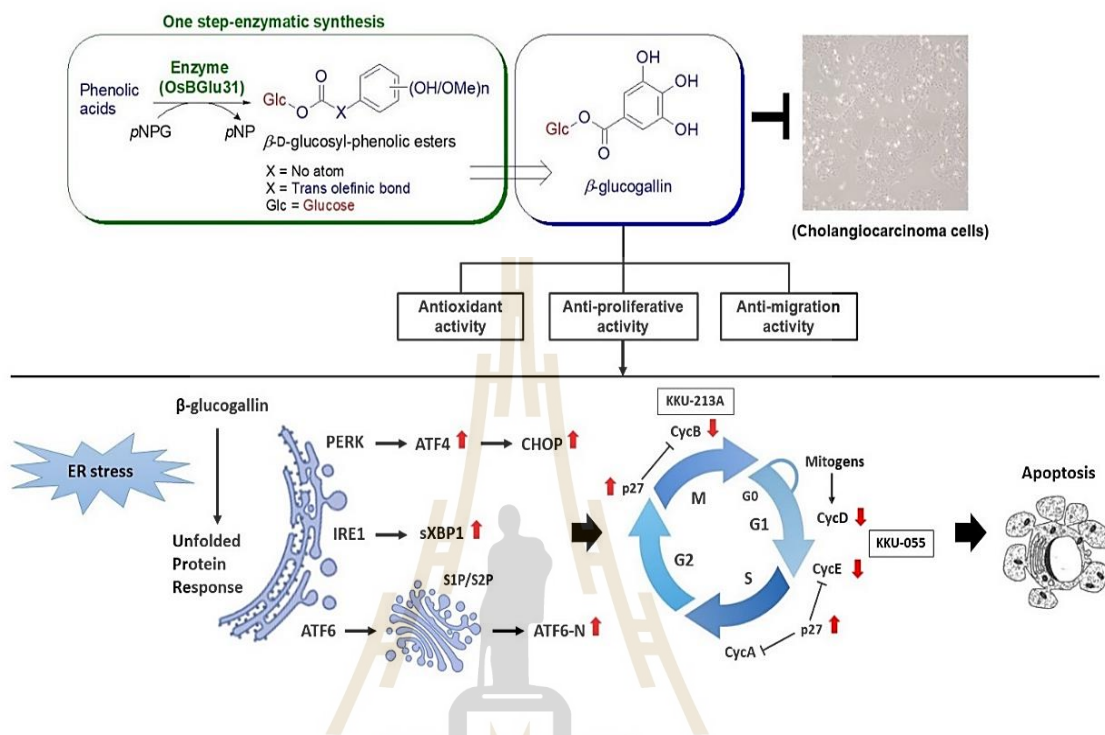
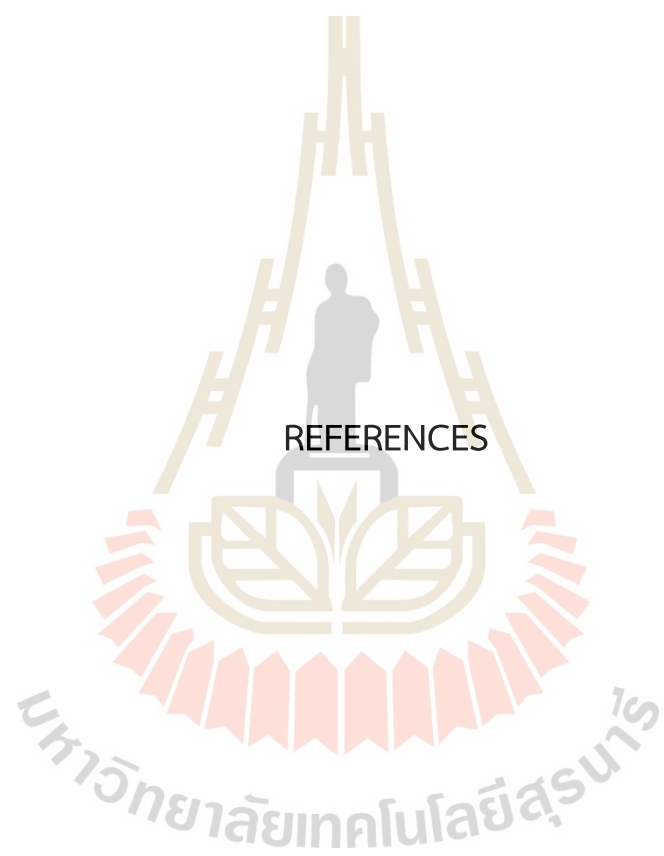


**Figure 5.1** Synthesis and production of phenolic acid glucosyl esters by rice Os9BGlu31 transglucosidase in one-step enzymatic synthesis and their effects in cholangiocarcinoma cells. The phenolic acid glucosyl esters display antioxidant, anti-proliferative, and anti-migration activity in cholangiocarcinoma cells. The inhibitory mechanism of  $\beta$ -glucogallin in cholangiocarcinoma cells are proposed.  $\beta$ -Glucogallin inhibited cholangiocarcinoma cell growth via ER stress-induced cell death by up-regulating of gene expression of ER-stress and unfolded protein response signaling markers, leading to inhibit cell cycle progression via down-regulating of gene expression of cell cycle regulators, then induce apoptotic pathway to promote apoptosis.



REFERENCES

## REFERENCES

- Adams, J. M., and Cory, S. (2007). The Bcl-2 apoptotic switch in cancer development and therapy. *Oncogene*, 26(9), 1324–1337. <https://doi.org/10.1038/sj.onc.1210220>
- Adari, B. R., Alavala, S., George, S. A., Meshram, H. M., Tiwari, A. K., and Sarma, A. V. S. (2016). Synthesis of rebaudioside-A by enzymatic transglycosylation of stevioside present in the leaves of *Stevia rebaudiana* Bertoni. *Food Chemistry*, 200, 154–158. <https://doi.org/https://doi.org/10.1016/j.foodchem.2016.01.033>
- Alimbetov, D., Askarova, S., Umbayev, B., Davis, T., and Kipling, D. (2018). Pharmacological targeting of cell cycle, apoptotic and cell adhesion signaling pathways implicated in chemoresistance of cancer cells. *International Journal of Molecular Sciences*, 19(6), 1–32. <https://doi.org/10.3390/ijms19061690>
- Alshareef, M. H., Hartland, E. L., and McCaffrey, K. (2021). Effectors targeting the unfolded protein response during intracellular bacterial infection. *Microorganisms*, 9(4), 1–12. <https://doi.org/10.3390/microorganisms9040705>
- Alves, M. J., Ferreira, I. C. F. R., Froufe, H. J. C., Abreu, R. M. V., Martins, A., and Pintado, M. (2013). Antimicrobial activity of phenolic compounds identified in wild mushrooms, SAR analysis, and docking studies. *Journal of Applied Microbiology*, 115(2), 346–357. <https://doi.org/10.1111/jam.12196>
- Andreasen, M. F., Kroon, P. A., Williamson, G., and Garcia-Conesa, M. T. (2001). Intestinal release and uptake of phenolic antioxidant diferulic acids. *Free Radical Biology and Medicine*, 31(3), 304–314. [https://doi.org/https://doi.org/10.1016/S0891-5849\(01\)00585-8](https://doi.org/https://doi.org/10.1016/S0891-5849(01)00585-8)
- Astolfi, L., Ghiselli, S., Guaran, V., Chicca, M., Simoni, E. D. I., Olivetto, E., Lelli, G., and Martini, A. (2013). Correlation of adverse effects of cisplatin administration in patients affected by solid tumours: a retrospective evaluation. *Oncology Reports*, 3(29), 1285–1292. <https://doi.org/10.3892/or.2013.2279>
- Bae, S., Yalamarti, B., and Kang, P. M. (2008). Role of caspase-independent apoptosis in

- cardiovascular diseases. *Frontiers in Bioscience*, *13*, 2495–2503.
- Baiya, S., Hua, Y., Ekkhara, W., and Ketudat-Cairns, J. R. (2014). Expression and enzymatic properties of rice (*Oryza sativa* L) monolignol  $\beta$ -glucosidases. *Plant Science*, *227*, 101–109. <https://doi.org/10.1016/j.plantsci.2014.07.009>
- Baiya, S., Mahong, B., Lee, S.-K., Jeon, J.-S., and Ketudat-Cairns, J. R. (2018). Demonstration of monolignol  $\beta$ -glucosidase activity of rice Os4BGlu14, Os4BGlu16 and Os4BGlu18 in *Arabidopsis thaliana* bglu45 mutant. *Plant Physiology and Biochemistry*, *127*, 223–230. <https://doi.org/10.1016/j.plaphy.2018.03.026>
- Balasundram, N., Sundram, K., and Samman, S. (2006). Phenolic compounds in plants and agri-industrial by-products: antioxidant activity, occurrence, and potential uses. *Food Chemistry*, *99*(1), 191–203. <https://doi.org/10.1016/j.foodchem.2005.07.042>
- Banales, J. M., Marin, J. J. G., Lamarca, A., Rodrigues, P. M., Khan, S. A., Roberts, L. R., Cardinale, V., Carpino, G., Andersen, J. B., Braconi, C., Calvisi, D. F., Perugorria, M. J., Fabris, L., Boulter, L., Macias, R. I. R., Gaudio, E., Alvaro, D., Gradilone, S. A., Strazzabosco, M., ... Gores, G. J. (2020). Cholangiocarcinoma 2020: the next horizon in mechanisms and management. *Nature Reviews Gastroenterology and Hepatology*, *17*(9), 557–588. <https://doi.org/10.1038/s41575-020-0310-z>
- Barnum, K. J., and O’Connell, M. J. (2014). Cell cycle regulation by checkpoints. In E. Noguchi and M. C. Gadaleta (Eds.), *Methods and Molecular Biology*. pp. 29-40. Springer New York. [https://doi.org/10.1007/978-1-4939-0888-2\\_2](https://doi.org/10.1007/978-1-4939-0888-2_2)
- Barros, J., Escamilla-Trevino, L., Song, L., Rao, X., Serrani-Yarce, J. C., Palacios, M. D., Engle, N., Choudhury, F. K., Tschaplinski, T. J., Venables, B. J., Mittler, R., and Dixon, R. A. (2019). 4-Coumarate 3-hydroxylase in the lignin biosynthesis pathway is a cytosolic ascorbate peroxidase. *Nature Communications*, *10*(1), 1–11. <https://doi.org/10.1038/s41467-019-10082-7>
- Besson, A., Hwang, H. C., Cicero, S., Donovan, S. L., Gurian-West, M., Johnson, D., Clurman, B. E., Dyer, M. A., and Roberts, J. M. (2007). Discovery of an oncogenic activity in p27<sup>Kip1</sup> that causes stem cell expansion and a multiple tumor phenotype. *Genes and Development*, *21*(14), 1731–1746.

<https://doi.org/10.1101/gad.1556607>

- Bhadra, K. (2022). A mini review on molecules inducing caspase-independent cell death: A new route to cancer therapy. *Molecules*, 27(19), 1–19. <https://doi.org/10.3390/molecules27196401>
- Bhattacharya, S. (2021). Clinical attestation and redox mechanism of ascorbic acid in the treatment of cancer. *Free Radicals and Antioxidants*, 11(1), 1–6. <https://doi.org/10.5530/fra.2021.1.1>
- Bhattarai, K. R., Chaudhary, M., Kim, H. R., and Chae, H. J. (2020). Endoplasmic reticulum (ER) stress response failure in diseases. *Trends in Cell Biology*, 30(9), 672–675. <https://doi.org/10.1016/j.tcb.2020.05.004>
- Binder, D., Schweisfurth, H., Grah, C., Schäper, C., Temmesfeld-wollbrück, B., Siebert, G., Suttorp, N., and Beinert, T. (2007). Docetaxel/gemcitabine or cisplatin/gemcitabine followed by docetaxel in the first-line treatment of patients with metastatic non-small cell lung cancer (NSCLC): results of a multicentre randomized phase II trial. *Cancer Chemotherapy Pharmacology*, 60, 143–150. <https://doi.org/10.1007/s00280-006-0358-7>
- Blechacz, B. R. A., and Gores, G. J. (2008). Cholangiocarcinoma. *Clinics in Liver Disease*, 12(1), 131–150. <https://doi.org/10.1016/j.cld.2007.11.003>
- Bourne, Y., and Henrissat, B. (2001). Glycoside hydrolases and glycosyltransferases: families and functional modules. *Current Opinion in Structural Biology*, 11(5), 593–600. [https://doi.org/https://doi.org/10.1016/S0959-440X\(00\)00253-0](https://doi.org/https://doi.org/10.1016/S0959-440X(00)00253-0)
- Brand-Williams, W., Cuvelier, M. E., and Berset, C. (1995). Use of a free radical method to evaluate antioxidant activity. *Food Science and Technology*, 28(1), 25–30. [https://doi.org/10.1016/S0023-6438\(95\)80008-5](https://doi.org/10.1016/S0023-6438(95)80008-5)
- Brindley, P. J., Bachini, M., Ilyas, S. I., Khan, S. A., Loukas, A., Sirica, A. E., Teh, B. T., Wongkham, S., and Gores, G. J. (2021). Cholangiocarcinoma. *Nature Reviews Disease Primers*, 7(1), 1–17. <https://doi.org/10.1038/s41572-021-00300-2>
- Buck, M. B., Pfizenmaier, K., and Knabbe, C. (2004). Antiestrogens induce growth inhibition by sequential activation of p38 mitogen-activated protein kinase and transforming growth Factor- $\beta$  pathways in human breast cancer cells. *Molecular*

- Endocrinology*, 18(7), 1643–1657. <https://doi.org/10.1210/me.2003-0278>
- Bujuq, N. A, Arar, S., and Khalil, R. (2018). Synthesis and cytotoxic activity of 4-O- $\beta$ -D-galactopyranosyl derivatives of phenolic acids esters. *Natural Product Research*, 32(22), 2663–2669. <https://doi.org/10.1080/14786419.2017.1375927>
- Cantarel, B. L., Coutinho, P. M., Rancurel, C., Bernard, T., Lombard, V., and Henrissat, B. (2009). The carbohydrate-active enzymes database (CAZy): an expert resource for glycogenomics. *Nucleic Acids Research*, 37, 233–238. <https://doi.org/10.1093/nar/gkn663>
- Carocho, M., and Ferreira, I. C. F. (2013). The role of phenolic compounds in the fight against cancer—a review. *Anti-Cancer Agents in Medicinal Chemistry*, 13(8), 1236–1258.
- Chaabane, W., User, S. D., El-Gazzah, M., Jaksik, R., Sajjadi, E., Rzeszowska-Wolny, J., and Łos, M. J. (2013). Autophagy, apoptosis, mitoptosis and necrosis: interdependence between those pathways and effects on cancer. *Archivum Immunologiae et Therapiae Experimentalis*, 61(1), 43–58. <https://doi.org/10.1007/s00005-012-0205-y>
- Chahar, M. K., Sharma, N., Dobhal, M. P., and Joshi, Y. C. (2011). Flavonoids: a versatile source of anticancer drugs. *Pharmacognosy Reviews*, 5(9), 1–12. <https://doi.org/10.4103/0973-7847.79093>
- Chandrasekara, A., and Shahidi, F. (2011). Bioactivities and antiradical properties of millet grains and hulls. *Journal of Agricultural and Food Chemistry*, 59(17), 9563–9571. <https://doi.org/10.1021/jf201849d>
- Chang, K. C., Laffin, B., Ponder, J., Énzöly, A., Németh, J., LaBarbera, D. V, and Petrash, J. M. (2013).  $\beta$ -Glucogallin reduces the expression of lipopolysaccharide-induced inflammatory markers by inhibition of aldose reductase in murine macrophages and ocular tissues. *Chemico-Biological Interactions*, 202(1), 283–287. <https://doi.org/10.1016/j.cbi.2012.12.001>
- Charoenwattanasatien, R., Pengthaisong, S., Breen, I., Mutoh, R., Sansenya, S., Hua, Y., Tankrathok, A., Wu, L., Songsirittthigul, C., Tanaka, H., Williams, S. J., Davies, G. J., Kurisu, G., and Cairns, J. R. K. (2016). Bacterial  $\beta$ -glucosidase reveals the structural

- and functional basis of genetic defects in human glucocerebrosidase 2 (GBA2). *ACS Chemical Biology*, 11(7), 1891–1900. <https://doi.org/10.1021/acscchembio.6b00192>
- Chen, M., Xia, L., and Xue, P. (2007). Enzymatic hydrolysis of corncob and ethanol production from cellulosic hydrolysate. *International Biodeterioration and Biodegradation*, 59(2), 85–89. <https://doi.org/10.1016/j.ibiod.2006.07.011>
- Chipuk, J. E., and Green, D. R. (2005). Do inducers of apoptosis trigger caspase-independent cell death? *Nature Reviews Molecular Cell Biology*, 6(3), 268–275. <https://doi.org/10.1038/nrm1573>
- Chowdhury, P., Dey, P., Ghosh, S., Sarma, A., and Ghosh, U. (2019). Reduction of metastatic potential by inhibiting EGFR/Akt/p38/ERK signaling pathway and epithelial-mesenchymal transition after carbon ion exposure is potentiated by PARP-1 inhibition in non-small-cell lung cancer. *BMC Cancer*, 19(1), 1–12. <https://doi.org/10.1186/s12885-019-6015-4>
- Christofferson, D. E., and Yuan, J. (2010). Necroptosis as an alternative form of programmed cell death. *Current Opinion in Cell Biology*, 22(2), 263–268. <https://doi.org/https://doi.org/10.1016/j.ceb.2009.12.003>
- Ciulu, M., Cádiz-Gurrea, de la L. M., and Segura-Carretero, A. (2018). Extraction and analysis of phenolic compounds in rice: a review. *Molecules*, 23(11), 1–20. <https://doi.org/10.3390/molecules23112890>
- Connell-Crowley, L., Harper, J. W., and Goodrich, D. W. (1997). Cyclin D1/Cdk4 regulates retinoblastoma protein-mediated cell cycle arrest by site-specific phosphorylation. *Molecular Biology of the Cell*, 8(2), 287–301. <https://doi.org/10.1091/mbc.8.2.287>
- Czabotar, P. E., Lessene, G., Strasser, A., and Adams, J. M. (2014). Control of apoptosis by the BCL-2 protein family: implications for physiology and therapy. *Nature Reviews Molecular Cell Biology*, 15(1), 49–63. <https://doi.org/10.1038/nrm3722>
- Czjzek, M., Cicek, M., Zamboni, V., Bevan, D. R., Henrissat, B., and Esen, A. (2000). The mechanism of substrate (aglycone) specificity in  $\beta$ -glucosidases is revealed by crystal structures of mutant maize  $\beta$ -glucosidase-DIMBOA, -DIMBOAGlc, and -

- dhurrin complexes. *Proceedings of the National Academy of Sciences of The United State of America*, 97(25), 13555–13560. <https://doi.org/10.1073/pnas.97.25.13555>
- Deng, J., Cheng, W., and Yang, G. (2011). A novel antioxidant activity index (AAU) for natural products using the DPPH assay. *Food Chemistry*, 125(4), 1430–1435. <https://doi.org/10.1016/j.foodchem.2010.10.031>
- Du, J., Cullen, J. J., and Buettner, G. R. (2012). Ascorbic acid: chemistry, biology and the treatment of cancer. *Biochimica et Biophysica Acta (BBA) - Reviews on Cancer*, 1826(2), 443–457. <https://doi.org/10.1016/j.bbcan.2012.06.003>
- El-Seedi, H. R., El-Said, A. M. A., Khalifa, S. A. M., Göransson, U., Bohlin, L., Borg-Karlson, A. K., and Verpoorte, R. (2012). Biosynthesis, natural sources, dietary intake, pharmacokinetic properties, and biological activities of hydroxycinnamic acids. *Journal of Agricultural and Food Chemistry*, 60(44), 10877–10895. <https://doi.org/10.1021/jf301807g>
- Ferreira, M. L., Rius, S. P., and Casati, P. (2012). Flavonoids: biosynthesis, biological functions, and biotechnological applications. *Frontiers in Plant Science*, 3, 1–15. <https://doi.org/10.3389/fpls.2012.00222>
- Gantt, R. W., Peltier-Pain, P., Cournoyer, W. J., and Thorson, J. S. (2011). Using simple donors to drive the equilibria of glycosyltransferase-catalyzed reactions. *Nature Chemical Biology*, 7(10), 685–691. <https://doi.org/10.1038/nchembio.638>
- Gao, X., Leone, G. W., and Wang, H. (2020). Cyclin D-CDK4/6 functions in cancer. In K. D. Tew and P. B. B. T. Fisher (Eds.), *Advanced Cancer Research* (Vol. 148, pp. 147–169). Academic Press. <https://doi.org/10.1016/bs.acr.2020.02.002>
- Ghasemzadeh, A., and Jaafar, H. Z. (2013). Profiling of phenolic compounds and their antioxidant and anticancer activities in pandan (*Pandanus amaryllifolius* Roxb.) extracts from different locations of Malaysia. *BMC Complementary and Alternative Medicine*, 13(1), 1–9. <https://doi.org/10.1186/1472-6882-13-341>
- Ghouri, Y. A., Mian, I., and Blechacz, B. (2015). Cancer review: cholangiocarcinoma. *Journal of Carcinogenesis*, 14(1), 1–10. <https://doi.org/10.4103/1477-3163.151940>
- Goufo, P., and Trindade, H. (2014). Rice antioxidants: phenolic acids, flavonoids,

- anthocyanins, proanthocyanidins, tocopherols, tocotrienols,  $\gamma$ -oryzanol, and phytic acid. *Food Science and Nutrition*, 2(2), 75–104. <https://doi.org/10.1002/fsn3.86>
- Hammer, M. B., Eleuch-Fayache, G., Schottlaender, L. V, Nehdi, H., Gibbs, J. R., Arepalli, S. K., Chong, S. B., Hernandez, D. G., Sailer, A., Liu, G., Mistry, P. K., Cai, H., Shrader, G., Sassi, C., Bouhlal, Y., Houlden, H., Hentati, F., Amouri, R., and Singleton, A. B. (2013). Mutations in GBA2 cause autosomal-recessive cerebellar ataxia with spasticity. *American Journal of Human Genetics*, 92(2), 245–251. <https://doi.org/10.1016/j.ajhg.2012.12.012>
- Han, J., Zhong, C. Q., and Zhang, D. W. (2011). Programmed necrosis: backup to and competitor with apoptosis in the immune system. *Nature Immunology*, 12(12), 1143–1149. <https://doi.org/10.1038/ni.2159>
- Hanahan, D. (2022). Hallmarks of cancer: new dimensions. *Cancer Discovery*, 12, 31–46. <https://doi.org/10.1158/2159-8290.CD-21-1059>
- Heitman, E., and Ingram, D. K. (2017). Cognitive and neuroprotective effects of chlorogenic acid. *Nutritional Neuroscience*, 20(1), 32–39. <https://doi.org/10.1179/1476830514Y.0000000146>
- Henrissat, B. (1991). A classification of glycosyl hydrolases based on amino acid sequence similarities. *Biochemical Journal*, 280(2), 309–316. <https://doi.org/10.1042/bj2800309>
- Henrissat, B., and Davies, G. J. (2000). Glycoside hydrolases and glycosyltransferases. Families, modules, and implications for genomics. *Plant Physiology*, 124(4), 1515–1519. <https://doi.org/10.1104/pp.124.4.1515>
- Hetz, C. (2012). The unfolded protein response: controlling cell fate decisions under ER stress and beyond. *Nature Reviews Molecular Cell Biology*, 13(2), 89–102. <https://doi.org/10.1038/nrm3270>
- Hetz, C., Zhang, K., and Kaufman, R. J. (2020). Mechanisms, regulation and functions of the unfolded protein response. *Nature Reviews Molecular Cell Biology*, 21(8), 421–438. <https://doi.org/10.1038/s41580-020-0250-z>
- Hofmann, K., Bucher, P., Falquet, L., and Bairoch, A. (1999). The PROSITE database, its

- status in 1999. *Nucleic Acids Research*, 27(1), 215–219. <https://doi.org/10.1093/nar/27.1.215>
- Hole, A. S., Rud, I., Grimmer, S., Sigl, S., Narvhus, J., and Sahlstrøm, S. (2012). Improved bioavailability of dietary phenolic acids in whole grain barley and oat groat following fermentation with probiotic *Lactobacillus acidophilus*, *Lactobacillus johnsonii*, and *Lactobacillus reuteri*. *Journal of Agricultural and Food Chemistry*, 60(25), 6369–6375. <https://doi.org/10.1021/jf300410h>
- Hommelaj, G., Withers, S. G., Chuenchor, W., Ketudat-Cairns, J. R., and Svasti, J. (2007). Enzymatic synthesis of cello-oligosaccharides by rice BGlu1  $\beta$ -glucosidase glycosynthase mutants. *Glycobiology*, 17(7), 744–753. <https://doi.org/10.1093/glycob/cwm039>
- Hruska, K. S., LaMarca, M. E., Scott, C. R., and Sidransky, E. (2008). Gaucher disease: Mutation and polymorphism spectrum in the glucocerebrosidase gene (GBA). *Human Mutation*, 29(5), 567–583. <https://doi.org/10.1002/humu.20676>
- Hua, Y., Sansenya, S., Saetang, C., Wakuta, S., and Ketudat-Cairns, J. R. (2013). Enzymatic and structural characterization of hydrolysis of gibberellin A4 glucosyl ester by a rice  $\beta$ -D-glucosidase. *Archives of Biochemistry and Biophysics*, 537(1), 39–48. <https://doi.org/10.1016/j.abb.2013.06.005>
- Hulo, N., Bairoch, A., Bulliard, V., Cerutti, L., De Castro, E., Langendijk-Genevaux, P. S., Pagni, M., and Sigrist, C. J. A. (2006). The PROSITE database. *Nucleic Acids Research*, 34, 227–230. <https://doi.org/10.1093/nar/gkj063>
- Hydbring, P., Malumbres, M., and Sicinski, P. (2016). Non-canonical functions of cell cycle cyclins and cyclin-dependent kinases. *Nature Reviews Molecular Cell Biology*, 17(5), 280–292. <https://doi.org/10.1038/nrm.2016.27>
- Ichim, G., and Tait, S. W. G. (2016). A fate worse than death: apoptosis as an oncogenic process. *Nature Reviews Cancer*, 16(8), 539–548. <https://doi.org/10.1038/nrc.2016.58>
- Irakli, M. N., Samanidou, V. F., Biliaderis, C. G., and Papadoyannis, I. N. (2012). Simultaneous determination of phenolic acids and flavonoids in rice using solid-phase extraction and RP-HPLC with photodiode. *Journal of Separation Science*,

- 35, 1603–1611. <https://doi.org/10.1002/jssc.201200140>
- Iriti, M., and Faoro, F. (2010). Bioactive chemicals and health benefits of grapevine products. In R. R. Watson and V. R. Preedy (Eds.), *Bioactive Foods in Promoting Health*, (pp. 581–620). Academic Press. <https://doi.org/https://doi.org/10.1016/B978-0-12-374628-3.00038-4>
- Isidan, A., Yenigun, A., Soma, D., Aksu, E., Lopez, K., Park, Y., Cross-Najafi, A., Li, P., Kundu, D., House, M. G., Chakraborty, S., Glaser, S., Kennedy, L., Francis, H., Zhang, W., Alpini, G., and Ekser, B. (2022). Development and characterization of human primary cholangiocarcinoma cell lines. *The American Journal of Pathology*, *192*(9), 1200–1217. <https://doi.org/10.1016/j.ajpath.2022.05.007>
- Jaiswal, M., LaRusso, N. F., Burgart, L. J., and Gores, G. J. (2000). Inflammatory cytokines induce DNA damage and inhibit DNA repair in cholangiocarcinoma cells by a nitric oxide-dependent mechanism. *Cancer Research*, *60*(1), 184–190.
- Jenkins, J., Lo Leggio, L., Harris, G., and Pickersgill, R. (1995).  $\beta$ -Glucosidase,  $\beta$ -galactosidase, family A cellulases, family F xylanases and two barley glycanases form a superfamily of enzymes with 8-fold  $\beta/\alpha$  architecture and with two conserved glutamates near the carboxy-terminal ends of  $\beta$ -strands four and seven. *FEBS Letters*, *362*(3), 281–285. [https://doi.org/10.1016/0014-5793\(95\)00252-5](https://doi.org/10.1016/0014-5793(95)00252-5)
- Julian, L. M., and Blais, A. (2015). Transcriptional control of stem cell fate by E2Fs and pocket proteins. *Frontiers in Genetics*, *6*, 1–15. <https://doi.org/10.3389/fgene.2015.00161>
- Kang, H. K., Seo, C. H., and Park, Y. (2015). The effects of marine carbohydrates and glycosylated compounds on human health. *International Journal of Molecular Sciences*, *16*, 6018–6056. <https://doi.org/10.3390/ijms16036018>
- Kang, Y. H., Yi, M. J., Kim, M. J., Park, M. T., Bae, S., Kang, C. M., Cho, C. K., Park, I. C., Park, M. J., Rhee, C. H., Hong, S. I., Chung, H. Y., Lee, Y. S., and Lee, S. J. (2004). Caspase-independent cell death by arsenic trioxide in human cervical cancer cells: reactive oxygen species-mediated poly(ADP-ribose) polymerase-1 activation signals apoptosis-inducing factor release from mitochondria. *Cancer Research*,

- 64(24), 8960–8967. <https://doi.org/10.1158/0008-5472.CAN-04-1830>
- Ketudat-Cairns, J. R., and Esen, A. (2010).  $\beta$ -Glucosidases. *Cellular and Molecular Life Sciences*, 67(20), 3389–3405. <https://doi.org/10.1007/s00018-010-0399-2>
- Ketudat-Cairns, J. R., Mahong, B., Baiya, S., and Jeon, J. S. (2015).  $\beta$ -Glucosidases: multitasking, moonlighting or simply misunderstood? *Plant Science*, 241, 246–259. <https://doi.org/10.1016/j.plantsci.2015.10.014>
- Ketudat-Cairns, J. R., Pengthaisong, S., Luang, S., Sansenya, S., Tankratok, A., and Svasti, J. (2012). Protein-carbohydrate interactions leading to hydrolysis and transglycosylation in plant glycoside hydrolase family 1 enzymes. *Journal of Applied Glycoscience*, 59(2), 51–62. <https://doi.org/10.5458/jag.jag.JAG-2011>
- Khan, H., Saeedi, M., Nabavi, S. M., Mubarak, M. S., and Bishayee, A. (2019). Glycosides from medicinal plants as potential anticancer agents: emerging trends towards future drugs. *Current Medicinal Chemistry*, 26(13), 2389–2406. <https://doi.org/10.2174/0929867325666180403145137>
- Khan, S. A., Tavolari, S., and Brandi, G. (2019). Cholangiocarcinoma: epidemiology and risk factors. *Liver International*, 39, 19–31. <https://doi.org/10.1111/liv.14095>
- Kim, R., Emi, M., and Tanabe, K. (2006). Role of mitochondria as the gardens of cell death. *Cancer Chemotherapy and Pharmacology*, 57(5), 545–553. <https://doi.org/10.1007/s00280-005-0111-7>
- Koga, J., Yazawa, M., Miyamoto, K., Yumoto, E., Kubota, T., Sakazawa, T., Hashimoto, S., Sato, M., and Yamane, H. (2021). Sphingadienine-1-phosphate levels are regulated by a novel glycoside hydrolase family 1 glucocerebrosidase widely distributed in seed plants. *Journal of Biological Chemistry*, 297(5), 1–18. <https://doi.org/10.1016/j.jbc.2021.101236>
- Komvongsa, J., Luang, S., Marques, J. V., Phasai, K., Davin, L. B., Lewis, N. G., and Ketudat-Cairns, J. R. (2015a). Active site cleft mutants of Os9BGlu31 transglucosidase modify acceptor substrate specificity and allow production of multiple kaempferol glycosides. *Biochimica et Biophysica Acta - General Subjects*, 1850(7), 1405–1414. <https://doi.org/10.1016/j.bbagen.2015.03.013>
- Komvongsa, J., Mahong, B., Phasai, K., Hua, Y., Jeon, J. S., and Ketudat-Cairns, J. R.

- (2015b). Identification of fatty acid glucose esters as Os9BGlu31 transglucosidase substrates in rice flag leaves. *Journal of Agricultural and Food Chemistry*, 63(44), 9764–9769. <https://doi.org/10.1021/acs.jafc.5b04105>
- Koul, H. K., Pal, M., and Koul, S. (2013). Role of p38 MAP kinase signal transduction in solid tumors. *Genes and Cancer*, 4(9), 342–359. <https://doi.org/10.1177/1947601913507951>
- Kroemer, G., Galluzzi, L., and Brenner, C. (2007). Mitochondrial membrane permeabilization in cell death. *Physiological Reviews*, 87(1), 99–163. <https://doi.org/10.1152/physrev.00013.2006>
- Kumar, B. S., Singh, S., and Verma, R. (2017). Anticancer potential of dietary vitamin D and ascorbic acid: a review. *Critical Reviews in Food Science and Nutrition*, 57(12), 2623–2635. <https://doi.org/10.1080/10408398.2015.1064086>
- Kumar, N., and Goel, N. (2019). Phenolic acids: natural versatile molecules with promising therapeutic applications. *Biotechnology Reports*, 24, 1–10. <https://doi.org/10.1016/j.btre.2019.e00370>
- Kunkel, T. A. (1985). Rapid and efficient site-specific mutagenesis without phenotypic selection. *Proceedings of the National Academy of Sciences*, 82(2), 488–492. <https://doi.org/10.1073/pnas.82.2.488>
- Kuntothom, T., Luang, S., Harvey, A. J., Fincher, G. B., Opassiri, R., Hrmova, M., and Ketudat-Cairns, J. R. (2009). Rice family GH1 glycoside hydrolases with  $\beta$ -D-glucosidase and  $\beta$ -D-mannosidase activities. *Archives of Biochemistry and Biophysics*, 491(1), 85–95. <https://doi.org/10.1016/j.abb.2009.09.004>
- Lairson, L. L., and Withers, S. G. (2004). Mechanistic analogies amongst carbohydrate modifying enzymes. *Chemical Communications*, 20, 2243–2248. <https://doi.org/10.1039/B406490A>
- Leal-Esteban, L. C., and Fajas, L. (2020). Cell cycle regulators in cancer cell metabolism. *Biochimica et Biophysica Acta (BBA) - Molecular Basis of Disease*, 1866(5), 1–10. <https://doi.org/10.1016/j.bbadis.2020.165715>
- Lee, J., Jang D. S., Kim, N. H., Lee, Y. M., Kim, J., and Kim, J. S. (2011). Galloyl glucoses from the seeds of *Cornus officinalis* with inhibitory activity against protein

- glycation, aldose reductase, and cataractogenesis *ex vivo*. *Biological and Pharmaceutical Bulletin*, *34*(3), 443–446. <https://doi.org/10.1248/bpb.34.443>
- Lee, J., Lee, J., Kim, S. J., and Kim, J. H. (2016). Quercetin-3-*O*-glucoside suppresses pancreatic cancer cell migration induced by tumor-deteriorated growth factors *in vitro*. *Oncology Reports*, *35*, 2473–2479. <https://doi.org/10.3892/or.2016.4598>
- Li, L., Chang, K. C., Zhou, Y., Shieh, B., Ponder, J., Abraham, A. D., Ali, H., Snow, A., Petrash, J. M., and LaBarbera, D. V. (2014). Design of an amide *N*-glycoside derivative of  $\beta$ -glucogallin: a stable, potent, and specific inhibitor of aldose reductase. *Journal of Medicinal Chemistry*, *57*(1), 71–77. <https://doi.org/10.1021/jm401311d>
- Li, X., Chen, D., Wang, G., and Lu, Y. (2015). Probing the interaction of human serum albumin with DPPH in the absence and presence of the eight antioxidants. *Spectrochimica Acta Part A: Molecular and Biomolecular Spectroscopy*, *137*, 1144–1152. <https://doi.org/10.1016/j.saa.2014.08.140>
- Lim, E. K., Doucet, C. J., Hou, B., Jackson, R. G., Abrams, S. R., and Bowles, D. J. (2005). Resolution of (+)-abscisic acid using an *Arabidopsis* glycosyltransferase. *Tetrahedron: Asymmetry*, *16*(1), 143–147. <https://doi.org/10.1016/j.tetasy.2004.11.062>
- Lim, S., and Kaldis, P. (2013). Cdks, cyclins and CKIs: roles beyond cell cycle regulation. *Development*, *140*(15), 3079–3093. <https://doi.org/10.1242/dev.091744>
- Limas, J. C., and Cook, J. G. (2019). Preparation for DNA replication: the key to a successful S phase. *FEBS Letters*, *593*(20), 2853–2867. <https://doi.org/10.1002/1873-3468.13619>
- Lin, P., and Lai, H. (2011). Bioactive compounds in rice during grain development. *Food Chemistry*, *127*(1), 86–93. <https://doi.org/10.1016/j.foodchem.2010.12.092>
- Liu, M. M., Ma, R. H., Ni, Z. J., Thakur, K., Cespedes-Acuña, C. L., Jiang, L., and Wei, Z. J. (2020). Apigenin 7-*O*-glucoside promotes cell apoptosis through the PTEN/PI3K/AKT pathway and inhibits cell migration in cervical cancer HeLa cells. *Food and Chemical Toxicology*, *146*, 1–14. <https://doi.org/10.1016/j.fct.2020.111843>

- Livak, K. J., and Schmittgen, T. D. (2001). Analysis of relative gene expression data using real-time quantitative PCR and the  $2^{-\Delta\Delta CT}$  method. *Methods*, 25(2001), 402–408. <https://doi.org/10.1006/meth.2001.1262>
- Llambi, F., Moldoveanu, T., Tait, S. W. G., Bouchier-Hayes, L., Temirov, J., McCormick, L. L., Dillon, C. P., and Green, D. R. (2011). A unified model of mammalian BCL-2 protein family interactions at the mitochondria. *Molecular Cell*, 44(4), 517–531. <https://doi.org/10.1016/j.molcel.2011.10.001>
- Loader, T. B., Taylor, C. G., Zahradka, P., and Jones, P. J. H. (2017). Chlorogenic acid from coffee beans: evaluating the evidence for a blood pressure–regulating health claim. *Nutrition Reviews*, 75(2), 114–133. <https://doi.org/10.1093/nutrit/nuw057>
- Lombard, V., Golaconda Ramulu, H., Drula, E., Coutinho, P. M., and Henrissat, B. (2014). The carbohydrate-active enzymes database (CAZy) in 2013. *Nucleic Acids Research*, 42, 490–495. <https://doi.org/10.1093/nar/gkt1178>
- Los, M., Mozoluk, M., Ferrari, D., Stepczynska, A., Stroh, C., Renz, A., Herceg, Z., Wang, Z. Q., and Schulze-Osthoff, K. (2002). Activation and caspase-mediated inhibition of PARP: a molecular switch between fibroblast necrosis and apoptosis in death receptor signaling. *Molecular Biology of the Cell*, 13(3), 978–988. <https://doi.org/10.1091/mbc.01-05-0272>
- Luang, S., Cho, J. I., Mahong, B., Opassiri, R., Akiyama, T., Phasai, K., Komvongsa, J., Sasaki, N., Hua, Y. L., Matsuba, Y., Ozeki, Y., Jeon, J. S., and Ketudat-Cairns, J. R. (2013). Rice Os9BGlu31 is a transglucosidase with the capacity to equilibrate phenylpropanoid, flavonoid, and phytohormone glycoconjugates. *Journal of Biological Chemistry*, 288(14), 10111–10123. <https://doi.org/10.1074/jbc.M112.423533>
- Ma, Y. L., Zhang, Y. S., Zhang, F., Zhang, Y. Y., Thakur, K., Zhang, J. G., and Wei, Z. J. (2019). Methyl protodioscin from *Polygonatum sibiricum* inhibits cervical cancer through cell cycle arrest and apoptosis induction. *Food and Chemical Toxicology*, 132, 1–9. <https://doi.org/10.1016/j.fct.2019.110655>
- Mandal, S. M., Chakraborty, D., and Dey, S. (2010). Phenolic acids act as signaling molecules in plant-microbe symbioses. *Plant Signaling and Behavior*, 5(4), 359–

368. <https://doi.org/10.4161/psb.5.4.10871>
- Mansoori, B., Mohammadi, A., Davudian, S., Shirjang, S., and Baradaran, B. (2017). The different mechanisms of cancer drug resistance: a brief review. *Tabriz University of Medical Sciences*, 7(3), 339–348. <https://doi.org/10.15171/apb.2017.041>
- Mao, J., Hu, Y., Ruan, L., Ji, Y., and Lou, Z. (2019). Role of endoplasmic reticulum stress in depression. *Molecular Medicine Report*, 20(6), 4774–4780. <https://doi.org/10.3892/mmr.2019.10789>
- Marana, S. R., Jacobs-Lorena, M., Terra, W. R., and Ferreira, C. (2001). Amino acid residues involved in substrate binding and catalysis in an insect digestive  $\beta$ -glycosidase. *Biochimica et Biophysica Acta (BBA) - Protein Structure and Molecular Enzymology*, 1545(1), 41–52. [https://doi.org/10.1016/S0167-4838\(00\)00260-0](https://doi.org/10.1016/S0167-4838(00)00260-0)
- Marchiosi, R., dos Santos, W. D., Constantin, R. P., de Lima, R. B., Soares, A. R., Finger-Teixeira, A., Mota, T. R., de Oliveira, D. M., Foletto-Felipe, M. P., Abrahão, J., and Ferrarese-Filho, O. (2020). Biosynthesis and metabolic actions of simple phenolic acids in plants. *Phytochemistry Reviews*, 19(4), 865–906. <https://doi.org/10.1007/s11101-020-09689-2>
- Martin, E., Schüle, R., Smets, K., Rastetter, A., Boukhris, A., Loureiro, J. L., Gonzalez, M. A., Mundwiller, E., Deconinck, T., Wessner, M., Jornea, L., Oteyza, A. C., Durr, A., Martin, J. J., Schöls, L., Mhiri, C., Lamari, F., Züchner, S., De Jonghe, P., ... Stevanin, G. (2013). Loss of function of glucocerebrosidase GBA2 is responsible for motor neuron defects in hereditary spastic paraplegia. *American Journal of Human Genetics*, 92(2), 238–244. <https://doi.org/10.1016/j.ajhg.2012.11.021>
- Martínez-Torres, A. C., Reyes-Ruiz, A., Benítez-Londoño, M., Franco-Molina, M. A., and Rodríguez-Padilla, C. (2018). IMMUNEPOTENT CRP induces cell cycle arrest and caspase-independent regulated cell death in HeLa cells through reactive oxygen species production. *BMC Cancer*, 18(1), 1–13. <https://doi.org/10.1186/s12885-017-3954-5>
- Matern, H., Boermans, H., Lottspeich, F., and Matern, S. (2001). Molecular cloning and expression of human bile acid  $\beta$ -glucosidase. *Journal of Biological Chemistry*,

- 276(41), 37929–37933. <https://doi.org/10.1074/jbc.M104290200>
- Mathiasen, I. S., Sergeev, I. N., Bastholm, L., Elling, F., Norman, A. W., and Jäättelä, M. (2002). Calcium and calpain as key mediators of apoptosis-like death induced by vitamin D compounds in breast cancer cells. *Journal of Biological Chemistry*, 277(34), 30738–30745. <https://doi.org/10.1074/jbc.M201558200>
- Matsuba, Y., Sasaki, N., Tera, M., Okamura, M., Abe, Y., Okamoto, E., Nakamura, H., Funabashi, H., Takatsu, M., Saito, M., Matsuoka, H., Nagasawa, K., and Ozeki, Y. (2010). A novel glucosylation reaction on anthocyanins catalyzed by acyl-glucose-dependent glucosyltransferase in the petals of carnation and delphinium. *The Plant Cell*, 22, 3374–3389. <https://doi.org/10.1105/tpc.110.077487>
- Mehmet, H. (2000). Caspases find a new place to hide. *Nature*, 403(6765), 29–30. <https://doi.org/10.1038/47377>
- Méndez-Liter, J. A., Tundidor, I., Nieto-Domínguez, M., de Toro, B. F., González-Santana, A., de Eugenio, L. I., Prieto, A., Asensio, J. L., Sánchez, C., and Martínez, M. J. (2019). Transglycosylation products generated by *Talaromyces amestolkiae* GH3  $\beta$ -glucosidases: effect of hydroxytyrosol, vanillin and its glucosides on breast cancer cells. *Microbial Cell Factories*, 18(1), 1–12. <https://doi.org/10.1186/s12934-019-1147-4>
- Miyahara, T., Sakiyama, R., Ozeki, Y., and Sasaki, N. (2013). Acyl-glucose-dependent glucosyltransferase catalyzes the final step of anthocyanin formation in *Arabidopsis*. *Journal of Plant Physiology*, 170(6), 619–624. <https://doi.org/10.1016/j.jplph.2012.12.001>
- Mizushima, N., and Yoshimori, T. (2007). How to Interpret LC3 Immunoblotting. *Autophagy*, 3(6), 542–545. <https://doi.org/10.4161/auto.4600>
- Moellering, E. R., and Benning, C. (2011). Galactoglycerolipid metabolism under stress: a time for remodeling. *Trends in Plant Science*, 16(2), 98–107. <https://doi.org/10.1016/j.tplants.2010.11.004>
- Moellering, E. R., Muthan, B., and Benning, C. (2010). Freezing tolerance in plants requires lipid remodeling at the outer chloroplast membrane. *Science*, 330(6001), 226–228. <https://doi.org/10.1126/science.1191803>

- Moradi, S. V., Hussein, W. M., Varamini, P., Simerska, P., and Toth, I. (2016). Glycosylation, an effective synthetic strategy to improve the bioavailability of therapeutic peptides. *Chemical Science*, 7, 2492–2500. <https://doi.org/10.1039/c5sc04392a>
- Morton, L. W., Caccetta, R. A., Puddey, I. B., and Croft, K. D. (2000). Chemistry and biological effects of dietary phenolic compounds: relevance to cardiovascular disease. *Clinical and Experimental Pharmacology and Physiology*, 27(3), 152–159. <https://doi.org/10.1046/j.1440-1681.2000.03214.x>
- Mullegger, J., Jahn, M., Chen, H. M., Mu, J., Warren, R. A. J., and Withers, S. G. (2005). Engineering of a thioglycosylase: randomized mutagenesis of the acid-base residue leads to the identification of improved catalysts. *Protein Engineering, Design and Selection*, 18(1), 33–40. <https://doi.org/10.1093/protein/gzi003>
- Nam, S. H., Park, J., Jun, W., Kim, D., Ko, J. A., Abd El-Aty, A., Choi, J. Y., Kim, D. I., and Yang, K. Y. (2017). Transglycosylation of gallic acid by using *Leuconostoc* glucansucrase and its characterization as a functional cosmetic agent. *AMB Express*, 7(1), 1–10. <https://doi.org/10.1186/s13568-017-0523-x>
- Nam, T. W., Yoo, C. I., Kim, H. T., Kwon, C. H., Park, J. Y., and Kim, Y. K. (2008). The flavonoid quercetin induces apoptosis and inhibits migration through a MAPK-dependent mechanism in osteoblasts. *Journal of Bone and Mineral Metabolism*, 26, 551–560. <https://doi.org/10.1007/s00774-008-0864-2>
- Naradun, N., Talabnin, K., Ayuttha, K. I., and Talabnin, C. (2022). Piperlongumine and bortezomib synergically inhibit cholangiocarcinoma via ER stress-induced cell death. *Naunyn-Schmiedeberg's Archives of Pharmacology*, 396(1), 109–120. <https://doi.org/10.1007/s00210-022-02305-4>
- Nishizaki, Y., Yasunaga, M., Okamoto, E., Okamoto, M., Hirose, Y., Yamaguchi, M., Ozeki, Y., and Sasaki, N. (2013). *p*-Hydroxybenzoyl-glucose is a zwitter donor for the biosynthesis of 7-polyacylated anthocyanin in delphinium. *The Plant Cell*, 25(10), 4150–4165. <https://doi.org/10.1105/tpc.113.113167>
- Niyonizigiye, I., Ngabire, D., Patil, M. P., Singh, A. A., and Kim, G. D. (2019). *In vitro* induction of endoplasmic reticulum stress in human cervical adenocarcinoma HeLa cells by fucoidan. *International Journal of Biological Macromolecules*, 137,

- 844–852. <https://doi.org/10.1016/j.ijbiomac.2019.07.043>
- Nokin, M., Bellier, J., Durieux, F., Peulen, O., Rademaker, G., Gabriel, M., Monseur, C., Charloteaux, B., Verbeke, L., Laere, S. Van, Roncarati, P., Herfs, M., Lambert, C., Scheijen, J., Schalkwijk, C., Colige, A., Caers, J., Delvenne, P., Turtoi, A., ... Bellahcène, A. (2019). Methylglyoxal, a glycolysis metabolite, triggers metastasis through MEK/ERK/SMAD1 pathway activation in breast cancer. *Breast Cancer Research*, *21*(11), 1–19. <https://doi.org/10.1186/s13058-018-1095-7>
- Opassiri, R., Hua, Y., Wara-Aswapati, O., Akiyama, T., Svasti, J., Esen, A., and Ketudat-Cairns, J. R. (2004).  $\beta$ -Glucosidase, exo- $\beta$ -glucanase and pyridoxine transglucosylase activities of rice BGLu1. *Biochemical Journal*, *379*(1), 125–131. <https://doi.org/10.1042/bj20031485>
- Opassiri, R., Ketudat-Cairns, J. R., Akiyama, T., Wara-Aswapati, O., Svasti, J., and Esen, A. (2003). Characterization of a rice  $\beta$ -glucosidase highly expressed in flower and germinating shoot. *Plant Science*, *165*(3), 627–638. [https://doi.org/10.1016/S0168-9452\(03\)00235-8](https://doi.org/10.1016/S0168-9452(03)00235-8)
- Opassiri, R., Maneesan, J., Akiyama, T., Pomthong, B., Jin, S., Kimura, A., and Ketudat-Cairns, J. R. (2010). Rice Os4BGLu12 is a wound-induced  $\beta$ -glucosidase that hydrolyzes cell wall- $\beta$ -glucan-derived oligosaccharides and glycosides. *Plant Science*, *179*(3), 273–280. <https://doi.org/10.1016/j.plantsci.2010.05.013>
- Opassiri, R., Pomthong, B., Onkoksoong, T., Akiyama, T., Esen, A., and Ketudat-Cairns, J. R. (2006). Analysis of rice glycosyl hydrolase family 1 and expression of Os4BGLu12  $\beta$ -glucosidase. *BMC Plant Biology*, *19*(6), 1–19. <https://doi.org/10.1186/1471-2229-6-33>
- Panawan, O., Silsirivanit, A., Chang, C. H., Putthisen, S., Boonnate, P., Yokota, T., Nishiyama-Ikeda, Y., Detarya, M., Sawanyawisuth, K., Kaewkong, W., Muisuk, K., Luang, S., Vaeteewoottacharn, K., Kariya, R., Yano, H., Komohara, Y., Ohta, K., Okada, S., Wongkham, S., and Araki, N. (2023). Establishment and characterization of a novel cancer stem-like cell of cholangiocarcinoma. *Cancer Science*, *114*(8), 3230–3246. <https://doi.org/10.1111/cas.15812>
- Pandey, R. P., Gurung, R. B., Parajuli, P., Koirala, N., Tuoi, L. T., and Sohng, J. K. (2014).

- Assessing acceptor substrate promiscuity of YjiC-mediated glycosylation toward flavonoids. *Carbohydrate Research*, 393, 26–31. <https://doi.org/10.1016/j.carres.2014.03.011>
- Park, C. M., and Song, Y. (2019). Luteolin and luteolin-7-O-glucoside protect against acute liver injury through regulation of inflammatory mediators and antioxidative enzymes in GalN/LPS-induced hepatitic ICR mice. *Nutrition Research and Practice*, 13(6), 473–479. <https://doi.org/10.4162/nrp.2019.13.6.473>
- Park, D. D., Phoomak, C., Xu, G., Olney, L. P., Tran, K. A., Park, S. S., Haigh, N. E., Luxardi, G., Lert-Itthiporn, W., Shimoda, M., Li, Q., Matoba, N., Fierro, F., Wongkham, S., Maverakis, E., and Lebrilla, C. B. (2020). Metastasis of cholangiocarcinoma is promoted by extended high-mannose glycans. *Proceedings of the National Academy of Sciences of The United State of America*, 117(14), 7633–7644. <https://doi.org/10.1073/pnas.1916498117>
- Park, S. Y., Ha, S. H., Lim, S. H., Jung, J. Y., Lee, S. M., Yeo, Y., and Kim, J. K. (2012). Determination of phenolic acids in Korean rice (*Oryza sativa* L.) cultivars using gas chromatography-time-of-flight mass spectrometry. *Food Science and Biotechnology*, 21(4), 1141–1148. <https://doi.org/10.1007/s10068-012-0149-3>
- Parr, A. J., and Bolwell, G. P. (2000). Phenols in the plant and in man. The potential for possible nutritional enhancement of the diet by modifying the phenols content or profile. *Journal of the Science of Food and Agriculture*, 80, 985–1012. [https://doi.org/10.1002/\(SICI\)1097-0010\(20000515\)80:7](https://doi.org/10.1002/(SICI)1097-0010(20000515)80:7)
- Patel, T. (2011). Cholangiocarcinoma-controversies and challenges. *Nature Reviews Gastroenterology and Hepatology*, 8(4), 189–200. <https://doi.org/10.1038/nrgastro.2011.20>
- Pengthaisong, S., and Ketudat-Cairns, J. R. (2014). Effects of active site cleft residues on oligosaccharide binding, hydrolysis, and glycosynthase activities of rice BGlu1 and its mutants. *Protein Science*, 23, 1738–1752. <https://doi.org/10.1002/pro.2556>
- Peracchi, A. (2001). Enzyme catalysis: removing chemically ‘essential’ residues by site-directed mutagenesis. *Trends in Biochemical Sciences*, 26(8), 497–503. [https://doi.org/10.1016/S0968-0004\(01\)01911-9](https://doi.org/10.1016/S0968-0004(01)01911-9)

- Pergolizzi, G., Dedola, S., and Field, R. A. (2017). Contemporary glycoconjugation chemistry. *Carbohydrate Chemistry*, 42, 1–46. <https://doi.org/10.1039/9781782626657-00001>
- Perillo, B., Donato, M. D., Pezone, A., Zazzo, E. D., Castoria, G., and Migliaccio, A. (2020). ROS in cancer therapy: the bright side of the moon. *Experimental and Molecular Medicine*, 52, 192–203. <https://doi.org/10.1038/s12276-020-0384-2>
- Pinlaor, S., Yongvanit, P., Hiraku, Y., Ma, N., Semba, R., Oikawa, S., Murata, M., Sripa, B., Sithithaworn, P., and Kawanishi, S. (2003). 8-Nitroguanine formation in the liver of hamsters infected with *Opisthorchis viverrini*. *Biochemical and Biophysical Research Communications*, 309(3), 567–571. <https://doi.org/10.1016/j.bbrc.2003.08.039>
- Pourakbari, R., Taher, S. M., Mosayyebi, B., Ayoubi-joshaghani, M. H., Ahmadi, H., and Aghebati-Maleki, L. (2020). Implications for glycosylated compounds and their anti-cancer effects. *International Journal of Biological Macromolecules*, 163, 1323–1332. <https://doi.org/10.1016/j.ijbiomac.2020.06.281>
- Puppala, M., Ponder, J., Suryanarayana, P., Reddy, G. B., Petrash, M., and Labarbera, D. (2012). The isolation and characterization of  $\beta$ -glucogallin as a novel aldose reductase inhibitor from *Emblica officinalis*. *PLoS ONE*, 7(4), 1–9. <https://doi.org/10.1371/journal.pone.0031399>
- Rather, M. Y., and Mishra, S. (2013).  $\beta$ -Glycosidases: an alternative enzyme based method for synthesis of alkyl-glycosides. *Sustainable Chemical Processes*, 1(7), 1–15. <https://doi.org/10.1186/2043-7129-1-7>
- Rattanachitthawat, S., Suwannalert, P., Riengrojpitak, S., Chaiyasut, C., and Pantuwatana, S. (2010). Phenolic content and antioxidant activities in red unpolished Thai rice prevents oxidative stress in rats. *Journal of Medicinal Plants Research*, 4(9), 796–801. <https://doi.org/10.5897/JMPR10.067>
- Razumilava, N., and Gores, G. J. (2014). Cholangiocarcinoma. *The Lancet*, 383(9935), 2168–2179. [https://doi.org/10.1016/S0140-6736\(13\)61903-0](https://doi.org/10.1016/S0140-6736(13)61903-0)
- Rehan, M. (2021). Biosynthesis of diverse class flavonoids via shikimate and phenylpropanoid pathway. In L. Q. Zepka, T. C. do Nascimento, and E. Jacob-

- Lopes (Eds.), *Bioactive compounds - biosynthesis, characterization and applications* (p. Ch. 6). IntechOpen. <https://doi.org/10.5772/intechopen.96512>
- Rempel, B. P., and Withers, S. G. (2008). Covalent inhibitors of glycosidases and their applications in biochemistry and biology. *Glycobiology*, *18*(8), 570–586. <https://doi.org/10.1093/glycob/cwn041>
- Rizvi, S., Eaton, J., Yang, J. D., Chandrasekhara, V., and Gores, G. J. (2018). Emerging technologies for the diagnosis of perihilar cholangiocarcinoma. *Seminar in Liver Disease*, *38*(2), 160–169. <https://doi.org/10.1055/s-0038-1655775>
- Rizvi, S., and Gores, G. J. (2013). Pathogenesis, diagnosis, and management of cholangiocarcinoma. *Gastroenterology*, *145*(6), 1215–1229. <https://doi.org/10.1053/j.gastro.2013.10.013>
- Rouyi, C., Baiya, S., Lee, S., Mahong, B., Jeon, J., and Ketudat-Cairns, J. R. (2014). Recombinant expression and characterization of the cytoplasmic rice  $\beta$ -Glucosidase Os1BGlu4. *PLoS One*, *9*(5), 1–13. <https://doi.org/10.1371/journal.pone.0096712>
- Sammar, M., Abu-Farich, B., Rayan, I., Falah, M., and Rayan, A. (2019). Correlation between cytotoxicity in cancer cells and free radical-scavenging activity: *in vitro* evaluation of 57 medicinal and edible plant extracts. *Oncology Letters* *18*(6), 6563–6571. <https://doi.org/10.3892/ol.2019.11054>
- Santana-Gálvez, J., Cisneros-Zevallos, L., and Jacobo-Velázquez, D. A. (2017). Chlorogenic acid: recent advances on its dual role as a food additive and a nutraceutical against metabolic syndrome. *Molecules* *22*(3), 1–21. <https://doi.org/10.3390/molecules22030358>
- Sasaki, N., Nishizaki, Y., Ozeki, Y., and Miyahara, T. (2014). The role of acyl-glucose in anthocyanin modifications. *Molecules*, *19*(11), 18747–18766. <https://doi.org/10.3390/molecules191118747>
- Seshadri, S., Akiyama, T., Opassiri, R., Kuaprasert, B., and Ketudat-Cairns, J. R. (2009). Structural and enzymatic characterization of Os3BGlu6, a rice  $\beta$ -glucosidase hydrolyzing hydrophobic glycosides and (1 $\rightarrow$ 3)- and (1 $\rightarrow$ 2)-linked disaccharides. *Plant Physiology*, *151*(1), 47–58. <https://doi.org/10.1104/pp.109.139436>

- Shao-qiang, L. I., Li-jian, L., Yun-peng, H. U. A., Bao-gang, P., Qiang, H. E., Ming-de, L. U., and Dong, C. (2009). Long-term outcome and prognostic factors of intrahepatic cholangiocarcinoma. *Chinese Medical Journal*, 122(19), 2286–2291. <https://doi.org/10.3760/cma.j.issn.0366-6999.2009.19.018>
- Shao, Y., and Bao, J. (2015). Polyphenols in whole rice grain : genetic diversity and health benefits. *Food Chemistry*, 180, 86–97. <https://doi.org/10.1016/j.foodchem.2015.02.027>
- Sharma, R., Cao, P., Jung, K. H., Sharma, M. K., and Ronald, P. C. (2013). Construction of a rice glycoside hydrolase phylogenomic database and identification of targets for biofuel research. *Frontiers in Plant Science*, 4(330), 1–15. <https://doi.org/10.3389/fpls.2013.00330>
- Shen, T., Cheng, X., Xia, C., Li, Q., Gao, Y., Pan, D., Zhang, X., Zhang, C., and Li, Y. (2019). Erlotinib inhibits colon cancer metastasis through inactivation of TrkB-dependent ERK signaling pathway. *Journal of Cellular Biochemistry*, 120, 11248–11255. <https://doi.org/10.1002/jcb.28400>
- Sherr, C. J., and Roberts, J. M. (1999). CDK inhibitors: positive and negative regulators of G1-phase progression. *Genes and Development*, 13(901), 1501–1512.
- Siloto, R. M. P., and Weselake, R. J. (2012). Site saturation mutagenesis: methods and applications in protein engineering. *Biocatalysis and Agricultural Biotechnology*, 1(3), 181–189. <https://doi.org/10.1016/j.bcab.2012.03.010>
- Silsirivanit, A., Prongvitaya, S., Sawanyawisuth, K., Wongkham, C., and Wongkham, S. (2013). Biomarkers in bile duct cancers: current status. *Srinagarind Medical Journal*, 27, 405–412. <https://li01.tci-thaijo.org/index.php/SRIMEDJ/article/view/11166>
- Silva, A. B., Koistinen, V. M., Mena, P., Bronze, M. R., Hanhineva, K., Sahlstrøm, S., Kitrytè, V., Moco, S., and Marja, A. (2020). Factors affecting intake, metabolism and health benefits of phenolic acids: do we understand individual variability? *European Journal of Nutrition*, 59(4), 1275–1293. <https://doi.org/10.1007/s00394-019-01987-6>
- Sithithaworn, P., Yongvanit, P., Duengngai, K., Kiatsopit, N., and Pairojkul, C. (2014). Roles

- of liver fluke infection as risk factor for cholangiocarcinoma. *Journal of Hepatobiliary Pancreatic Science*, 21(5), 301–308. <https://doi.org/10.1002/jhbp.62>
- Small, W., Bacon, M. A., Bajaj, A., Chuang, L. T., Fisher, B. J., Harkenrider, M. M., Jhingran, A., Kitchener, H. C., Mileskin, L. R., Viswanathan, A. N., and Gaffney, D. K. (2017). Cervical cancer: a global health crisis. *Cancer*, 123, 2404–2412. <https://doi.org/10.1002/cncr.30667>
- Smiljkovic, M., Stanisavljevic, D., Stojkovic, D., Petrovic, I., Vicentic, J. M., Popovic, J., Grdadolnik, S. G., Markovic, D., Sankovic-Barbice, S., Glamoclija, J., Stevanovic, M., and Sokovic, M. (2017). Apigenin-7-O-glucoside versus apigenin: insight into the modes of anticandidal and cytotoxic actions. *EXCLI Journal*, 16, 795–807. <https://doi.org/10.17179/excli2017-300>
- Sripa, B., Bethony, J. M., Sithithaworn, P., Kaewkes, S., Mairiang, E., Loukas, A., Mulvenna, J., Laha, T., Hotez, P. J., and Brindley, P. J. (2011). Opisthorchiasis and Opisthorchis-associated cholangiocarcinoma in Thailand and Laos. *Acta Tropica*, 120, 158–168. <https://doi.org/10.1016/j.actatropica.2010.07.006>
- Sripa, B., Kaewkes, S., Sithithaworn, P., Mairiang, E., Laha, T., Smout, M., Pairojkul, C., Bhudhisawasdi, V., Tesana, S., Thinkamrop, B., Bethony, J. M., Loukas, A., and Brindley, P. J. (2007). Liver fluke induces cholangiocarcinoma. *PLoS Medicine*, 4(7), 1148–1155. <https://doi.org/10.1371/journal.pmed.0040201>
- Sripa, B., Leungwattanawanit, S., Nitta, T., Wongkham, C., Bhudhisawasdi, V., Puapairoj, A., Sripa, C., and Miwa, M. (2005). Establishment and characterization of an opisthorchiasis-associated cholangiocarcinoma cell line (KKU-100). *World Journal of Gastroenterology*, 11(22), 3392–3397. <https://doi.org/10.3748/wjg.v11.i22.3392>
- Sripa, B., and Pairojkul, C. (2008). Cholangiocarcinoma: lessons from Thailand. *Current Opinion in Gastroenterology*, 24(3), 349–356. <https://doi.org/10.1097/MOG.0b013e3282fbf9b3>
- Sripa, B., Seubwai, W., Vaeteewoottacharn, K., Sawanyawisuth, K., Silsirivanit, A., Kaewkong, W., Muisuk, K., Dana, P., Phoomak, C., Lert-itthiporn, W., Luvira, V., Pairojkul, C., Teh, B. T., Wongkham, S., Okada, S., and Chamgramol, Y. (2020). Functional and genetic characterization of three cell lines derived from a single

- tumor of an *Opisthorchis viverrini*-associated cholangiocarcinoma patient. *Human Cell*, 33(3), 695–708. <https://doi.org/10.1007/s13577-020-00334-w>
- Sun, Q., Lu, N. N., and Feng, L. (2018). Apigetrin inhibits gastric cancer progression through inducing apoptosis and regulating ROS-modulated STAT3/JAK2 pathway. *Biochemical and Biophysical Research Communications*, 498(1), 164–170. <https://doi.org/10.1016/j.bbrc.2018.02.009>
- Sun, Y. S., Thakur, K., Hu, F., Cespedes-Acuña, C. L., Zhang, J. G., and Wei, Z. J. (2020). Icariside II suppresses cervical cancer cell migration through JNK modulated matrix metalloproteinase-2/9 inhibition *in vitro* and *in vivo*. *Biomedicine and Pharmacotherapy*, 125, 1–12. <https://doi.org/10.1016/j.biopha.2020.110013>
- Tait, S. W. G., and Green, D. R. (2008). Caspase-independent cell death: leaving the set without the final cut. *Oncogene*, 27(50), 6452–6461. <https://doi.org/10.1038/onc.2008.311>
- Talabnin, C., Talabnin, K., and Wongkham, S. (2020). Enhancement of piperlongumine chemosensitivity by silencing heme oxygenase-1 expression in cholangiocarcinoma cell lines. *Oncology Letters*, 20(3), 2483–2492. <https://doi.org/10.3892/ol.2020.11784>
- Tan, C. P., Lu, Y. Y., Ji, L. N., and Mao, Z. W. (2014). Metallomics insights into the programmed cell death induced by metal-based anticancer compounds. *Metallomics*, 6(5), 978–995. <https://doi.org/10.1039/c3mt00225j>
- Tang, B. O., Liang, W., Liao, Y., Li, Z., Wang, Y., and Yan, C. (2019). PEA15 promotes liver metastasis of colorectal cancer by upregulating the ERK/MAPK signaling pathway. *Oncology Reports*, 41, 43–56. <https://doi.org/10.3892/or.2018.6825>
- Tepsiri, N., Chaturat, L., Sripan, B., Namwat, W., Wongkham, S., Bhudhisawasdi, V., and Tassaneeyakul, W. (2005). Drug sensitivity and drug resistance profiles of human intrahepatic cholangiocarcinoma cell lines. *World Journal of Gastroenterology*, 11(18), 2748–2753. <https://doi.org/10.3748/wjg.v11.i18.2748>
- Teze, D., Hendrickx, J., Czjzek, M., Ropartz, D., Sanejouand, Y. H., Tran, V., Tellier, C., and Dion, M. (2014). Semi-rational approach for converting a GH1  $\beta$ -glycosidase into a  $\beta$ -transglycosidase. *Protein Engineering, Design and Selection*, 27(1), 13–19.

<https://doi.org/10.1093/protein/gzt057>

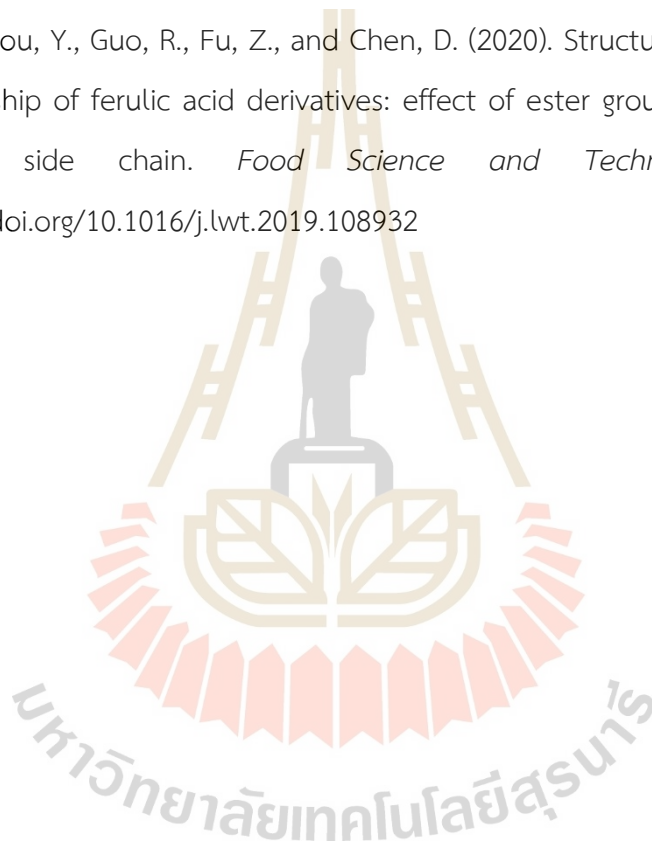
- Teze, D., Hendrickx, J., Dion, M., Tellier, C., Woods, V. L., Tran, V., and Sanejouand, Y. (2013). Conserved water molecules in family 1 glycosidases: a DXMS and molecular dynamics study. *Biochemistry*, *52*(34), 5900–5910. <https://doi.org/10.1021/bi400260b>
- Thanan, R., Murata, M., Pinlaor, S., Sithithaworn, P., Khuntikeo, N., Tangkanakul, W., Hiraku, Y., Oikawa, S., Yongvanit, P., and Kawanishi, S. (2008). Urinary 8-Oxo-7,8-dihydro-2'-deoxyguanosine in patients with parasite infection and effect of antiparasitic drug in relation to cholangiocarcinogenesis. *Cancer Epidemiology, Biomarkers and Prevention*, *17*(3), 518–524. <https://doi.org/10.1158/1055-9965.EPI-07-2717>
- Thapa, S. B., Pandey, R. P., Bashyal, P., Yamaguchi, T., and Sohng, J. K. (2019). Cascade biocatalysis systems for bioactive naringenin glucosides and quercetin rhamnoside production from sucrose. *Applied Microbiology and Biotechnology*, *103*(19), 7953–7969. <https://doi.org/10.1007/s00253-019-10060-5>
- Thongsom, S., Suginta, W., Lee, K. J., Choe, H., and Talabnin, C. (2017). Piperlongumine induces G2/M phase arrest and apoptosis in cholangiocarcinoma cells through the ROS-JNK-ERK signaling pathway. *Apoptosis*, *22*(11), 1473–1484. <https://doi.org/10.1007/s10495-017-1422-y>
- Tian, S., Akamura, K., and Kayahara, H. (2004). Analysis of phenolic compounds in white rice, brown rice, and germinated brown rice. *Journal of Agricultural and Food Chemistry*, *52*, 4808–4813. <https://doi.org/10.1021/jf049446f>
- Tran, L. T., Blay, V., Luang, S., Eurtivong, C., Choknud, S., González-Díaz, H., and Ketudat-Cairns, J. R. (2019). Engineering faster transglycosidases and their acceptor specificity. *Green Chemistry*, *21*(10), 2823–2836. <https://doi.org/10.1039/c9gc00621d>
- Tsao, R. (2010). Chemistry and biochemistry of dietary polyphenols. *Nutrients*, *2*, 1231–1246. <https://doi.org/10.3390/nu2121231>
- Upadhyay, R., and Rao, L. J. M. (2013). An outlook on chlorogenic acids-occurrence, chemistry, technology, and biological activities. *Critical Reviews in Food Science*

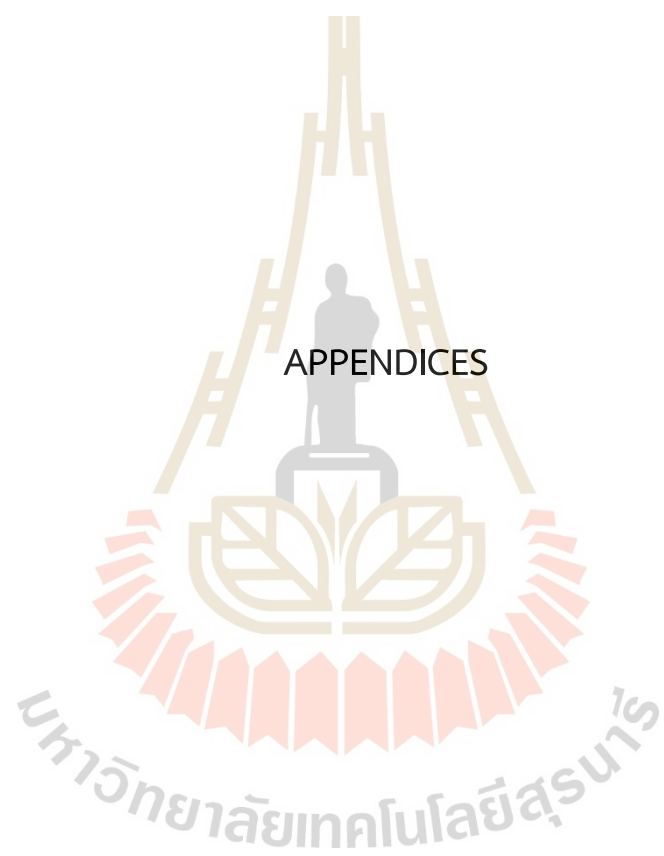
- and Nutrition*, 53(9), 968–984. <https://doi.org/10.1080/10408398.2011.576319>
- Uphoff, C. C., Denkmann, S. A., and Drexler, H. G. (2012). Treatment of mycoplasma contamination in cell cultures with plasmocin. *Journal of Biomedicine and Biotechnology*, 2012, 1–8. <https://doi.org/10.1155/2012/267678>
- Valle, J., Wasan, H., Palmer, D. H., Cunningham, D., Anthoney, A., Maraveyas, A., Madhusudan, S., Iveson, T., Hughes, S., Pereira, S. P., Roughton, M., and Bridgewater, J. (2010). Cisplatin plus gemcitabine versus gemcitabine for biliary tract cancer. *New England Journal of Medicine*, 362(14), 1273–1281. <https://doi.org/10.1056/NEJMoa0908721>
- van Gorkom, G. N., Lookermans, E. L., van Elssen, C. H., and Bos, G. M. (2019). The effect of vitamin C (ascorbic acid) in the treatment of patients with cancer: a systematic review. *Nutrients*, 11(5), 1–15. <https://doi.org/10.3390/nu11050977>
- Velmurugan, B. K., Lin, J. T., Mahalakshmi, B., Chuang, Y. C., Lin, C. C., Lo, Y. S., Hsieh, M. J., and Chen, M. K. (2020). Luteolin-7-O-glucoside inhibits oral cancer cell migration and invasion by regulating matrix metalloproteinase-2 expression and extracellular signal-regulated kinase pathway. *Biomolecules*, 10(4), 1–16. <https://doi.org/10.3390/biom10040502>
- Verma, D. K., and Srivastav, P. P. (2020). Bioactive compounds of rice (*Oryza sativa* L): review on paradigm and its potential benefit in human health. *Trends in Food Science and Technology*, 97, 355–365. <https://doi.org/10.1016/j.tifs.2020.01.007>
- Vichai, V., and Kirtikara, K. (2006). Sulforhodamine B colorimetric assay for cytotoxicity screening. *Nature Protocols*, 1(3), 1112–1116. <https://doi.org/10.1038/nprot.2006.179>
- Vivekanandhan, D. K., Verma, P. R. P., and Singh, S. K. (2016). Emerging technologies for improving bioavailability of polyphenols. *Current Nutrition and Food Science*, 12(1), 12–22.
- Vo, T. K., Ta, Q. T. H., Chu, Q. T., Nguyen, T. T., and Vo, V. G. (2020). Anti-hepatocellular-cancer activity exerted by  $\beta$ -sitosterol and  $\beta$ -sitosterol-glucoside from *Indigofera zollingeriana* Miq. *Molecules*, 25(13), 1–14. <https://doi.org/10.3390/molecules25133021>

- Wakuta, S., Hamada, S., Ito, H., Imai, R., Mori, H., Matsuura, H., Nabeta, K., and Matsui, H. (2011). Comparison of enzymatic properties and gene expression profiles of two tuberonic acid glucoside  $\beta$ -glucosidases from *Oryza sativa* L. *Journal of Applied Glycoscience*, *58*(2), 67–70. [https://doi.org/10.5458/jag.jag.JAG-2010\\_013](https://doi.org/10.5458/jag.jag.JAG-2010_013)
- Wang, C., Qi, R., and Xu, Z. (2023). Glycosyl radical-based synthesis of C-glycoamino acids and C-glycopeptides. *Chemistry-A European Journal*, *29*(21), 1–8. <https://doi.org/10.1002/chem.202203689>
- Wang, J., Silva, J. P., Gustafsson, C. M., Rustin, P., and Larsson, N. G. (2001). Increased *in vivo* apoptosis in cells lacking mitochondrial DNA gene expression. *Proceedings of the National Academy of Sciences*, *98*(7), 4038–4043. <https://doi.org/10.1073/pnas.061038798>
- Wang, Z., Liu, Y., and Cui, Y. (2005). Pathways to caspase activation. *Cell Biology International*, *29*(7), 489–496. <https://doi.org/10.1016/j.cellbi.2005.04.001>
- Wang, Z. (2021). Regulation of cell cycle progression by growth factor-induced cell signaling. *Cells*, *10*(12), 1–23. <https://doi.org/10.3390/cells10123327>
- Wei, J., Lv, X., Lu, Y., Yang, G., Fu, L., Yang, L., Wang, J., Gao, J., Cheng, S., Duan, Q., Jin, C., and Li, X. (2013). Glycosynthase with broad substrate specificity-an efficient biocatalyst for the construction of oligosaccharide library. *European Journal of Organic Chemistry*, *2013*, 2414–2419. <https://doi.org/10.1002/ejoc.201201507>
- Wodrich, A. P. K., Scott, A. W., Shukla, A. K., Harris, B. T., and Giniger, E. (2022). The unfolded protein responses in health, aging, and neurodegeneration: recent advances and future considerations. *Frontiers in Molecular Neuroscience*, *15*, 1–27. <https://doi.org/10.3389/fnmol.2022.831116>
- Woo, H. J., Kang, H. K., Nguyen, T. T. H., Kim, G. E., Kim, Y. M., Park, J. S., Kim, D., Cha, J., Moon, Y. H., Nam, S. H., Xia, Y., Kimura, A., and Kim, D. (2012). Synthesis and characterization of ampelopsin glucosides using dextransucrase from *Leuconostoc mesenteroides* B-1299CB4: glucosylation enhancing physicochemical properties. *Enzyme and Microbial Technology*, *51*(6–7), 311–318. <https://doi.org/10.1016/j.enzmictec.2012.07.014>
- Xu, L., Chen, S., and Bergan, R. C. (2006). MAPKAPK2 and HSP27 are downstream

- effectors of p38 MAP kinase-mediated matrix metalloproteinase type 2 activation and cell invasion in human prostate cancer. *Oncogene*, *25*(21), 2987–2998. <https://doi.org/10.1038/sj.onc.1209337>
- Yang, H., Villani, R. M., Wang, H., Simpson, M. J., Roberts, M. S., Tang, M., and Liang, X. (2018). The role of cellular reactive oxygen species in cancer chemotherapy. *Journal of Experimental and Clinical Cancer Research*, *37*(266), 1–10. <https://doi.org/10.1186/s13046-018-0909-x>
- Yongvanit, P., Pinlaor, S., and Bartsch, H. (2012). Oxidative and nitrative DNA damage: key events in opisthorchiasis-induced carcinogenesis. *Parasitology International*, *61*(1), 130–135. <https://doi.org/10.1016/j.parint.2011.06.011>
- Yue, S., Zhang, P., Zhu, Y., Li, N. G., Chen, Y., Li, J., Zhang, S., Jin, R. Y., Yan, H., Shi, X. Q., Tang, Y. P., and Duan, J. A. (2019). A ferulic acid derivative FXS-3 inhibits proliferation and metastasis of human lung cancer A549 cells via positive JNK signaling pathway and negative ERK/p38, AKT/mTOR and MEK/ERK signaling pathways. *Molecules*, *24*(11), 1–12. <https://doi.org/10.3390/molecules24112165>
- Zabalza, A., Orcaray, L., Fernández-Escalada, M., Zulet-González, A., and Royuela, M. (2017). The pattern of shikimate pathway and phenylpropanoids after inhibition by glyphosate or quinate feeding in pea roots. *Pesticide Biochemistry and Physiology*, *141*, 96–102. <https://doi.org/10.1016/j.pestbp.2016.12.005>
- Zaupa, M., Calani, L., Rio, D. D., Brighenti, F., and Pellegrini, N. (2015). Characterization of total antioxidant capacity and (poly) phenolic compounds of differently pigmented rice varieties and their changes during domestic cooking. *Food Chemistry*, *187*, 338–347. <https://doi.org/10.1016/j.foodchem.2015.04.055>
- Zelig, U., Kapelushnik, J., Moreh, R., Mordechai, S., and Nathan, I. (2009). Diagnosis of cell death by means of infrared spectroscopy. *Biophysical Journal*, *97*(7), 2107–2114. <https://doi.org/10.1016/j.bpj.2009.07.026>
- Zhang, L., Zhang, T., Chang, M., Lu, M., Liu, R., Jin, Q., and Wang, X. (2019). Effects of interaction between  $\alpha$ -tocopherol, oryzanol, and phytosterol on the antiradical activity against DPPH radical. *LWT-Food Science and Technology*, *112*, 1–8. <https://doi.org/10.1016/j.lwt.2019.05.104>

- Zhang, Y. Y., Zhang, F., Zhang, Y. S., Thakur, K., Zhang, J. G., Liu, Y., Kan, H., and Wei, Z. J. (2019). Mechanism of juglone-induced cell cycle arrest and apoptosis in Ishikawa human endometrial cancer cells. *Journal of Agricultural and Food Chemistry*, 67(26), 7378–7389. <https://doi.org/10.1021/acs.jafc.9b02759>
- Zheng, S., Zhu, Y., Zhao, Z., Wu, Z., Okanurak, K., and Lv, Z. (2017). Liver fluke infection and cholangiocarcinoma: a review. *Parasitology Research*, 116, 11–19. <https://doi.org/10.1007/s00436-016-5276-y>
- Zheng, Y., Zhou, Y., Guo, R., Fu, Z., and Chen, D. (2020). Structure-antioxidant activity relationship of ferulic acid derivatives: effect of ester groups at the end of the carbon side chain. *Food Science and Technology*, 120, 1–7. <https://doi.org/10.1016/j.lwt.2019.108932>





APPENDICES

## APPENDIX A

### PROTEIN PURIFICATION AND GLYCOSYLATED PRODUCTS

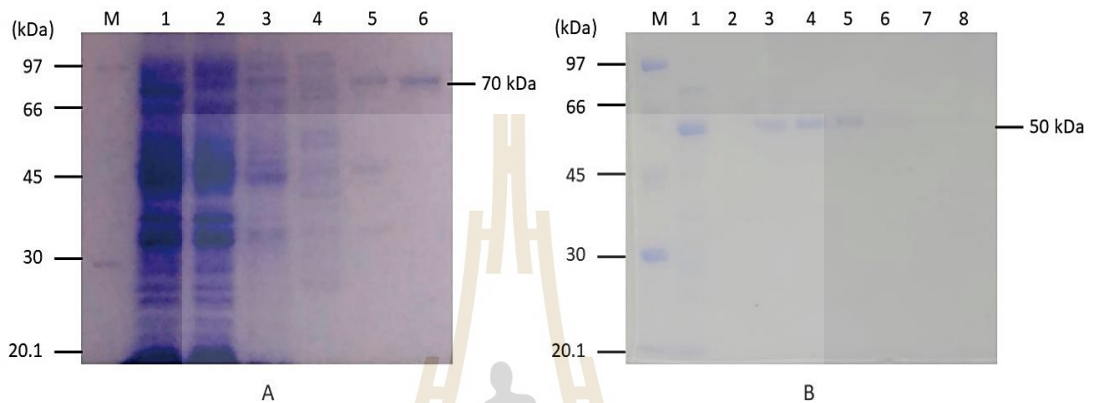


**Figure A.1** SDS-PAGE analysis of Os9BGlu31 wild type purification fractions. (A) Os9BGlu31 wild type was purified by 1<sup>st</sup> IMAC Sepharose with Co<sup>2+</sup> equilibrated resin. Lane M = molecular weight marker, lane 1 = soluble crude enzyme, lane 2 = flow through, lane 3 = W0 (unbound protein with equilibration buffer), lane 4 = W10 (10 mM imidazole), lane 5 = W20 (20 mM imidazole), lane 6 = E250 (His-tag-Os9BGlu31 eluted with 250 mM imidazole). (B) Os9BGlu31 wild type was purified by 2<sup>nd</sup> IMAC Sepharose with Co<sup>2+</sup> equilibrated resin after TEV cleavage from the tags. Lane M = molecular weight marker, lane 1 = protein after cleavage, lane 2 = flow through, lane 3 = E0<sub>1</sub>, lane 4 = E0<sub>2</sub>, lane 5 = E0<sub>3</sub>, lane 6 = E0<sub>4</sub>, lane 7 = E5<sub>1</sub>, lane 8 = E5<sub>2</sub>.

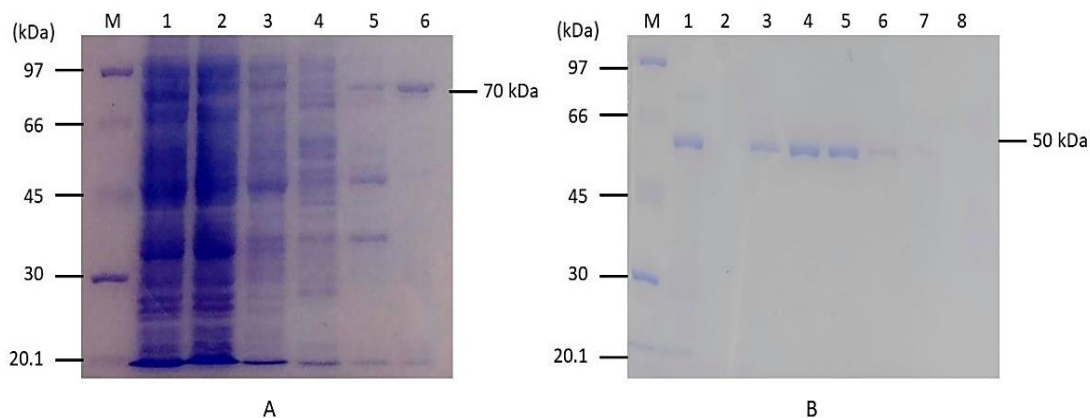


**Figure A.2** SDS-PAGE analysis of Os9BGlu31 W243H purification fractions. (A) Os9BGlu31 W243H was purified by 1<sup>st</sup> IMAC Sepharose with Co<sup>2+</sup> equilibrated resin. Lane M = molecular weight marker, lane 1 = soluble crude enzyme, lane 2 = flow through, lane 3 = W0 (unbound protein with equilibration buffer), lane 4 = W10 (10 mM imidazole), lane 5 = W20 (20 mM imidazole), lane 6 = E250 (His-tag-Os9BGlu31 eluted with 250 mM imidazole). (B) Os9BGlu31 W243H was purified by 2<sup>nd</sup> IMAC Sepharose with Co<sup>2+</sup> equilibrated resin after TEV cleavage from the tags. Lane M = molecular weight marker, lane 1 = protein after cleavage, lane 2 = flow through, lane 3 = E0<sub>1</sub>, lane 4 = E0<sub>2</sub>, lane 5 = E0<sub>3</sub>, lane 6 = E0<sub>4</sub>, lane 7 = E5<sub>1</sub>, lane 8 = E5<sub>2</sub>.

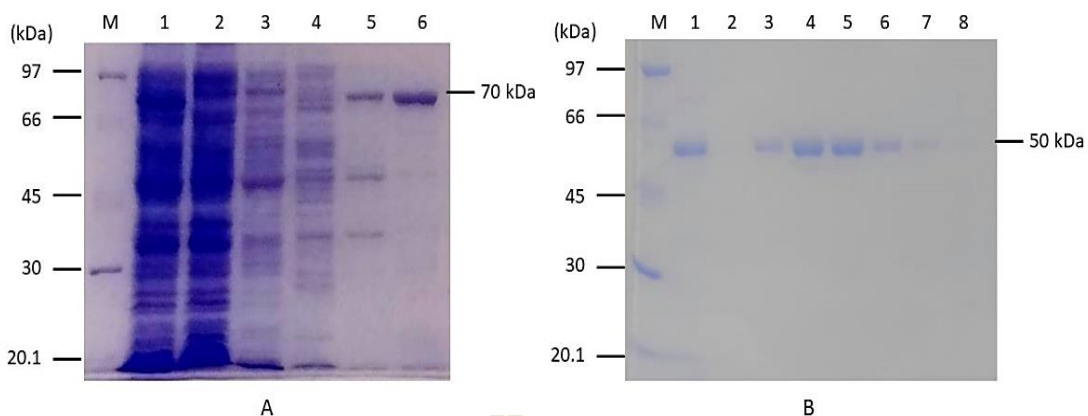


**Figure A.3** SDS-PAGE analysis of Os9BGlu31 W243N purification fractions. (A) Os9BGlu31 W243N was purified by 1<sup>st</sup> IMAC Sepharose with Co<sup>2+</sup> equilibrated resin. Lane M = molecular weight marker, lane 1 = soluble crude enzyme, lane 2 = flow through, lane 3 = W0 (unbound protein with equilibration buffer), lane 4 = W10 (10 mM imidazole), lane 5 = W20 (20 mM imidazole), lane 6 = E250 (His-tag-Os9BGlu31 eluted with 250 mM imidazole). (B) Os9BGlu31 W243N was purified by 2<sup>nd</sup> IMAC Sepharose with Co<sup>2+</sup> equilibrated resin after TEV cleavage from the tags. Lane M = molecular weight marker, lane 1 = protein after cleavage, lane 2 = flow through, lane 3 = E0<sub>1</sub>, lane 4 = E0<sub>2</sub>, lane 5 = E0<sub>3</sub>, lane 6 = E0<sub>4</sub>, lane 7 = E5<sub>1</sub>, lane 8 = E5<sub>2</sub>.

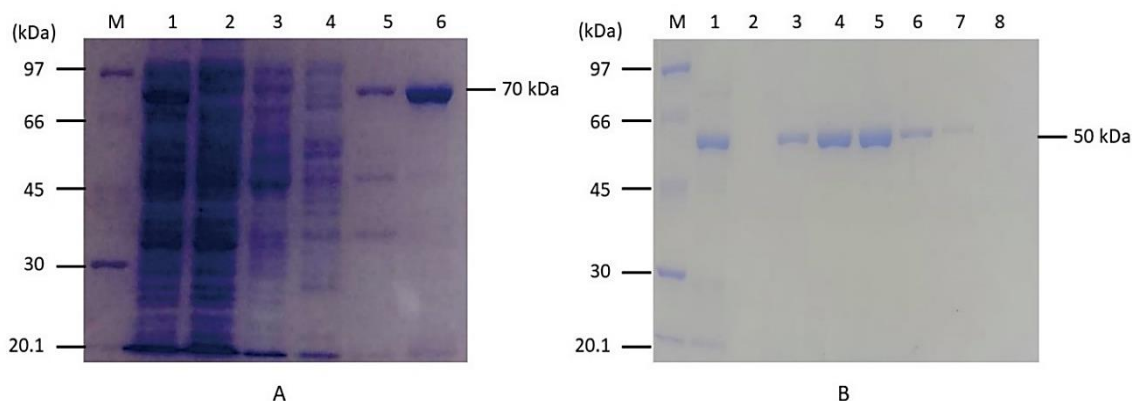


**Figure A.4** SDS-PAGE analysis of Os9BGlu31 W243L purification fractions. (A) Os9BGlu31 W243L was purified by 1<sup>st</sup> IMAC Sepharose with Co<sup>2+</sup> equilibrated resin. Lane M = molecular weight marker, lane 1 = soluble crude enzyme, lane 2 = flow through, lane 3 = W0 (unbound protein with equilibration buffer), lane 4 = W10 (10 mM imidazole), lane 5 = W20 (20 mM imidazole), lane 6 = E250 (His-tag-Os9BGlu31 eluted with 250 mM imidazole). (B) Os9BGlu31 W243L was purified by 2<sup>nd</sup> IMAC Sepharose with Co<sup>2+</sup> equilibrated resin after TEV cleavage from the tags. Lane M = molecular weight marker, lane 1 = protein after cleavage, lane 2 = flow through, lane 3 = E0<sub>1</sub>, lane 4 = E0<sub>2</sub>, lane 5 = E0<sub>3</sub>, lane 6 = E0<sub>4</sub>, lane 7 = E5<sub>1</sub>, lane 8 = E5<sub>2</sub>.

**Table A.1** Retention time of transglucosylation products in the enzymatic reactions with several glucosyl acceptors after separation by UHPLC.

Substrates (Glucosyl acceptors)	MF	MW (g/mol)	RT (min)	Retention time of products (min)		
				glucosyl- ester	glucoside	bis- glucoside
Ferulic acid	C <sub>10</sub> H <sub>10</sub> O <sub>4</sub>	194.18	10.2	8.2	7.4	6.3
Vanillic acid	C <sub>8</sub> H <sub>8</sub> O <sub>4</sub>	168.14	8.5	6.7	5.9	4.7
4-Hydroxybenzoic acid	C <sub>7</sub> H <sub>6</sub> O <sub>3</sub>	138.12	7.8	6.2	4.9	3.3
<i>p</i> -Coumaric acid	C <sub>9</sub> H <sub>8</sub> O <sub>3</sub>	164.16	9.7	7.8	6.9	5.9
<i>trans</i> -Cinnamic acid	C <sub>9</sub> H <sub>8</sub> O <sub>2</sub>	148.15	13.4	10.3	-	-
Syringic acid	C <sub>9</sub> H <sub>10</sub> O <sub>5</sub>	198.17	8.7	7	6.5	5.5
Sinapic acid	C <sub>11</sub> H <sub>12</sub> O <sub>5</sub>	224.21	10.3	8.3	7.8	-
Gallic acid	C <sub>7</sub> H <sub>6</sub> O <sub>3</sub>	170.12	3.8	2.8	5.6	-

## APPENDIX B

### PHENOLIC ACID GLUCOSYL ESTERS AND THEIR AGLYCONES

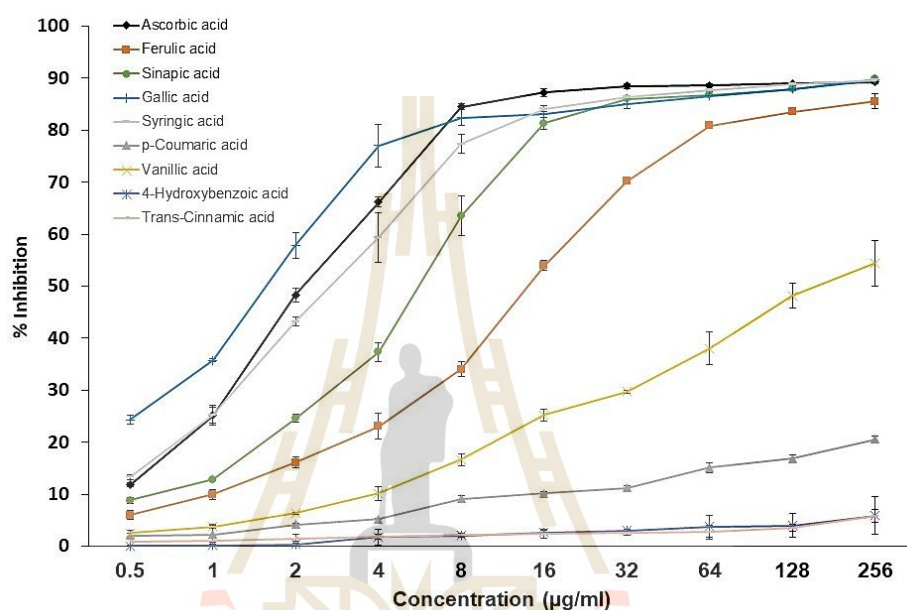


**Figure B.1** Antioxidant activity of phenolic acids. The radical scavenging activity was determined by DPPH assay. The values are expressed as mean  $\pm$  SD (shown as error bars) of three independent experiments.

**Table B.1** IC<sub>50</sub> values of antioxidant activity of phenolic acids. The values are expressed as mean  $\pm$  SD (shown as error bars) of three independent experiments.

Glycones	IC <sub>50</sub>	Glycones	IC <sub>50</sub>
Ascorbic acid	2.35 $\pm$ 0.05 $\mu$ g/ml		
Ferulic acid	14.50 $\pm$ 0.46 $\mu$ g/ml	<i>p</i> -Coumaric acid	> 256 $\mu$ g/ml
Sinapic acid	5.56 $\pm$ 0.21 $\mu$ g/ml	Vanillic acid	> 256 $\mu$ g/ml
Gallic acid	1.58 $\pm$ 0.09 $\mu$ g/ml	4-Hydroxybenzoic acid	> 256 $\mu$ g/ml
Syringic acid	2.86 $\pm$ 0.12 $\mu$ g/ml	<i>trans</i> -Cinnamic acid	> 256 $\mu$ g/ml

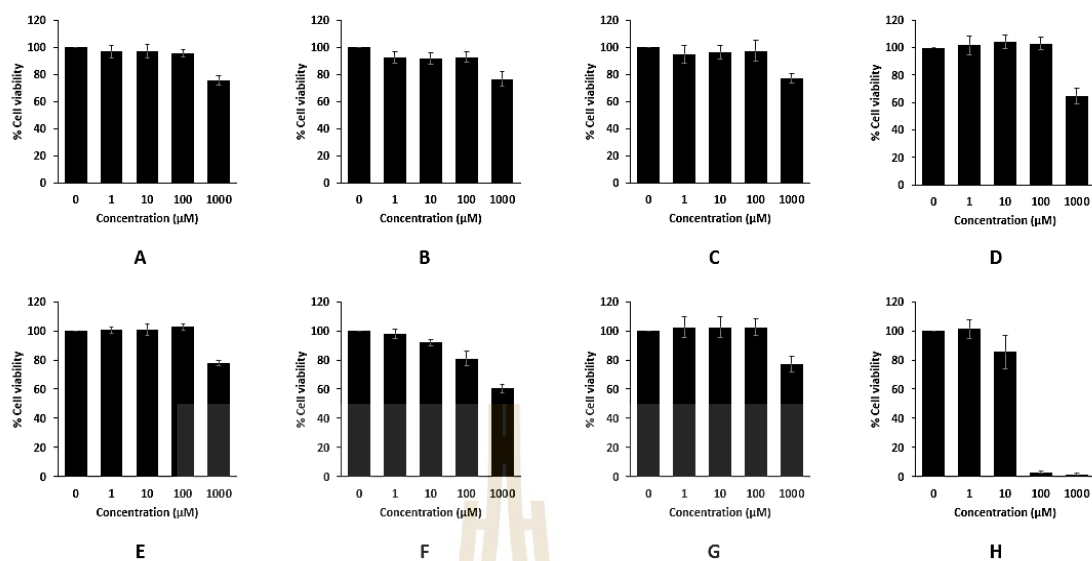


**Figure B.2** Inhibitory effect of phenolic acids on cell proliferation of KKU-213A at 24 h. (A) ferulic acid, (B) vanillic-acid, (C) 4-hydroxybenzoic acid, (D) *p*-coumaric acid, (E) *trans*-cinnamic acid, (F) syringic acid, (G) sinapic acid, and (H) gallic acid. The cell viability was determined by the SRB assay. The values are expressed as mean  $\pm$  SD (shown as error bars) of three independent experiments.

**Table B.2** IC<sub>50</sub> values of inhibitory effect of  $\beta$ -glucogallin in cholangiocarcinoma cells at 24, 48 and 72 h. The values are expressed as mean  $\pm$  SD of three independent experiments.

CCA Cells	Incubation time	IC <sub>50</sub> values (µM)
KKU-213A	24 h	67.3 $\pm$ 1.3
	48 h	57.8 $\pm$ 1.6
	72 h	51.7 $\pm$ 0.4
KKU-055	24 h	19.8 $\pm$ 1.3
	48 h	18.1 $\pm$ 0.7
	72 h	17.6 $\pm$ 1.7
KKU-100	24 h	178.7 $\pm$ 4.1
	48 h	170.9 $\pm$ 4.9
	72 h	140.7 $\pm$ 1.6

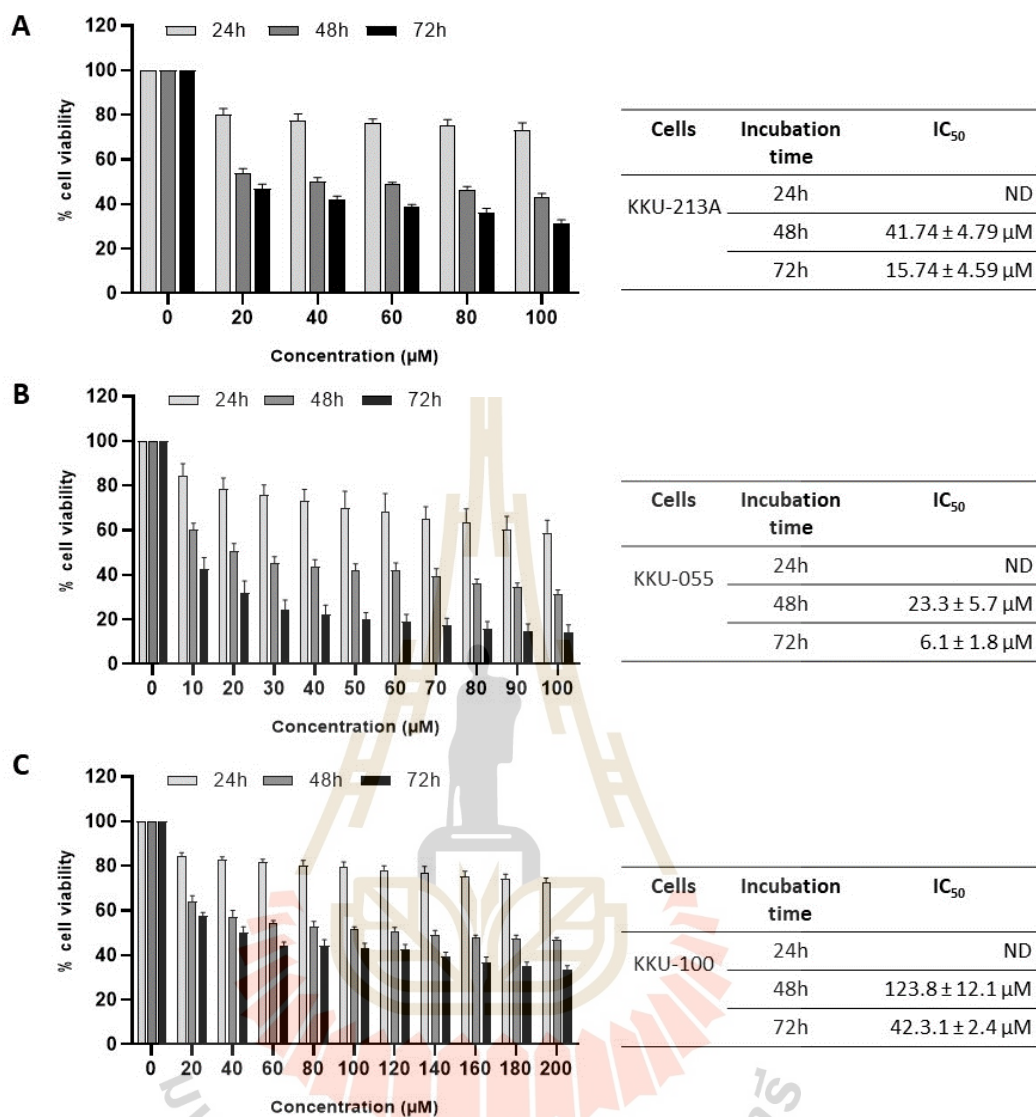


**Figure B.3** Inhibitory effect of 5-fluorouracil in (A) KKU-213A, (B) KKU-055, and (C) KKU-100 at 24, 48 and 72 h. The cell viability was determined by SRB assay. The values are expressed as mean ± SD (shown as error bars) of three independent experiments.



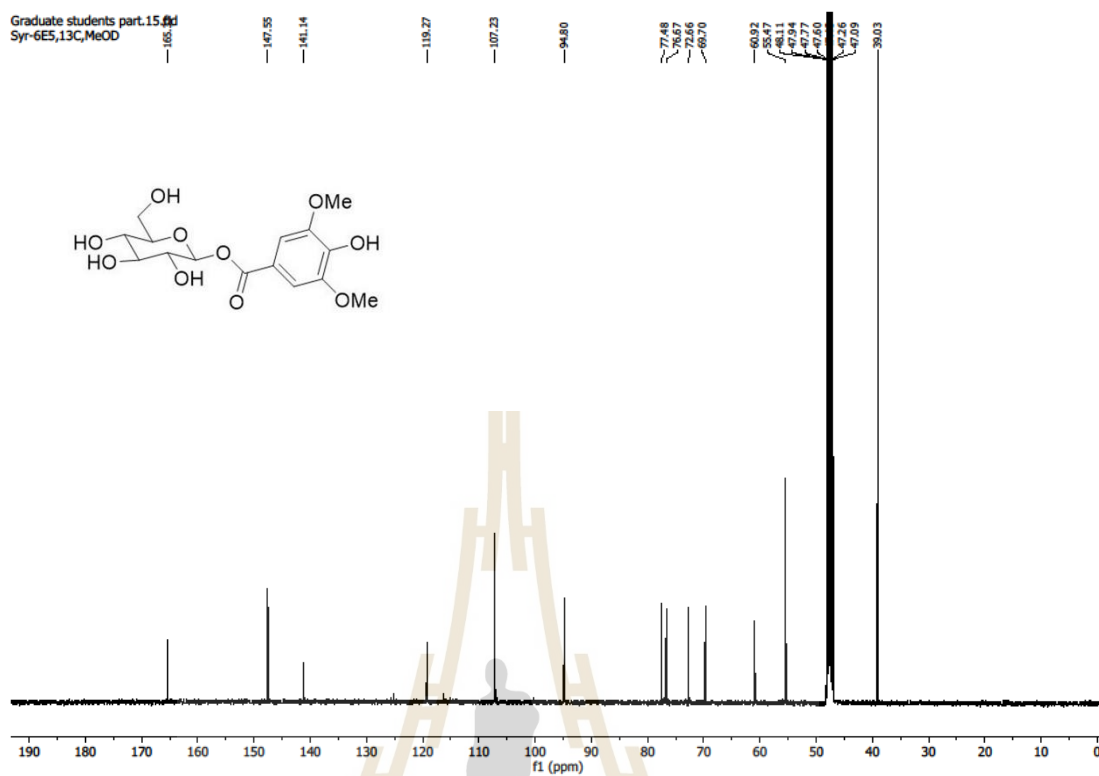
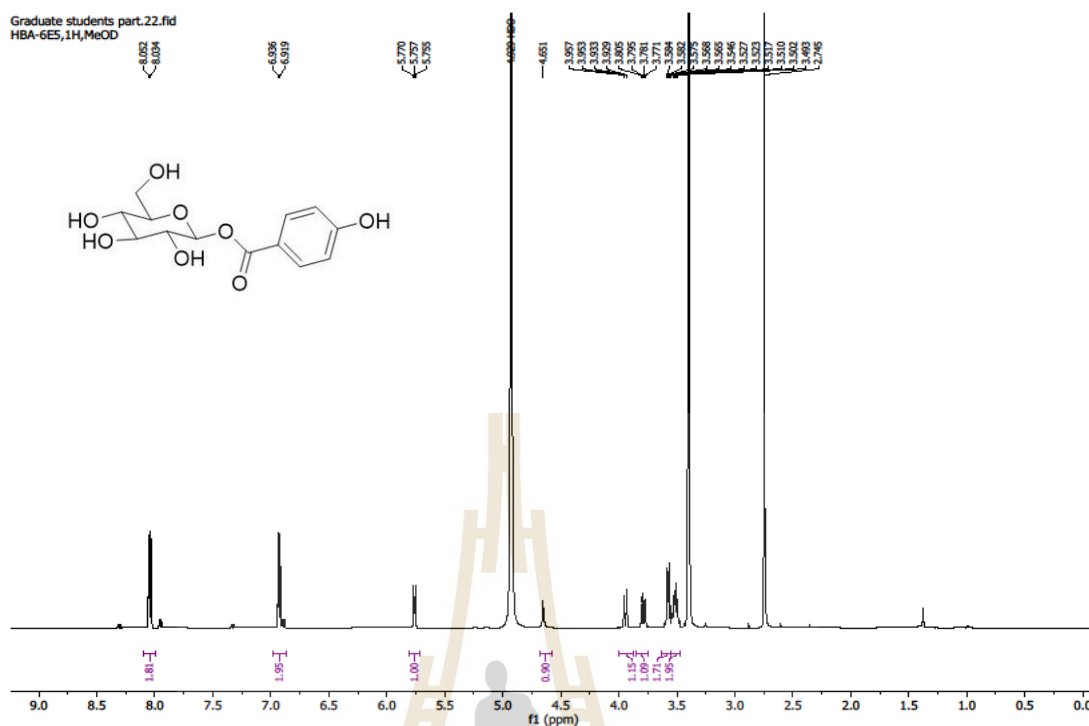


Figure C.2  $^{13}\text{C}$ -NMR (125 MHz,  $\text{CD}_3\text{OD}$ ) spectra of syringic acid glucosyl ester. Solvent:  $\text{CD}_3\text{OD}$ , Frequency: 125 MHz.





**Figure C.3**  $^1\text{H-NMR}$  (500 MHz,  $\text{CD}_3\text{OD}$ ) spectra of 4-hydroxybenzoic acid glucosyl ester. Solvent:  $\text{CD}_3\text{OD}$ , Frequency: 500 MHz.

#### Experimental section:

(4-Hydroxybenzoic acid glucosyl ester):  $^1\text{H NMR}$  (500 MHz,  $\text{CD}_3\text{OD}$ )  $\delta$  8.04 (d,  $J = 8.8$  Hz, 2H), 6.93 (d,  $J = 8.8$  Hz, 2H), 5.76 (d,  $J = 7.8$  Hz, 1H), 4.65 (s, 1H), 3.94 (dd,  $J = 12.2, 2.0$  Hz, 1H), 3.79 (dd,  $J = 12.1, 4.7$  Hz, 1H), 3.63 – 3.55 (m, 2H), 3.55 – 3.47 (m, 2H);  $^{13}\text{C NMR}$  (125 MHz,  $\text{CD}_3\text{OD}$ )  $\delta$  165.38, 162.63, 131.90, 120.15, 114.81, 94.59, 77.45, 76.72, 72.68, 69.71, and 60.94.

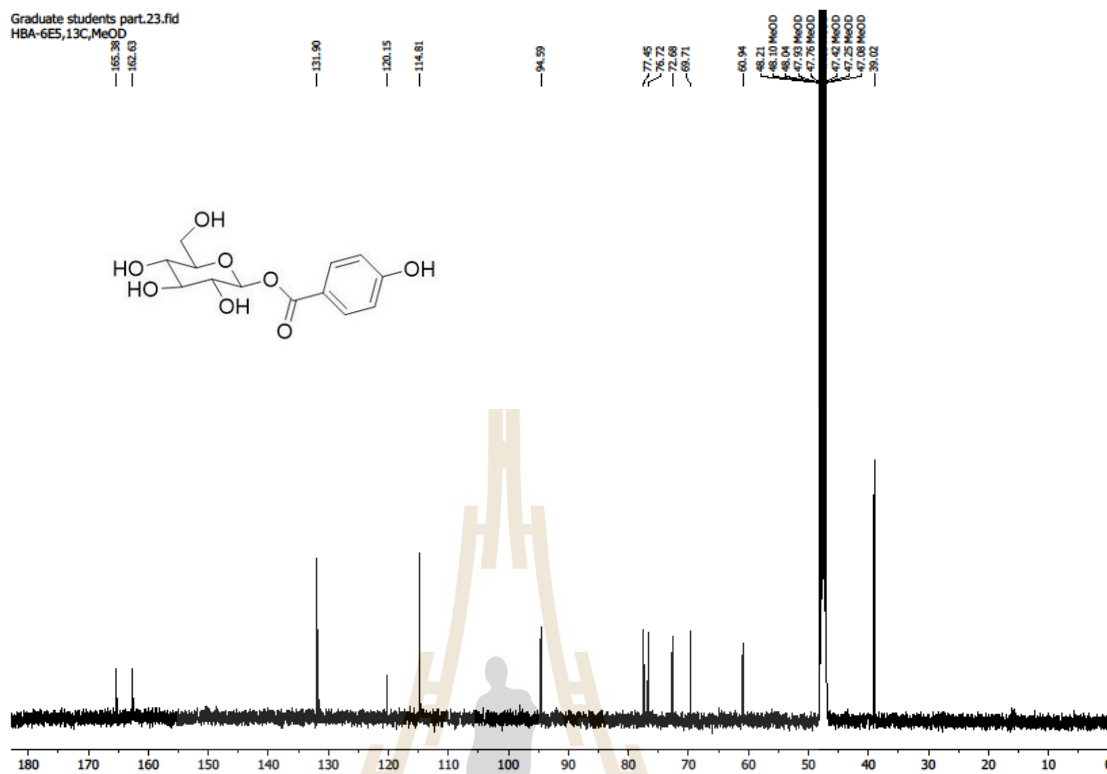


Figure C.4  $^{13}\text{C-NMR}$  (125 MHz,  $\text{CD}_3\text{OD}$ ) spectra of 4-hydroxybenzoic acid glucosyl ester.

Solvent:  $\text{CD}_3\text{OD}$ , Frequency: 125 MHz.



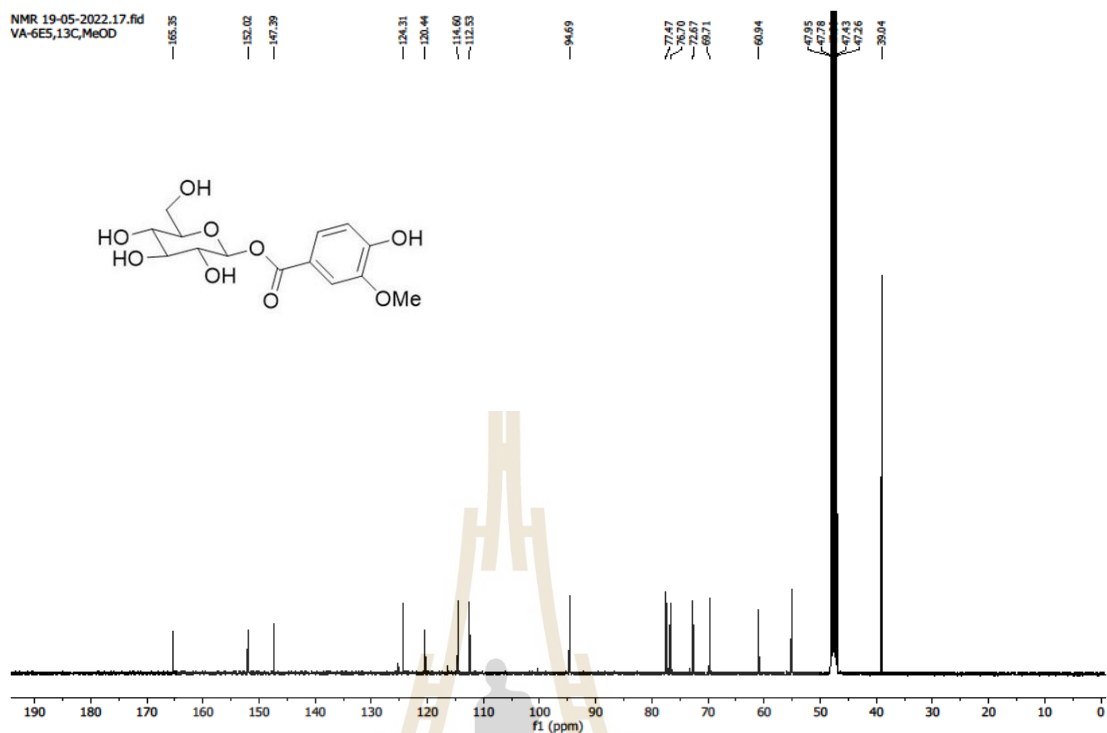


Figure C.6  $^{13}\text{C}$ -NMR (125 MHz,  $\text{CD}_3\text{OD}$ ) spectra of vanillic acid glucosyl ester. Solvent:  $\text{CD}_3\text{OD}$ , Frequency: 125 MHz.



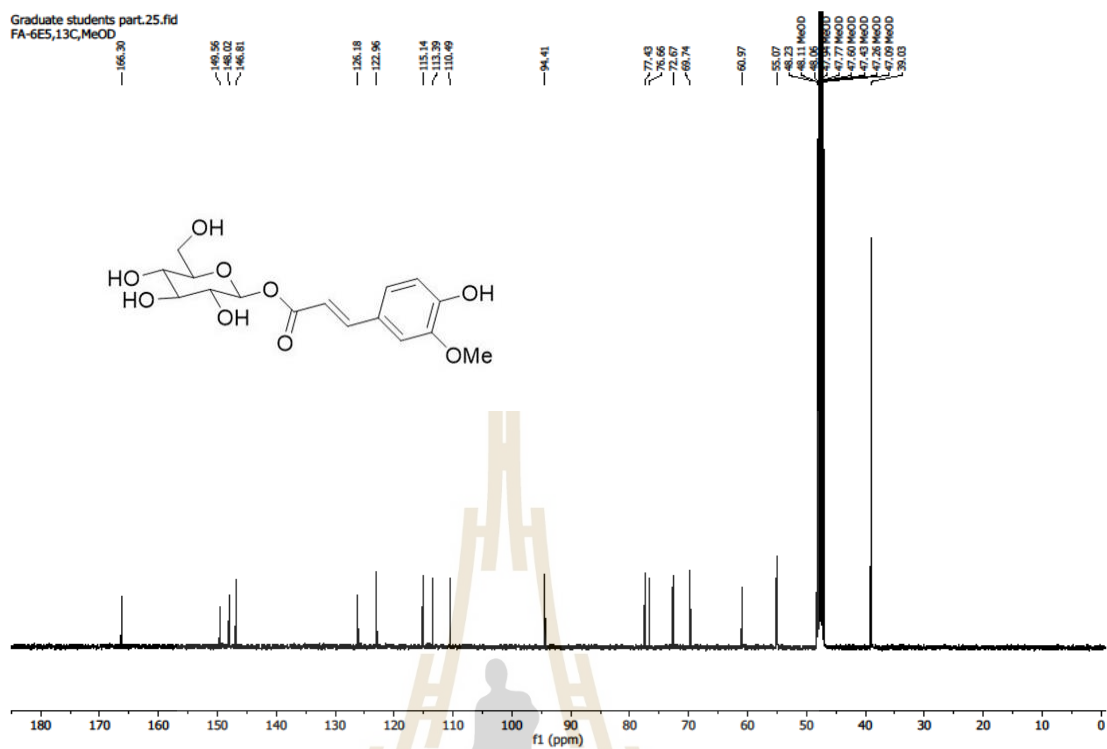
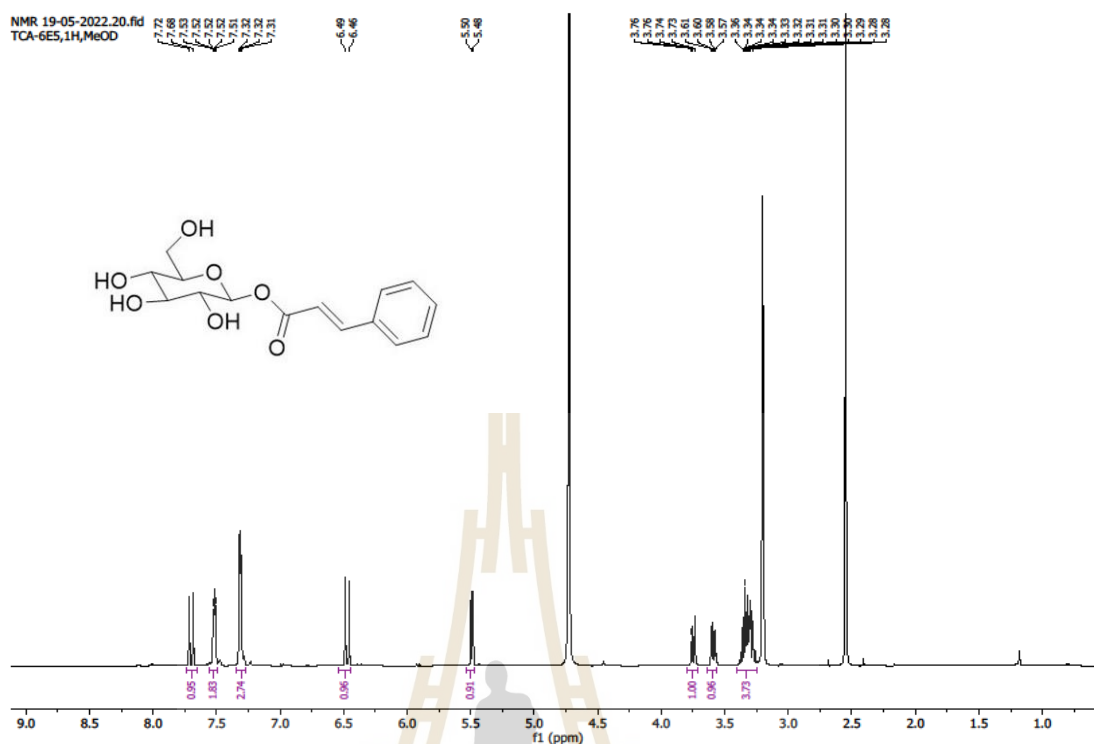


Figure C.8  $^{13}\text{C}$ -NMR (125 MHz,  $\text{CD}_3\text{OD}$ ) spectra of ferulic acid glucosyl ester. Solvent:  $\text{CD}_3\text{OD}$ , Frequency: 125 MHz.





**Figure C.9**  $^1\text{H-NMR}$  (500 MHz,  $\text{CD}_3\text{OD}$ ) spectra of *trans*-cinnamic acid glucosyl ester. Solvent:  $\text{CD}_3\text{OD}$ , Frequency: 500 MHz.

#### Experimental section:

(*trans*-cinnamic acid glucosyl ester):  $^1\text{H NMR}$  (500 MHz,  $\text{CD}_3\text{OD}$ )  $\delta$  7.70 (d,  $J = 16.0$  Hz, 1H), 7.52 (dd,  $J = 6.6, 2.9$  Hz, 2H), 7.35 – 7.27 (m, 3H), 6.47 (d,  $J = 16.0$  Hz, 1H), 5.49 (d,  $J = 7.7$  Hz, 1H), 3.75 (dd,  $J = 12.1, 2.1$  Hz, 1H), 3.59 (dd,  $J = 12.1, 4.9$  Hz, 1H), and 3.41 – 3.25 (m, 4H);  $^{13}\text{C NMR}$  (125 MHz,  $\text{CD}_3\text{OD}$ )  $\delta$  165.70, 146.23, 134.21, 130.40, 128.68, 127.97, 116.88, 94.54, 77.47, 76.62, 72.63, 69.71, and 60.94.

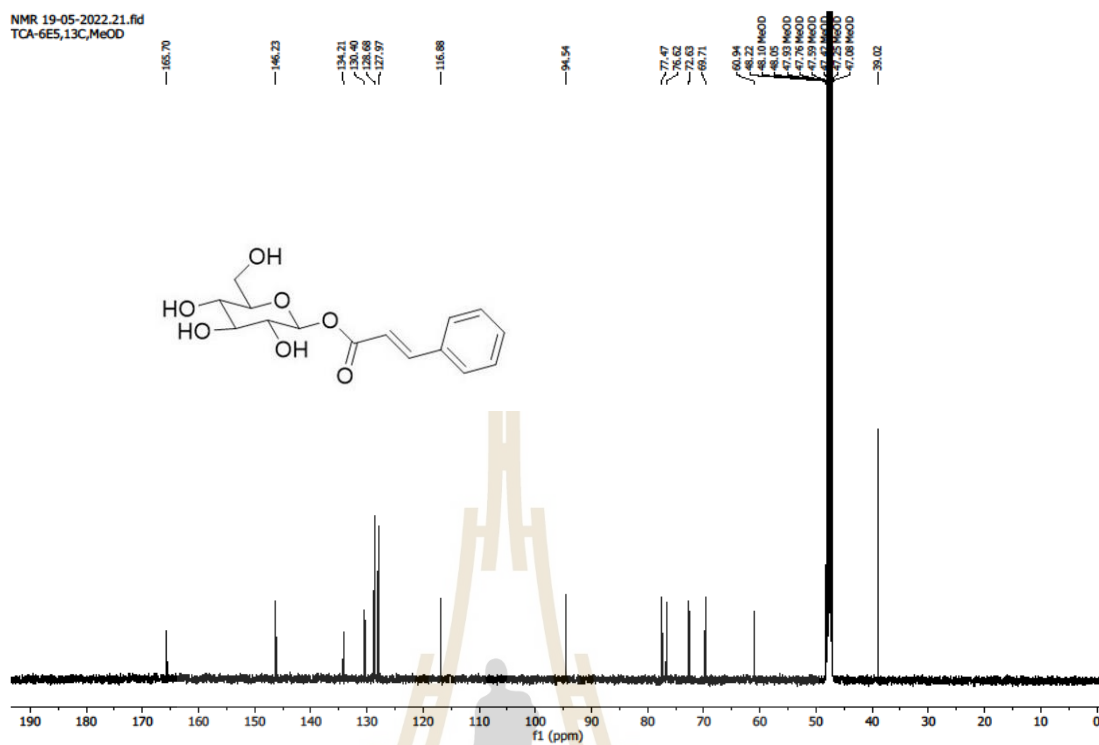


Figure C.10  $^{13}\text{C}$ -NMR (125 MHz,  $\text{CD}_3\text{OD}$ ) spectra of *trans*-cinnamic acid glucosyl ester. Solvent:  $\text{CD}_3\text{OD}$ , Frequency: 125 MHz.



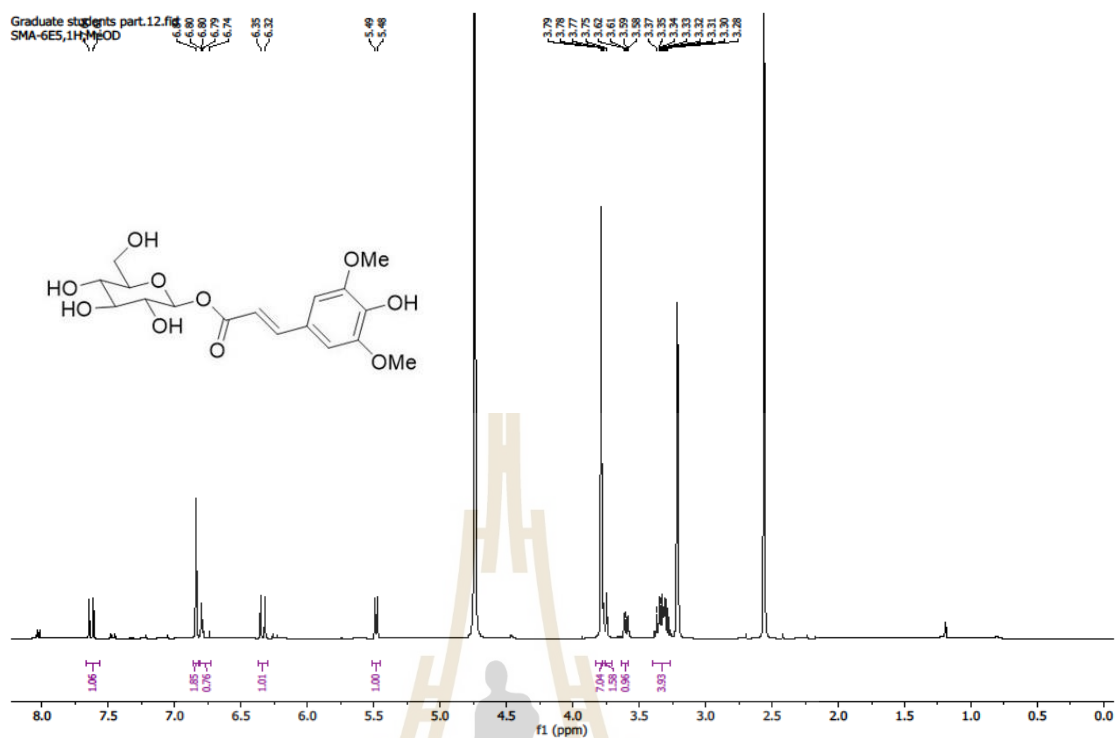


Figure C.11  $^1\text{H-NMR}$  (500 MHz,  $\text{CD}_3\text{OD}$ ) spectra of sinapic acid glucosyl ester. Solvent:  $\text{CD}_3\text{OD}$ , Frequency: 500 MHz.

#### Experimental section:

(Sinapic acid glucosyl ester):  $^1\text{H NMR}$  (500 MHz,  $\text{CD}_3\text{OD}$ )  $\delta$  7.63 (d,  $J = 15.8$  Hz, 1H), 6.84 (s, 2H), 6.79 (d,  $J = 5.9$  Hz, 1H), 6.34 (d,  $J = 15.9$  Hz, 1H), 5.48 (d,  $J = 7.7$  Hz, 1H), 3.78 (s,  $J = 4.2$  Hz, 6H), 3.75 (m, 1H), 3.60 (dd,  $J = 12.1, 4.9$  Hz, 1H), and 3.40 – 3.26 (m, 4H);  $^{13}\text{C NMR}$  (125 MHz,  $\text{CD}_3\text{OD}$ )  $\delta$  166.22, 148.12, 147.03, 138.58, 125.64, 125.10, 115.11, 113.83, 105.73, 94.43, 77.44, 76.66, 72.68, 69.74, 60.97, and 55.46.

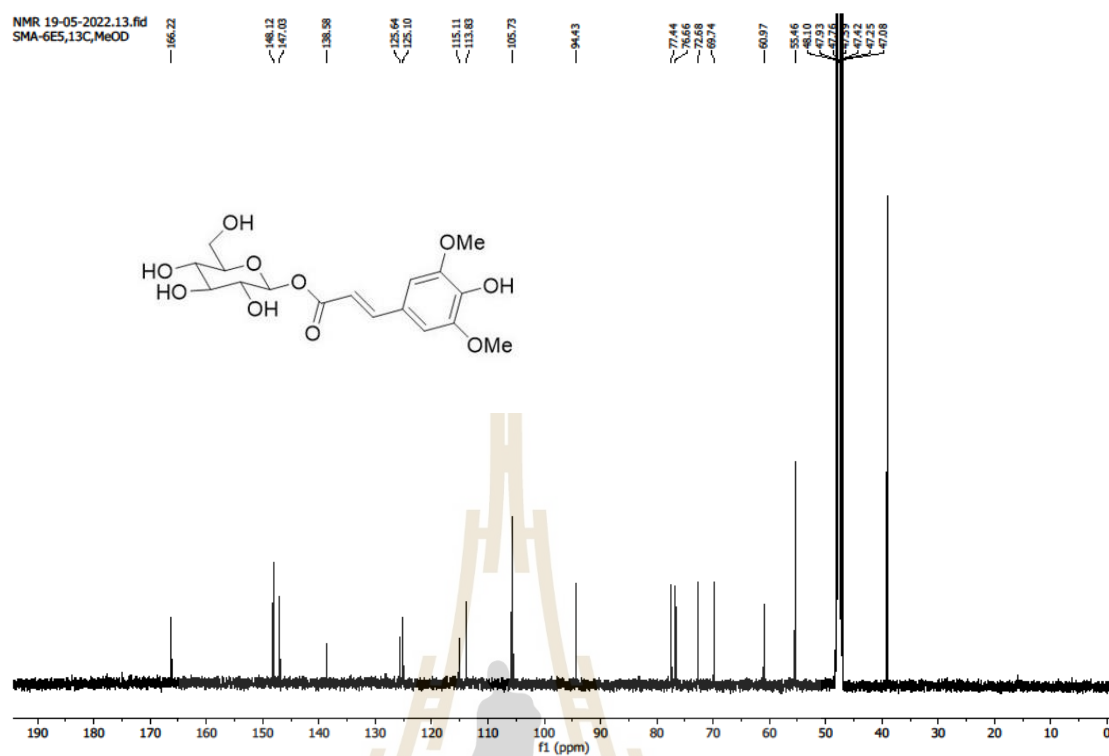
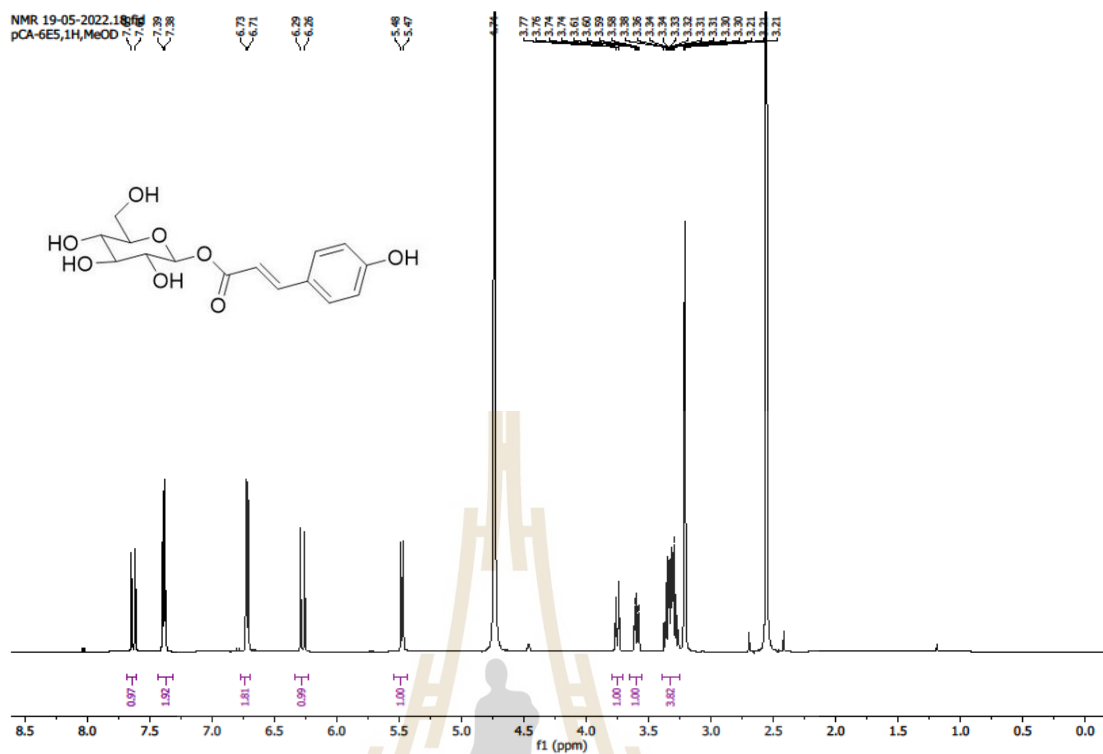


Figure C.12  $^{13}\text{C}$ -NMR (125 MHz,  $\text{CD}_3\text{OD}$ ) spectra of sinapic acid glucosyl ester. Solvent:  $\text{CD}_3\text{OD}$ , Frequency: 125 MHz.



**Figure C.13**  $^1\text{H-NMR}$  (500 MHz,  $\text{CD}_3\text{OD}$ ) spectra of *p*-coumaric acid glucosyl ester. Solvent:  $\text{CD}_3\text{OD}$ , Frequency: 500 MHz.

#### Experimental section:

(*p*-Coumaric acid glucosyl ester):  $^1\text{H NMR}$  (500 MHz,  $\text{CD}_3\text{OD}$ )  $\delta$  7.63 (d,  $J = 15.9$  Hz, 1H), 7.38 (d,  $J = 8.6$  Hz, 2H), 6.72 (d,  $J = 8.6$  Hz, 2H), 6.27 (d,  $J = 15.9$  Hz, 1H), 5.48 (d,  $J = 7.8$  Hz, 1H), 3.75 (dd,  $J = 12.1, 2.0$  Hz, 1H), 3.59 (dd,  $J = 12.1, 4.8$  Hz, 1H), and 3.39 – 3.25 (m, 4H);  $^{13}\text{C NMR}$  (125 MHz,  $\text{CD}_3\text{OD}$ )  $\delta$  166.32, 160.19, 146.54, 129.98, 125.63, 115.49, 113.08, 94.39, 77.43, 76.64, 72.65, 69.73, and 60.96.

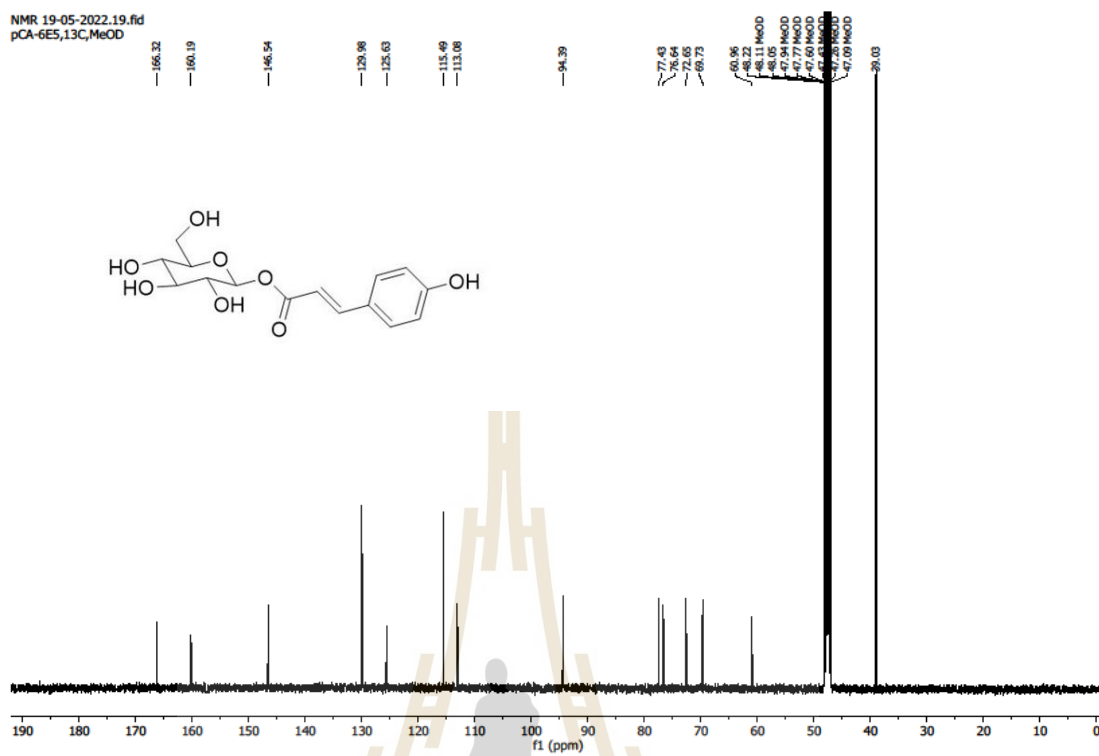


Figure C.14  $^{13}\text{C}$ -NMR (125 MHz,  $\text{CD}_3\text{OD}$ ) spectra of *p*-coumaric acid glucosyl ester.  
Solvent:  $\text{CD}_3\text{OD}$ , Frequency: 125 MHz.



## APPENDIX D

### PUBLICATIONS AND ACHIEVEMENT

**Publications:** <https://scholar.google.com/citations?hl=en&user=06nKzQMAAAAJ>

1. Sutanti, V., **Suyanto, E.**, Mufidah, M., and Kurnianingsih, N. (2020). Diversity of sub-gingival fluids microbiota compositions in periodontitis and rheumatoid arthritis patients: A case study. *Brazilian Research in Pediatric Dentistry and Integrated Clinic* 20:1-8. doi : 10.1590/pboci.2020.107
2. Fatchiyah, F., Meidinna, HN., **Suyanto, E.** (2020). The cyanidin-3-O-glucoside of black rice Inhibit the interaction of HMG-CoA and HMG-CoA reductase: three and two-dimension structure. *Proceedings Journal of Physics Conference Series* 1665(2020) 012005. doi : 10.1088/1742-6596/1665/1/012005
3. **Suyanto, E.**, Fatchiyah, F. (2021). Predominant bacterial diversity in rheumatoid arthritis rat after treated with caprine CSN1S2 protein. *Journal of Tropical Life Science* 11(2):121-131. doi : 10.11594/jtls.11.02.01
4. Fatchiyah, F., Safitri, A., Palis, CN., Sari, DRT., **Suyanto, E.**, Fajriani, S., Kurnianingsih, N., Nugraha, Y., Sitaresmi, T., Kusbiantoro, B., Ketudat-Cairns, JR., (2023). Bioactive compound profile and their biological activities of endogenous black rice from Java and East Nusa Tenggara. *CyTA Journal of Food* 21(1):159-170. doi : 10.1080/19476337.2023.2173306
5. Gorantla, JN., Choknud, S., **Suyanto, E.**, Win, HH., Hua, Y., Santi, M., Wangngae, S., Kamkaew, A., Ketudat-Cairns, M., Rojanathammanee, L., Ketudat-Cairns, JR. (2023). Semi-synthesis of phenolic-amides and their cytotoxicity against THP-1, HeLa, HepG2 and MCF-7 cell lines. *Natural Products Research* (published 1 August 2023)
6. **Suyanto, E.**, Gorantla, JN., Santi, M., Fatchiyah, F., Ketudat-Cairns, M., Talabnin, C., Ketudat-Cairns, JR. (2023). Enzymatic synthesis of phenolic acid glucosyl esters to test activities on cholangiocarcinoma cells. *Applied Microbiology and Biotechnology* 108(1):1-13. doi : 10.1007/s00253-023-12895-5

**Conferences:**

1. **Oral presentation** in the 11<sup>st</sup> International Conference on Global Resource Conservation (ICGRC) 2020, Malang, Indonesia (28-29 July 2020)
2. **Invited speaker** in the 3<sup>rd</sup> International Seminar on Smart Molecules of Natural Resources (ISSMART) - Asian Federation of Biotechnology (AFOB) 2021, Malang, Indonesia (25-26 August 2021)
3. **Poster presentation** in the 16<sup>th</sup> International online Mini-Symposium of The Protein Society of Thailand (PST) 2021, Chiang Mai, Thailand (17-18 November 2021)
4. **Oral presentation** in the 1<sup>st</sup> IRN international conference (IRNIC) 2022, Nakhon Ratchasima, Thailand (21-22 July 2022)
5. **Oral presentation** in the 4<sup>th</sup> International Seminar on Smart Molecules of Natural Resources (ISSMART) - Asian Federation of Biotechnology (AFOB) 2022, Malang, Indonesia (24-25 August 2022)
6. **Oral presentation** in the Science Postgrad Annual Research Conference (SPARC) 2023, Nakhon Ratchasima, Thailand (18 March 2023)
7. **Invited speaker** in the 5<sup>th</sup> International Seminar on Smart Molecules of Natural Resources (ISSMART) - Asian Federation of Biotechnology (AFOB) 2023, Malang, Indonesia (17-18 October 2023)
8. **Poster presentation** in the 30<sup>th</sup> FAOBMB-8<sup>th</sup> BMB conference 2023, Bangkok, Thailand (22-25 November 2023)

**Achievement:**

1. One Research One Graduate (OROG) Scholarship awardee
2. Best participant award in the 4<sup>th</sup> International Seminar on Smart Molecule of Natural Resources (ISSMART) - Asian Federation of Biotechnology (AFOB) 2022, Indonesia (24-25 August 2022)
3. Best oral presentation award in the Science Postgrad Annual Research Conference (SPARC) 2023, Thailand (18 March 2023)

## CURRICULUM VITAE

**Name** : Eko Suyanto

**Date of birth** : January 31<sup>st</sup>, 1986

**Place of birth** : Sidoarjo, East Java, Indonesia

**Education** :

2020 to 2023 Doctor of Philosophy (Ph.D) in Biochemistry and Biochemical Technology under supervision of Prof. Dr. James R. Ketudat-Cairns, School of Chemistry, Institute of Science, Suranaree University of Technology, Thailand

2012 to 2015 Master of Science (M.Sc) in Biology, Biology department, Faculty of Biology, Universitas Gadjah Mada, Indonesia

2005 to 2010 Bachelor of Science (S.Si) in Biology, Biology department, Faculty of Biology, Universitas Gadjah Mada, Indonesia



มหาวิทยาลัยเทคโนโลยีสุรนารี